

1 **Dental microwear textures differ in pigs with overall similar diets but fed with different**  
2 **seeds**

3 Margot Louail<sup>1\*</sup>, Stéphane Ferchaud<sup>2</sup>, Antoine Souron<sup>3</sup>, Axelle E.C. Walker<sup>1</sup>, Gildas Merceron<sup>1</sup>

4

5 1. PALEVOPRIM, UMR 7262 CNRS and University of Poitiers, 86073 Poitiers Cedex 9, France

6 2. GenESI, UE 1372 INRAE, 86480 Rouillé, France

7 3. PACEA, UMR 5199 CNRS and University of Bordeaux, 33615 Pessac Cedex, France

8 \*Corresponding author

9 Email address:

10 \*[margot.louail@univ-poitiers.fr](mailto:margot.louail@univ-poitiers.fr)

11 [stephane.ferchaud@inrae.fr](mailto:stephane.ferchaud@inrae.fr)

12 [antoine.souron@u-bordeaux.fr](mailto:antoine.souron@u-bordeaux.fr)

13 [axelle.walker@univ-poitiers.fr](mailto:axelle.walker@univ-poitiers.fr)

14 [gildas.merceron@univ-poitiers.fr](mailto:gildas.merceron@univ-poitiers.fr)

15

16 Abstract

17           The thick-enameled, bunodont dentition shared by most early hominins has traditionally  
18 been interpreted as reflecting durophagy, especially in the robust genus *Paranthropus*.  
19 However, subsequent works on dental microwear textures (DMT) and biogeochemical  
20 compositions have challenged this hypothesis. Some authors argued that their robust  
21 morphology might have been driven by the consumption of mechanically challenging  
22 resources during periods of food scarcity. An experimental baseline using a model taxon with  
23 bunodont, thick-enameled cheek teeth, could help better interpret DMT and test hypotheses  
24 regarding the consumption of mechanically challenging foods that could be fallback foods.  
25 Besides, earlier studies have shown that DMT can track subtle dietary variations in extant taxa.  
26 This study aims at testing the hypothesis that the consumption of various seeds has an impact  
27 on DMT of bunodont mammals despite similar overall diets. Trials were conducted on four  
28 groups of domestic pigs (*Sus scrofa*) all fed on mixed cereal and soy flours: the control group  
29 received only flours (n = 12), and the three others were supplemented with either 20 % corn  
30 kernels (n = 6), 30 % barley seeds (n = 5), or 10 hazelnuts in shell per day (n = 6). We studied  
31 phases I and II facets on first molars and on fourth deciduous premolars, and applied a  
32 subsampling surface strategy to identify discriminative parameters among dietary groups.  
33 Principal Component Analyses show that DMT differ between pigs fed on different types of  
34 seeds. Our results also demonstrate that combining both crushing and shearing facets into  
35 analyses improves dietary discriminations. This study shows that variables that contribute most  
36 to dietary discriminations as selected from the subsampling strategy are mainly height  
37 parameters. These results thus support the idea that the consumption of seeds has an impact  
38 on the relief of surface textures.

39

40 Keywords: suids, bunodont, omnivorous, feeding experiments

## 41 **1. Introduction**

42 Ecological constraints associated with feeding and foraging can exert key selective  
43 pressures among animals, leading to physiological, morphological, and/or behavioral  
44 adaptations (e.g., Bels and Herrel, 2019). Thus, investigating the diets of extinct species  
45 contributes to a better understanding of how their morphological diversity can be related to  
46 feeding adaptive traits (Codron et al., 2008; Cerling et al., 2011; Winkler et al., 2013). Dietary  
47 inferences have primarily been based on functional interpretations of craniomandibular and  
48 dental morphologies (Anthony and Kay, 1993; Ungar, 2002; Damuth and Janis, 2011).  
49 However, if trophic morphology may help us to identify gross dietary habits, it tells us more  
50 about what an extinct species was capable to eat than the precise composition of its diet  
51 (Lister, 2013; Tütken et al., 2013; Gailer et al., 2016; van Casteren et al., 2019). Dietary habits  
52 and feeding adaptations are not equivalent, and it has been shown that some species do not  
53 actually, or very rarely, eat items to which their trophic morphology seems to be adapted. Some  
54 apparently specialized feeders have in fact a more diversified diet than expected given their  
55 morphology. This phenomenon, known as “Liem’s Paradox”, was first demonstrated (Liem,  
56 1980) for cichlid fish. It has been proposed as well among other taxa, notably primates (Remis,  
57 2002; Lambert et al., 2004; Norconk and Veres, 2011; Sayers, 2013; Grine and Daegling,  
58 2017). A mismatch between craniomandibular and dental morphology and dietary habits has  
59 also been described among extant and extinct suids (Harris and Cerling, 2002; Souron, 2017;  
60 Lazagabaster, 2019). To explain some apparent discrepancies between dental morphologies  
61 and diets, notably in some primate species, resources now commonly referred as “fallback  
62 foods” (FBFs) have received considerable attention (Robinson and Wilson, 1998; Yamashita,  
63 1998; Lambert et al., 2004; Marshall and Wrangham, 2007). FBFs are defined as resources  
64 that are particularly consumed during periods of food scarcity, when preferred items are scarce  
65 or unavailable (Marshall et al., 2009). Such items, generally mechanically challenging, have  
66 been recognized as potential selective drivers of trophic morphologies or behaviors, notably  
67 among primates (MacArthur and Pianka, 1966; Robinson and Wilson, 1998; Potts, 2004). They

68 received much more attention in recent years (Altmann, 2009; Constantino and Wright, 2009;  
69 Constantino et al., 2009; Lucas et al., 2009; Marshall et al., 2009; Wrangham et al., 2009).

70 Numerous studies advocated for the importance of FBFs as key selective agents in the  
71 evolution of early hominins, particularly to understand the discrepancy between dietary habits  
72 inferred from dental microwear and dental morphologies (Laden and Wrangham, 2005; Scott  
73 et al., 2005; Dominy et al., 2008; Ungar et al., 2008; Constantino et al., 2009; Strait et al.,  
74 2009). The thick-enameled, bunodont cheek teeth shared by most early hominins has  
75 traditionally been considered as reflecting durophagy, especially in the robust genus  
76 *Paranthropus* whose diet was thought to be mainly composed of hard foods such as nuts and  
77 seeds (Robinson, 1954). This interpretation based on craniomandibular and dental  
78 morphology have led to the vision that *Paranthropus* were specialized feeders. However, later  
79 works focusing on enamel biogeochemical compositions and dental microwear textures have  
80 challenged this hypothesis. Notably, they show contrasting patterns between eastern and  
81 southern African *Paranthropus* and overlapping diets between some hominins (e.g., Ungar and  
82 Sponheimer, 2011; Martin et al., 2020). Some authors have suggested robust morphologies  
83 might have been driven by the consumption of mechanically challenging foods during “fallback”  
84 episodes of resource stress (e.g., Ungar and Daegling, 2013). However, without an  
85 experimental baseline using model taxa with similar bunodont, thick-enameled dentition, it has  
86 proven difficult to interpret DMT of early hominins and to test hypotheses regarding their  
87 fallback strategies. Moreover, such an experimental baseline would also be helpful to test  
88 hypotheses regarding the relationship between craniomandibular and dental morphologies  
89 and the consumption of FBFs among suids with seasonal/opportunistic feeding behaviors  
90 (Lazagabaster, 2019).

91 Besides enamel biogeochemical composition, dental microwear texture analysis  
92 (DMTA) is one of the few proxies that inform us about what was actually eaten by an extinct  
93 species. Indeed, microscopic marks on enamel surfaces are highly dependent on the  
94 mechanical properties and inner biosilica content of the masticated foods, although exogenous



95 abrasive particles may also contribute to toothwear (Teaford and Oyen, 1989; Lucas, 2004;  
96 Hua et al., 2015; Xia et al., 2015; Daegling et al., 2016; Merceron et al., 2016; Teaford et al.,  
97 2017; Winkler et al., 2020; see also Lucas et al., 2013; van Casteren et al., 2018). Microwear  
98 textures have a fast turnover rate so that DMTA records the diet of an animal a few weeks or  
99 months before death (Teaford and Oyen, 1989; Romero et al., 2012; Winkler et al., this  
100 volume). DMTA has proved its efficiency in assessing the diets of extant primate species (Scott  
101 et al., 2006, 2012; Krueger et al., 2008; Percher et al., 2017) and has been widely used for  
102 paleodietary reconstructions (Scott et al., 2005; Merceron et al., 2006, 2009, this volume;  
103 Ungar et al., 2008; Martin et al., 2018; Peterson et al., 2018). DMTA can then provide insights  
104 into ecological niche partitioning and dietary overlap between sympatric species, thus  
105 contributing to a better understanding of inter- and intraspecific competition (Teaford and  
106 Runestad, 1992; Ramdarshan et al., 2011; Merceron et al., 2014; Hofman-Kamińska et al.,  
107 2018; Martin et al., 2018; Percher et al., 2017; Aiba et al., 2019). Moreover, studies have shown  
108 that DMTA can reflect subtle dietary variations within species or populations, such as seasonal,  
109 social or sexual differences (Teaford and Robinson, 1989; Merceron et al., 2010; Berlioz et al.,  
110 2017; Percher et al., 2017). However, the mechanisms of dental microwear formation are still  
111 highly debated (Lucas et al., 2013, 2014; Xia et al., 2015; van Casteren et al., 2018, 2020;  
112 Teaford et al., 2020; Winkler et al., 2020) and little is known about whether microwear patterns  
113 can reflect small proportions of foods such as FBFs in an individual's diet. These limitations  
114 are crucial elements that need to be investigated to better interpret microwear textures of  
115 extinct species, notably among early hominins. Controlled-food experiments are assumed to  
116 reduce the dietary variability and thus enable targeting the effect of specific resources on dental  
117 microwear textures. In recent years, there have been an increasing number of studies with  
118 controlled feeding experiments (Teaford and Oyen, 1989; Hoffman et al., 2015; Calandra et  
119 al., 2016; Merceron et al., 2016; Ramdarshan et al., 2016, 2017; Ackermans et al., 2018, 2020;  
120 Zykov et al., 2018; Martin et al., 2019, this volume; Winkler et al., 2019, this volume; Schulz-  
121 Kornas et al., 2020). Most studies focused on herbivorous mammals and there is no work  
122 focusing on DMT variations of controlled-fed omnivorous mammals with bunodont, thick-

123 enameled dentition and similar overall diets (but see Teaford and Oyen, 1989; Teaford et al.,  
124 2017, this volume). Few works analyzed DMT variations among extant and extinct suids that  
125 exhibit this morphology, but they all point to the need of further studies for a better  
126 understanding of the relationship between dental microwear patterns and feeding behaviors  
127 (Ward and Mainland, 1999; Souron et al., 2015; Ungar et al., 2017; Yamada et al., 2018;  
128 Lazagabaster, 2019). Thus, such a controlled-feeding study is particularly interesting for  
129 helping the interpretation of DMT patterns among extant and extinct suids, as well as among  
130 early hominins and for a better understanding of niche partitioning between them.

131 In the present study, we investigate DMT variations on 29 domestic pigs (*Sus scrofa*),  
132 issued from controlled feeding experiments. We aim to test the hypothesis that the  
133 consumption of various types of seeds leads to significant differences of DMT despite similar  
134 overall diets. Recent in vivo and in vitro experimental studies have shown contrasting results  
135 about whether the consumption of hard seeds impacts dental microwear but none focused on  
136 standard measures of overall microwear textures (Teaford et al., 2020; van Casteren et al.,  
137 2020). Because high texture complexity (*Asfc*) has been related to the consumption of hard  
138 and/or brittle items, such as seeds, nuts, woody browse, hard fruits or bones (Scott et al., 2006,  
139 2012; Schubert et al., 2010; Daegling et al., 2011), we expect that pigs fed on the hardest  
140 seeds would show more complex textures than pigs fed on softer seeds, and even more than  
141 pigs fed only on flours. Besides, because pigs had a large part of their diet in common, and  
142 considering previous studies by Francisco et al. (2018a, 2018b), we expect that using the  
143 whole set of discriminative texture parameters selected from their surface sampling strategy  
144 will highlight dietary discriminations depending on the type of seeds consumed. Moreover, we  
145 hypothesize that combining both phase I (shearing) and phase II (crushing) facets will improve  
146 these discriminations.

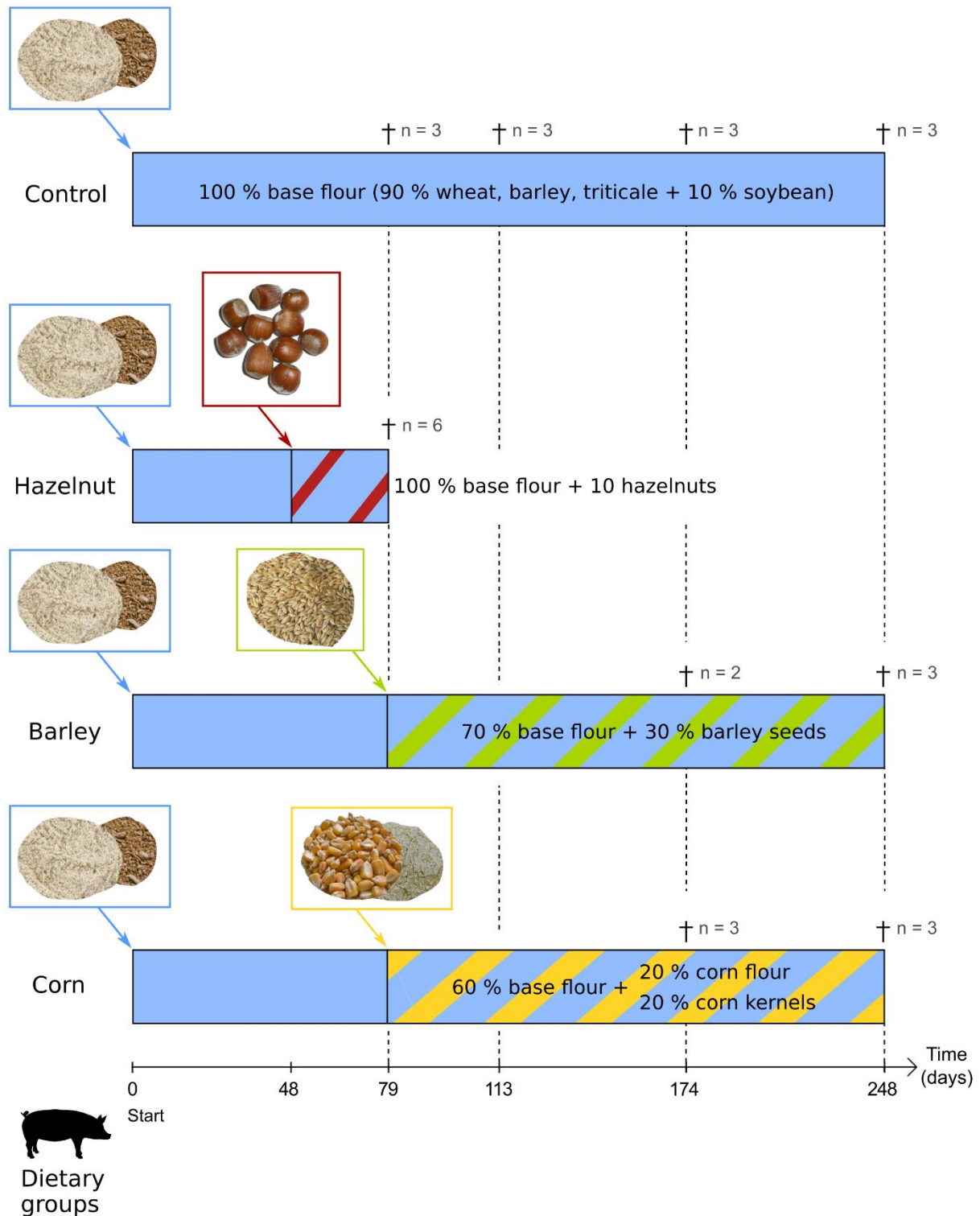
147

## 148 **2. Material and methods**

## 149 2.1. Controlled-food trials

150 The controlled-food experiments were carried out at the experimental unit UE1372  
151 GenESI (Pigs innovative breeding experimental Facility, Vienne, France; DOI:  
152 10.15454/1.5572415481185847E12) of the INRAE (*Institut national de recherche pour*  
153 *l'agriculture, l'alimentation et l'environnement*). Trials were conducted on domestic pigs (*Sus*  
154 *scrofa*; large-white cross breed Piétrain) and were designed by G.M. and S.F (agreement  
155 number: APAFiS 155/2015012117162897, *Ministère de l'Enseignement Supérieur et de la*  
156 *Recherche*). We considered a total of 29 juvenile pigs fed with four different diets *ad libitum*  
157 (Figure 1). Pigs were weaned about 28 days old and were raised on concrete floors. Each  
158 animal had access to an individual trough. They were kept together in groups of five to six pigs  
159 according to their dedicated diet. Before they were given their dedicated diets, they were all  
160 fed daily with a dry base diet (manufactured by ALICOOP) composed of 90 % of wheat  
161 (*Triticum* spp.), barley (*Hordeum vulgare*), and triticale (x *Triticosecale*) flour, and 10 % of  
162 soybean (*Glycine max*) flour. This period of homogenization of surface textures lasted at least  
163 48 days. The control group (n = 12) was then fed exclusively with the same base diet described  
164 above for at least another 30 days before death. This base diet, composed of ground cereal  
165 and soy seeds (Table 1), is expected to have little impact on dental microwear textures and  
166 represents a baseline for comparing dietary signals among the experimental groups. However,  
167 these base flours contain the outer parts of the grains and therefore imply higher abrasivity  
168 than finer flours. The three other groups then received seeds of different size and hardness  
169 (Table 2) in addition to the base diet. A 4-day period of adaptation to the new diet (with a  
170 progressive intake of seeds) was carried out on these three groups just before the dietary  
171 switch. The corn group (n = 6) was fed with 60 % of the base diet and 20 % of corn (*Zea mays*)  
172 flour, supplemented with 20 % (as dry matter weight) of corn kernels. The barley group (n = 5)  
173 was fed with 30 % of barley seeds and 70 % of the base diet. These two groups of pigs received  
174 their dedicated diet for at least another 95 days before death. The hazelnut group (n = 6) was  
175 fed with the same amount of flours than the control group and received 10 hazelnuts in shell

176 (*Corylus avellana*; endosperm and shell used but leafy involucre removed, Figure 1) per pig  
177 each day for another 30 days, during the month before slaughter. Due to a lack of homogeneity  
178 in hardness measurements in literature, we considered the mean force required for cracking  
179 the seed as an indicator for seed hardness (rupture force decreasing from hazelnuts to barley  
180 seeds; Table 2). Indeed, hardness is frequently defined as the resistance of a surface to  
181 deforming under indentation, and is usually measured as the ratio of rupture force to indented  
182 area (Lucas, 2004); rupture force thus helps estimate the hardness of the seeds. Each flour  
183 (including the base diet) was sieved through mesh of 1.25 mm and 0.5 mm diameter. The  
184 wheat, barley and triticale flour is composed of approximately 25 % particles above 1.25 mm  
185 diameter and 35 % below 0.5 mm. The soybean flour is composed of approximately 60 %  
186 particles above 1.25 mm diameter and less than 10 % below 0.5 mm (Table 2). Consequently,  
187 because the base diet is composed of an important amount of particles above 1.25 mm, it  
188 would be inappropriate to consider the pigs fed only on flours as a model for soft-food eaters.  
189 The corn flour, only given to the corn group, is composed of less than 20 % particles above  
190 1.25 mm diameter and 43 % below 0.5 mm (Table 2). Each group was approximately sex-  
191 balanced (Table S1). None of the pigs lost weight during the experiments. As planned by the  
192 experimental unit, pigs were slaughtered from six and a half months to nine and a half months  
193 old when they reached their target weight (about 150–200 kg; females slaughtered a month  
194 after males) and were all sold for meat (Figure 1; see Table S1 for details). Pig skulls were  
195 then boiled for 4 hours in water to remove the flesh, and dried in an oven for 24 hours at 40  
196 °C.



197  
 198 **Figure 1.** Graphical representation of the controlled-feeding experimental design conducted  
 199 on domestic pigs (*Sus scrofa*). Food items given to pigs are represented in blue (base diet: 90  
 200 % wheat, barley and triticale flour + 10 % soybean flour), red and blue (100 % base diet + 10  
 201 hazelnuts in shell per day), green and blue (70 % base diet + 30 % barley seeds), and yellow  
 202 and blue (60 % base diet + 20 % corn flour + 20 % corn kernels). Period of homogenization of  
 203 surface textures lasted at least 48 days. A 4-day period of adaptation to the new diet (not

204 represented on the figure) was carried out just before the dietary switch. Each time point  
 205 specified by † indicate feeding duration before slaughter (and number of pigs slaughtered).

206

207 **Table 1.** Particle size distribution within the flours given to pigs. The base diet given to all  
 208 dietary groups is composed of 90 % wheat, barley, and triticale flour and 10 % of soybean  
 209 flour. The corn flour is only given to the corn group (20 % of the diet).

Flour	Total sieved weight	< 0.5 mm	0.5 mm – 1.25 mm	> 1.25 mm
Wheat, barley, triticale (g)	1024	383	391	250
<b>Wheat, barley, triticale (%)</b>	<b>100</b>	<b>37.4</b>	<b>38.2</b>	<b>24.4</b>
Soybean (g)	840	75	255	510
<b>Soybean (%)</b>	<b>100</b>	<b>8.9</b>	<b>30.4</b>	<b>60.7</b>
Corn (g)	955	411	376	168
<b>Corn (%)</b>	<b>100</b>	<b>43</b>	<b>39.4</b>	<b>17.6</b>

210

211 **Table 2.** Summary statistics (mean and standard deviation SD) for dimensions (length of major  
 212 and minor axes), density and hardness index of each seed type. Dimensions are averaged  
 213 from 30 measured seeds. Densities are estimated from weights of 30 seeds for corn kernels  
 214 and hazelnuts, and from number of seeds in 20 g for barley. Mean rupture forces are averaged  
 215 from two studies for each type of seeds: hazelnut (Ercisli et al., 2011; Delprete and Sesana,  
 216 2014), corn (Tran et al., 1981; Kalkan et al., 2011), and barley (Markowski et al., 2010; Nouri  
 217 Jangi et al., 2011).

Seed	Major axis (mm)		Minor axis (mm)		Density (seeds/kg)	Rupture force (N)
	Mean	SD	Mean	SD		
Barley	8.93	0.89	3.64	0.31	22,500	140.51
Corn	12.75	0.91	8.18	0.53	3,333	164.42
Hazelnut	20.56	1.51	19.22	0.72	375	331.26

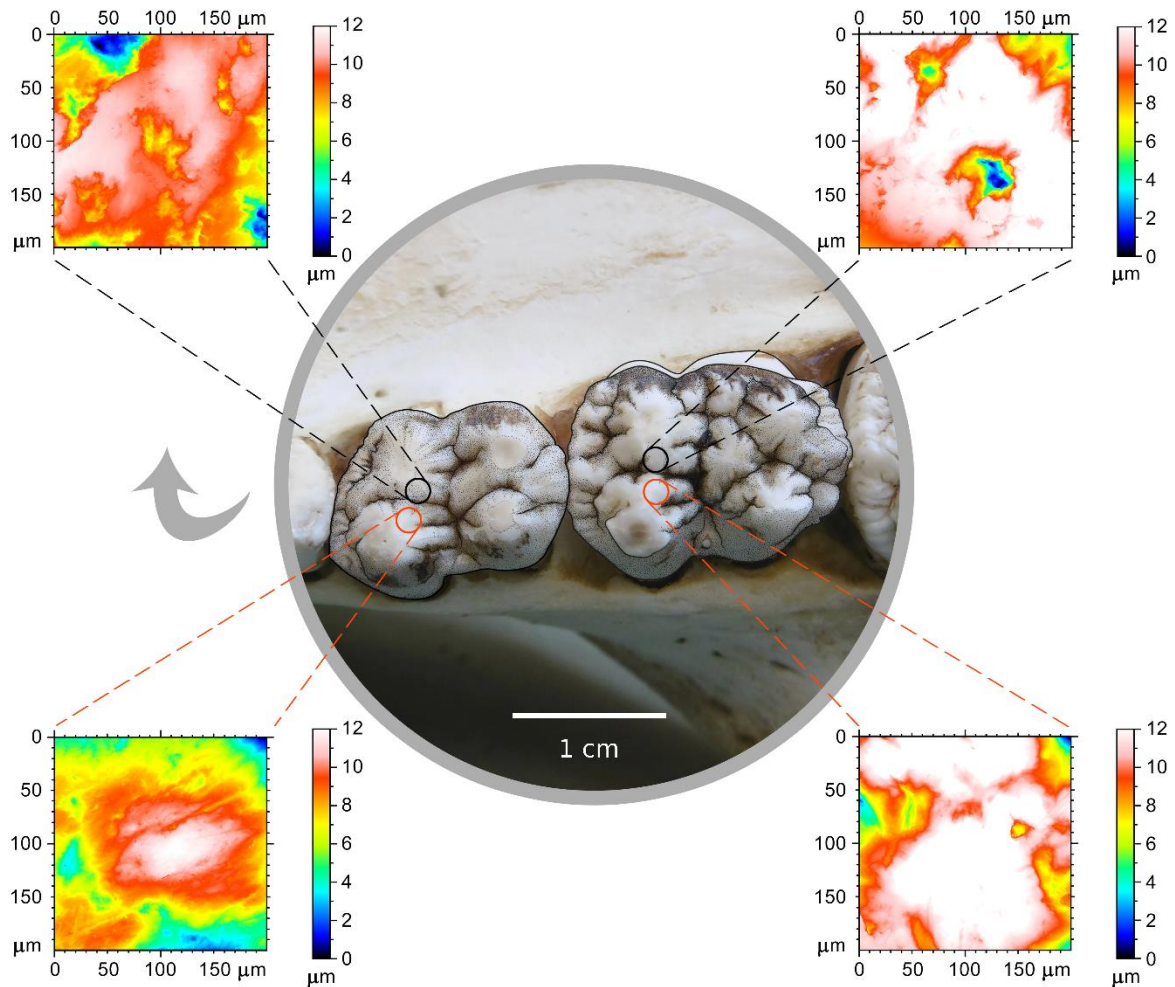
218

## 219 **2.2. Molding, scanning, and processing of the surfaces**

220 This study focused on lower and upper first molars (Figure 2) because molars are the  
 221 most studied teeth when analyzing dental microwear in paleodietary investigations. We  
 222 considered the first ones as the second molars were not fully erupted by the end of the  
 223 experiments. None of the molars showed dentin exposure, or only slightly on some buccal  
 224 cusp apices, corresponding to early stages of wear (stages b-c following Rolett and Chiu,  
 225 1994). We also analyzed deciduous upper fourth premolars (Figure 2) because they are more

226 worn than molars and are thus expected to be more functional, and consequently to carry a  
227 more pronounced dietary signal than molars. Moreover, deciduous fourth premolars are  
228 molariform (see Figure 2) and display the same wear pattern, including phase I and phase II  
229 dental facets. All crushing and shearing facets were visible on premolars, islets of dentin were  
230 visible and wear facets on mesial cusps tended to coalesce (stages d-e following Rolett and  
231 Chiu, 1994). We did not analyze lower fourth deciduous premolars because they are heavily  
232 worn. Each tooth surface was cleaned with cotton swabs soaked with a 3 % bleach solution  
233 (NaOCl) to remove organic matter, dust, and dirt, and then generously rinsed with distilled  
234 water. Once dry, occlusal surfaces were molded with polyvinylsiloxane (Regular Body  
235 President, ref. 6015 - ISO 4823, medium consistency, polyvinylsiloxane addition-type, Coltene  
236 Whaledent). We studied both one shearing (phase I) and one crushing (phase II) facet of the  
237 same tooth (Figure 2). Each facet was carefully cut on the silicon impression (negative replica)  
238 and scanned as flat as possible using "TRIDENT", a white-light confocal profilometer Leica  
239 DCM8 with a 100x objective housed at the PALEVOPRIM lab, CNRS and University of Poitiers,  
240 France (Numerical aperture = 0.90; Working distance = 0.9 mm; Leica Microsystems). Each  
241 scanned surface was pre-processed using LeicaMap v8.0 (Leica Microsystems;  
242 MountainsMap, Digital Surf). Surfaces were inverted along the z-axis and non-measured  
243 points (< 3 %) were filled with a smooth shape (Laplacian filter) calculated from neighboring  
244 points. A morphological filter was applied to remove artifacts such as aberrant peaks  
245 (Merceron et al., 2016) and surfaces were then leveled. A 200 × 200 μm (1551 × 1551 pixels)  
246 leveled area was automatically generated at the center of each surface. In case of adhering  
247 dirt particles, the extracted area was shifted aside to get the particles out of the field of  
248 selection. In the worst case, the particles were manually erased using a user-defined contour  
249 on few scans and replaced with a smooth shape calculated from neighboring points. If adhering  
250 dirt particles exceed 10 μm, the specimen was cleaned and scanned again until there was no  
251 dirt on the surface.

252



253  
 254 **Figure 2.** Exemplary occlusal views of right upper first molar (right) and fourth deciduous  
 255 premolar (left) and topography (false color elevation map) of one individual for each scanned  
 256 crushing and shearing facet. Localizations of one shearing and one crushing facet are depicted  
 257 in red and black circles, respectively. The arrow is oriented mesio-lingually.

258

### 259 **2.3. Acquisition of textural parameters**

260 We generated two sets of data for each scanned surface: 1) Scale-Sensitive Fractal  
 261 Analysis parameters (SSFA; Scott et al., 2006); 2) parameters obtained using a statistical  
 262 routine introduced by Francisco et al. (2018a, 2018b), including most parameters (some  
 263 modified) from the international standard ISO 25178. Prior to the calculation of SSFA-  
 264 parameters, a second-order least square polynomial surface (PS2) was subtracted from each  
 265 surface to remove the concavity of dental facets in order to better visualize the relief due to  
 266 microwear. Parameters obtained with the statistical routine are measured on surfaces



267 subtracted from an eighth-order least square polynomial surface (PS8) because it enhances  
268 roughness clarity (Francisco et al., 2018b).

269 1) SSFA-parameters were calculated using LeicaMap v. 8.0. We considered four  
270 texture variables for this study: Area-scale fractal complexity (*Asfc*), exact proportion of Length-  
271 scale anisotropy of relief (*epLsar* (*Sfrac*) in LeicaMap v8.0), Scale of maximum fractal  
272 complexity (*Smfc*), Heterogeneity of Area-scale fractal complexity (*HAsfc*, calculated through  
273 36 cells). Complexity (*Asfc*) measures the surface roughness at a given scale. Anisotropy  
274 (*epLsar*) quantifies the orientation concentration of surface roughness. *Smfc* estimates the  
275 scale at which maximal complexity is calculated. *HAsfc* measures the variation of complexity  
276 of subsampled parts of the surface (6 × 6 blocks in this study). Detailed descriptions of these  
277 parameters can be found in Scott et al. (2006).

278 2) The sampling method described by Francisco et al. (2018a, 2018b) generates 256  
279 sub-surfaces of 256 × 256 pixels per scanned surface. It produces one global value (on the  
280 whole 200 × 200 μm surface) per parameter and different statistics per parameter from the 256  
281 sub-surfaces batch. Sixteen height, spatial, and topological parameters are generated (Table  
282 S2). Nine statistics per parameter and per surface (composed of 256 sub-surfaces) are  
283 extracted: mean and median, skewness and kurtosis, standard deviation, means of the *n*  
284 values above and below the first and third quartiles, means of the 25 % lowest and highest  
285 values (Table S3). It thus generates a set of 160 variables (combination of statistics and  
286 parameters plus the global value). Francisco et al.'s routine (2018a, 2018b) is run  
287 independently for each of the two types of facets (crushing and shearing) to target the most  
288 discriminative variables among samples (Tables S4, S9, S14). The routine starts with a Box-  
289 Cox transformation and ends with the extraction of the three best discriminative variables after  
290 running Fisher's LSD tests (Figure S1A). We followed here Merceron et al.'s (this volume)  
291 implementation (Figure S1B): after LSD tests, each set (for crushing and shearing facets) of  
292 discriminative variables is ordered by decreasing number of significant differences between  
293 the four feeding groups of pigs (Figure S1B, Box 1). Then, we computed the geometric mean,

294 rather than the arithmetic one, of significant p-values ( $p < 0.05$ ) per variable because the  
295 arithmetic mean can be overly influenced by high values (Figure S1B, Box 2). We extracted  
296 the variable with the lowest mean p-value for each parameter for each of the two sets on  
297 crushing and shearing facets (Figure S1B, Box 4). Finally, 8 and 14 variables are extracted on  
298 lower molars (respectively on crushing and shearing facets; Table S5), 13 and 12 variables  
299 are extracted on upper molars (respectively on crushing and shearing facets; Table S10) and  
300 15 and 3 variables are extracted on upper deciduous premolars (respectively on crushing and  
301 shearing facets; Table S15).

## 302 **2.4. Statistical analyses**

303 All statistical analyses were conducted in the R statistical environment (R Core Team,  
304 2019, v3.6.2). Using the discriminative variables gathered from the sampling method, we  
305 performed six Principal Component Analyses (PCA; packages “FactoMineR”, “ggplot2” and  
306 “factoextra”) on each of the two types of facets on lower molars, upper molars, and upper  
307 deciduous premolars. Additionally, three PCA were produced combining both crushing and  
308 shearing facets on lower molars, upper molars, and upper deciduous premolars (Figure S1B,  
309 Box 5). SSFA-parameters (*Asfc*, *epLsar*, *HAsfc*, and *Smfc*) on each of the two types of facets  
310 were then inserted into PCA as supplementary variables (Figure S1B, Box 6). Contrary to  
311 variables gathered from the sampling method, SSFA-parameters had no influence on the PC  
312 computations but they were used to help interpret the distributions.

313 Analyses of variance (one-way ANOVAs) were performed on the PC coordinates to  
314 detect significant differences among the four controlled-fed groups. PC coordinates were Box-  
315 Cox transformed to meet the ANOVA assumptions of homoscedasticity and normality of the  
316 residual errors. Then, we conducted two post-hoc tests (package “agricolae”) to detect  
317 significant differences between dietary groups (Tables S6-S8, S11-S13, S16-S18): Tukey’s  
318 Honest Significant Difference test (HSD) and Fisher’s Least Significant Difference test (LSD);

319 less conservative than Tukey's HSD). In case of violation of the assumptions, an alternative  
320 Kruskal-Wallis test was run followed with a post-hoc Dunn's test.

321

### 322 **3. Results**

#### 323 **3.1. Lower molars**

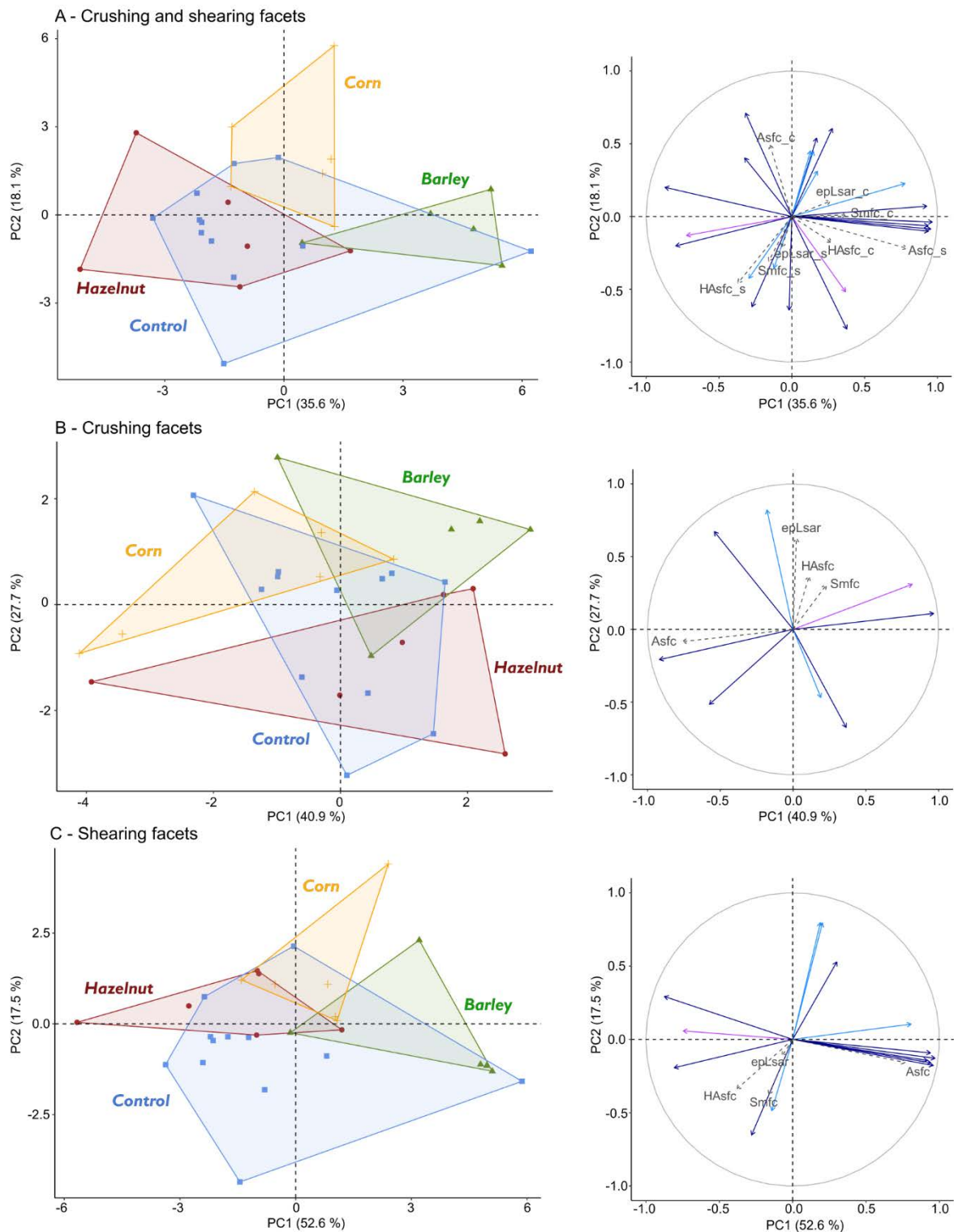
324 When combining crushing and shearing lower molar facets in the PCA, the most  
325 contributing variables along PC1 are from shearing facets and represent in majority dispersion  
326 statistics of height parameters (Figure S2). Along PC2, the most contributing variables are  
327 equally issued from crushing and shearing facets. They mainly represent dispersion statistics  
328 but also central (contributing about 20 % to PC2) and distribution (about 10 %) of height  
329 parameters. PC1 is twice as informative as PC2: PC1 and PC2 explain respectively 35.6 %  
330 and 18.1 % of the variance (Figure S2). Significant differences between dietary groups are  
331 observed only on PC1 and PC2 axes (Table S6). Added as supplementary variables, *Asfc*  
332 (SSFA-parameter) of shearing facets is positively correlated with PC1 values, and *Asfc* of  
333 crushing facets is positively correlated with PC2 values (Figure 3).

334 Pigs fed with barley seeds show the highest PC1 values. Hazelnut-fed pigs and the  
335 control group exhibit significantly lower PC1 values, meaning they show less complex enamel  
336 surfaces on molar shearing facets than the barley-fed pigs ( $p < 0.002$  and  $p < 0.004$ ,  
337 respectively; Figure 3, Table S6). Dispersion statistics of the absolute value of the smallest  
338 height *Sv* and median height *Smd*, and percentage of nearly horizontal faces *Sh*, all on  
339 shearing facets, contribute to pull these two groups toward low PC1 values (Figure 3, Figure  
340 S2). Pigs fed with corn kernels tend to express intermediate PC1 values. Barley-fed pigs  
341 display higher values of complexity *Asfc* on shearing facets (supplementary variable)  
342 compared to all other groups (Figure 3).

343

344 Along PC2, corn kernel-fed pigs show high values whereas the three other groups all  
345 display lower values (Figure 3). They tend to show high values of complexity *Asfc* on crushing  
346 facets, as reflected by the positive correlation of this supplementary to PC2 (Figure 3). The  
347 corn group is significantly different from the control one ( $p < 0.03$ , Table S6), and from the two  
348 other groups of seed-eaters according to LSD ( $p < 0.02$ ; but  $p < 0.10$  according to HSD, Table  
349 S6). The control group and hazelnut-fed pigs are overlapping along both PCs.

350 When considering only one type of facets, the discriminations between the DMT of  
351 lower molars of three groups of seed-eating pigs are weaker than when combining both types  
352 of facets (Figure 3). Using parameters on crushing facets only, the barley-fed group slightly  
353 overlaps with the two other groups of seed-eaters but significant differences are observed  
354 (along PC1,  $p < 0.05$  between barley-fed and corn-fed pigs, and along PC2,  $p < 0.04$  between  
355 barley-fed and hazelnut-fed pigs; Table S7). The hazelnut-fed and the corn-fed groups seem  
356 well distinct but significant difference is only observed with LSD (along PC1,  $p = 0.04$ ; Table  
357 S7). Control pigs overlap with the three groups of seed-eaters but tend to be distinct from  
358 barley-fed pigs ( $p = 0.04$  with LSD along PC2; Table S7). Parameters on shearing facets only  
359 allow to discriminate barley-fed pigs from the other groups (along PC1:  $p < 0.004$  between  
360 barley-fed and hazelnut-fed pigs,  $p < 0.005$  between barley-fed and control pigs; along PC2:  $p$   
361  $< 0.02$  between barley-fed and corn-fed pigs according to Dunn's test; Table S8). Indeed, four  
362 out of five individuals of the barley group display high values along PC1 whereas the other  
363 groups show lower values along PC1 (except for one individual of the control group). Corn-fed  
364 pigs and hazelnut-fed pigs are slightly overlapping along both PCs. The control group tends to  
365 show the lowest values along PC2 and is significantly different from the hazelnut group ( $p =$   
366  $0.01$ , Dunn's test; Table S8) and from the corn group ( $p = 0.002$ , Dunn's test; Table S8).



367

368 **Figure 3.** Distributions of individuals (left) and correlation circle (right) along PC1 and PC2 of  
 369 the four dietary groups based on dental wear parameters from both crushing and shearing  
 370 lower first molar facets (A), on crushing facets alone (B) and on shearing facets alone (C).  
 371 Dietary groups: ●: 100 % base flours + 10 hazelnuts in shell a day, ▲: 70 % base flours + 30  
 372 % barley seeds, +: 60 % base flours + 20 % corn flour + 20 % corn kernels, ■: 100 % base  
 373 flours. Active variables (filled arrows): height (dark blue), spatial (light blue), and topological  
 374 (purple) parameters. SSFA-parameters added as supplementary variables (gray dotted

375 arrows). Suffixes “\_c”: crushing facets, “\_s”: shearing facets. See Figure S7 to visualize the  
376 distributions using sexes as another grouping factor.

377

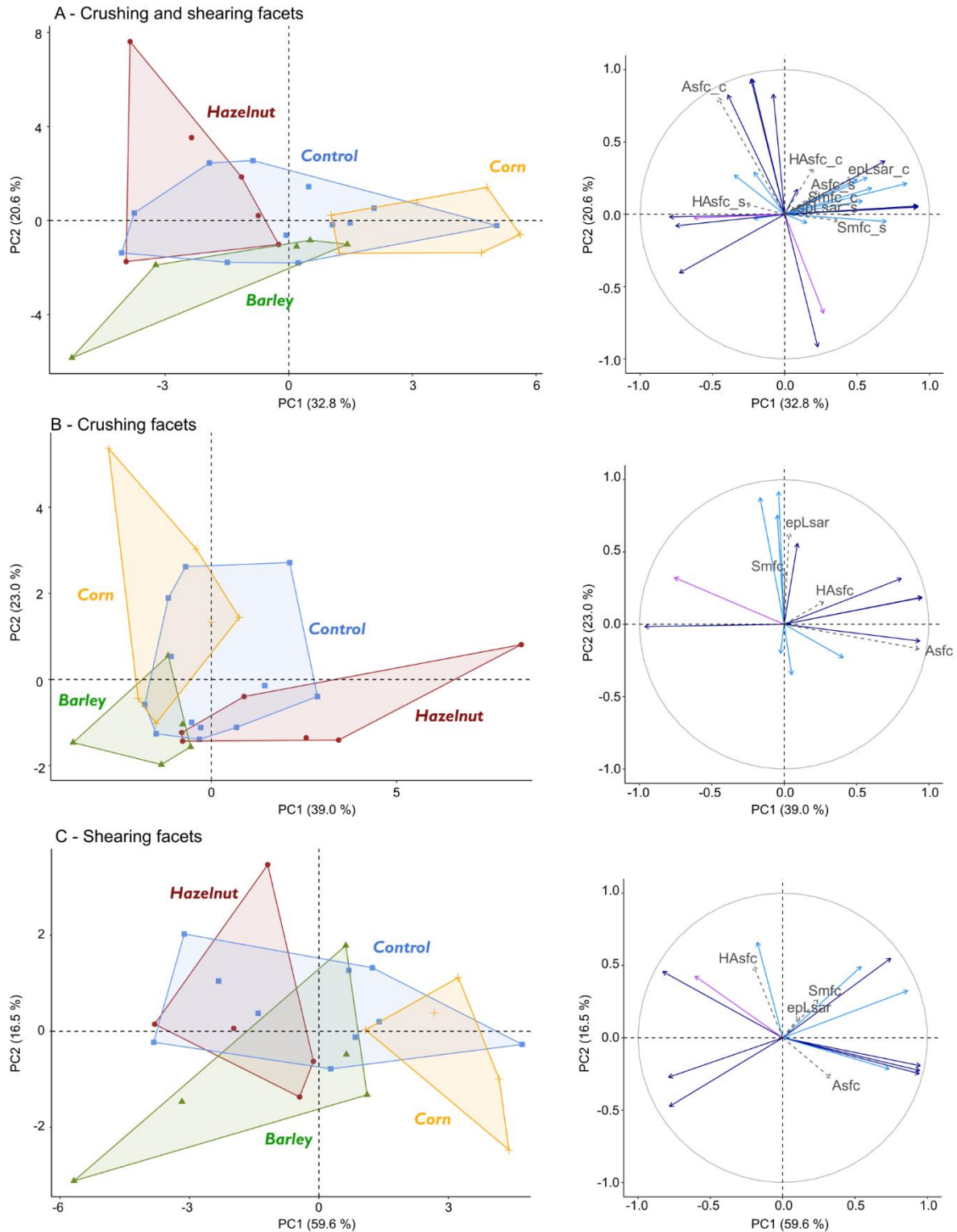
### 378 **3.2. Upper molars**

379 When combining crushing and shearing facets on upper molars, PC1 explains about  
380 30 % of the variance, PC2 about 20 % (Figure S3). Along PC1, the most contributing variables  
381 are mainly issued from shearing facets and mainly represent dispersion statistics of height  
382 parameters. Along PC2, parameters on crushing facets are the most contributing variables.  
383 They represent central and dispersion statistics of height parameters, but the median of the  
384 percentage of nearly horizontal faces (*Sh*), a topological parameter, contributes almost 10 %  
385 to the observed variance. No significant differences are observed on other PCs (Table S11).  
386 Added as supplementary variables, the anisotropy of crushing facets (*epLsar\_c*) is positively  
387 correlated with PC1 values, and *Asfc* of crushing facets is positively correlated with PC2 values  
388 (Figure 4).

389 Along PC1, hazelnut fed-pigs show low values, and barley-fed pigs display on average  
390 low values but with a large inter-individual dispersion (Figure 4). Corn-fed pigs display the  
391 highest PC1 values and are strongly distinct from hazelnut-fed pigs ( $p < 0.002$ , Table S11),  
392 and well distinct from the two other groups as well ( $p < 0.03$ , Table S11). This reflects more  
393 complex molar shearing surfaces among corn kernel fed-pigs. The anisotropy SSFA-  
394 parameter *epLsar* of crushing facets tends to reflect a trend toward textures with more parallel  
395 striations associated with high values along PC1, whereas the most contributing variables to  
396 this PC are from shearing facets. Numerous SSFA-parameters, notably related to complexity,  
397 are also positively associated to PC1. Control pigs are highly variable along PC1 but do not  
398 show extreme values along PC2, suggesting low complexity on crushing upper molar facets,  
399 similarly to lower molars. Hazelnut-fed pigs show the highest PC2 values but with high inter-  
400 individual dispersion (Figure 4). Notably, first quartiles of arithmetic mean of the absolute value  
401 of the height *Sa* and of height standard deviation *Sq*, and the median of the relative area *Sdar*  
402 (developed area/projected area), all compiled on crushing facets, contribute to pull the

403 hazelnut-fed group toward high PC2 values (Figure 4, Figure S3). *Asfc* on crushing facets,  
404 positively associated with PC2, reflects a tendency to more complex surfaces on pigs fed with  
405 hazelnuts (Figure 4). Barley-fed pigs show intermediate to low values along PC2 and are  
406 significantly different from hazelnut-fed pigs along this component ( $p < 0.03$ , Table S11).

407         When considering one type of facets, the dietary discrimination is weaker than when  
408 considering both types (Figure 4). However, regarding parameters on crushing facets only, the  
409 three groups of seed-eating pigs tend to exhibit different microwear patterns. Hazelnut-fed pigs  
410 display complex surfaces and tend to be discriminated from the two other groups fed with  
411 seeds, especially from the corn-fed group. However, significant differences are only observed  
412 with LSD between hazelnut-fed and corn-fed pigs (both  $p < 0.02$ ; Table S12). Barley-fed pigs  
413 exhibit low values on both PCs and are well discriminated from the hazelnut-fed group along  
414 PC1 ( $p < 0.02$ ; Table S12) and from corn-fed pigs along PC2 ( $p < 0.02$ ; Table S12). Regarding  
415 shearing facets only, only pigs fed with corn kernels are well distinct from the three other  
416 groups (along PC1:  $p < 0.02$  between corn-fed and hazelnut-fed pigs,  $p < 0.03$  between corn-  
417 fed and barley-fed pigs, and  $p = 0.01$  between corn fed and control pigs with LSD but  $p = 0.05$   
418 with HSD; Table S13).



419

420 **Figure 4.** Distributions of individuals (left) and correlation circle (right) along PC1 and PC2 of  
 421 the four dietary groups on both crushing and shearing upper first molar facets (A), on crushing  
 422 facets alone (B), and on shearing facets alone (C). Dietary groups: ●: 100 % base flours + 10  
 423 hazelnuts in shell a day, ▲: 70 % base flours + 30 % barley seeds, +: 60 % base flours + 20  
 424 % corn flour + 20 % corn kernels, ■: 100 % base flours. Active variables (filled arrows): height  
 425 (dark blue), spatial (light blue), and topological (purple) parameters. SSFA-parameters added



426 as supplementary variables (gray dotted arrows). Suffixes “\_c”: crushing facets, “\_s”: shearing  
427 facets. See Figure S8 to visualize the distributions using sexes as another grouping factor.

428

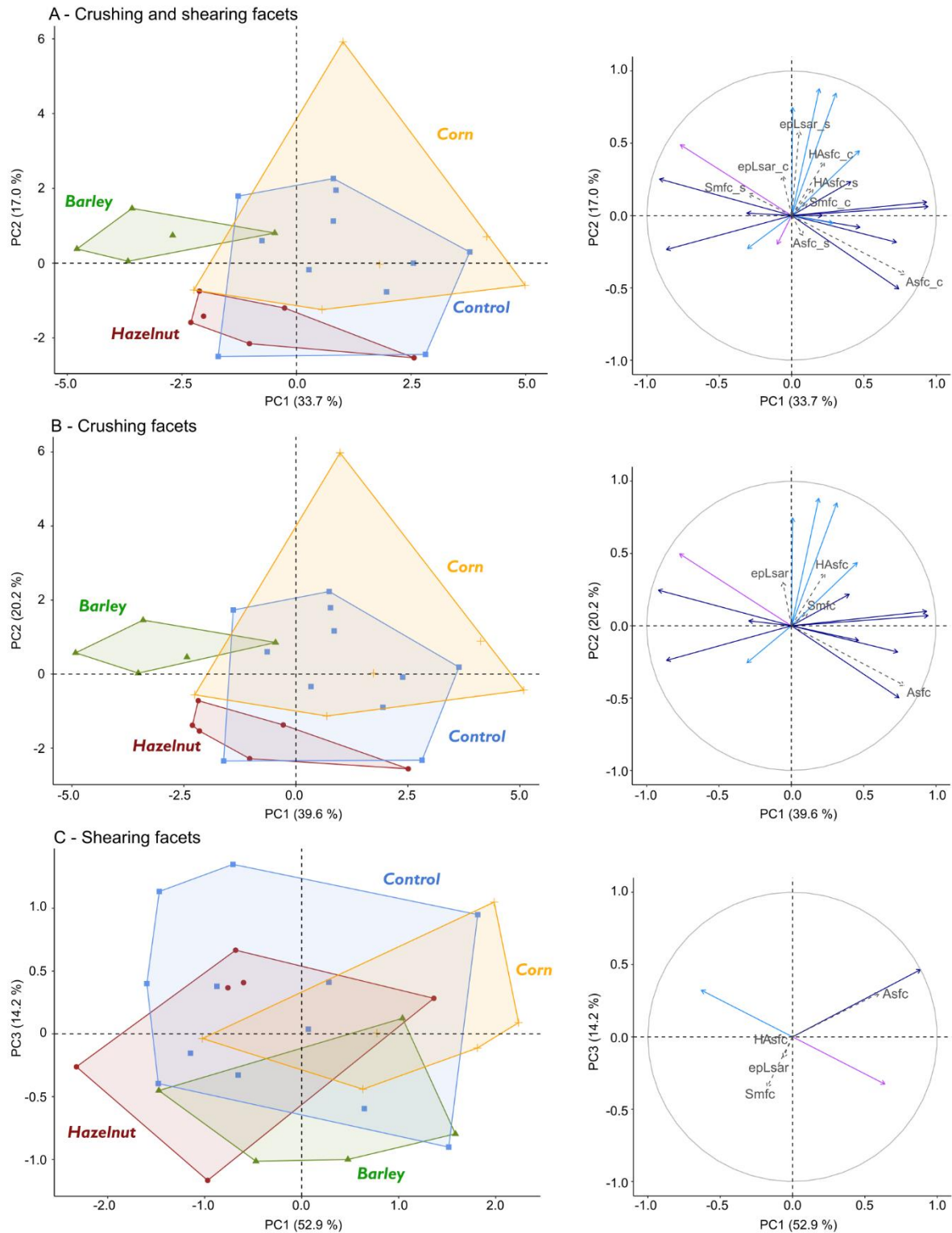
### 429 **3.3. Upper deciduous premolars**

430 Principal component analysis on upper fourth deciduous premolars shows that  
431 parameters on crushing facets contribute the most to both PC1 and PC2 (Figure S4).  
432 Significant differences between dietary groups are observed on PC1 and PC2, as well as on  
433 PC3 (Table S16). PC1 explains 33.7 % of the variance observed and is twice as informative  
434 as PC2 (Figure S4). No parameter on shearing facets substantially contributes to PC1. The  
435 most contributing variables along PC1 are dispersion statistics of height parameters on  
436 crushing facets, but the mean percentage of nearly horizontal faces *Sh* (on crushing facets), a  
437 topological parameter, contributes almost 10 % to PC1. Added as supplementary variable,  
438 *Asfc* of crushing facets is positively correlated with PC1 (Figure 5). Along this PC, barley-fed  
439 pigs are well distinct from control and corn-fed pigs (both  $p < 0.002$ , Table S16). Barley-fed  
440 pigs show the lowest PC1 values and corn-fed pigs exhibit the highest PC1 values (Figure 5).  
441 Specifically, the 25 % highest values of absolute smallest height *Sv* as well as the mean  
442 percentage of nearly horizontal faces *Sh*, both measured on crushing facets, contribute to pull  
443 barley-fed pigs toward low PC1 values (Figure S4). Dispersion statistics of the arithmetic mean  
444 of the absolute of the heights *Sa* and height standard deviation *Sq* of crushing facets contribute  
445 to pull the corn group toward high PC1 values.

446 PC2 explains 17 % of the variance and provides complementary information to PC1.  
447 The most contributing variables to PC2 mainly represent dispersion statistics of spatial  
448 parameters on crushing facets. Although no parameter on shearing facet substantially  
449 contributes to PC2, *epLsar* on shearing facets is positively associated to this component. The  
450 relative area *Sdar* (height parameter) and percentage of nearly horizontal faces *Sh*, both on  
451 crushing facets, contribute as well, albeit to a lesser extent. Along PC2, hazelnut-fed pigs show  
452 the lowest values and are well distinct from the three other groups ( $p < 0.03$ , Table S16).

453 Dispersion statistics of spatial parameters contribute to pull the control, the barley-fed, and the  
454 corn-fed groups toward high PC2 values. Control pigs and corn-fed pigs show similar values  
455 along both PC1 and PC2 axes (Figure 5). PC3 (Figure S5), which explains 12.8 % of the  
456 variance, provides few complementary discriminative information, but only for distinguishing  
457 the control group from the corn-fed group ( $p < 0.02$ , Table S16). However, control pigs still  
458 overlap with corn-fed pigs, as well as with hazelnut-fed pigs.

459         When considering only one type of facets, the PCA using parameters on crushing  
460 facets provides highly similar results (most contributing variables to PCs and distribution of  
461 individuals) to the PCA using both types of facets (Figure 5; see also Figures S5 and S6).  
462 Along PC1, barley-fed pigs differ from corn-fed ( $p < 0.002$ ) and control pigs ( $p < 0.003$ ), and  
463 from hazelnut-fed pigs along PC2 ( $p < 0.04$ ; Table S17). The hazelnut and the corn groups  
464 differ significantly along PC2 ( $p < 0.04$ ; Table S17). On shearing facets, only PC1 tends to  
465 show differences between dietary groups ( $p = 0.08$ ; Table S18). No differences are observed  
466 on PC2 ( $p > 0.3$ ) or PC3 ( $p > 0.1$ ). The PCA biplot on shearing facets shows that all groups  
467 are strongly overlapping. The hazelnut-fed pigs differ from corn-fed pigs along PC1 but only  
468 according to LSD ( $p = 0.02$ ). In contrast to molars, the combination of facets on upper fourth  
469 deciduous premolars does not improve the dietary discrimination compared to analyses that  
470 consider only crushing facets. However, combining both types of facets does not mask the  
471 discriminations.



472

473 **Figure 5.** Distributions of individuals (left) and correlation circle (right) of the four dietary groups  
 474 along PC1 and PC2 on both crushing and shearing upper fourth deciduous premolar facets  
 475 (A), along PC1 and PC2 on crushing facets alone (B) and along PC1 and PC4 on shearing  
 476 facets alone (C). Dietary groups: ●: 100 % base flours + 10 hazelnuts in shell a day, ▲: 70 %  
 477 base flours + 30 % barley seeds, +: 60 % base flours + 20 % corn flour + 20 % corn kernels,  
 478 ■: 100 % base flours. Active variables (filled arrows): height (dark blue), spatial (light blue) and  
 479 topological (purple) parameters. SSFA-parameters added as supplementary variables (gray

480 dotted arrows). Suffixes “\_c”: crushing facets, “\_s”: shearing facets. See Figure S9 to visualize  
481 the distributions using sexes as another grouping factor.

482

## 483 **4. Discussion**

### 484 **4.1. DMT in controlled-fed pigs and dietary overlapping among hominins**

485         The present study analyzed DMT variations of controlled-fed pigs characterized by  
486 bunodont, thick-enameled cheek teeth. To our knowledge, this is the first work proposing an  
487 experimental baseline with a model taxon for interpreting DMT variations among extinct taxa  
488 with bunodont dentition and similar tooth wear pattern, such as suids or primates. We focused  
489 here on four dietary groups: pigs were all fed with the same flours (at least 60 % of the diet),  
490 supplemented with different types of seeds for three groups. While those pigs had overall  
491 similar diets, our results highlight significant differences in their DMT. In line with several  
492 studies on wild caught specimens (Teaford and Robinson, 1989; Merceron et al., 2010; Berlioz  
493 et al., 2017; Percher et al., 2017), this work strongly supports that DMT reflect intra-specific  
494 and even intra-population minor variations in dietary habits. Moreover, although van Casteren  
495 et al. (2020) recently argued that “hard plant tissues barely influence dental microwear  
496 textures”, we show that controlled-fed pigs exhibit significant differences in DMT depending on  
497 the type of seeds consumed. Nonetheless, our results have some limitations, notably because  
498 the feeding groups were given different concentrations of seeds so we cannot disentangle the  
499 respective impacts of seed structure and seed concentrations on DMT.

500         This work is of particular interest for reconstructing dietary habits of early hominins, for  
501 whom several studies have suggested overlapping diets that may have differed mainly  
502 regarding fallback foods consumed during periods of food scarcity (Ungar, 2004; Scott et al.,  
503 2005; Ungar and Sponheimer, 2011; Ungar et al., 2012; Ungar and Daegling, 2013). Works  
504 based on enamel stable carbon isotopes and dental microwear textures have challenged the  
505 hypothesis of durophagy and specialized diets within the *Paranthropus* genus as driving the  
506 selection of their robust craniomandibular and dental morphology (see references below),

507 conversely to their “gracile” contemporaneous early *Homo* considered as generalists (e.g.,  
508 Wood and Strait, 2004). In addition to highlighting overlapping diets between some early  
509 hominins, these works show strongly different patterns between the eastern and the southern  
510 African species of *Paranthropus* (e.g., Sponheimer et al., 2006; Ungar et al., 2008; Ungar and  
511 Sponheimer, 2011; Martin et al., 2020). On the one hand, eastern African *P. boisei* exhibit  
512 stable carbon isotope compositions indicative of a dominant C<sub>4</sub> diet, most likely composed of  
513 grasses and/or sedges (Cerling et al., 2011, 2013; Wynn et al., 2020). Analyses of their dental  
514 microwear show low texture complexity, providing no evidence that they regularly consumed  
515 hard foods and would rather advocate for an abrasive diet composed of silica-bearing  
516 herbaceous monocots, *i.e.*, grasses, sedges (Ungar et al., 2008, 2012). Among alternative  
517 hypotheses, the ingestion of dust and grit with foods has been proposed as severely impacting  
518 the enamel surface and as driving the selection of robust morphologies (Madden, 2014).  
519 Southern African *P. robustus*, on the other hand, exhibit stable carbon isotopic compositions  
520 consistent with a mixed or dominant C<sub>3</sub> diet (Lee-Thorp et al., 1994; Sponheimer et al., 2006;  
521 Caley et al., 2018; Lüdecke et al., 2018; see also Balter et al., 2012). They show the highest  
522 average value of texture complexity compared to other early hominins, as well as a broad  
523 range of individual variation (Scott et al., 2005; Peterson et al., 2018). This distribution has  
524 been suggested to be more comparable to extant primates that occasionally rely on hard items  
525 as FBFs (Ungar and Sponheimer, 2011). Consequently, these studies suggest that robust  
526 craniomandibular and dental morphologies might have been favored by an occasional  
527 consumption of mechanically challenging FBFs critical for survival.

528         The present controlled-food experiments are not directly comparable with data from  
529 wild populations (either past or present-day species) as diets in the wild are much more diverse  
530 than controlled diets in experimental settings. Those experiments nevertheless highlight our  
531 understanding of the relations between dietary variations and dental microwear textures, and  
532 consequently improve our interpretations on the role of feeding habits upon niche partitioning  
533 among early hominins.

534 **4.2. Improving dietary discriminations using a surface sampling strategy and combining**  
535 **phase I and phase II facets**

536 The surface sampling strategy used in this study exploits different statistics for a whole  
537 set of standard texture parameters measured on 256 sub-surfaces per scanned surface and  
538 allows detection of the most discriminative parameters among several dietary groups  
539 (Francisco et al., 2018a, 2018b). Rather than considering variables independently, we  
540 performed Principal Component Analyses with the most discriminative variables selected from  
541 the sampling strategy (see Material and Methods and Figure S1). Our results show that this  
542 approach allows detection of significant differences in dental microwear textures among  
543 different groups of controlled-fed pigs with overall similar diets. In every analysis, we show that  
544 most discriminative variables are dispersion and distribution statistics of surface texture  
545 parameters, rather than central tendency statistics (mean or median). Dispersion statistics are  
546 the most contributing variables to PCs (Figures S1, S2, S3), which thus have the potential to  
547 discriminate groups with slight differences in diet. Several data analysis (not only in DMTA)  
548 have pointed out that quantiles, distribution or dispersion among samples may yield more  
549 significant differences than central tendencies (Plavcan and Cope, 2001; Ragni et al., 2017;  
550 Merceron et al., this volume; see also Lambrechtsen et al., 1999; Brewer and Pickle, 2002;  
551 Phillips et al., 2005; Cox et al., 2013; Krzywinski and Altman, 2014). We suggest that  
552 dispersion statistics of standard parameters, and not only central tendencies, are of particular  
553 interest for DMTA studies focusing on taxa with subtle dietary variations. It is also worth noting  
554 that some of the observed dietary discriminations are not mirrored by the global value of SSFA-  
555 parameters added as supplementary variables into PCAs. Notably, the distinction on upper  
556 molars of pigs fed with barley seeds is not reflected by any SSFA-parameter, and that is also  
557 the case for the distinction of hazelnut-fed pigs on upper deciduous premolars. These  
558 observations thus reinforce the relevance of using a wider set of texture parameters to target  
559 significant differences among animals with overall similar diets. In the same way that earlier  
560 studies using 2D dental microwear methods were able to discriminate a species from others

561 by the frequency of the occurrence of few large pits per surface (e.g., Solounias and  
562 Semprebon, 2002; Merceron et al., 2005), the sampling strategy chosen here may allow to  
563 discriminate the species not by the central tendency values of a given parameter, but by its  
564 distribution shape or its value at the quartile  $Q_n$ .

565         PCAs highlight that parameters measured on both crushing and shearing facets bear  
566 discriminant dietary signals. Considering only one type of facets on upper or lower molars  
567 allows discriminating one group of seed-eaters from another (or from the two others), but does  
568 not reveal significant differences (observed with both HSD and LSD) among all three groups  
569 of seed-eaters. In contrast, when combining the two types of facets, the differences among the  
570 three groups of seed-eaters are even stronger and are significant with both post-hoc tests.  
571 Consequently, combining data from crushing and shearing facets on molars leads to a better  
572 discrimination among all three groups of seed-eaters. When considering the upper deciduous  
573 premolars, the combination of two dental facet types does not lead to a better discrimination  
574 than when considering only crushing facets. Nevertheless, including shearing facets in the  
575 analysis does not mask the dietary signal on upper deciduous premolars. Thus, this study  
576 supports recent results showing that the combination of facet types may improve the resolution  
577 of dietary reconstructions (Arman et al., 2019; Merceron et al., this volume). While crushing  
578 facets are mostly considered in DMT analyses on early hominins because they are thought to  
579 be more discriminant than shearing ones among primates (Krueger et al., 2008), we argue that  
580 both types of facets should be considered for future studies (see Martin et al., 2019; Merceron  
581 et al., this volume).

582

### 583 **4.3. DMT variations depending on the presence and type of seeds consumed**

584         Because high texture complexity has been related to hard food consumption (Scott et  
585 al., 2006, 2012; Schubert et al., 2010; Daegling et al., 2011), we expected that the highest  
586 complexity values would correspond to the harder dietary item consumed (but see

587 Ramdarshan et al., 2016). Thus, pigs fed on hazelnuts in shell should exhibit more complex  
588 textures than corn and barley-fed pigs (Table 2), and even more in comparison to control pigs.  
589 However, earlier works have pointed out that surface complexity alone might not be a strong  
590 indicator for the hardness of seeds consumed, because their consumption does not  
591 necessarily generate the expected complex surfaces on enamel (Ramdarshan et al., 2016;  
592 van Casteren et al., 2020). Our results on lower molars, indeed, show that pigs fed on  
593 hazelnuts exhibit facets that appear to be about as complex as those of pigs fed only on flours,  
594 and pigs fed on barley (the less resistant seeds) show more complex shearing facets than the  
595 other dietary groups. However, on upper molars, barley-fed pigs do not show the most complex  
596 facets. Thus, the complexity of enamel surfaces does not seem associated with seed hardness  
597 in this study. Besides the hardness of the seeds consumed, other factors should also be  
598 considered to better understand the relationships between seed consumption and texture  
599 complexity (e.g., seed size, particle size after mastication, number of seeds in one bolus, seed  
600 digestibility; see Lucas, 2004). For example, it has been suggested that food resources of  
601 smaller particle size might require higher bite force for oral processing than larger ones (Lucas,  
602 2004), as well as bolus containing high amount of small resources (van Casteren et al., 2020).  
603 In the present study, we did not control for these factors, and we used seeds of different  
604 hardness and size, and representing different proportions of the diet depending on the feeding  
605 groups. Thus, we cannot identify which factor predominantly influences the differences among  
606 the groups. Nevertheless, we show overall that DMT are impacted by seed consumption and  
607 that they differ between the three groups of seed-eating pigs.

608         PCAs and ANOVAs on PC coordinates show significant differences in DMT of the three  
609 groups of pigs fed on seeds. The dietary discrimination is, however, weaker on both upper and  
610 lower molars than on upper deciduous premolars. Wear facets on upper and lower molars  
611 were barely developed and not all crushing and shearing facets were developed, although  
612 every individual showed distinct facets at their early stages of formation, notably on mesial  
613 cusps. Molars of pigs are erupted between 4 to 6 months old (Legge, 2013) and were thus



614 probably in full occlusion only a few weeks before death, particularly among pigs fed with  
615 hazelnuts (slaughtered at 195 days old). This could explain that, contrary to what is found on  
616 deciduous premolars, there is no difference in dental microwear complexity between crushing  
617 and shearing facets on molars. This would have been expected because of their different  
618 implications in mastication with more occlusal pitting on phase II homologous facets involved  
619 into grinding and crushing of foods, conversely to phase I facets involved in slicing food items  
620 with lateral movements. This difference between facets is observed on upper deciduous  
621 premolars because, being erupted at about 25 days old (Tucker and Widowski, 2009), they  
622 were fully functional at the time pigs received their dedicated diet. To sum up, our results show  
623 a stronger dietary discrimination among the three groups of seed-eaters on the worn upper  
624 deciduous premolars than on the barely worn molars.

625         While the present study shows significant differences in DMT between pigs fed on  
626 different seeds, we observe that control pigs fed only on flours are highly overlapping with one  
627 or two groups of seed-eaters. This is actually not surprising because, in addition to the high  
628 proportion of diet these groups have in common, the flours contained an important number of  
629 particles above 1.25 mm in diameter (24 % for the wheat flour, 61 % for the soy flour; Table  
630 2). Indeed, feeding pigs with finely ground flours is not possible because it would lead to gastric  
631 damages, such as ulcers, that would affect animal well-being. These flours, rich in millimetric  
632 seed fragments, explain why the texture complexity is overall high, even in the control group.  
633 Moreover, Winkler et al. (2020) recently showed that angular quartz particles lead to complex  
634 surfaces. Although it is not clear if this also applies on softer seed particles, such as corn  
635 fragments, it is likely that numerous particles in the flours are angular. This might contribute to  
636 the overall complexity among pigs in this study.

637         Altogether, our results are in line with a recent in vivo experiment on captive capuchin  
638 monkeys (*Sapajus apella*; Teaford et al., 2020), which demonstrates that hard food  
639 consumption impacts tooth wear by generating new features on wear facet in a very short  
640 period of time (3-4 hours). We here provide novel information that complements their study as

641 we considered texture parameters. We show overall that dispersion statistics of height  
642 parameters are, in majority, the variables that most contribute to PCs. This is congruent with  
643 Schulz-Kornas et al.'s (2019) study on Western chimpanzees who showed that some height  
644 parameters (on crushing and shearing facets) differ depending on nut consumption. Our  
645 results thus support the hypothesis that the consumption of different seeds generates  
646 differences on DMT highlighted by parameters related to surface height profiles.

647

## 648 **5. Conclusions**

649         The present study aimed at testing the hypothesis that the consumption of various types  
650 of seeds has an impact on dental microwear textures despite overall similar diets. Controlled  
651 feeding trials were conducted on four dietary groups of domestic pigs which exhibit thick-  
652 enameled, bunodont cheek teeth. Such an experimental baseline might help the interpretation  
653 of DMT patterns among extinct bunodont species of suids or primates with overlapping dietary  
654 signals. This could greatly contribute to discussions regarding the consumption of  
655 mechanically challenging resources that could be fallback foods for early hominins.

656         We used a subsampling surface strategy that measures different statistics for a whole  
657 set of texture parameters. We performed Principal Component Analyses on shearing (phase  
658 I) and crushing (phase II) facets independently, as well as by combining the two types of facets.  
659 Our results show that controlled-fed pigs exhibit significant differences in their DMT patterns  
660 depending on the type of seeds consumed. This study shows that both phase I and II facets  
661 bear discriminant dietary signals and that considering both types of facets in the analyses  
662 improves dietary discriminations. These discriminations are not mirrored by standard Scale  
663 Sensitive Fractal Analysis (SSFA) parameters in every case when added as supplementary  
664 variables, substantiating the efficiency of the subsampling surface strategy to detect significant  
665 differences among groups with a high proportion of diet in common. The variables selected  
666 from the subsampling strategy that most contribute to dietary discriminations represent in

667 majority dispersion statistics of height parameters. Thus, these results show that dispersion  
668 statistics have the potential to distinguish DMT among groups with overall similar diets, and  
669 support the hypothesis that the consumption of seeds has an impact on texture parameters  
670 related to surface relief.

671

## 672 **Acknowledgments**

673 The authors thank R. Marquet, notably for preparing pigs' crania and mandibles after slaughter,  
674 and the staff from the GenESI experimental unit. We also thank S. Riffaut for drawing Figure  
675 2. This study was funded by the ANR project Diet-Scratches (ANR-17-CE27-0002-02, PIs: G.  
676 Merceron and S. Ferchaud; French Agency for Research), the ALIHOM project ([project](#)  
677 [n°210389](#), *Nouvelle-Aquitaine* region, France, PI: G. Merceron) and the *Ministère de*  
678 *l'Enseignement supérieur, de la Recherche et de l'Innovation* (France). The authors thank G.  
679 Reynaud and L. Painault (PALEVOPRIM, Poitiers, France) for administrative guidance, and  
680 G. Thiery (PALEVOPRIM, Poitiers, France) and X. Milhet (Pprime institute, Poitiers, France)  
681 for discussion. We thank two anonymous reviewers and the editors whose comments greatly  
682 improved the initial version of the manuscript.

683

684 **References**

685

686 Ackermans, N.L., Winkler, D.E., Schulz-Kornas, E., Kaiser, T.M., Müller, D.W.H., Kircher, P.R.,  
687 Hummel, J., Clauss, M., Hatt, J.-M., 2018. Controlled feeding experiments with diets of  
688 different abrasiveness reveal slow development of mesowear signal in goats (*Capra*  
689 *aegagrus hircus*). *Journal of Experimental Biology* 221, jeb186411.  
690 <https://doi.org/10.1242/jeb.186411>

691 Ackermans, N.L., Winkler, D.E., Martin, L.F., Kaiser, T.M., Clauss, M., Hatt, J.-M., 2020. Dust  
692 and grit matter: abrasives of different size lead to opposing dental microwear textures  
693 in experimentally fed sheep (*Ovis aries*). *Journal of Experimental Biology* 223,  
694 jeb220442. <https://doi.org/10.1242/jeb.220442>

695 Aiba, K., Miura, S., Kubo, M.O., 2019. Dental microwear texture analysis in two ruminants,  
696 Japanese serow (*Capricornis crispus*) and sika deer (*Cervus nippon*), from Central  
697 Japan. *Mammal Study* 44, 183–192. <https://doi.org/10.3106/ms2018-0081>

698 Altmann, S.A., 2009. Fallback foods, eclectic omnivores, and the packaging problem.  
699 *American Journal of Physical Anthropology* 140, 615–629.  
700 <https://doi.org/10.1002/ajpa.21097>

701 Anthony, M.R.L., Kay, R.F., 1993. Tooth form and diet in ateline and alouattine primates;  
702 reflections on the comparative method. *American Journal of Science* 293, 356–382.  
703 <https://doi.org/10.2475/ajs.293.A.356>

704 Arman, S.D., Prowse, T.A.A., Couzens, A.M.C., Ungar, P.S., Prideaux, G.J., 2019.  
705 Incorporating intraspecific variation into dental microwear texture analysis. *Journal of*  
706 *the Royal Society Interface* 16, 20180957. <https://doi.org/10.1098/rsif.2018.0957>

707 Balter, V., Braga, J., Télouk, P., Thackeray, J.F., 2012. Evidence for dietary change but not  
708 landscape use in South African early hominins. *Nature* 489, 558–560.  
709 <https://doi.org/10.1038/nature11349>

710 Bels, V., Herrel, A., 2019. Feeding, a Tool to Understand Vertebrate Evolution Introduction to  
711 “Feeding in Vertebrates,” in: Bels, V., Whishaw, I.Q. (Eds.), Feeding in Vertebrates:  
712 Evolution, Morphology, Behavior, Biomechanics, Fascinating Life Sciences. Springer  
713 International Publishing, Cham, pp. 1–18. [https://doi.org/10.1007/978-3-030-13739-](https://doi.org/10.1007/978-3-030-13739-7_1)  
714 [7\\_1](https://doi.org/10.1007/978-3-030-13739-7_1)

715 Berlioz, E., Azorit, C., Blondel, C., Ruiz, M.S.T., Merceron, G., 2017. Deer in an arid habitat:  
716 dental microwear textures track feeding adaptability. *Hystrix, the Italian Journal of*  
717 *Mammalogy* 28, 222–230. <https://doi.org/10.4404/hystrix-28.2-12048>

718 Brewer, C.A., Pickle, L., 2002. Evaluation of Methods for Classifying Epidemiological Data on  
719 Choropleth Maps in Series. *Annals of the Association of American Geographers* 92,  
720 662–681. <https://doi.org/10.1111/1467-8306.00310>

721 Calandra, I., Zub, K., Szafrńska, P.A., Zalewski, A., Merceron, G., 2016. Silicon-based plant  
722 defences, tooth wear and voles. *Journal of Experimental Biology* 219, 501–507.  
723 <https://doi.org/10.1242/jeb.134890>

724 Caley, T., Extier, T., Collins, J.A., Schefuß, E., Dupont, L., Malaizé, B., Rossignol, L., Souron,  
725 A., McClymont, E.L., Jimenez-Espejo, F.J., García-Comas, C., Eynaud, F., Martinez,  
726 P., Roche, D.M., Jorry, S.J., Charlier, K., Wary, M., Gourves, P.-Y., Billy, I., Giraudeau,  
727 J., 2018. A two-million-year-long hydroclimatic context for hominin evolution in  
728 southeastern Africa. *Nature* 560, 76–79. <https://doi.org/10.1038/s41586-018-0309-6>

729 Cerling, T.E., Mbu, E., Kirera, F.M., Manthi, F.K., Grine, F.E., Leakey, M.G., Sponheimer, M.,  
730 Uno, K.T., 2011. Diet of *Paranthropus boisei* in the early Pleistocene of East Africa.  
731 *Proceedings of the National Academy of Sciences* 108, 9337–9341.  
732 <https://doi.org/10.1073/pnas.1104627108>

733 Cerling, T.E., Manthi, F.K., Mbu, E.N., Leakey, L.N., Leakey, M.G., Leakey, R.E., Brown,  
734 F.H., Grine, F.E., Hart, J.A., Kaleme, P., Roche, H., Uno, K.T., Wood, B.A., 2013.  
735 Stable isotope-based diet reconstructions of Turkana Basin hominins. *Proceedings of*  
736 *the National Academy of Sciences* 110, 10501–10506.  
737 <https://doi.org/10.1073/pnas.1222568110>

738 Codron, D., Brink, J.S., Rossouw, L., Clauss, M., Codron, J., Lee-Thorp, J.A., Sponheimer, M.,  
739 2008. Functional differentiation of African grazing ruminants: an example of specialized  
740 adaptations to very small changes in diet. *Biological Journal of the Linnean Society* 94,  
741 755–764. <https://doi.org/10.1111/j.1095-8312.2008.01028.x>

742 Constantino, P.J., Wright, B.W., 2009. The importance of fallback foods in primate ecology and  
743 evolution. *American Journal of Physical Anthropology* 140, 599–602.  
744 <https://doi.org/10.1002/ajpa.20978>

745 Constantino, P.J., Lucas, P.W., Lee, J.J.-W., Lawn, B.R., 2009. The influence of fallback foods  
746 on great ape tooth enamel. *American Journal of Physical Anthropology* 140, 653–660.  
747 <https://doi.org/10.1002/ajpa.21096>

748 Cox, C., Schneider, M.F., Muñoz, A., 2013. Quantiles of Residual Survival, in: Lee, M.-L.T.,  
749 Gail, M., Pfeiffer, R., Satten, G., Cai, T., Gandy, A. (Eds.), *Risk Assessment and*  
750 *Evaluation of Predictions, Lecture Notes in Statistics*. Springer, New York, NY, pp. 87–  
751 103. [https://doi.org/10.1007/978-1-4614-8981-8\\_6](https://doi.org/10.1007/978-1-4614-8981-8_6)

752 Daegling, D.J., McGraw, W.S., Ungar, P.S., Pampush, J.D., Vick, A.E., Bitty, E.A., 2011. Hard-  
753 object feeding in sooty mangabeys (*Cercocebus atys*) and interpretation of early  
754 hominin feeding ecology. *PLoS ONE* 6, e23095.  
755 <https://doi.org/10.1371/journal.pone.0023095>

756 Daegling, D.J., Hua, L.-C., Ungar, P.S., 2016. The role of food stiffness in dental microwear  
757 feature formation. *Archives of Oral Biology* 71, 16–23.  
758 <https://doi.org/10.1016/j.archoralbio.2016.06.018>

759 Damuth, J., Janis, C.M., 2011. On the relationship between hypsodonty and feeding ecology  
760 in ungulate mammals, and its utility in palaeoecology. *Biological Reviews* 86, 733–758.  
761 <https://doi.org/10.1111/j.1469-185X.2011.00176.x>

762 Delprete, C., Sesana, R., 2014. Mechanical characterization of kernel and shell of hazelnuts:  
763 proposal of an experimental procedure. *Journal of Food Engineering* 124, 28–34.  
764 <https://doi.org/10.1016/j.jfoodeng.2013.09.027>

765 Dominy, N.J., Vogel, E.R., Yeakel, J.D., Constantino, P., Lucas, P.W., 2008. Mechanical  
766 properties of plant underground storage organs and implications for dietary models of  
767 early hominins. *Evolutionary Biology* 35, 159–175. [https://doi.org/10.1007/s11692-008-](https://doi.org/10.1007/s11692-008-9026-7)  
768 9026-7

769 Ercisli, S., Ozturk, I., Kara, M., Kalkan, F., Seker, H., Duyar, O., Erturk, Y., 2011. Physical  
770 properties of hazelnuts. *International Agrophysics* 25, 115–121.

771 Francisco, A., Blondel, C., Brunetière, N., Ramdarshan, A., Merceron, G., 2018a. Enamel  
772 surface topography analysis for diet discrimination. A methodology to enhance and  
773 select discriminative parameters. *Surface Topography: Metrology and Properties* 6,  
774 015002. <https://doi.org/10.1088/2051-672X/aa9dd3>

775 Francisco, A., Brunetière, N., Merceron, G., 2018b. Gathering and analyzing surface  
776 parameters for diet identification purposes. *Technologies* 6, 75.  
777 <https://doi.org/10.3390/technologies6030075>

778 Gailer, J.P., Calandra, I., Schulz-Kornas, E., Kaiser, T.M., 2016. Morphology is not destiny:  
779 discrepancy between form, function and dietary adaptation in bovid cheek teeth.  
780 *Journal of Mammalian Evolution* 23, 369–383. [https://doi.org/10.1007/s10914-016-](https://doi.org/10.1007/s10914-016-9325-1)  
781 9325-1

782 Grine, F.E., Daegling, D.J., 2017. Functional morphology, biomechanics and the retrodiction  
783 of early hominin diets. *Comptes Rendus Palevol* 16, 613–631.  
784 <https://doi.org/10.1016/j.crv.2017.01.005>

785 Harris, J.M., Cerling, T.E., 2002. Dietary adaptations of extant and Neogene African suids.  
786 *Journal of Zoology* 256, 45–54. <https://doi.org/10.1017/S0952836902000067>

787 Hoffman, J.M., Fraser, D., Clementz, M.T., 2015. Controlled feeding trials with ungulates: a  
788 new application of in vivo dental molding to assess the abrasive factors of microwear.  
789 *Journal of Experimental Biology* 218, 1538–1547. <https://doi.org/10.1242/jeb.118406>

790 Hofman-Kamińska, E., Merceron, G., Bocherens, H., Makowiecki, D., Piličiauskienė, G.,  
791 Ramdarshan, A., Berlioz, E., Kowalczyk, R., 2018. Foraging habitats and niche  
792 partitioning of European large herbivores during the Holocene – Insights from 3D dental

793 microwear texture analysis. *Palaeogeography, Palaeoclimatology, Palaeoecology* 506,  
794 183–195. <https://doi.org/10.1016/j.palaeo.2018.05.050>

795 Hua, L.-C., Brandt, E.T., Meullenet, J.-F., Zhou, Z.-R., Ungar, P.S., 2015. Technical note: An  
796 in vitro study of dental microwear formation using the BITE Master II chewing machine.  
797 *American Journal of Physical Anthropology* 158, 769–775.  
798 <https://doi.org/10.1002/ajpa.22823>

799 Kalkan, F., Kara, M., Bastaban, S., Turgut, N., 2011. Strength and frictional properties of  
800 popcorn kernel as affected by moisture content. *International Journal of Food*  
801 *Properties* 14, 1197–1207. <https://doi.org/10.1080/10942911003637319>

802 Krueger, K.L., Scott, J.R., Kay, R.F., Ungar, P.S., 2008. Technical note: Dental microwear  
803 textures of “Phase I” and “Phase II” facets. *American Journal of Physical Anthropology*  
804 137, 485–490. <https://doi.org/10.1002/ajpa.20928>

805 Krzywinski, M., Altman, N., 2014. Visualizing samples with box plots. *Nature Methods* 11, 119–  
806 120. <https://doi.org/10.1038/nmeth.2813>

807 Laden, G., Wrangham, R., 2005. The rise of the hominids as an adaptive shift in fallback foods:  
808 Plant underground storage organs (USOs) and australopith origins. *Journal of Human*  
809 *Evolution* 49, 482–498. <https://doi.org/10.1016/j.jhevol.2005.05.007>

810 Lambert, J.E., Chapman, C.A., Wrangham, R.W., Conklin-Brittain, N.L., 2004. Hardness of  
811 cercopithecine foods: Implications for the critical function of enamel thickness in  
812 exploiting fallback foods. *American Journal of Physical Anthropology* 125, 363–368.  
813 <https://doi.org/10.1002/ajpa.10403>

814 Lambrechtsen, J., Rasmussen, F., Hansen, H., Jacobsen, I., 1999. Tracking and factors  
815 predicting rising in ‘tracking quartile’ in blood pressure from childhood to adulthood:  
816 Odense Schoolchild Study. *Journal of Human Hypertension* 13, 385–391.  
817 <https://doi.org/10.1038/sj.jhh.1000836>

818 Lazagabaster, I.A., 2019. Dental microwear texture analysis of Pliocene Suidae from Hadar  
819 and Kanapoi in the context of early hominin dietary breadth expansion. *Journal of*  
820 *Human Evolution* 132, 80–100. <https://doi.org/10.1016/j.jhevol.2019.04.010>



821 Lee-Thorp, J.A., van der Merwe, N.J., Brain, C.K., 1994. Diet of *Australopithecus robustus* at  
822 Swartkrans from stable carbon isotopic analysis. *Journal of Human Evolution* 27, 361–  
823 372. <https://doi.org/10.1006/jhev.1994.1050>

824 Legge, A.J., 2013. 'Practice with Science': Molar Tooth Eruption Ages in Domestic, Feral and  
825 Wild Pigs (*Sus scrofa*). *International Journal of Osteoarchaeology*.  
826 [https://onlinelibrary.wiley.com/pb-](https://onlinelibrary.wiley.com/pb-assets/assets/10991212/Anthony_Legge_Final_Paper.pdf)  
827 [assets/assets/10991212/Anthony\\_Legge\\_Final\\_Paper.pdf](https://onlinelibrary.wiley.com/pb-assets/assets/10991212/Anthony_Legge_Final_Paper.pdf) (accessed 16 September  
828 2020)

829 Liem, K.F., 1980. Adaptive significance of intra- and interspecific differences in the feeding  
830 repertoires of cichlid fishes. *American Zoologist* 20, 295–314.  
831 <https://doi.org/10.1093/icb/20.1.295>

832 Lister, A.M., 2013. The role of behaviour in adaptive morphological evolution of African  
833 proboscideans. *Nature* 500, 331–334. <https://doi.org/10.1038/nature12275>

834 Lucas, P.W., 2004. *Dental Functional Morphology: How Teeth Work*, 1st ed. Cambridge  
835 University Press. <https://doi.org/10.1017/CBO9780511735011>

836 Lucas, P.W., Constantino, P.J., Chalk, J., Ziscovici, C., Wright, B.W., Fragaszy, D.M., Hill,  
837 D.A., Lee, J.J.-W., Chai, H., Darvell, B.W., Lee, P.K.D., Yuen, T.D.B., 2009. Indentation  
838 as a technique to assess the mechanical properties of fallback foods. *American Journal*  
839 *of Physical Anthropology* 140, 643–652. <https://doi.org/10.1002/ajpa.21026>

840 Lucas, P.W., Omar, R., Al-Fadhalah, K., Almusallam, A.S., Henry, A.G., Michael, S., Thai, L.A.,  
841 Watzke, J., Strait, D.S., Atkins, A.G., 2013. Mechanisms and causes of wear in tooth  
842 enamel: implications for hominin diets. *Journal of The Royal Society Interface* 10,  
843 20120923. <https://doi.org/10.1098/rsif.2012.0923>

844 Lucas, P.W., Casteren, A. van, Al-Fadhalah, K., Almusallam, A.S., Henry, A.G., Michael, S.,  
845 Watzke, J., Reed, D.A., Diekwisch, T.G.H., Strait, D.S., Atkins, A.G., 2014. The role of  
846 dust, grit and phytoliths in tooth wear. *Annals Zoologici Fennici* 51, 143–152.  
847 <https://doi.org/10.5735/086.051.0215>

848 Lüdecke, T., Kullmer, O., Wacker, U., Sandrock, O., Fiebig, J., Schrenk, F., Mulch, A., 2018.  
849 Dietary versatility of Early Pleistocene hominins. *Proceedings of the National Academy*  
850 *of Sciences USA* 115, 13330–13335. <https://doi.org/10.1073/pnas.1809439115>

851 MacArthur, R.H., Pianka, E.R., 1966. On optimal use of a patchy environment. *The American*  
852 *Naturalist* 100, 603–609. <https://doi.org/10.1086/282454>

853 Madden, R.H., 2014. *Hypsodonty in Mammals: Evolution, Geomorphology and the Role of*  
854 *Earth Surface Processes*. Cambridge University Press, Cambridge.  
855 <https://doi.org/10.1017/CBO9781139003384>

856 Markowski, M., Majewska, K., Kwiatkowski, D., Malkowski, M., Burdylo, G., 2010. Selected  
857 geometric and mechanical properties of barley (*Hordeum vulgare* L.) grain.  
858 *International Journal of Food Properties* 13, 890–903.  
859 <https://doi.org/10.1080/10942910902908888>

860 Marshall, A.J., Wrangham, R.W., 2007. Evolutionary consequences of fallback foods.  
861 *International Journal of Primatology* 28, 1219–1235. [https://doi.org/10.1007/s10764-](https://doi.org/10.1007/s10764-007-9218-5)  
862 [007-9218-5](https://doi.org/10.1007/s10764-007-9218-5)

863 Marshall, A.J., Boyko, C.M., Feilen, K.L., Boyko, R.H., Leighton, M., 2009. Defining fallback  
864 foods and assessing their importance in primate ecology and evolution. *American*  
865 *Journal of Physical Anthropology* 140, 603–614. <https://doi.org/10.1002/ajpa.21082>

866 Martin, F., Plastiras, C.-A., Merceron, G., Souron, A., Boissarie, J.-R., 2018. Dietary niches of  
867 terrestrial cercopithecines from the Plio-Pleistocene Shungura Formation, Ethiopia:  
868 evidence from Dental Microwear Texture Analysis. *Scientific Reports* 8, 14052.  
869 <https://doi.org/10.1038/s41598-018-32092-z>

870 Martin, J.E., Tacail, T., Braga, J., Cerling, T.E., Balter, V., 2020. Calcium isotopic ecology of  
871 Turkana Basin hominins. *Nature Communications* 11, 3587.  
872 <https://doi.org/10.1038/s41467-020-17427-7>

873 Martin, L.F., Winkler, D., Tütken, T., Codron, D., De Cuyper, A., Hatt, J.-M., Clauss, M., 2019.  
874 The way wear goes: phytolith-based wear on the dentine–enamel system in guinea

875 pigs (*Cavia porcellus*). Proceedings of the Royal Society B: Biological Sciences 286,  
876 20191921. <https://doi.org/10.1098/rspb.2019.1921>

877 Martin, L.F., Krause, L., Ulbricht, A., Winkler, D.E., Codron, D., Kaiser, T.M., Müller, J.,  
878 Hummel, J., Clauss, M., Hatt, J.-M., Schulz-Kornas, E., this volume. Dental wear at  
879 macro- and microscopic scale in rabbits fed diets of different abrasiveness.  
880 Palaeogeography, Palaeoclimatology, Palaeoecology.

881 Merceron, G., Blondel, C., De Bonis, L., Koufos, G.D., Viriot, L., 2005. A new method of dental  
882 microwear analysis: Application to extant primates and *Ouranopithecus macedoniensis*  
883 (Late Miocene of Greece). *Palaios* 20, 551–561.  
884 <https://doi.org/10.2110/palo.2004.p04-17>

885 Merceron, G., Taylor, S., Scott, R., Chaimanee, Y., Jaeger, J.-J., 2006. Dietary  
886 characterization of the hominoid *Khoratpithecus* (Miocene of Thailand): evidence from  
887 dental topographic and microwear texture analyses. *Naturwissenschaften* 93, 329–  
888 333. <https://doi.org/10.1007/s00114-006-0107-0>

889 Merceron, G., Scott, J., Scott, R.S., Geraads, D., Spassov, N., Ungar, P.S., 2009. Folivory or  
890 fruit/seed predation for *Mesopithecus*, an earliest colobine from the Late Miocene of  
891 Eurasia? *Journal of Human Evolution* 57, 732–738.  
892 <https://doi.org/10.1016/j.jhevol.2009.06.009>

893 Merceron, G., Escarguel, G., Angibault, J.-M., Verheyden-Tixier, H., 2010. Can dental  
894 microwear textures record inter-individual dietary variations? *PLoS ONE* 5, e9542.  
895 <https://doi.org/10.1371/journal.pone.0009542>

896 Merceron, G., Hofman-Kamińska, E., Kowalczyk, R., 2014. 3D dental microwear texture  
897 analysis of feeding habits of sympatric ruminants in the Białowieża Primeval Forest,  
898 Poland. *Forest Ecology and Management* 328, 262–269.  
899 <https://doi.org/10.1016/j.foreco.2014.05.041>

900 Merceron, G., Ramdarshan, A., Blondel, C., Boisserie, J.-R., Brunetiere, N., Francisco, A.,  
901 Gautier, D., Milhet, X., Novello, A., Pret, D., 2016. Untangling the environmental from

902 the dietary: dust does not matter. *Proceedings of the Royal Society B: Biological*  
903 *Sciences* 283, 20161032. <https://doi.org/10.1098/rspb.2016.1032>

904 Merceron, G., Kallend, A., Francisco, A., Louail, M., Martin, F., Plastiras, C.-F., Thiery, G.,  
905 Noûs, C., Boisserie, J.-R., this volume. Further away with dental microwear analysis:  
906 food resource partitioning among Plio-Pleistocene monkeys from the Shungura  
907 Formation, Ethiopia. *Palaeogeography, Palaeoclimatology, Palaeoecology*.

908 Norconk, M.A., Veres, M., 2011. Physical properties of fruit and seeds ingested by primate  
909 seed predators with emphasis on sakis and bearded sakis. *The Anatomical Record*  
910 294, 2092–2111. <https://doi.org/10.1002/ar.21506>

911 Nouri Jangi, A., Mortazavi, S.A., Tavakoli, M., Ghanbari, A., Tavakolipour, H., Haghayegh,  
912 G.H., 2011. Comparison of mechanical and thermal properties between two varieties  
913 of barley (*Hordeum vulgare* L.) grains. *Australian Journal of Agricultural Engineering* 2,  
914 132–139.

915 Percher, A.M., Merceron, G., Nsi Akoue, G., Galbany, J., Romero, A., Charpentier, M.J., 2017.  
916 Dental microwear textural analysis as an analytical tool to depict individual traits and  
917 reconstruct the diet of a primate. *American Journal of Physical Anthropology* 165, 123–  
918 138. <https://doi.org/10.1002/ajpa.23337>

919 Peterson, A., Abella, E.F., Grine, F.E., Teaford, M.F., Ungar, P.S., 2018. Microwear textures  
920 of *Australopithecus africanus* and *Paranthropus robustus* molars in relation to  
921 paleoenvironment and diet. *Journal of Human Evolution* 119, 42–63.  
922 <https://doi.org/10.1016/j.jhevol.2018.02.004>

923 Phillips, B.D., Metz, W.C., Nieves, L.A., 2005. Disaster threat: Preparedness and potential  
924 response of the lowest income quartile. *Global Environmental Change Part B:*  
925 *Environmental Hazards* 6, 123–133. <https://doi.org/10.1016/j.hazards.2006.05.001>

926 Plavcan, J.M., Cope, D.A., 2001. Metric variation and species recognition in the fossil record.  
927 *Evolutionary Anthropology* 10, 204–222. <https://doi.org/10.1002/evan.20001>

928 Potts, R., 2004. Paleoenvironmental basis of cognitive evolution in great apes. *American*  
929 *Journal of Primatology* 62, 209–228. <https://doi.org/10.1002/ajp.20016>

930 Ragni, A.J., Teaford, M.F., Ungar, P.S., 2017. A molar microwear texture analysis of pitheciid  
931 primates. *American Journal of Primatology* 79, e22697.  
932 <https://doi.org/10.1002/ajp.22697>

933 Ramdarshan, A., Alloing-Séguier, T., Merceron, G., Marivaux, L., 2011. The primate  
934 community of Cachoeira (Brazilian Amazonia): A model to decipher ecological  
935 partitioning among extinct species. *PLoS ONE* 6, e27392.  
936 <https://doi.org/10.1371/journal.pone.0027392>

937 Ramdarshan, A., Blondel, C., Brunetière, N., Francisco, A., Gautier, D., Surault, J., Merceron,  
938 G., 2016. Seeds, browse, and tooth wear: a sheep perspective. *Ecology and Evolution*  
939 6, 5559–5569. <https://doi.org/10.1002/ece3.2241>

940 Ramdarshan, A., Blondel, C., Gautier, D., Surault, J., Merceron, G., 2017. Overcoming  
941 sampling issues in dental tribology: Insights from an experimentation on sheep.  
942 *Palaeontologia Electronica* 20, 1–19. <https://doi.org/10.26879/762>

943 Remis, M.J., 2002. Food preferences among captive western gorillas (*Gorilla gorilla gorilla*)  
944 and chimpanzees (*Pan troglodytes*). *International Journal of Primatology* 23, 231–249.  
945 <https://doi.org/10.1023/A:1013837426426>

946 Robinson, B.W., Wilson, D.S., 1998. Optimal foraging, specialization, and a solution to Liem's  
947 paradox. *The American Naturalist* 151, 223–235. <https://doi.org/10.1086/286113>

948 Robinson, J.T., 1954. Prehominid dentition and hominid evolution. *Evolution* 8, 324–334.  
949 <https://doi.org/10.1111/j.1558-5646.1954.tb01499.x>

950 Rolett, B.V., Chiu, M., 1994. Age estimation of prehistoric pigs (*Sus scrofa*) by molar eruption  
951 and attrition. *Journal of Archaeological Science* 21, 377–386.  
952 <https://doi.org/10.1006/jasc.1994.1036>

953 Romero, A., Galbany, J., Juan, J.D., Pérez-Pérez, A., 2012. Brief communication: Short- and  
954 long-term in vivo human buccal–dental microwear turnover. *American Journal of*  
955 *Physical Anthropology* 148, 467–472. <https://doi.org/10.1002/ajpa.22054>

956 Sayers, K., 2013. On folivory, competition, and intelligence: generalisms, overgeneralizations,  
957 and models of primate evolution. *Primates* 54, 111–124.  
958 <https://doi.org/10.1007/s10329-012-0335-1>

959 Schubert, B.W., Ungar, P.S., DeSantis, L.R.G., 2010. Carnassial microwear and dietary  
960 behaviour in large carnivorans: Carnivoran dental microwear. *Journal of Zoology* 280,  
961 257–263. <https://doi.org/10.1111/j.1469-7998.2009.00656.x>

962 Schulz-Kornas, E., Stuhlträger, J., Clauss, M., Wittig, R.M., Kupczik, K., 2019. Dust affects  
963 chewing efficiency and tooth wear in forest dwelling Western chimpanzees (*Pan*  
964 *trogodytes verus*). *American Journal of Physical Anthropology* 169, 66–77.  
965 <https://doi.org/10.1002/ajpa.23808>

966 Schulz-Kornas, E., Winkler, D.E., Clauss, M., Carlsson, J., Ackermans, N.L., Martin, L.F.,  
967 Hummel, J., Müller, D.W.H., Hatt, J.-M., Kaiser, T.M., 2020. Everything matters: Molar  
968 microwear texture in goats (*Capra aegagrus hircus*) fed diets of different abrasiveness.  
969 *Palaeogeography, Palaeoclimatology, Palaeoecology* 552, 109783.  
970 <https://doi.org/10.1016/j.palaeo.2020.109783>

971 Scott, R.S., Ungar, P.S., Bergstrom, T.S., Brown, C.A., Grine, F.E., Teaford, M.F., Walker, A.,  
972 2005. Dental microwear texture analysis shows within-species diet variability in fossil  
973 hominins. *Nature* 436, 693–695. <https://doi.org/10.1038/nature03822>

974 Scott, R.S., Ungar, P.S., Bergstrom, T.S., Brown, C.A., Childs, B.E., Teaford, M.F., Walker, A.,  
975 2006. Dental microwear texture analysis: technical considerations. *Journal of Human*  
976 *Evolution* 51, 339–349. <https://doi.org/10.1016/j.jhevol.2006.04.006>

977 Scott, R.S., Teaford, M.F., Ungar, P.S., 2012. Dental microwear texture and anthropoid diets.  
978 *American Journal of Physical Anthropology* 147, 551–579.  
979 <https://doi.org/10.1002/ajpa.22007>

980 Solounias, N., Semprebon, G., 2002. Advances in the reconstruction of ungulate  
981 ecomorphology with application to early fossil equids. *American Museum Novitates*  
982 3366, 1–49

983 Souron, A., 2017. Diet and Ecology of Extant and Fossil Wild Pigs, in: Melletti, M., Meijaard,  
984 E. (Eds.), Ecology, Conservation and Management of Wild Pigs and Peccaries.  
985 Cambridge University Press, pp. 29–38. <https://doi.org/10.1017/9781316941232.005>

986 Souron, A., Merceron, G., Blondel, C., Brunetière, N., Colyn, M., Hofman-Kamińska, E.,  
987 Boisserie, J.-R., 2015. Three-dimensional dental microwear texture analysis and diet  
988 in extant Suidae (Mammalia: Cetartiodactyla). *Mammalia* 79, 279–291.  
989 <https://doi.org/10.1515/mammalia-2014-0023>

990 Sponheimer, M., Passey, B.H., de Ruiter, D.J., Guatelli-Steinberg, D., Cerling, T.E., Lee-  
991 Thorp, J.A., 2006. Isotopic evidence for dietary variability in the early hominin  
992 *Paranthropus robustus*. *Science* 314, 980–982.  
993 <https://doi.org/10.1126/science.1133827>

994 Strait, D.S., Weber, G.W., Neubauer, S., Chalk, J., Richmond, B.G., Lucas, P.W., Spencer,  
995 M.A., Schrein, C., Dechow, P.C., Ross, C.F., Grosse, I.R., Wright, B.W., Constantino,  
996 P., Wood, B.A., Lawn, B., Hylander, W.L., Wang, Q., Byron, C., Slice, D.E., Smith, A.L.,  
997 2009. The feeding biomechanics and dietary ecology of *Australopithecus africanus*.  
998 *Proceedings of the National Academy of Sciences* 106, 2124–2129.  
999 <https://doi.org/10.1073/pnas.0808730106>

1000 Teaford, M.F., Oyen, O.J., 1989. In vivo and in vitro turnover in dental microwear. *American*  
1001 *Journal of Physical Anthropology* 80, 447–460.  
1002 <https://doi.org/10.1002/ajpa.1330800405>

1003 Teaford, M.F., Robinson, J.G., 1989. Seasonal or ecological differences in diet and molar  
1004 microwear in *Cebus nigrivittatus*. *American Journal of Physical Anthropology* 80, 391–  
1005 401. <https://doi.org/10.1002/ajpa.1330800312>

1006 Teaford, M.F., Runestad, J.A., 1992. Dental microwear and diet in Venezuelan primates.  
1007 *American Journal of Physical Anthropology* 88, 347–364.  
1008 <https://doi.org/10.1002/ajpa.1330880308>

1009 Teaford, M.F., Ungar, P.S., Taylor, A.B., Ross, C.F., Vinyard, C.J., 2017. In vivo rates of dental  
1010 microwear formation in laboratory primates fed different food items. *Biosurface and*  
1011 *Biotribology* 3, 166–173. <https://doi.org/10.1016/j.bsbt.2017.11.005>

1012 Teaford, M.F., Ungar, P.S., Taylor, A.B., Ross, C.F., Vinyard, C.J., 2020. The dental microwear  
1013 of hard-object feeding in laboratory *Sapajus apella* and its implications for dental  
1014 microwear formation. *American Journal of Physical Anthropology* 171, 439–455.  
1015 <https://doi.org/10.1002/ajpa.24000>

1016 Tran, T.L., deMan, J.M., Rasper, V.F., 1981. Measurement of corn kernel hardness. *Canadian*  
1017 *Institute of Food Science and Technology Journal* 14, 42–48.  
1018 [https://doi.org/10.1016/S0315-5463\(81\)72675-0](https://doi.org/10.1016/S0315-5463(81)72675-0)

1019 Tucker, A.L., Widowski, T.M., 2009. Normal profiles for deciduous dental eruption in domestic  
1020 piglets: Effect of sow, litter, and piglet characteristics. *Journal of Animal Science* 87,  
1021 2274–2281. <https://doi.org/10.2527/jas.2008-1498>

1022 Tütken, T., Kaiser, T.M., Vennemann, T., Merceron, G., 2013. Opportunistic feeding strategy  
1023 for the earliest Old World hypsodont equids: Evidence from stable isotope and dental  
1024 wear proxies. *PLoS ONE* 8, e74463. <https://doi.org/10.1371/journal.pone.0074463>

1025 Ungar, P., 2002. Reconstructing the Diets of Fossil Primates, in: Plavcan, J.M., Kay, R.F.,  
1026 Jungers, W.L., van Schaik, C.P. (Eds.), *Reconstructing Behavior in the Primate Fossil*  
1027 *Record*. Springer US, Boston, MA, pp. 261–296. [https://doi.org/10.1007/978-1-4615-](https://doi.org/10.1007/978-1-4615-1343-8_7)  
1028 [1343-8\\_7](https://doi.org/10.1007/978-1-4615-1343-8_7)

1029 Ungar, P., 2004. Dental topography and diets of *Australopithecus afarensis* and early *Homo*.  
1030 *Journal of Human Evolution* 46, 605–622. <https://doi.org/10.1016/j.jhevol.2004.03.004>

1031 Ungar, P.S., Daegling, D.J., 2013. The Functional Morphology of Jaws and Teeth: Implications  
1032 for Understanding Early Hominin Dietary Adaptations, in: Sponheimer, M., Lee-Thorp,  
1033 J.A., Reed, K.E., Ungar, P. (Eds.), *Early Hominin Paleoecology*. University Press of  
1034 Colorado, pp. 203–250. <https://doi.org/10.5876/9781607322252:c060>

1035 Ungar, P.S., Sponheimer, M., 2011. The diets of early hominins. *Science* 334, 190–193.  
1036 <https://doi.org/10.1126/science.1207701>



- 1037 Ungar, P.S., Grine, F.E., Teaford, M.F., 2008. Dental microwear and diet of the Plio-  
1038 Pleistocene hominin *Paranthropus boisei*. PLoS ONE 3, e2044.  
1039 <https://doi.org/10.1371/journal.pone.0002044>
- 1040 Ungar, P.S., Krueger, K.L., Blumenschine, R.J., Njau, J., Scott, R.S., 2012. Dental microwear  
1041 texture analysis of hominins recovered by the Olduvai Landscape Paleoanthropology  
1042 Project, 1995–2007. Journal of Human Evolution 63, 429–437.  
1043 <https://doi.org/10.1016/j.jhevol.2011.04.006>
- 1044 Ungar, P.S., Abella, E.F., Burgman, J.H.E., Lazagabaster, I.A., Scott, J.R., Delezene, L.K.,  
1045 Manthi, F.K., Plavcan, J.M., Ward, C.V., 2017. Dental microwear and Pliocene  
1046 paleocommunity ecology of bovids, primates, rodents, and suids at Kanapoi. Journal  
1047 of Human Evolution 140, 102315. <https://doi.org/10.1016/j.jhevol.2017.03.005>
- 1048 van Casteren, A., Lucas, P.W., Strait, D.S., Michael, S., Bierwisch, N., Schwarzer, N., Al-  
1049 Fadhalah, K.J., Almusallam, A.S., Thai, L.A., Saji, S., Shekeban, A., Swain, M.V., 2018.  
1050 Evidence that metallic proxies are unsuitable for assessing the mechanics of microwear  
1051 formation and a new theory of the meaning of microwear. Royal Society Open Science  
1052 5, 171699. <https://doi.org/10.1098/rsos.171699>
- 1053 van Casteren, A. van, Wright, E., Kupczik, K., Robbins, M.M., 2019. Unexpected hard-object  
1054 feeding in Western lowland gorillas. American Journal of Physical Anthropology 170,  
1055 433–438. <https://doi.org/10.1002/ajpa.23911>
- 1056 van Casteren, A., Strait, D.S., Swain, M.V., Michael, S., Thai, L.A., Philip, S.M., Saji, S., Al-  
1057 Fadhalah, K., Almusallam, A.S., Shekeban, A., McGraw, W.S., Kane, E.E., Wright,  
1058 B.W., Lucas, P.W., 2020. Hard plant tissues do not contribute meaningfully to dental  
1059 microwear: evolutionary implications. Scientific Reports 10, 582.  
1060 <https://doi.org/10.1038/s41598-019-57403-w>
- 1061 Ward, J., Mainland, I.L., 1999. Microwear in modern rooting and stall-fed pigs: the potential of  
1062 dental microwear analysis for exploring pig diet and management in the past.  
1063 Environmental Archaeology 4, 25–32. <https://doi.org/10.1179/env.1999.4.1.25>

- 1064 Winkler, D.E., Schulz, E., Calandra, I., Gailer, J.-P., Landwehr, C., Kaiser, T.M., 2013.  
1065 Indications for a dietary change in the extinct Bovid genus *Myotragus* (Plio-Holocene,  
1066 Mallorca, Spain). *Geobios* 46, 143–150. <https://doi.org/10.1016/j.geobios.2012.10.010>
- 1067 Winkler, D.E., Andrianasolo, T.H., Andriamandimbarisoa, L., Ganzhorn, J.U.,  
1068 Rakotondranary, S.J., Kaiser, T.M., Schulz-Kornas, E., 2016. Tooth wear patterns in  
1069 black rats (*Rattus rattus*) of Madagascar differ more in relation to human impact than  
1070 to differences in natural habitats. *Ecology and Evolution* 6, 2205–2215.  
1071 <https://doi.org/10.1002/ece3.2048>
- 1072 Winkler, D.E., Schulz-Kornas, E., Kaiser, T.M., De Cuyper, A., Clauss, M., Tütken, T., 2019.  
1073 Forage silica and water content control dental surface texture in guinea pigs and  
1074 provide implications for dietary reconstruction. *Proceedings of the National Academy*  
1075 *of Sciences USA* 116, 1325–1330. <https://doi.org/10.1073/pnas.1814081116>
- 1076 Winkler, D.E., Tütken, T., Schulz-Kornas, E., Kaiser, T.M., Müller, J., Leichliter, J., Weber, K.,  
1077 Hatt, J.-M., Clauss, M., 2020. Shape, size, and quantity of ingested external abrasives  
1078 influence dental microwear texture formation in guinea pigs. *Proceedings of the*  
1079 *National Academy of Sciences USA* 117, 22264–22273.  
1080 <https://doi.org/10.1073/pnas.2008149117>
- 1081 Winkler, D.E., Schulz-Kornas, E., Kaiser, T.M., Codron, D., Leichliter, J., Hummel, J., Martin,  
1082 L.F., Clauss, M., Tütken, T., this volume. The turnover of dental microwear texture:  
1083 Testing the “last supper” effect in small mammals in a controlled feeding experiment.  
1084 *Palaeogeography, Palaeoclimatology, Palaeoecology*.
- 1085 Wood, B., Strait, D., 2004. Patterns of resource use in early *Homo* and *Paranthropus*. *Journal*  
1086 *of Human Evolution* 46, 119–162. <https://doi.org/10.1016/j.jhevol.2003.11.004>
- 1087 Wrangham, R., Cheney, D., Seyfarth, R., Sarmiento, E., 2009. Shallow-water habitats as  
1088 sources of fallback foods for hominins. *American Journal of Physical Anthropology* 140,  
1089 630–642. <https://doi.org/10.1002/ajpa.21122>
- 1090 Wynn, J.G., Alemseged, Z., Bobe, R., Grine, F.E., Negash, E.W., Sponheimer, M., 2020.  
1091 Isotopic evidence for the timing of the dietary shift toward C4 foods in eastern African

1092           *Paranthropus*. Proceeding of the National Academy of Sciences USA 117, 21978–  
1093           21984. <https://doi.org/10.1073/pnas.2006221117>

1094   Xia, J., Zheng, J., Huang, D., Tian, Z.R., Chen, L., Zhou, Z., Ungar, P.S., Qian, L., 2015. New  
1095           model to explain tooth wear with implications for microwear formation and diet  
1096           reconstruction. Proceedings of the National Academy of Sciences USA 112, 10669–  
1097           10672. <https://doi.org/10.1073/pnas.1509491112>

1098   Yamada, E., Kubo, M.O., Kubo, T., Kohno, N., 2018. Three-dimensional tooth surface texture  
1099           analysis on stall-fed and wild boars (*Sus scrofa*). PLoS ONE 13, e0204719.  
1100           <https://doi.org/10.1371/journal.pone.0204719>

1101   Yamashita, N., 1998. Functional dental correlates of food properties in five Malagasy lemur  
1102           species. American Journal of Physical Anthropology 106, 169–188.  
1103           [https://doi.org/10.1002/\(SICI\)1096-8644\(199806\)106:2<169::AID-AJPA5>3.0.CO;2-L](https://doi.org/10.1002/(SICI)1096-8644(199806)106:2<169::AID-AJPA5>3.0.CO;2-L)

1104   Zykov, S.V., Kropacheva, Yu.E., Smirnov, N.G., Dimitrova, Yu.V., 2018. Molar microwear of  
1105           narrow-headed vole (*Microtus gregalis* Pall., 1779) depending on the feed  
1106           abrasiveness. Doklady Biological Sciences 478, 16–18.  
1107           <https://doi.org/10.1134/S0012496618010052>

1108

1109 **Table S1.** Detailed description of the controlled-feeding experiments per individual. 1: female, 2:  
 1110 uncastrated male, 3: castrated male.

Dietary group	Specimen number	Birth date	Sex	Start of trial (date)	Age at dietary switch (days)	Age at slaughter (days)	Total feeding duration (days)	Feeding duration after dietary switch (days)
Hazelnut	870601	13/12/2018	2	08/04/2019	163	194	78	30
	870603	13/12/2018	2	08/04/2019	163	194	78	30
	870609	13/12/2018	2	08/04/2019	163	194	78	30
	870610	13/12/2018	1	08/04/2019	163	194	78	30
	870645	12/12/2018	1	08/04/2019	164	195	78	30
	870649	12/12/2018	1	08/04/2019	164	195	78	30
Barley	812073	17/06/2018	1	28/07/2018	120	215	174	95
	811925	13/06/2018	3	28/07/2018	124	293	248	169
	812003	15/06/2018	1	28/07/2018	122	291	248	169
	812078	17/06/2018	3	28/07/2018	120	289	248	169
	812031	14/06/2018	3	28/07/2018	123	218	174	95
Corn	812046	14/06/2018	3	28/07/2018	123	218	174	95
	812049	14/06/2018	3	28/07/2018	123	218	174	95
	812068	17/06/2018	1	28/07/2018	120	215	174	95
	811916	13/06/2018	1	28/07/2018	124	293	248	169
	811958	14/06/2018	3	28/07/2018	123	292	248	169
	812020	14/06/2018	1	28/07/2018	123	292	248	169
Base	811924	13/06/2018	3	28/07/2018		219	174	
	812004	15/06/2018	3	28/07/2018		217	174	
	812074	17/06/2018	3	28/07/2018		215	174	
	811949	14/06/2018	1	28/07/2018		292	248	
	812026	14/06/2018	1	28/07/2018		292	248	
	812036	14/06/2018	1	28/07/2018		292	248	
	870614	13/12/2018	2	08/04/2019		194	78	
	870619	13/12/2018	2	08/04/2019		194	78	
	870641	12/12/2018	2	08/04/2019		195	78	
	870623	13/12/2018	1	08/04/2019		229	113	
	870638	12/12/2018	1	08/04/2019		230	113	
870640	12/12/2018	1	08/04/2019		230	113		

1111

1112

1113

1114 **Table S2.** Discriminative parameters considered in this study for surface analysis using the routine  
 1115 described in Francisco et al. (2018a, 2018b) (see supplementary materials for detailed descriptions of  
 1116 the parameters).

Parameter	Description	Type
Sa	Arithmetic mean height <sup>1</sup>	Height
Sp	Maximum peak height <sup>1</sup>	
Sq	Root-mean-square-height <sup>1</sup>	
Sv	Maximum pit height <sup>1</sup>	
Ssk	Skewness <sup>1</sup>	
Sku	Kurtosis <sup>1</sup>	
Sdar	Relative area (developed area/projected area, Sdar = Sdr - 1)	
Sm	Mean height	
Smd	Median height	
Rmax	Semi-major axis of the $f_{ACF}$ ellipsis <sup>2</sup>	
Sal	Autocorrelation length, semi-minor axis of the $f_{ACF}$ ellipsis <sup>1, 2</sup>	
Stri	Rmax/Sal ratio <sup>1, 2</sup>	
b.sl	Highest slope of $f_{ACF}$ at the distance $r_s$ from the origin	
r.sl	b.sl/s.sl ratio	
s.sl	Smallest slope of $f_{ACF}$ at the distance $r_s$ from the origin	
Sh	Percentage of quasi-horizontal faces	Topological

1117 <sup>1</sup>ISO 25178 parameters in their more or less modified form. <sup>2</sup>Because some surfaces exhibit long  
 1118 wavelengths, the default value  $s = 0.2$  is a bit low and the parameter is redefined as the average for  $s =$   
 1119  $0.3, 0.4, \text{ and } 0.5$ .

1120

1121 **Table S3.** Statistics considered in this study for surface analysis using the routine described in Francisco  
 1122 et al. (2018a, 2018b).

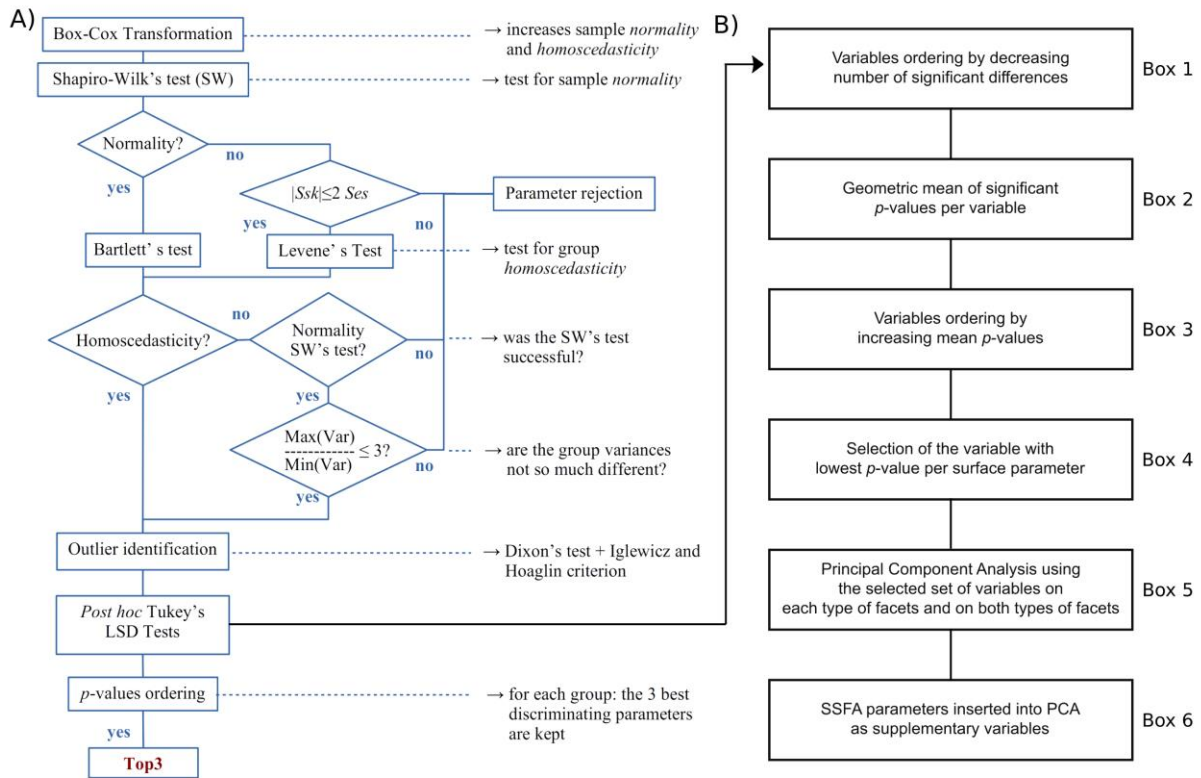
Statistic	Description	Statistic category
G	One value per surface	Global
Mean	Mean of $n$ values	Central
Median	Median of $n$ values	Central
Skw	Skewness of $n$ values	Distribution
Kurt	Kurtosis of $n$ values	Distribution
min.25	Mean of the 25 % lowest values among $n$ values	Dispersion
max.25	Mean of the 25 % highest values among $n$ values	Dispersion
fst.25	Value at the first quartile of the distribution of $n$ values	Dispersion
lst.25	Value at the third quartile of the distribution of $n$ values	Dispersion

1123

1124

1125

1126



1127  
 1128  
 1129  
 1130

**Figure S1.** Steps of the procedure developed by Francisco et al. (2018a, 2018b) and implementation (B) made by Merceron et al. (this volume) and in this study. Modified from Francisco et al. (2018b) and Merceron et al. (this volume).

1131 **Table S4.** Variables per parameter recognized as discriminative among the four lots on lower first molar  
 1132 facets (crushing and shearing) using the routine shown in Francisco et al. (2018a, 2018b).

Phase II (crushing) lower molar facets			Phase I (shearing) lower molar facets		
fst.25_Sh	max.25_Sh	SdaG	fst.25_Sh	max.25_Sku	min.25_Smd
fst.25_Sdar	max.25_Sv	skw_r.sl	fst.25_r.sl	max.25_Sm	min.25_Sp
fst.25_Sku	mea_Sh	skw_Sal	fst.25_Rmax	max.25_Sp	min.25_Sq
ShG	med_Sh	skw_Sp	fst.25_Sa	max.25_Sq	min.25_Stri
kurt_r.sl	med_Sdar	SpG	fst.25_Sal	max.25_Stri	min.25_Sv
kurt_Sp	med_Sv	std_Sh	fst.25_Sdar	max.25_Sv	RmaG
lst.25_Sh	min.25_Sdar	std_r.sl	fst.25_Sm	mea_Sh	SaG
lst.25_Smd	min.25_Sku	std_Sp	fst.25_Smd	mea_r.sl	SalG
lst.25_Sv			fst.25_Sp	mea_Rmax	SdaG
			fst.25_Sq	mea_Sa	SkuG
			fst.25_Stri	mea_Sdar	skw_Sh
			fst.25_Sv	mea_Sp	skw_Rmax
			ShG	mea_Sq	skw_Sa
			kurt_Sh	mea_Stri	skw_Sdar
			kurt_r.sl	mea_Sv	skw_Smd
			kurt_Rmax	med_Sh	skw_Sq
			kurt_Sa	med_r.sl	skw_Ssk
			kurt_Sdar	med_Rmax	skw_Stri
			kurt_Sq	med_Sa	SqG
			kurt_Stri	med_Sal	std_Sh
			lst.25_Sh	med_Sdar	std_Rmax
			lst.25_r.sl	med_Sp	std_Sa
			lst.25_Sa	med_Sq	std_Sal
			lst.25_Sdar	med_Stri	std_Sdar
			lst.25_Sm	med_Sv	std_Sku
			lst.25_Sp	min.25_Sh	std_Sm
			lst.25_Sq	min.25_r.sl	std_Smd
			lst.25_Stri	min.25_Rmax	std_Sp
			lst.25_Sv	min.25_Sa	std_Sq
			max.25_Sh	min.25_Sal	std_Ssk
			max.25_Rmax	min.25_Sdar	std_Stri
			max.25_Sa	min.25_Sm	
			max.25_Sdar		

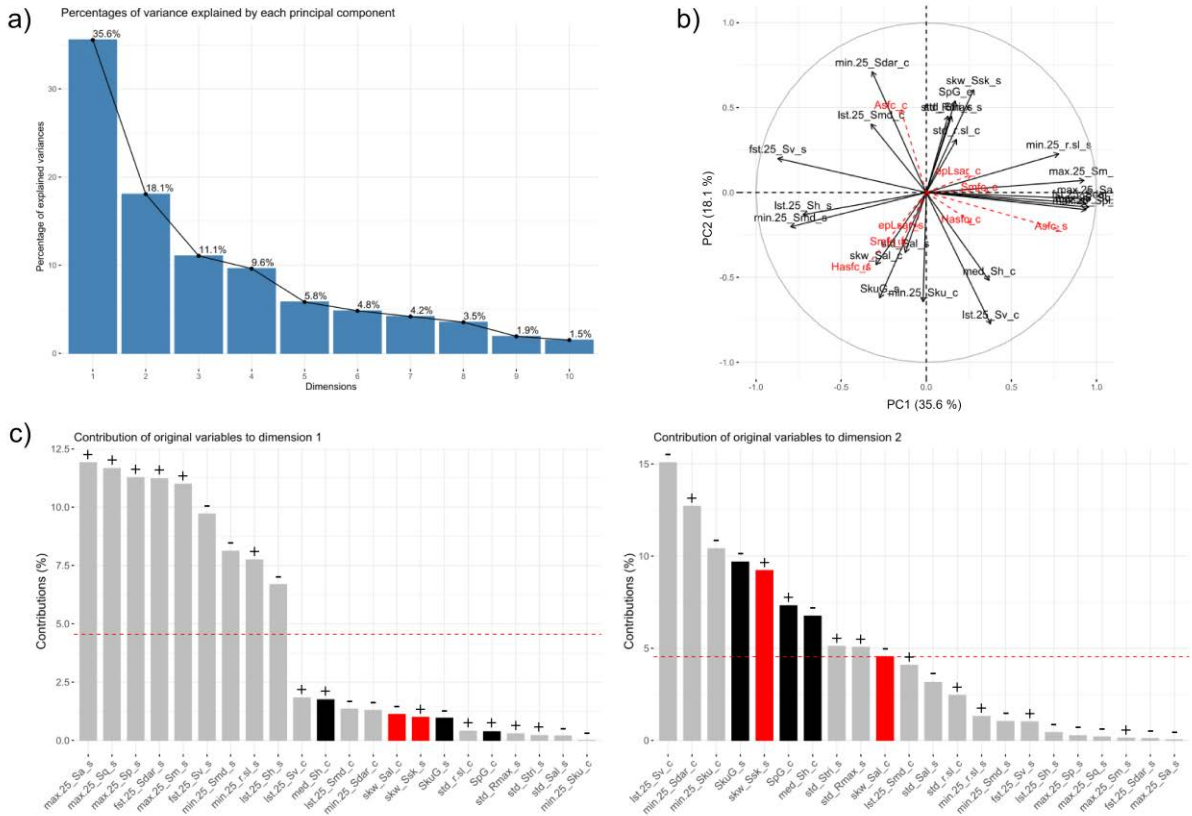
1133

1134

1135 **Table S5.** The most discriminative variables per parameters selected from the whole set of variables  
 1136 showing at least one significant difference among the four lots on lower first molar facets (crushing and  
 1137 shearing).

Facet	Variable	Parameter	Type	Statistic	Statistic category
Crushing	SpG	Sp	Height	global	Global
	med_Sh	Sh	Topological	median	Central
	min.25_Sku	Sku	Height	min.25	Dispersion
	min.25_Sdar	Sdar	Height	min.25	Dispersion
	lst.25_Sv	Sv	Height	lst.25	Dispersion
	std_r.sl	r.sl	Spatial	std	Dispersion
	skw_Sal	Sal	Spatial	skewness	Distribution
	lst.25_Smd	Smd	Height	lst.25	Dispersion
Shearing	max.25_Sa	Sa	Height	max.25	Dispersion
	max.25_Sq	Sq	Height	max.25	Dispersion
	fst.25_Sdar	Sdar	Height	fst.25	Dispersion
	max.25_Sp	Sp	Height	max.25	Dispersion
	lst.25_Sh	Sh	Topological	lst.25	Dispersion
	fst.25_Sv	Sv	Height	fst.25	Dispersion
	max.25_Sm	Sm	Height	max.25	Dispersion
	min.25_r.sl	r.sl	Spatial	min.25	Dispersion
	std_Rmax	Rmax	Spatial	standard deviation	Dispersion
	std_Sal	Sal	Spatial	standard deviation	Dispersion
	min.25_Smd	Smd	Height	min.25	Dispersion
	std_Stri	Stri	Spatial	standard deviation	Dispersion
	SkuG	Sku	Height	global	Dispersion
	skw_Ssk	Ssk	Height	skewness	Distribution





1138

1139 **Figure S2.** Principal Component Analysis based on the 23 most discriminative variables issued from  
 1140 both crushing (phase II) and shearing (phase I) facets on lower first molars. a) Percentage of variance  
 1141 explained by each principal component. b) Correlation circle between PC1 and PC2 with SSFA-  
 1142 parameters as supplementary variables (dotted red arrows). c) Contribution of each variable to PC1  
 1143 (left) and PC2 (right) in percentage and direction (positive: +, negative: -). Suffixes “\_c” and “\_s” refer to  
 1144 crushing and shearing facets, respectively. Black columns: central/global statistic, gray: dispersion  
 1145 statistics, red: distribution statistics. Dotted red line: expected average value if the contributions were  
 1146 uniform; any variable below this line could be considered negligible in contributing to the dimension.

1147

1148 **Table S6.** Analysis of variances on PC coordinates from PCA on crushing and shearing facets of lower  
 1149 first molars and combined HSD (above diagonal) and LSD (below diagonal) post hoc tests. Only p-  
 1150 values below a 10 % level of significance are given for post hoc tests.

		Df	SS	MS	F	p
PC1	Effect	3	24.09	8.031	6.95	0.0015
	Residuals	25	28.89	1.156		
PC2	Effect	3	49.23	16.410	3.547	0.0288
	Residuals	25	115.67	4.627		
PC3	Effect	3	0.401	0.1338	0.392	0.76
	Residuals	25	8.535	0.3414		
PC4	Effect	3	8.66	2.886	1.896	0.156
	Residuals	25	38.05	1.522		
PC5	Effect	3	0.768	0.2559	0.223	0.879
	Residuals	25	28.643	1.1457		

1151

1152

1153

LSD		HSD			
		Hazelnut	Barley	Control	Corn
PC1	Hazelnut		0.0015		
	Barley	0.0003		0.0035	
	Control		0.0007		
	Corn	0.0638	0.0262		
PC2	Hazelnut				0.0691
	Barley				
	Control				0.0275
	Corn	0.0155	0.0245	0.0057	

1154

1155 **Table S7.** Analysis of variances on PC coordinates from PCA on crushing facets of lower first molars  
 1156 and combined HSD (above diagonal) and LSD (below diagonal) post hoc tests. Only p-values below a  
 1157 10 % level of significance are given for post hoc tests.

		Df	SS	MS	F	p
PC1	Effect	3	152.9	50.95	3.014	0.0489
	Residuals	25	422.7	16.91		
PC2	Effect	3	53.37	17.79	3.277	0.0376
	Residuals	25	135.74	5.43		

1158

LSD		HSD			
		Hazelnut	Barley	Control	Corn
PC1	Hazelnut				
	Barley				0.0489
	Control		0.0805		
	Corn	0.0370	0.0106		
PC2	Hazelnut		0.0370		
	Barley	0.0079			
	Control		0.0361		
	Corn	0.0519			

1159

1160 **Table S8.** Analysis of variances on PC coordinates from PCA on shearing facets of lower first molars  
 1161 and combined HSD (above diagonal) and LSD (below diagonal) post hoc tests. A Kruskal-Wallis is run  
 1162 on PC2 followed with a Dunn's test. Only p-values below a 10 % level of significance are given for post  
 1163 hoc tests.

ANOVA		Df	SS	MS	F	p
PC1	Effect	3	43.11	14.37	6.303	0.0025
	Residuals	25	56.99	2.28		

1164

Kruskal-Wallis	Df	$\chi^2$	p
PC2	3	10.898	0.0123

1165

LSD		HSD			
		Hazelnut	Barley	Control	Corn
PC1	Hazelnut		0.0031		
	Barley	0.0006		0.0049	
	Control		0.0009		
	Corn	0.0696	0.0435		

1166

Dunn		Hazelnut	Barley	Control	Corn
PC2	Hazelnut				
	Barley				
	Control	0.0135			
	Corn		0.0190	0.0020	

1167

1168 **Table S9** Variables per parameter recognized as discriminative among the four lots on upper first molar  
 1169 facets (crushing and shearing) using the routine shown in Francisco et al. (2018a, 2018b).

Phase II (crushing) upper molar facets			Phase I (shearing) upper molar facets		
fst.25_Sh	max.25_Sq	min.25_Stri	fst.25_Rmax	max.25_Sku	min.25_Sku
fst.25_Sdar	mea_Sh	min.25_Sv	fst.25_Sa	max.25_Sv	min.25_Smd
fst.25_Stri	mea_r.sl	RmaG	fst.25_Sal	mea_Sa	min.25_Sp
fst.25_Sv	mea_Sa	SaG	fst.25_Sku	mea_Sal	min.25_Sq
ShG	mea_Sdar	SdaG	fst.25_Smd	mea_Sku	min.25_Ssk
kurt_s.sl	mea_Sp	skw_b.sl	fst.25_Sp	mea_Ssk	SaG
lst.25_Sh	mea_Sq	skw_s.sl	fst.25_Sq	med_r.sl	SalG
lst.25_Rmax	mea_Sv	skw_Sa	fst.25_Ssk	med_Rmax	SkuG
lst.25_Sa	med_Sh	skw_Sal	kurt_s.sl	med_Sa	skw_s.sl
lst.25_Sdar	med_Rmax	skw_Sm	kurt_Sa	med_Sal	skw_Sa
lst.25_Sp	med_Sa	SpG	kurt_Sq	med_Sku	skw_Sq
lst.25_Sq	med_Sdar	SqG	lst.25_Rmax	med_Sp	SskG
lst.25_Stri	med_Sp	std_r.sl	lst.25_Sa	med_Sq	std_Sh
lst.25_Sv	med_Sq	std_Sdar	lst.25_Sku	med_Ssk	std_Sal
max.25_r.sl	med_Stri	std_Sp	lst.25_Sq	min.25_Sa	std_Sku
max.25_S	med_Sv	std_Sv	max.25_Sal	min.25_Sal	std_Ssk
max.25_Sdar	min.25_Sh	StrG			
max.25_Sp	min.25_Sdar				

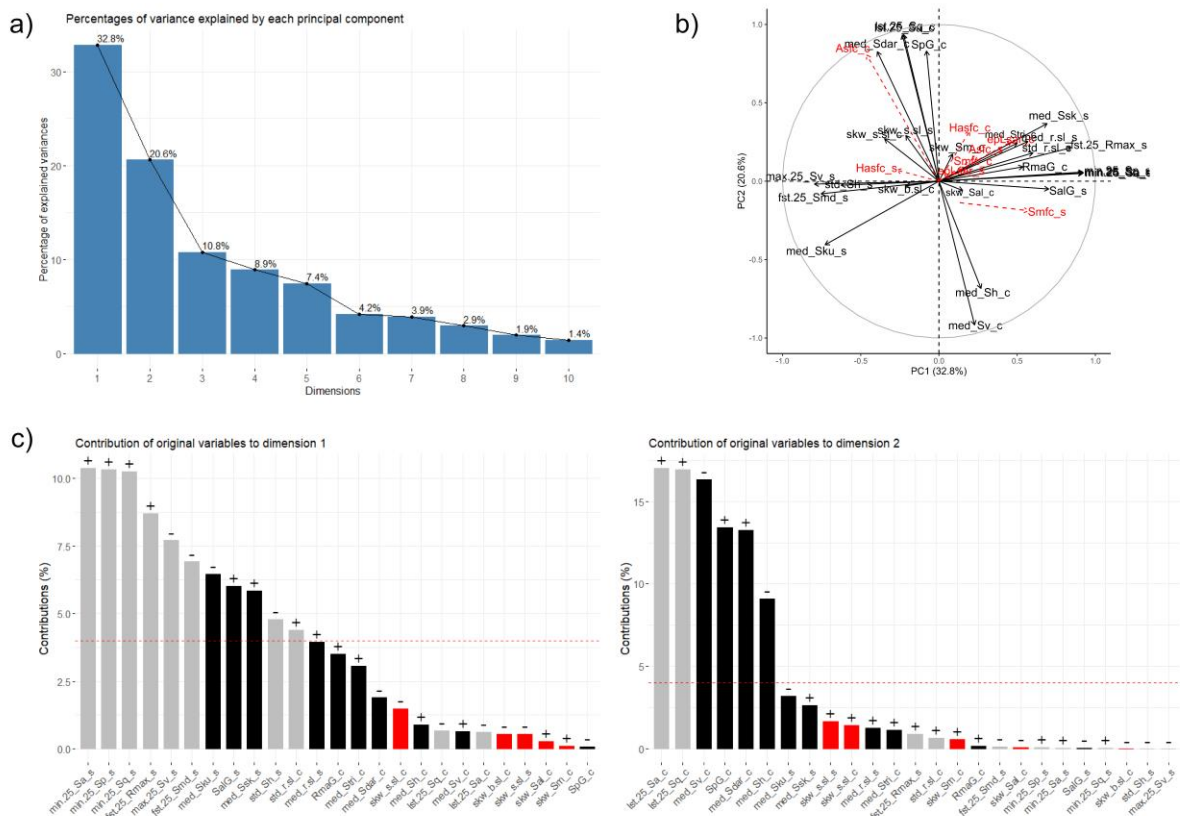
1170

1171

1172 **Table S10.** The most discriminative variables per parameter are selected from the whole set of variables  
 1173 showing at least one significant difference among the four lots on upper first molar facets (crushing and  
 1174 shearing).

Facet	Variable	Parameter	Type	Statistic	Statistic category
Crushing	med_Stri	Stri	Spatial	median	central
	skw_Sal	Sal	Spatial	skewness	distribution
	skw_b.sl	b.sl	Spatial	skewness	distribution
	skw_s.sl	s.sl	Spatial	skewness	distribution
	med_Sh	Sh	Topological	median	central
	med_Sdar	Sdar	Height	median	central
	RmaG	Rmax	Spatial	global	global
	std_r.sl	r.sl	Spatial	standard deviation	dispersion
	SpG	Sp	Height	global	global
	med_Sv	Sv	Height	median	central
	lst.25_Sq	Sq	Height	lst.25	dispersion
	lst.25_Sa	Sa	Height	lst.25	dispersion
	skw_Sm	Sm	Height	skewness	distribution
Shearing	min.25_Sp	Sp	Height	min.25	dispersion
	min.25_Sq	Sq	Height	min.25	dispersion
	med_Sku	Sku	Height	median	central
	min.25_Sa	Sa	Height	min.25	dispersion
	max.25_Sv	Sv	Height	max.25	dispersion
	fst.25_Rmax	Rmax	Spatial	fst.25	dispersion
	med_Ssk	Ssk	Height	median	central
	SalG	Sal	Spatial	global	global
	skw_s.sl	s.sl	Spatial	skewness	distribution
	med_r.sl	r.sl	Spatial	median	central
	fst.25_Smd	Smd	Height	fst.25	dispersion
	std_Sh	Sh	Topological	standard deviation	dispersion

1175



1176

1177 **Figure S3.** Principal Component Analysis based on the 25 most discriminative variables issued from  
 1178 both crushing (phase II) and shearing (phase I) facets on upper first molars. a) Percentage of variance  
 1179 explained by each principal component. b) Correlation circle between PC1 and PC2 with SSFA-  
 1180 parameters as supplementary variables (red dotted arrows). c) Contribution of each variable to PC1  
 1181 (left) and PC2 (right) in percentage and direction (positive: +, negative: -). Suffixes “\_c” and “\_s”  
 1182 refer to crushing and shearing facets, respectively. Black columns: central/global statistic, gray:  
 1183 dispersion statistics, red: distribution statistics. Dotted red line: expected average value if the  
 1184 contributions were uniform; any variable below this line could be considered negligible in contributing  
 1185 to the dimension.

1185

1186 **Table S11.** Analysis of variances on PC coordinates from PCA on upper first molars and combined HSD  
 1187 (above diagonal) and LSD (below diagonal) post hoc tests. Only p-values below a 10 % level of  
 1188 significance are given for post hoc tests.

		Df	SS	MS	F	p
PC1	Effect	3	103.3	34.44	6.406	0.0023
	Residuals	25	134.4	5.38		
PC2	Effect	3	19.73	6.577	3.299	0.0368
	Residuals	25	49.84	1.994		
PC3	Effect	3	0.782	0.2607	0.69	0.567
	Residuals	25	9.449	0.3779		
PC4	Effect	3	0.6138	0.2046	1.86	0.162
	Residuals	25	2.7507	0.1100		
PC5	Effect	3	17.92	5.973	1.01	0.405
	Residuals	25	147.84	5.914		

1189

1190

1191

		HSD			
LSD		Hazelnut	Barley	Control	Corn
PC1	Hazelnut				0.0022
	Barley				0.0133
	Control				0.0246
	Corn	0.0004	0.0027	0.0051	
PC2	Hazelnut		0.0215		
	Barley	0.0044			
	Control		0.0389		
	Corn		0.0982		

1192

1193 **Table S12.** Analysis of variances on PC coordinates from PCA on crushing facets of upper first molars  
 1194 and combined HSD (above diagonal) and LSD (below diagonal) post hoc tests. Only p-values below a  
 1195 10 % level of significance are given for post hoc tests.

		Df	SS	MS	F	p
PC1	Effect	3	4.829	1.6096	4.15	0.0162
	Residuals	25	9.696	0.3878		
PC2	Effect	3	0.9605	0.3202	4.13	0.0165
	Residuals	25	1.9379	0.0775		

1196

		HSD			
LSD		Hazelnut	Barley	Control	Corn
PC1	Hazelnut		0.0160		0.0570
	Barley	0.0032			
	Control	0.0639	0.0714		
	Corn	0.0126			
PC2	Hazelnut				0.0771
	Barley				0.0171
	Control		0.0377		
	Corn	0.0175	0.0035		

1197

1198 **Table S13.** Analysis of variances on PC coordinates from PCA on shearing facets of upper first molars  
 1199 and combined HSD (above diagonal) and LSD (below diagonal) post hoc tests. Only p-values below a  
 1200 10 % level of significance are given for post hoc tests.

		Df	SS	MS	F	p
PC1	Effect	3	219.2	73.05	4.851	0.0102
	Residuals	21	316.2	15.06		
PC2	Effect	3	6.248	2.083	1.39	0.274
	Residuals	21	31.478	1.499		

1201

		HSD			
LSD		Hazelnut	Barley	Control	Corn
PC1	Hazelnut				0.0129
	Barley				0.0231
	Control				0.0500
	Corn	0.0026	0.0048	0.0110	

1202

1203

1204 **Table S14.** Variables per parameter recognized as discriminative among the four lots on upper fourth  
 1205 deciduous premolar facets (crushing and shearing) using the routine shown in Francisco et al. (2018a,  
 1206 2018b).

Phase II (crushing) upper premolar facets			Phase I (shearing) upper premolar facets		
fst.25_Sh	max.25_Rmax	min.25_Sm	lst.25_Smd	skw_Sh	skw_Sal
fst.25_r.sl	max.25_Sa	min.25_Smd			
fst.25_Sa	max.25_Sdar	min.25_Sp			
fst.25_Sdar	max.25_Sm	min.25_Sq			
fst.25_Sm	max.25_Smd	min.25_Sv			
fst.25_Sp	max.25_Sp	r.sG			
fst.25_Sq	max.25_Sq	SaG			
fst.25_Sv	max.25_Stri	SdaG			
ShG	max.25_Sv	skw_b.sl			
kurt_b.sl	mea_Sh	skw_Rmax			
kurt_Rmax	mea_r.sl	skw_Sdar			
kurt_Sa	mea_Rmax	skw_Sku			
kurt_Sdar	mea_Sa	skw_Sp			
kurt_Sku	mea_Sdar	skw_Sq			
kurt_Smd	mea_Smd	skw_Stri			
kurt_Sp	mea_Sp	skw_Sv			
kurt_Sq	mea_Sq	SqG			
kurt_Ssk	mea_Stri	std_Sh			
kurt_Stri	mea_Sv	std_r.sl			
lst.25_Sh	med_Sh	std_Rmax			
lst.25_r.sl	med_r.sl	std_Sa			
lst.25_Rmax	med_Sa	std_Sal			
lst.25_Sa	med_Sdar	std_Sdar			
lst.25_Sdar	med_Sp	std_Sm			
lst.25_Sm	med_Sq	std_Smd			
lst.25_Smd	med_Sv	std_Sp			
lst.25_Sp	min.25_Sh	std_Sq			
lst.25_Sq	min.25_r.sl	std_Stri			
lst.25_Stri	min.25_Sa	std_Sv			
lst.25_Sv	min.25_Sal	SvG			
max.25_Sh	min.25_Sdar				
max.25_r.sl					

1207

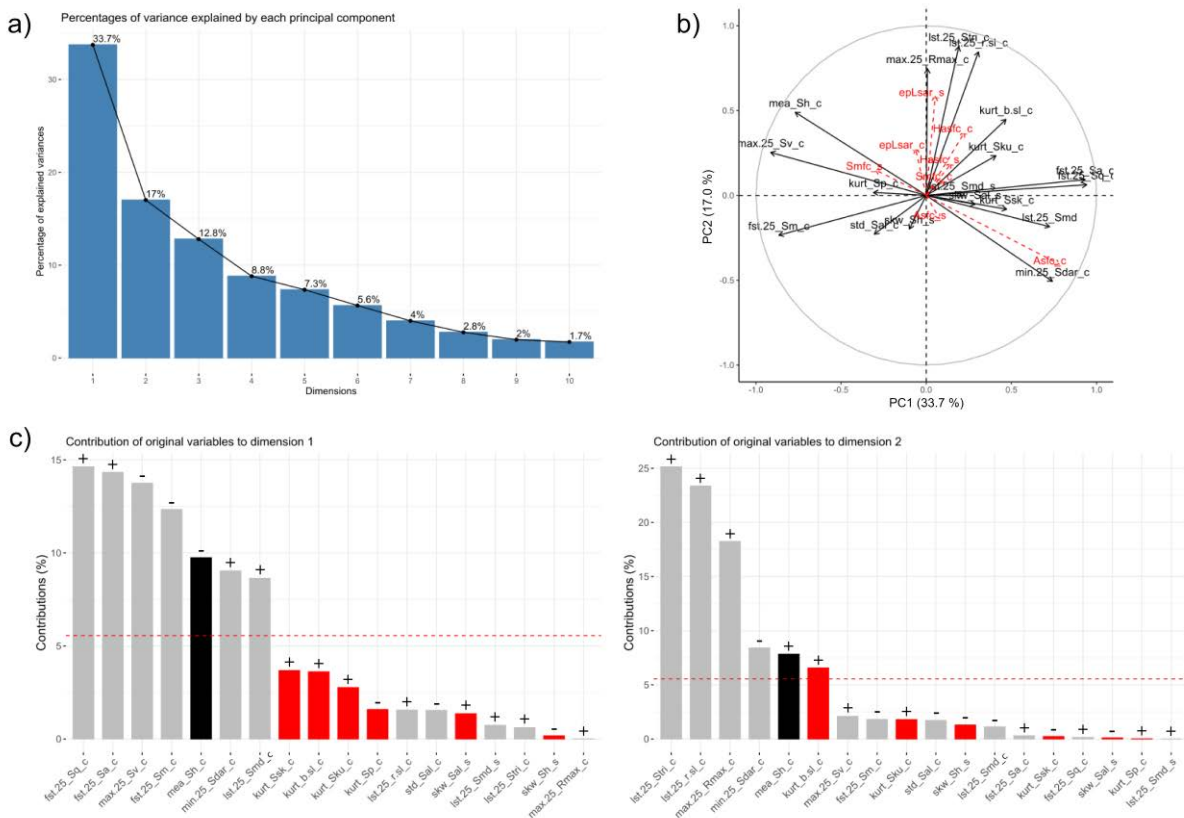
1208

1209 **Table S15.** The most discriminative variables per parameter are selected from the whole set of variables  
 1210 showing at least one significant difference among the four lots on fourth upper deciduous premolar  
 1211 facets (crushing and shearing).

Facet	Variable	Parameter	Type	Statistic	Statistic category
Crushing	min.25_Sdar	Sdar	Height	min.25	dispersion
	mea_Sh	Sh	Topological	mean	central
	kurt_Sp	Sp	Height	kurtosis	distribution
	max.25_Sv	Sv	Height	max.25	dispersion
	lst.25_r.sl	r.sl	Spatial	lst.25	dispersion
	fst.25_Sq	Sq	Height	fst.25	dispersion
	fst.25_Sa	Sa	Height	fst.25	dispersion
	std_Sal	Sal	Spatial	standard deviation	dispersion
	lst.25_Stri	Stri	Spatial	lst.25	dispersion
	fst.25_Sm	Sm	Height	fst.25	dispersion
	kurt_Sku	Sku	Height	kurtosis	distribution
	lst.25_Smd	Smd	Height	lst.25	dispersion
	max.25_Rmax	Rmax	Spatial	max.25	dispersion
	kurt_b.sl	b.sl	Spatial	kurtosis	distribution
kurt_Ssk	Ssk	Height	kurtosis	distribution	
Shearing	skw_Sal	Sal	Spatial	skewness	distribution
	lst.25_Smd	Smd	Height	lst.25	dispersion
	skw_Sh	Sh	Topological	skewness	distribution

1212

1213



1214



1215 **Figure S4.** Principal Component Analysis based on the 19 most discriminative variables issued from  
 1216 both crushing (phase II) and shearing (phase I) facets on upper fourth deciduous premolars. a)  
 1217 Percentage of variance explained by each principal component. b) Correlation circle between PC1 and  
 1218 PC2 with SSFA-parameters as supplementary variables (red dotted arrows). c) Contribution of each  
 1219 variable to PC1 (left) and PC2 (right) in percentage and direction (positive: +, negative: -). Suffixes “\_c”  
 1220 and “\_s” refer to crushing and shearing facets, respectively. Black columns: central/global statistic, gray:  
 1221 dispersion statistics, red: distribution statistics. Dotted red line: expected average value if the  
 1222 contributions were uniform; any variable below this line could be considered negligible in contributing to  
 1223 the dimension.

1224

1225 **Table S16.** Analysis of variances on PC coordinates from PCA on upper fourth deciduous premolars  
 1226 and combined HSD (above diagonal) and LSD (below diagonal) post hoc tests. A Kruskal-Wallis is run  
 1227 on PC3 followed with a Dunn’s test. Only p-values below a 10 % level of significance are given for post  
 1228 hoc tests.

ANOVA		Df	SS	MS	F	p
PC1	Effect	3	16.92	5.640	8.247	0.0006
	Residuals	24	16.41	0.684		
PC4	Effect	3	1.662	0.5539	0.498	0.687
	Residuals	24	26.708	1.1128		
PC5	Effect	3	2.862	0.9542	1.142	0.352
	Residuals	24	20.052	0.8355		

1229

Kruskal-Wallis	Df	$\chi^2$	p
PC2	3	9.8919	0.0195
PC3	3	13.903	0.0030

1230

LSD		Hazelnut	Barley	Control	Corn
PC1	Hazelnut				
	Barley	0.0267		0.0012	0.0010
	Control	0.0840	0.0002		
	Corn	0.0432	0.0002		

1231

Dunn		Hazelnut	Barley	Control	Corn
PC2	Hazelnut				
	Barley	0.0018			
	Control	0.0055			
	Corn	0.0209			
PC3	Hazelnut				
	Barley	0.0017			
	Control		0.0130		
	Corn	0.0014		0.0119	

1232

1233 **Table S17.** Analysis of variances on PC coordinates from PCA on crushing facets of upper fourth  
 1234 deciduous premolars and combined HSD (above diagonal) and LSD (below diagonal) post hoc tests.  
 1235 Only p-values below a 10 % level of significance are given for post hoc tests.

		Df	SS	MS	F	p
PC1	Effect	3	21.25	7.082	7.539	0.0010

	Residuals	24	22.55	0.939		
PC2	Effect	3	3.836	1.2785	3.999	0.0192
	Residuals	24	7.673	0.3197		
PC3	Effect	3	4.48	1.4935	2.641	0.0724
	Residuals	24	13.57	0.5654		

1236

LSD		HSD			
		Hazelnut	Barley	Control	Corn
PC1	Hazelnut				
	Barley	0.0476		0.0023	0.0017
	Control	0.0785	0.0004		
	Corn	0.0358	0.0003		
PC2	Hazelnut		0.0302	0.0691	0.0373
	Barley	0.0064			
	Control	0.0156			
	Corn	0.0080			
PC3	Hazelnut				
	Barley				
	Control				0.0875
	Corn	0.0592		0.0202	

1237

1238 **Table S18.** Analysis of variances on PC coordinates from PCA on shearing facets of upper fourth  
 1239 deciduous premolars and combined HSD (above diagonal) and LSD (below diagonal) post hoc tests.  
 1240 Only p-values below a 10 % level of significance are given for post hoc tests.

		Df	SS	MS	F	p
PC1	Effect	3	5.242	1.7473	2.481	0.0843
	Residuals	25	17.607	0.7043		
PC3	Effect	3	1.437	0.4789	2.202	0.1130
	Residuals	25	5.438	0.2175		

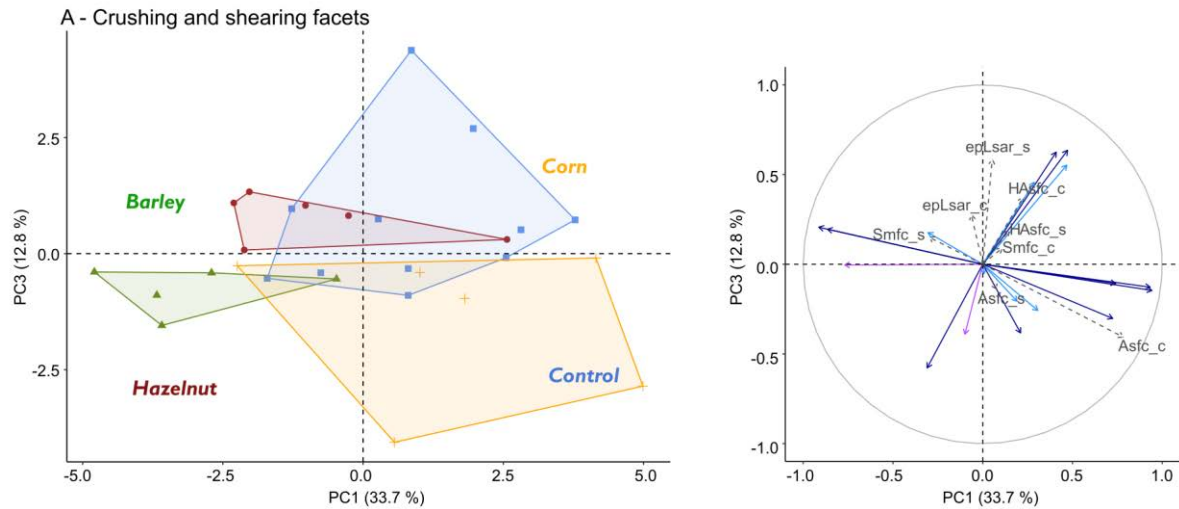
1241

1242

LSD		HSD			
		Hazelnut	Barley	Control	Corn
PC1	Hazelnut				0.0847
	Barley				
	Control				
	Corn	0.0194		0.0346	
PC3	Hazelnut				
	Barley	0.0798		0.0852	
	Control		0.0195		
	Corn		0.0563		

1243

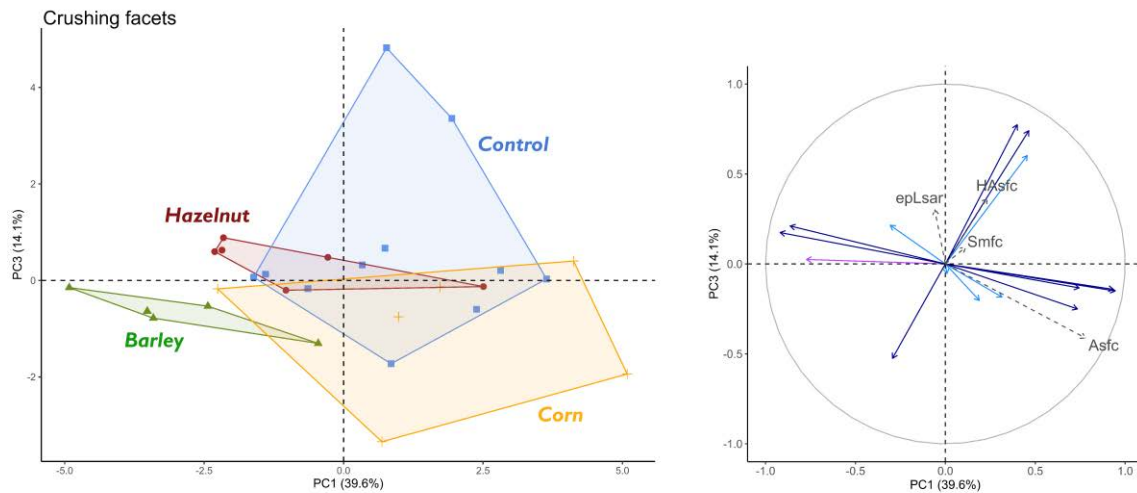
1244



1245  
 1246 **Figure S5.** Distribution of individuals (left) and correlation circle (right) along PC1 and PC3 of the four  
 1247 dietary groups on both crushing and shearing facets of upper deciduous premolars. Dietary groups: ●:  
 1248 100 % base flours +10 hazelnuts in shell a day, ▲: 70 % base flours + 30 % barley seeds, +: 60 % base  
 1249 flours + 20 % corn flour + 20 % corn kernels, ■: 100 % base flours. Active variables (filled arrows): height  
 1250 (dark blue), spatial (light blue), and topological (purple) parameters. SSFA parameters added as  
 1251 supplementary variables (gray dotted arrows). Suffixes “\_c”: crushing facets, “\_s”: shearing facets.

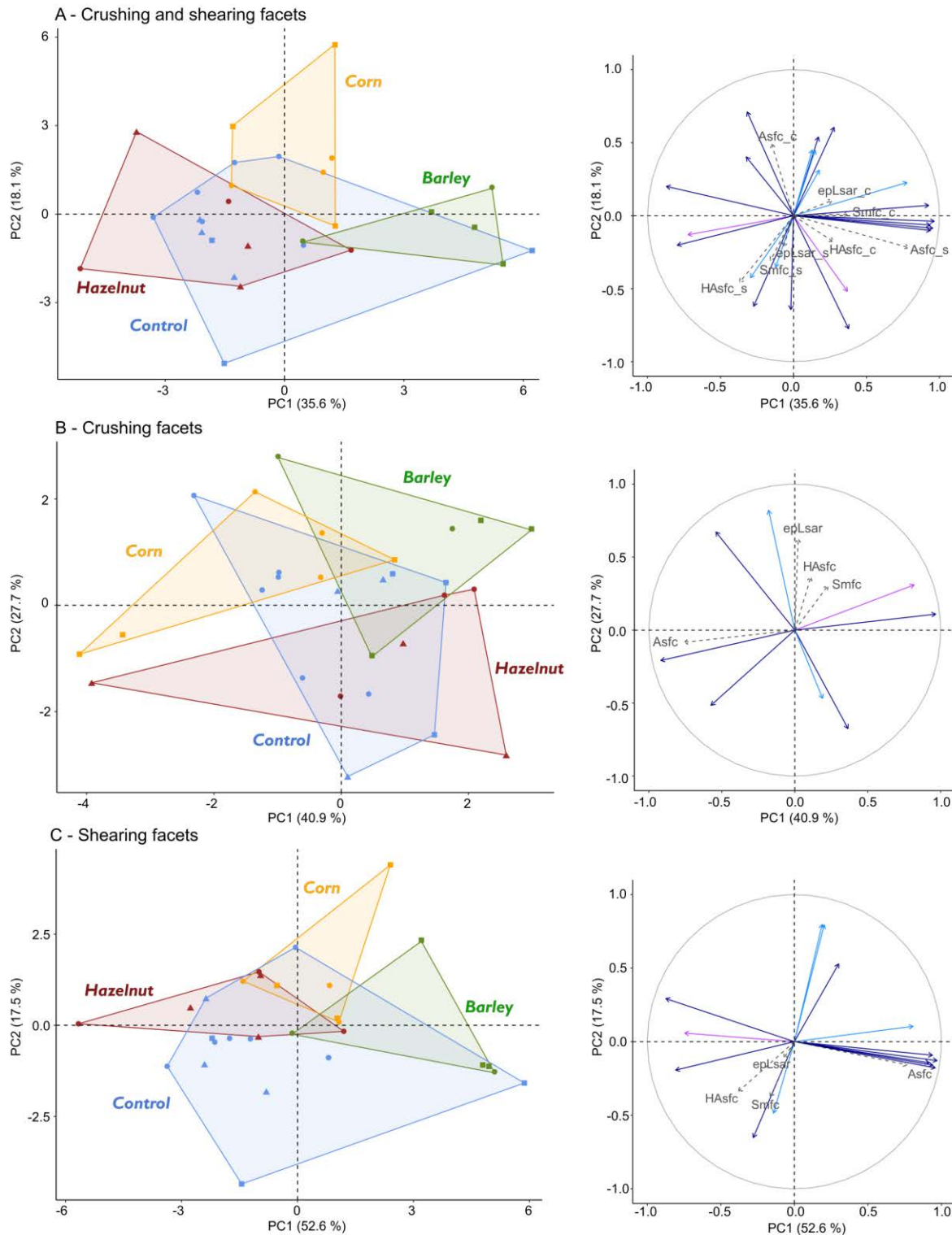
1252

1253



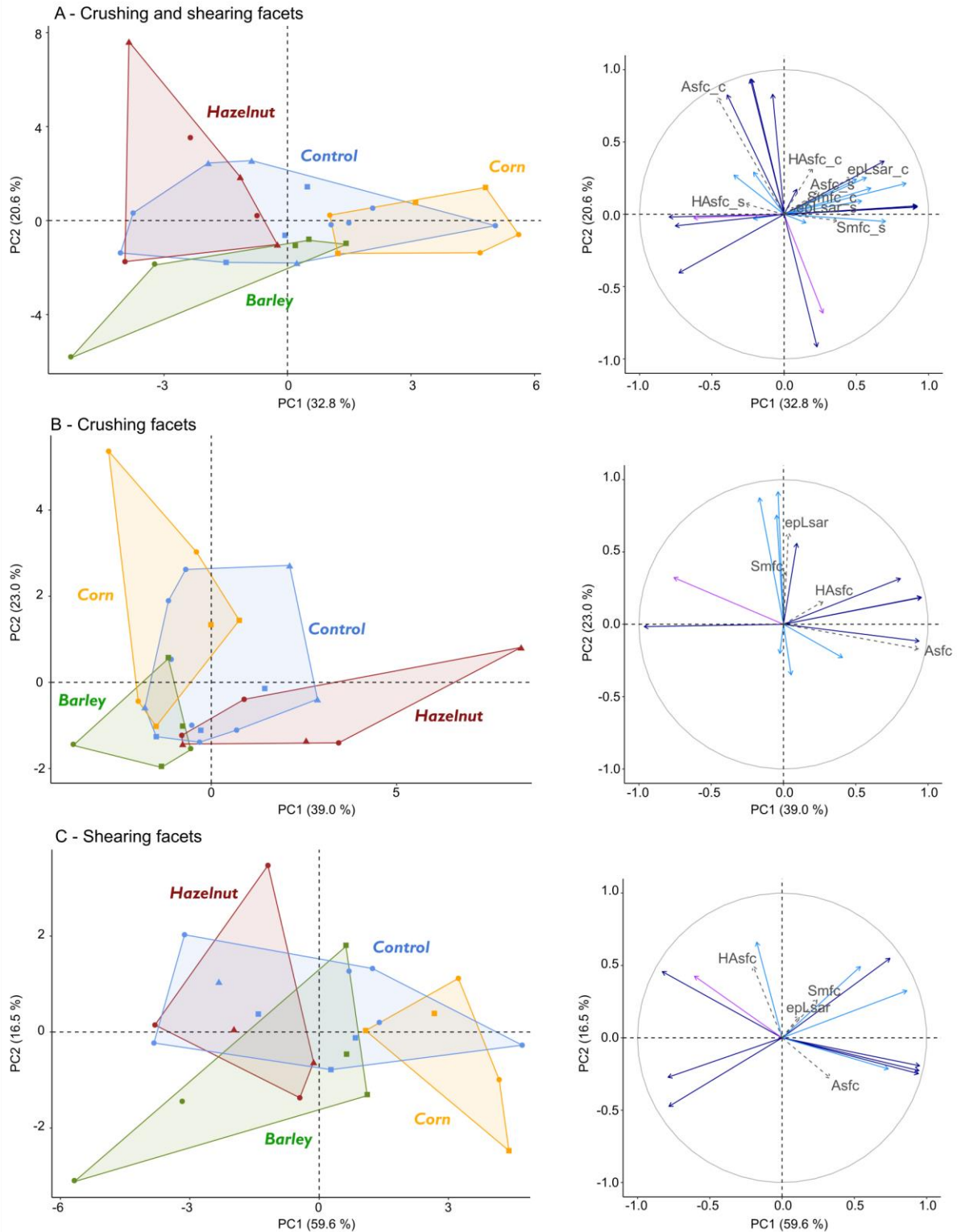
1254  
 1255 **Figure S6.** Distribution of individuals (left) and correlation circle (right) along PC1 and PC3 of the four  
 1256 dietary groups on crushing facets of upper deciduous premolars. Dietary groups: ●: 100 % base flours  
 1257 +10 hazelnuts in shell a day, ▲: 70 % base flours + 30 % barley seeds, +: 60 % base flours + 20 % corn  
 1258 flour + 20 % corn kernels, ■: 100 % base flours. Active variables (filled arrows): height (dark blue), spatial  
 1259 (light blue) and topological (purple) parameters. SSFA parameters added as supplementary variables  
 1260 (gray dotted arrows).

1261



1262

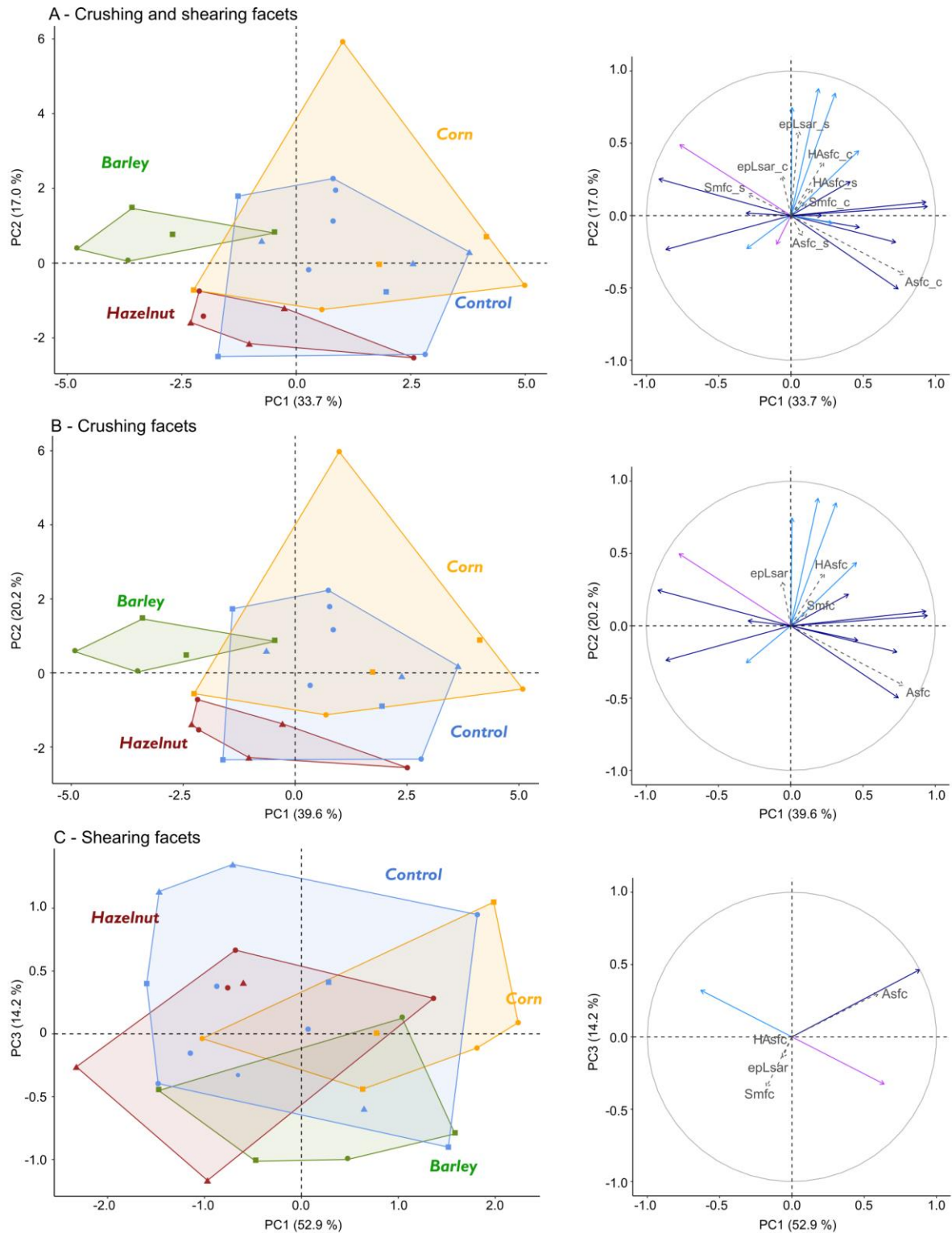
1263 Figure **S7**. Distributions of individuals (left) and correlation circle (right) along PC1 and PC2 of the four  
 1264 dietary groups on both crushing and shearing lower first molar facets (A), on crushing facets alone (B),  
 1265 and on shearing facets alone (C). Dietary groups: 100 % base flours + 10 hazelnuts in shell a day (red),  
 1266 70 % base flours + 30 % barley seeds (green), 60 % base flours + 20 % corn flour + 20 % corn kernels  
 1267 (yellow), 100 % base flours (blue). Sexes: ●: females, ▲: uncastrated males, ■: castrated males. Active  
 1268 variables (filled arrows): height (dark blue), spatial (light blue), and topological (purple) parameters.  
 1269 SSFA-parameters added as supplementary variables (gray dotted arrows). Suffixes “\_c”: crushing  
 1270 facets, “\_s”: shearing facets.



1271

1272 Figure S8. Distributions of individuals (left) and correlation circle (right) along PC1 and PC2 of the four  
 1273 dietary groups on both crushing and shearing upper first molar facets (A), on crushing facets alone (B),  
 1274 and on shearing facets alone (C). Dietary groups: 100 % base flours + 10 hazelnuts in shell a day (red),  
 1275 70 % base flours + 30 % barley seeds (green), 60 % base flours + 20 % corn flour + 20 % corn kernels  
 1276 (yellow), 100 % base flours (blue). Sexes: ●: females, ▲: uncastrated males, ■: castrated males. Active  
 1277 variables (filled arrows): height (dark blue), spatial (light blue), and topological (purple) parameters.  
 1278 SSFA-parameters added as supplementary variables (gray dotted arrows). Suffixes “\_c”: crushing  
 1279 facets, “\_s”: shearing facets.





1280

1281 Figure **S9**. Distributions of individuals (left) and correlation circle (right) along PC1 and PC2 of the four  
 1282 dietary groups on both crushing and shearing upper fourth deciduous premolar facets (A), on crushing  
 1283 facets alone (B), and on shearing facets alone (C). Dietary groups: 100 % base flours + 10 hazelnuts in  
 1284 shell a day (red), 70 % base flours + 30 % barley seeds (green), 60 % base flours + 20 % corn flour +  
 1285 20 % corn kernels (yellow), 100 % base flours (blue). Sexes: ●: females, ▲: uncastrated males, ■:  
 1286 castrated males. Active variables (filled arrows): height (dark blue), spatial (light blue), and topological  
 1287 (purple) parameters. SSFA-parameters added as supplementary variables (gray dotted arrows).  
 1288 Suffixes “\_c”: crushing facets, “\_s”: shearing facets.

1289

1290

1291 **Appendix 1**

1292 Photosimulations and false color elevation maps of scanned shearing and crushing facets on first lower

1293 and upper molars and on upper fourth deciduous premolars of the four dietary groups: control, hazelnut,

1294 barley and corn.

1295

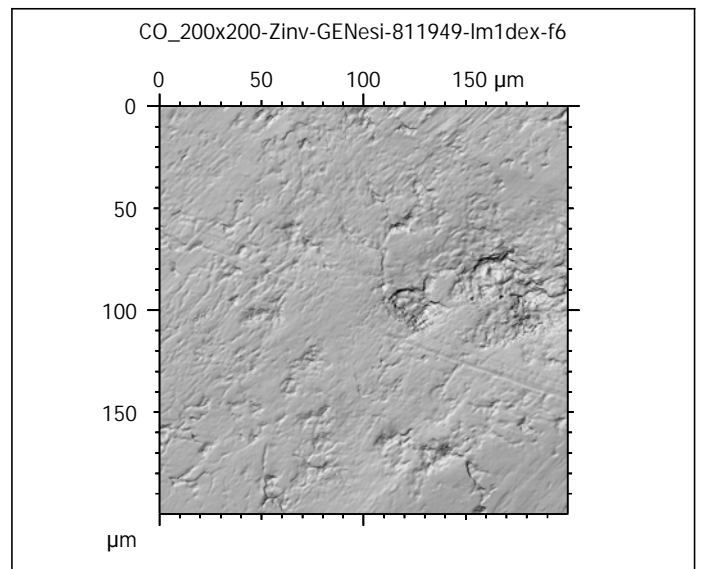
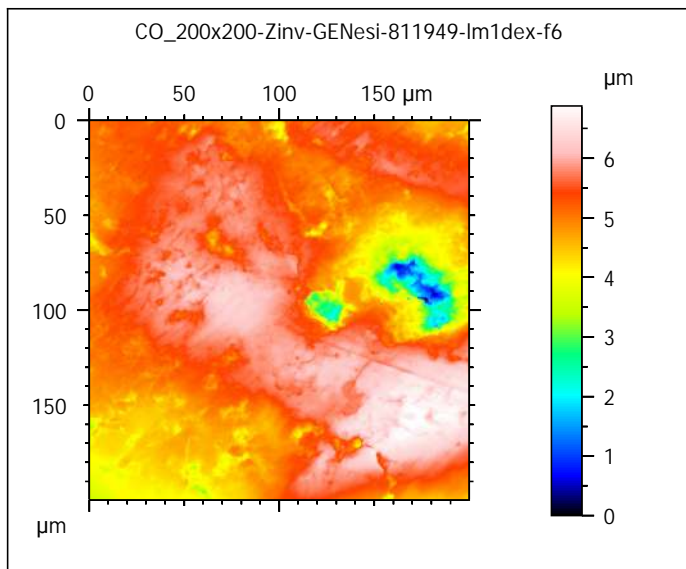
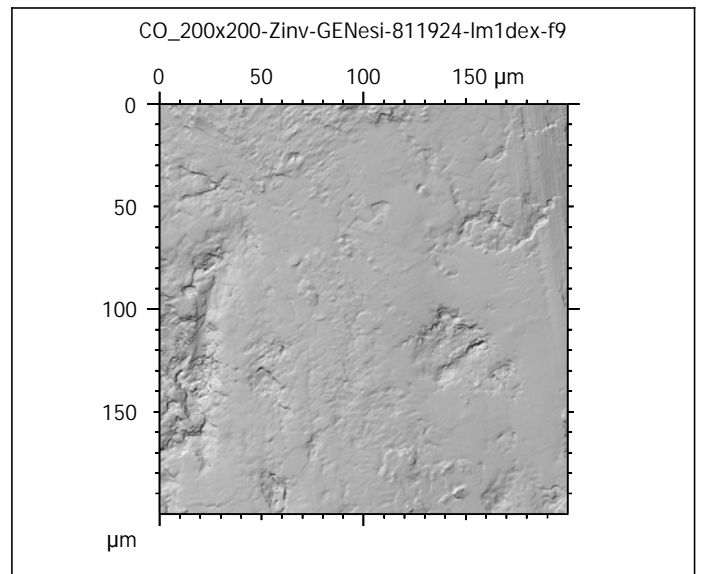
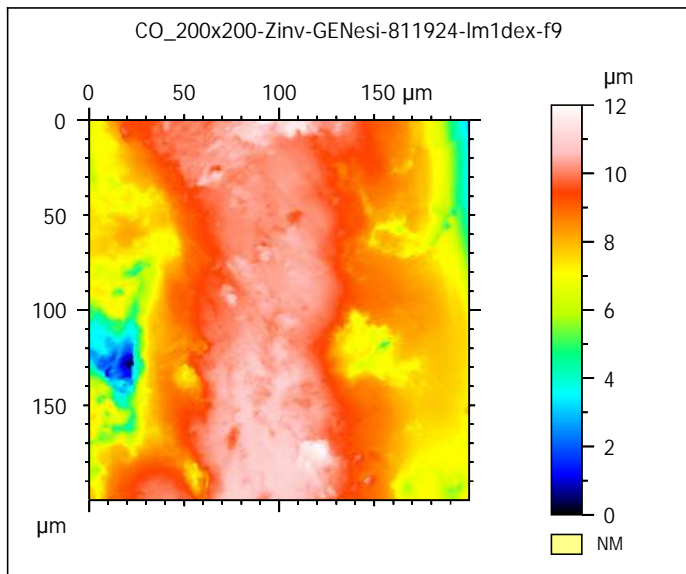
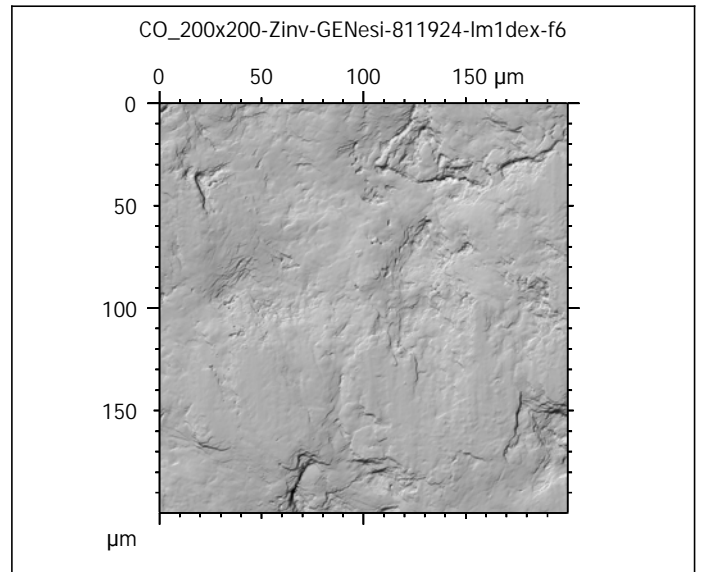
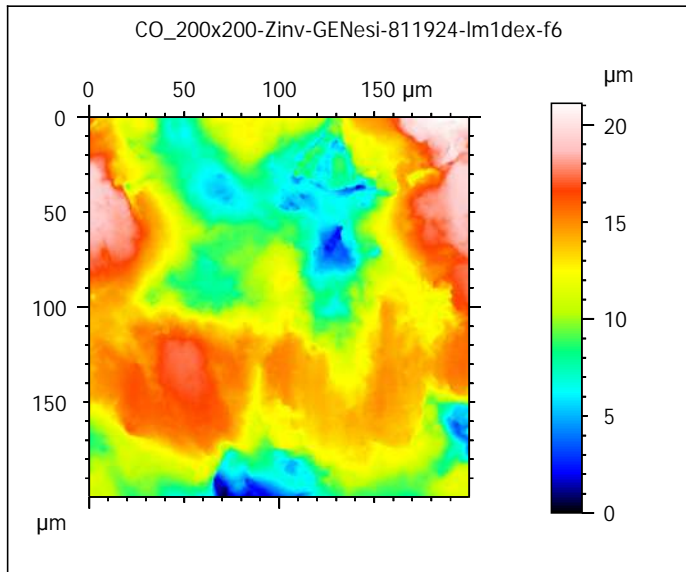
1296

Photosimulations and false color elevation maps of scanned shearing and crushing facets on molars and deciduous premolars of the **control group** (100% flours)

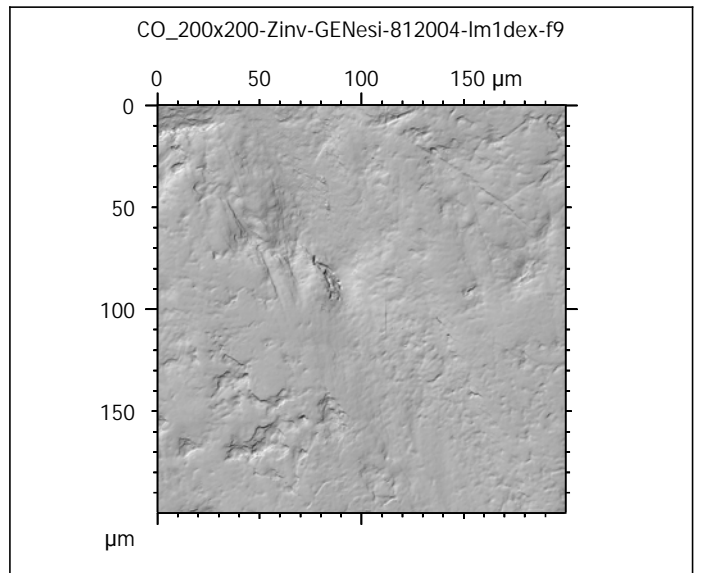
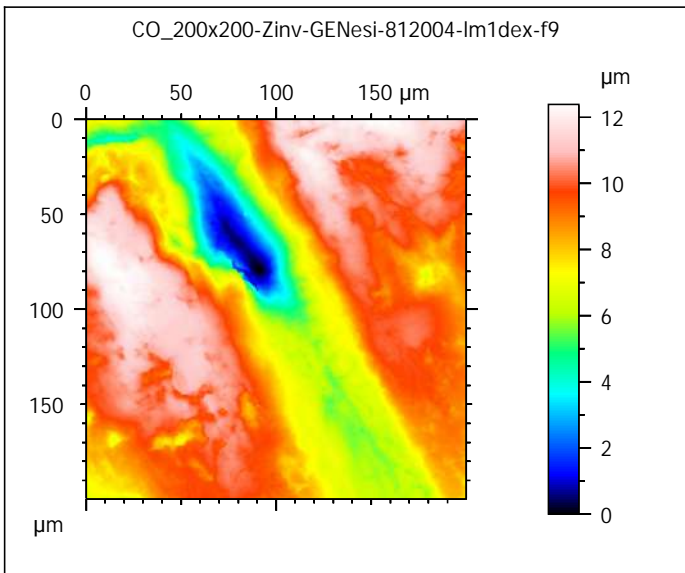
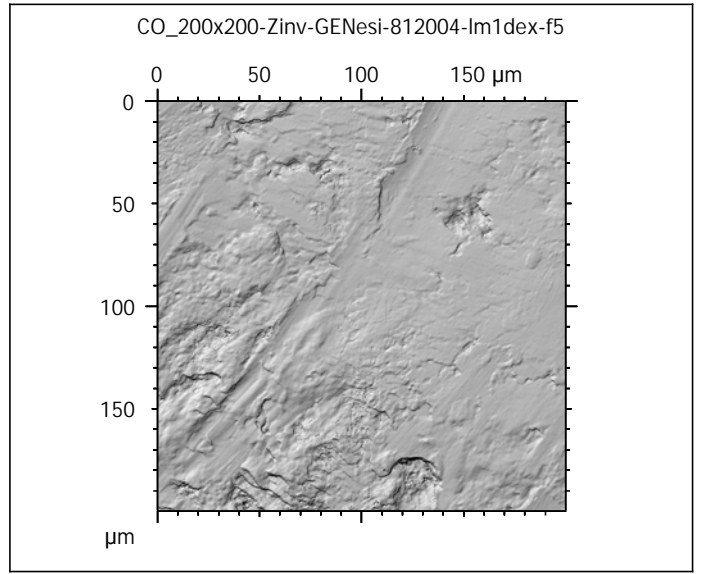
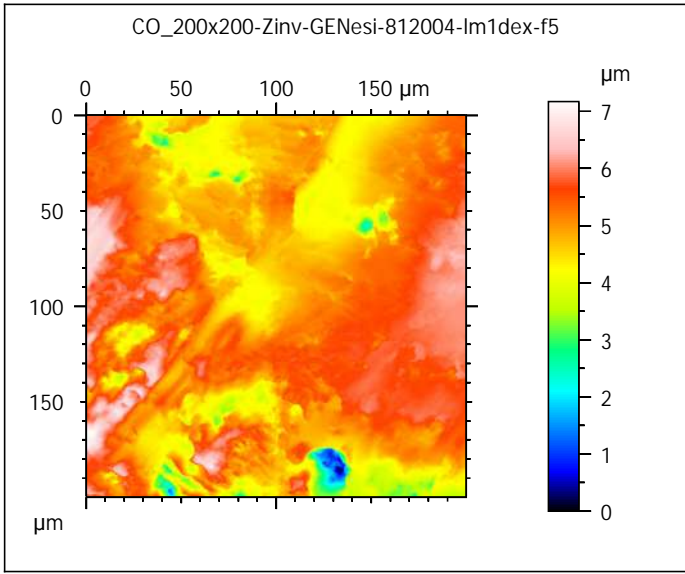
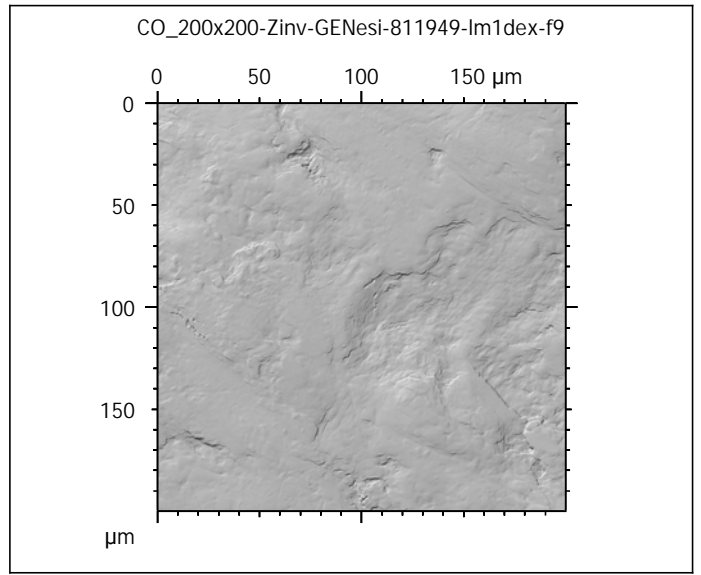
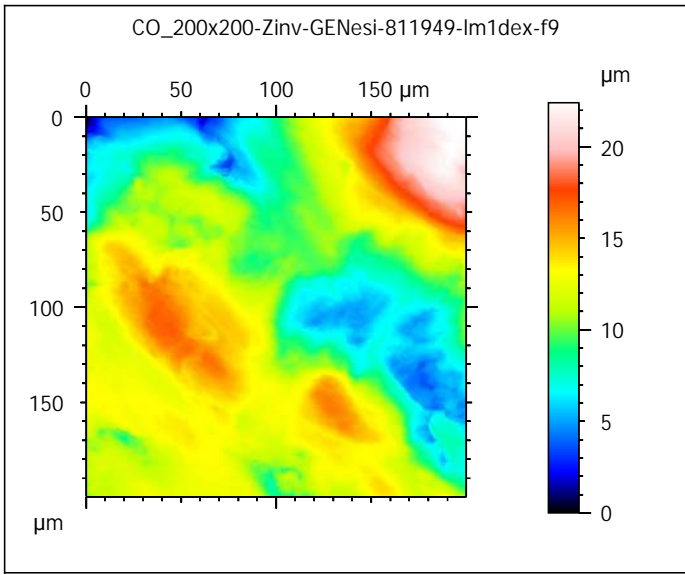
scanned at the PALEVOPRIM lab by M. Louail, University of Poitiers, France with "TRIDENT", white light confocal microscope Leica DCM8 - April 2020  
ALIHOM Project (Région Nouvelle Aquitaine, France), ANR Diet-Scratches

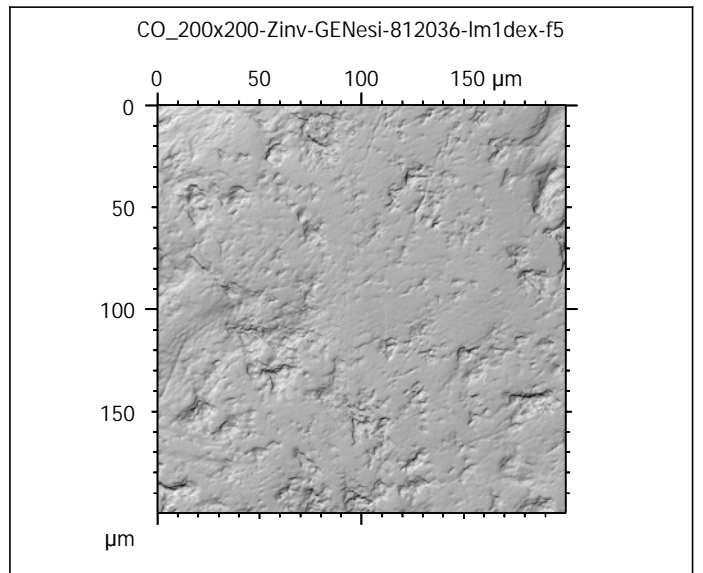
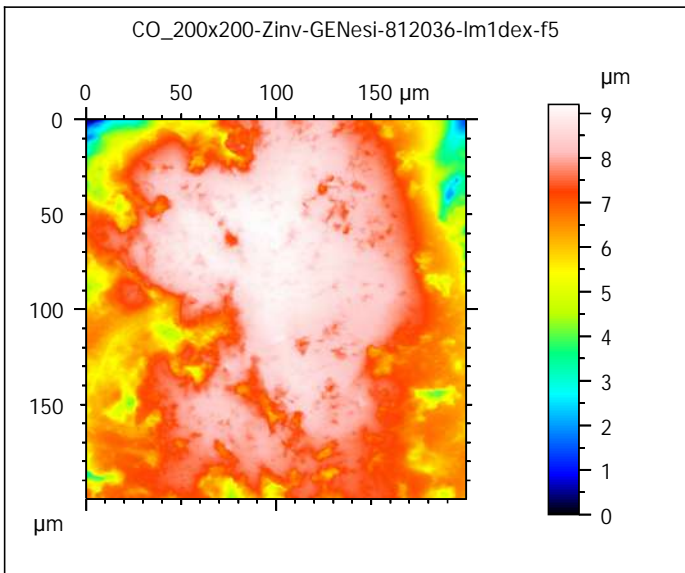
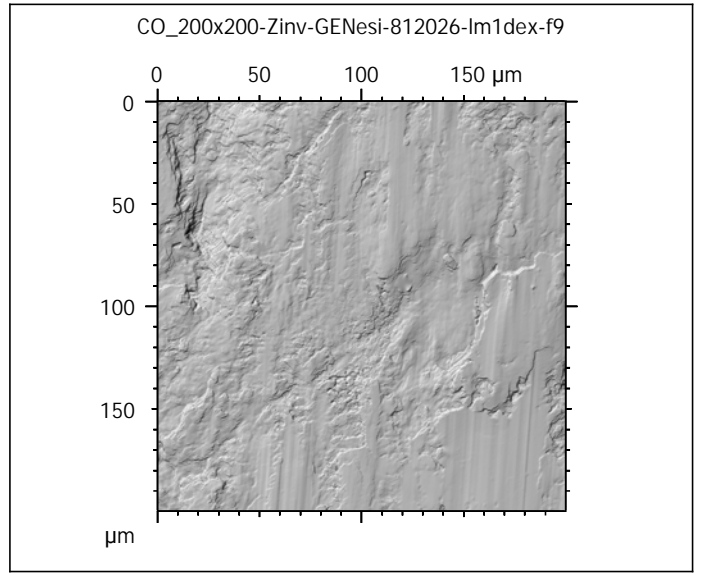
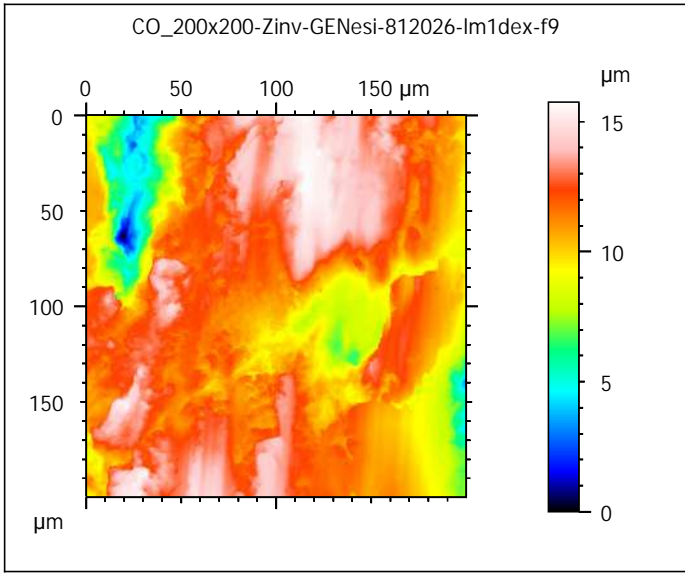
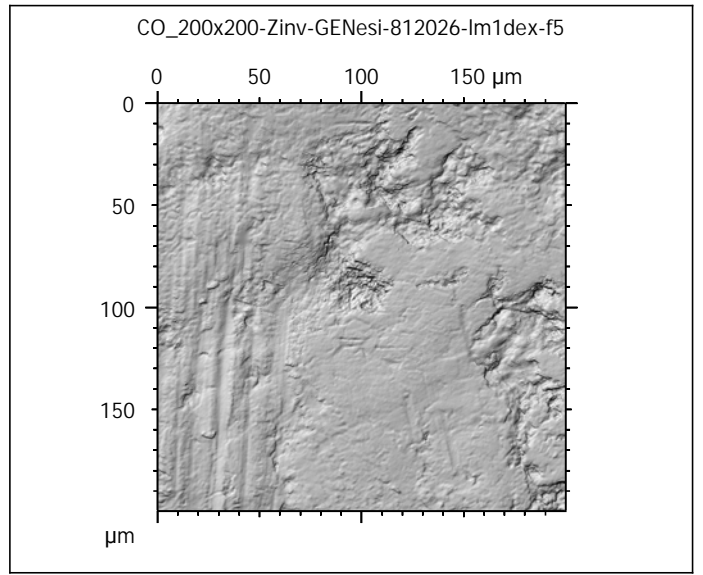
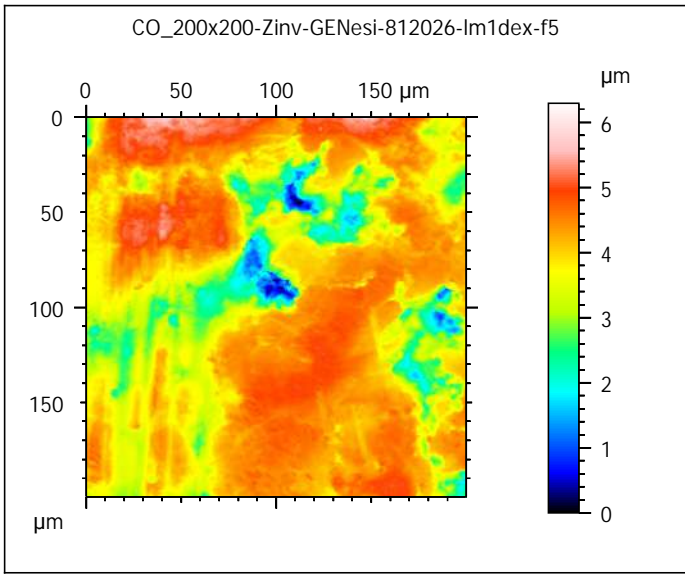
**DIET-SCRATCHES**

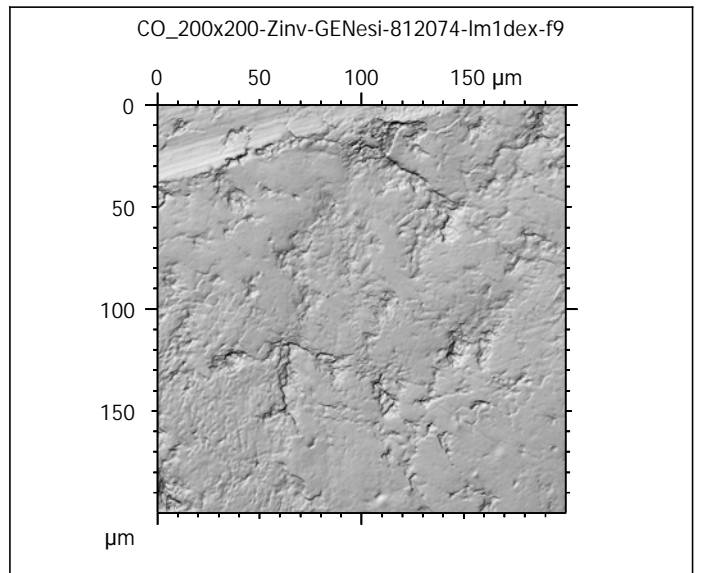
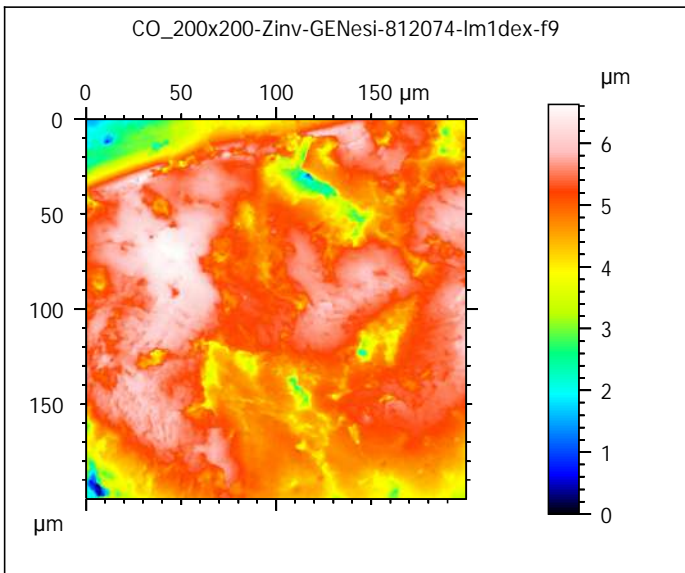
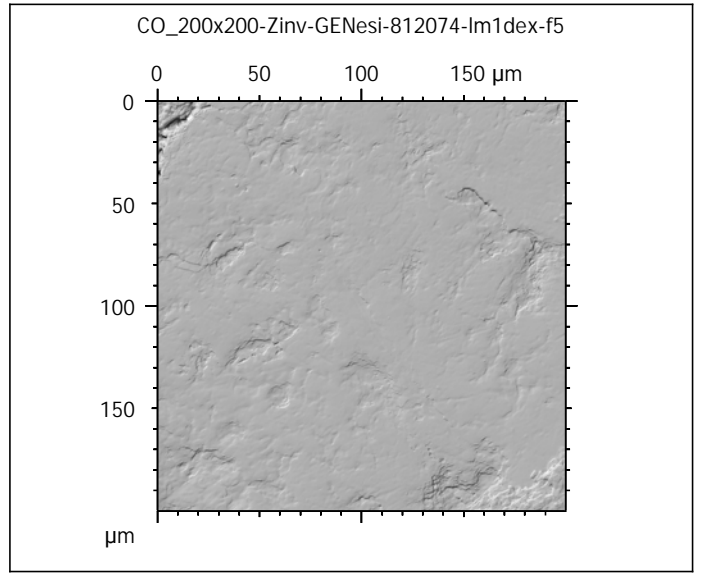
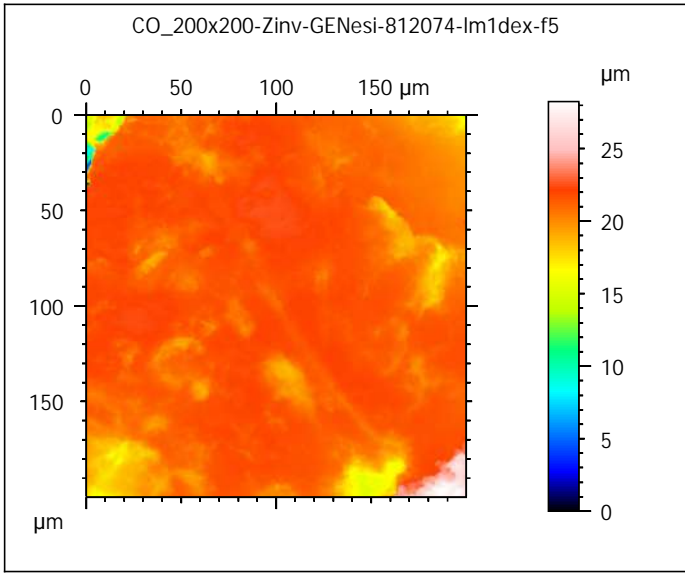
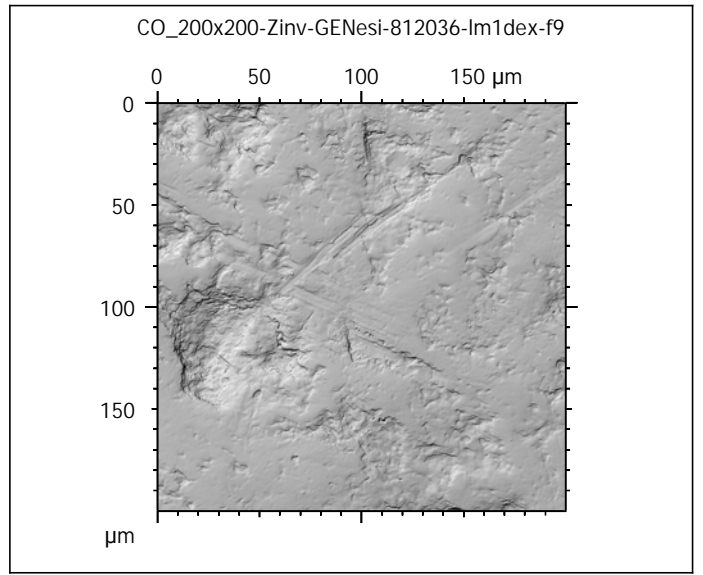
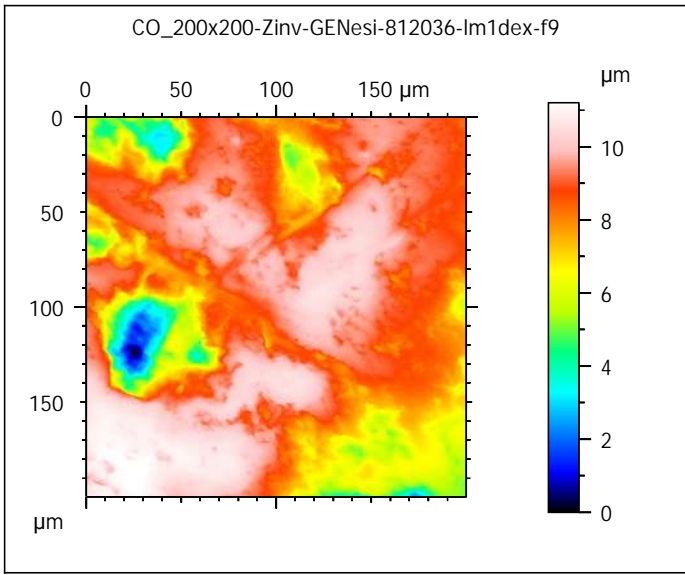
ANR-17-CE27-0002  
PIs: G. Merceron & S. Ferchaud



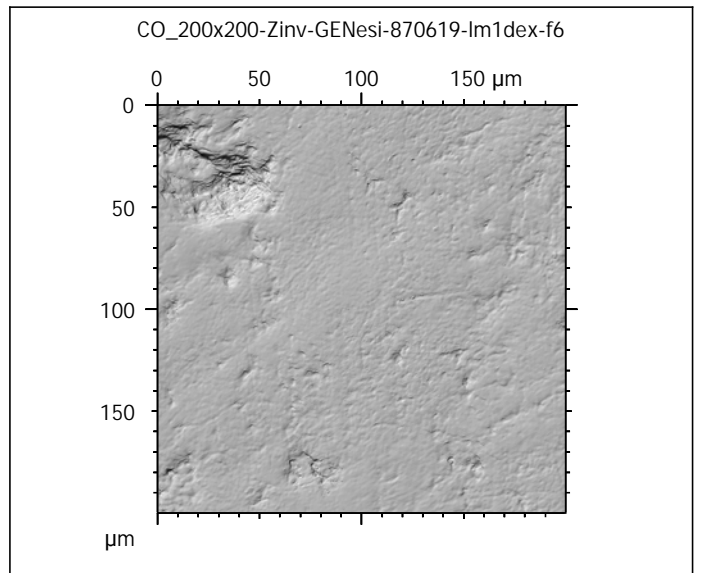
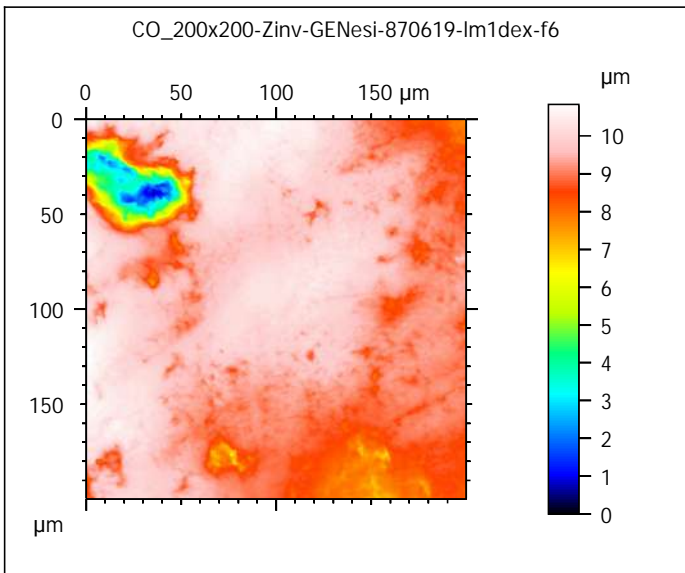
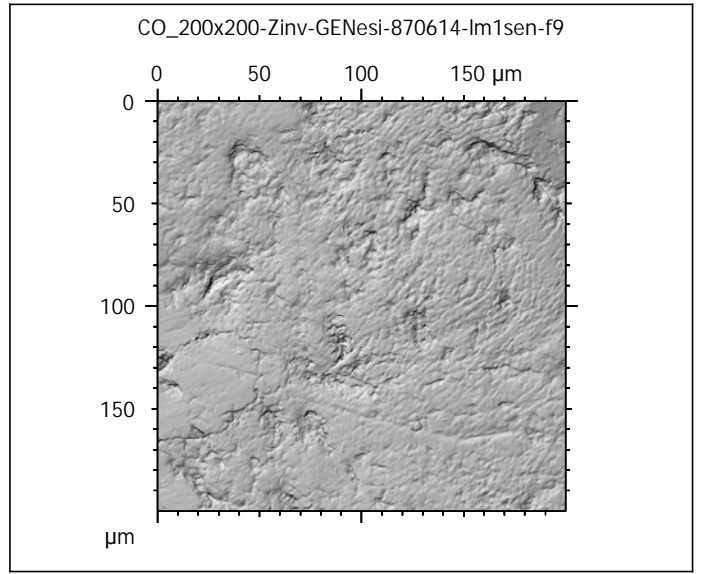
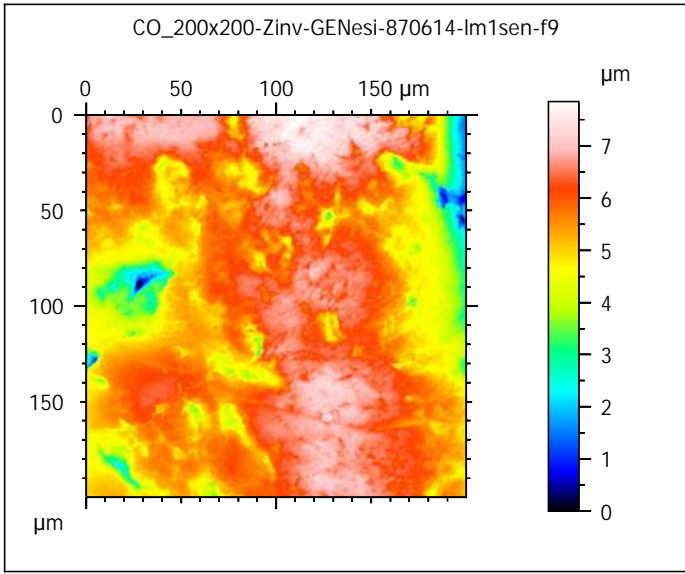
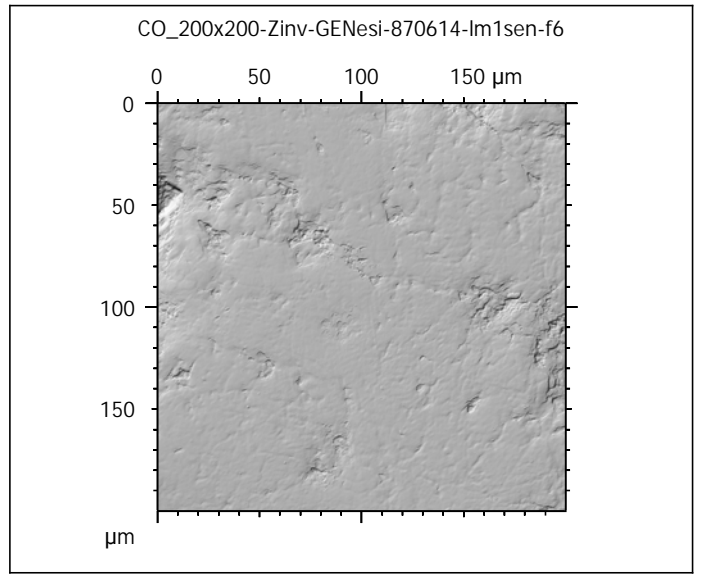
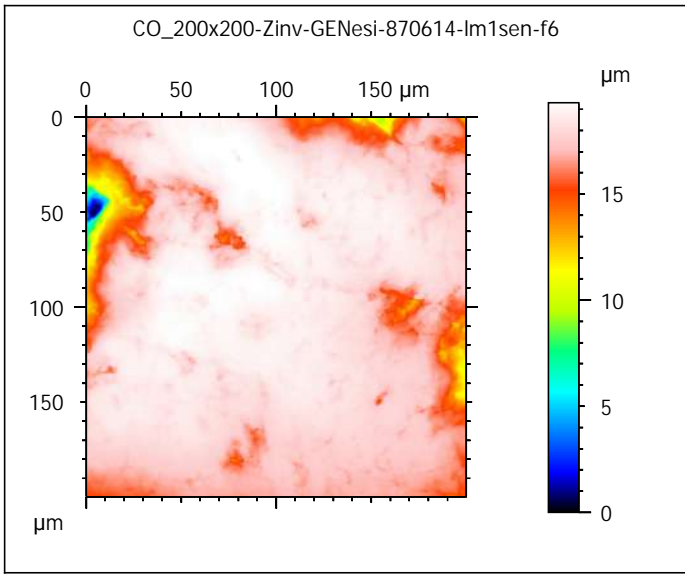


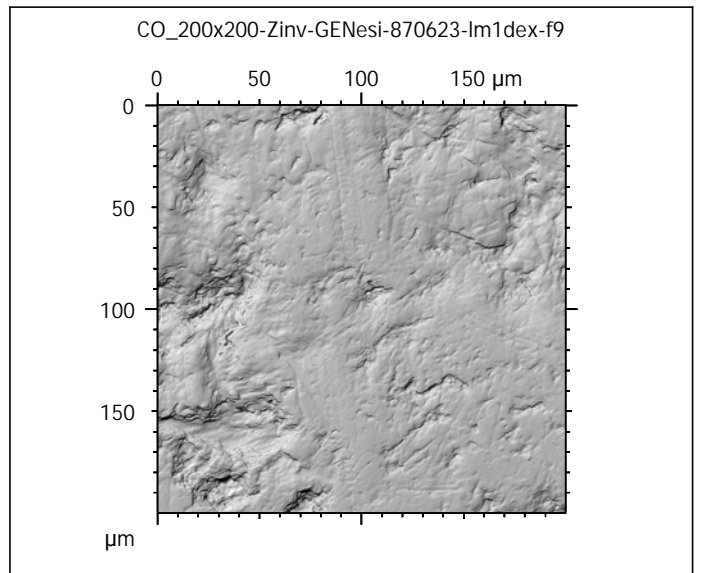
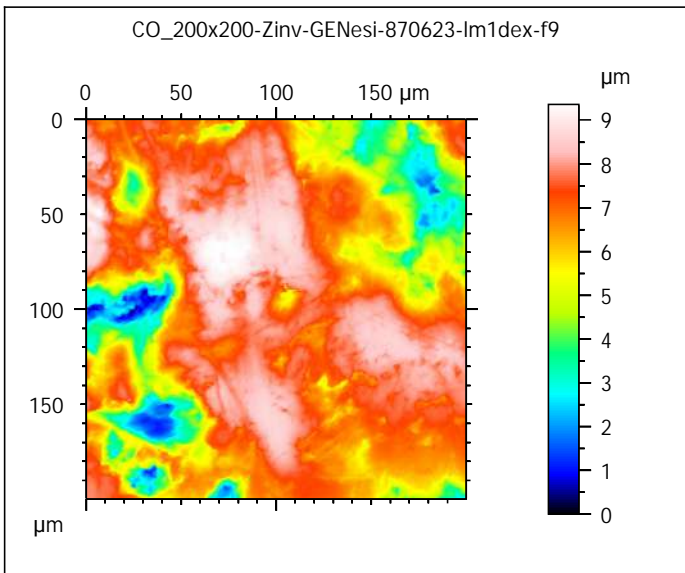
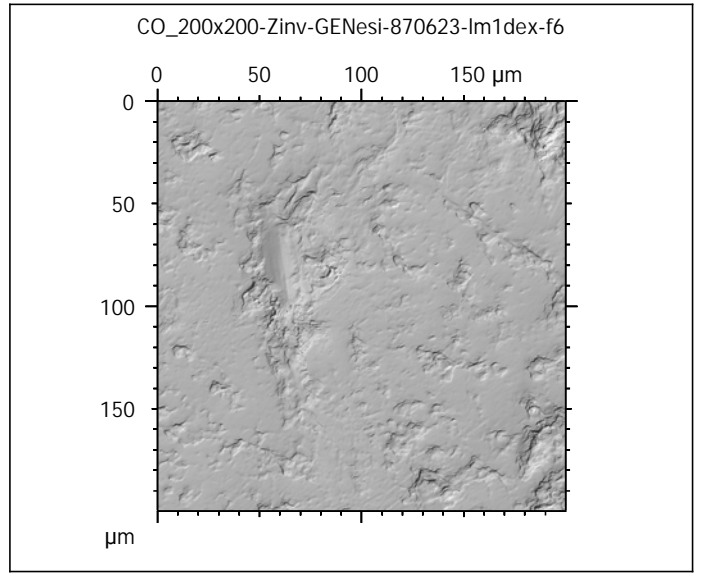
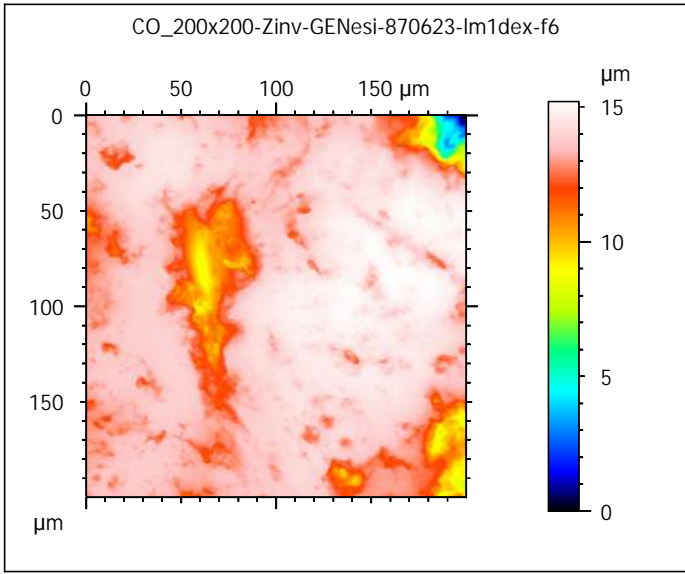
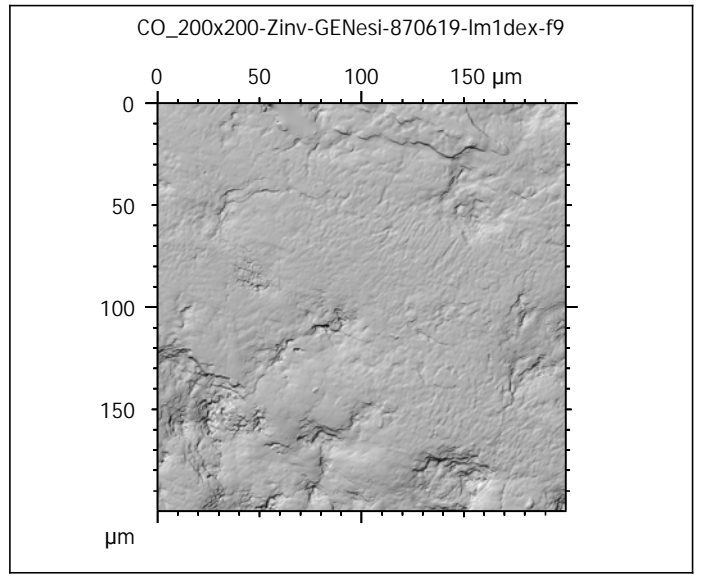
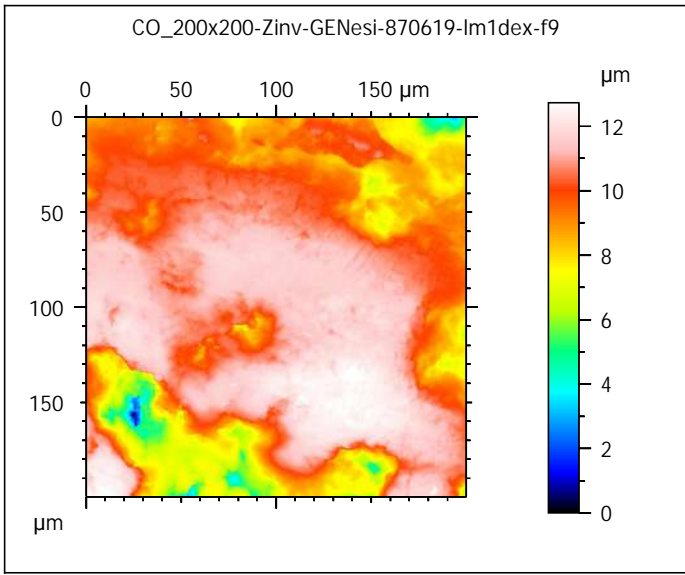


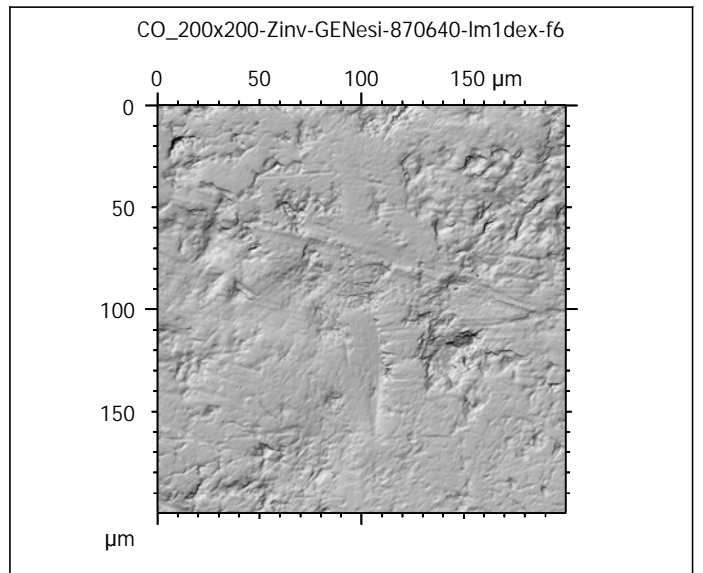
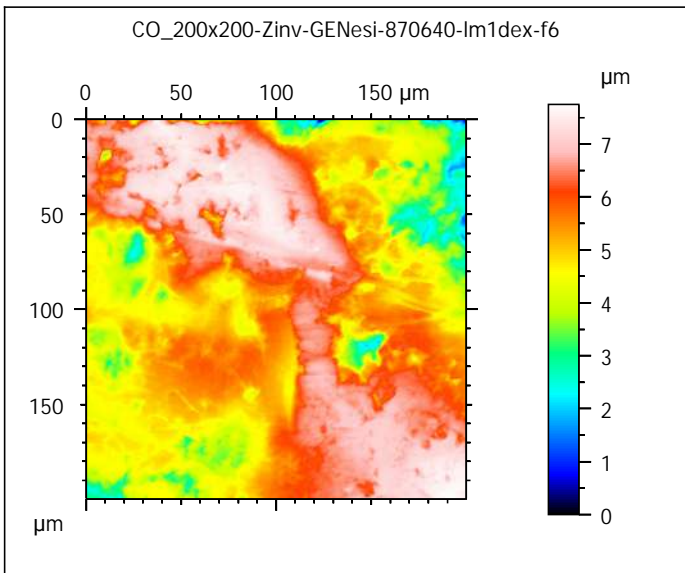
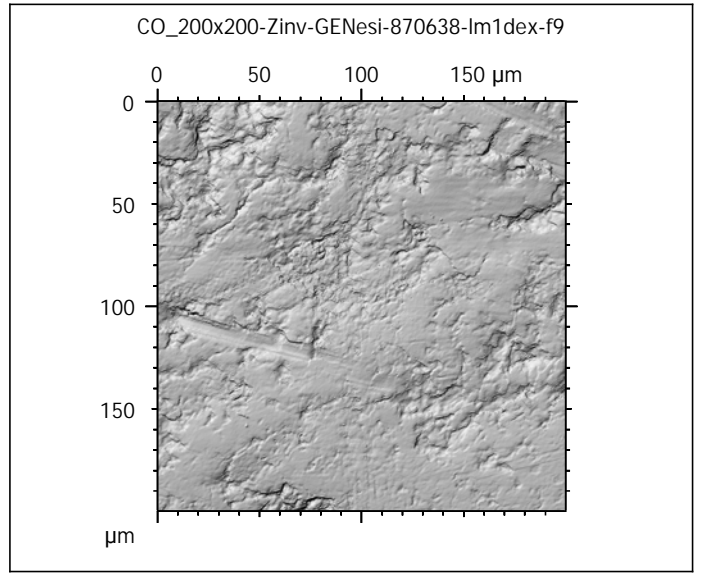
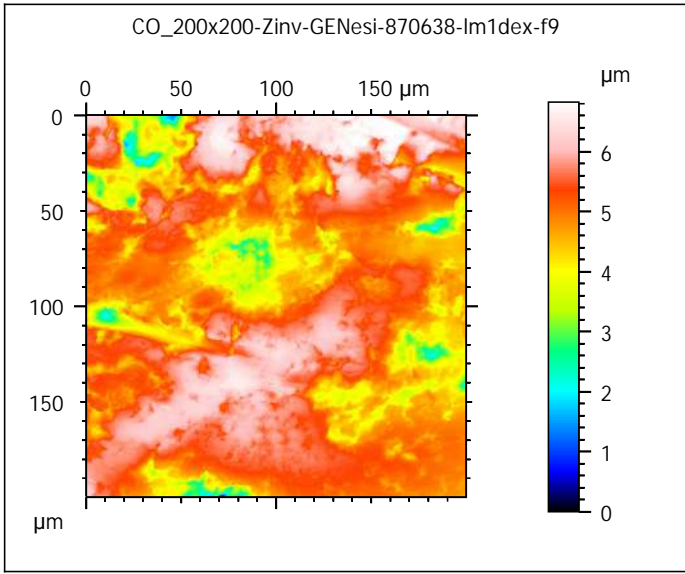
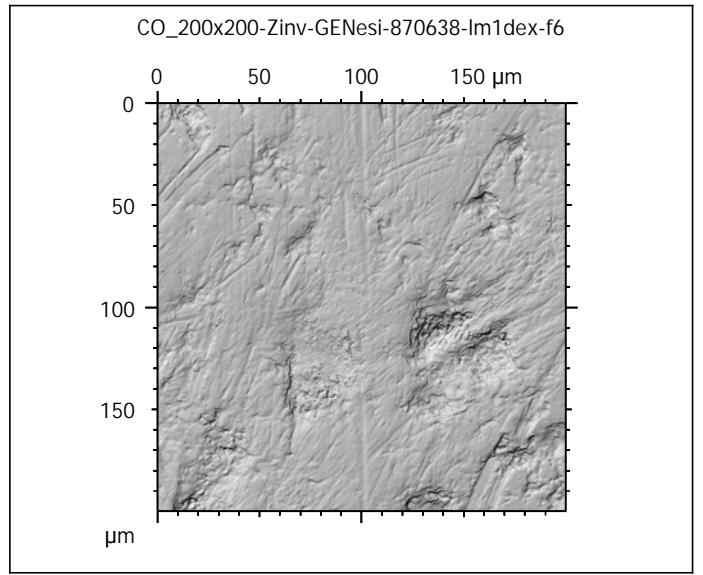
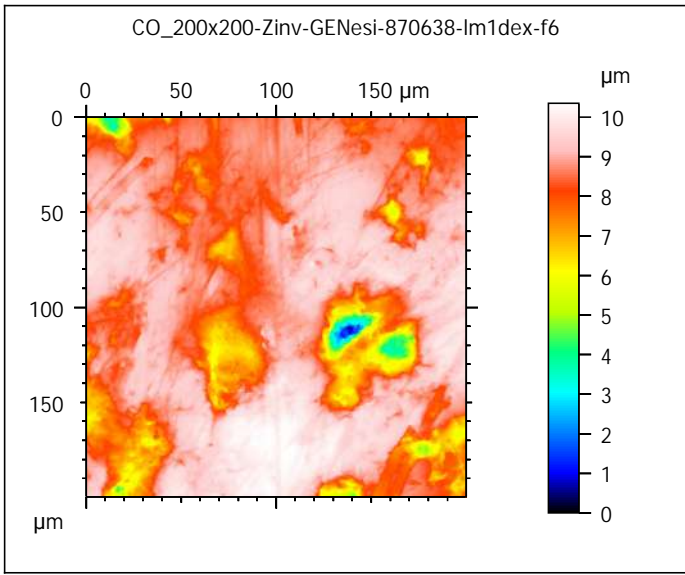




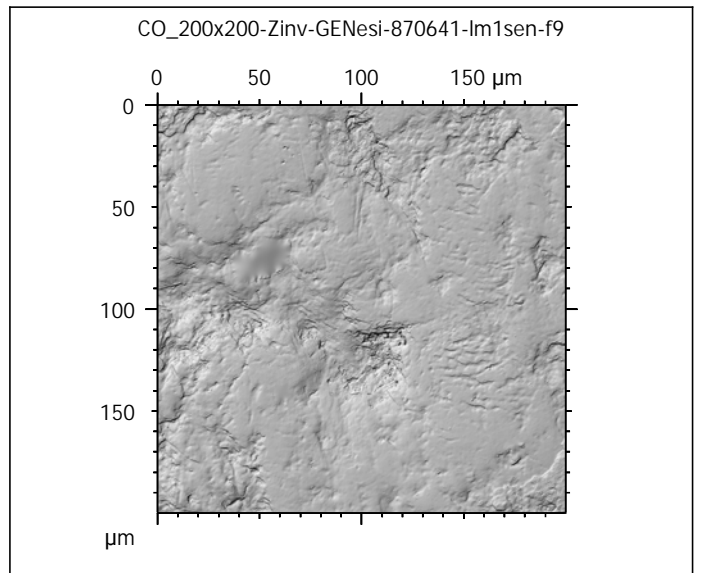
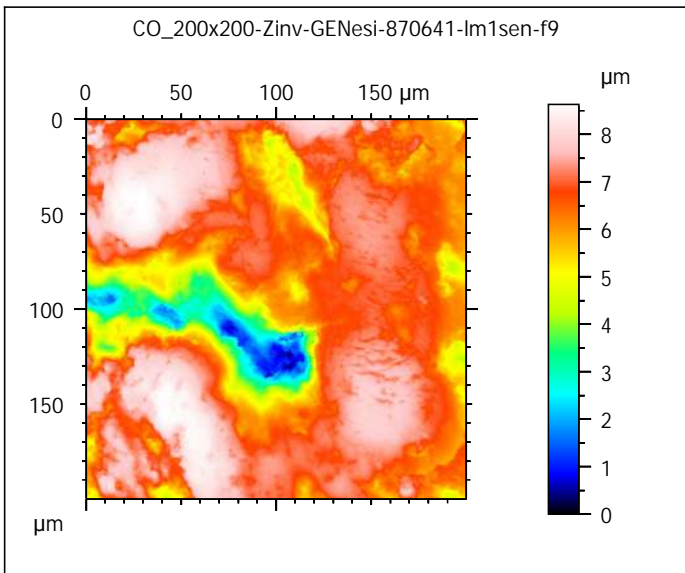
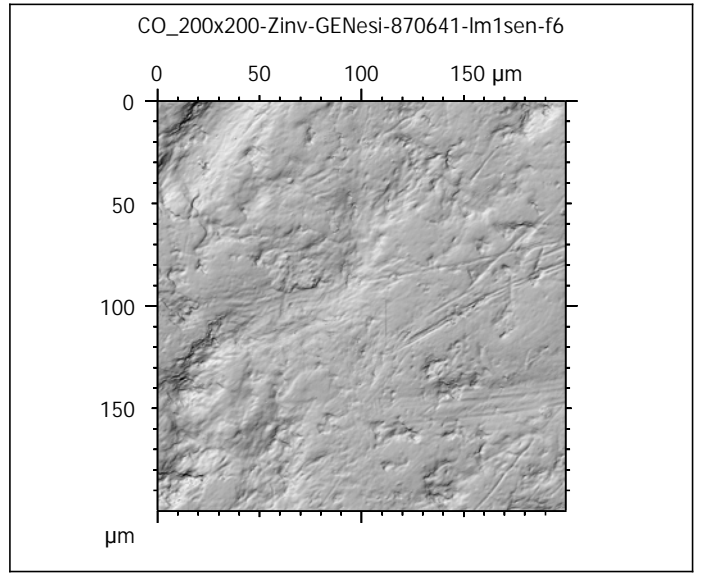
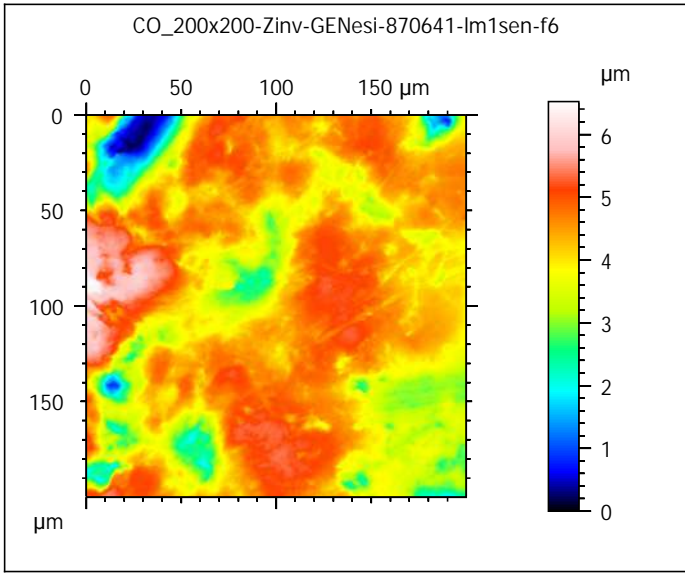
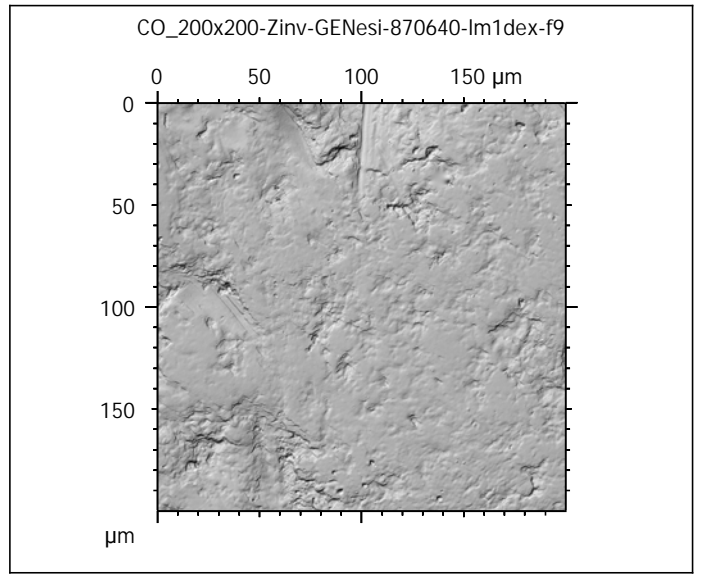
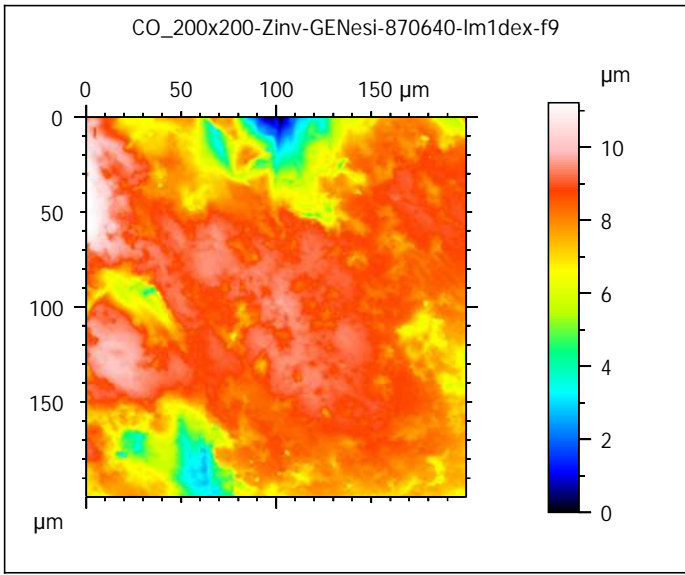


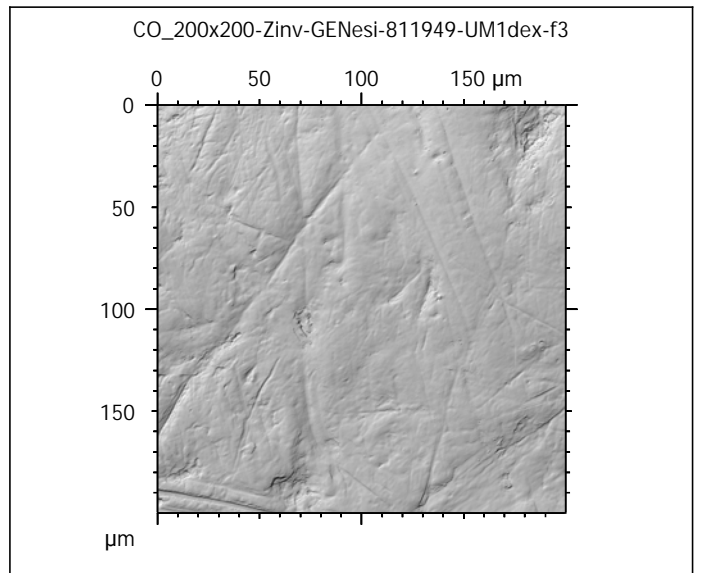
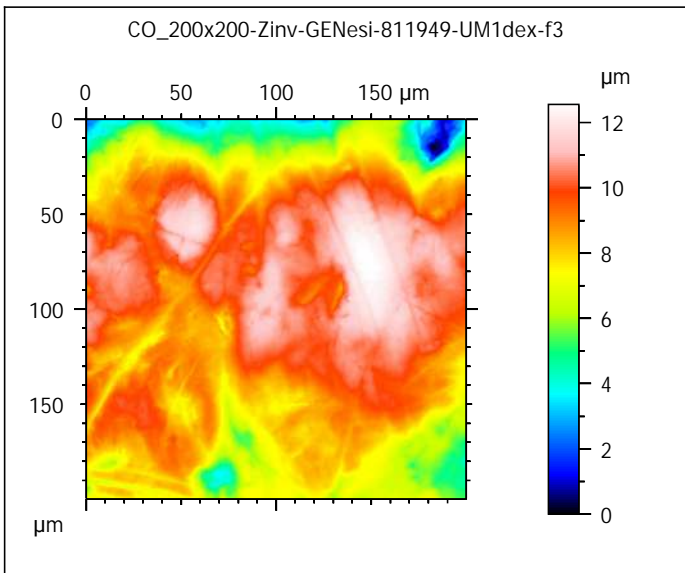
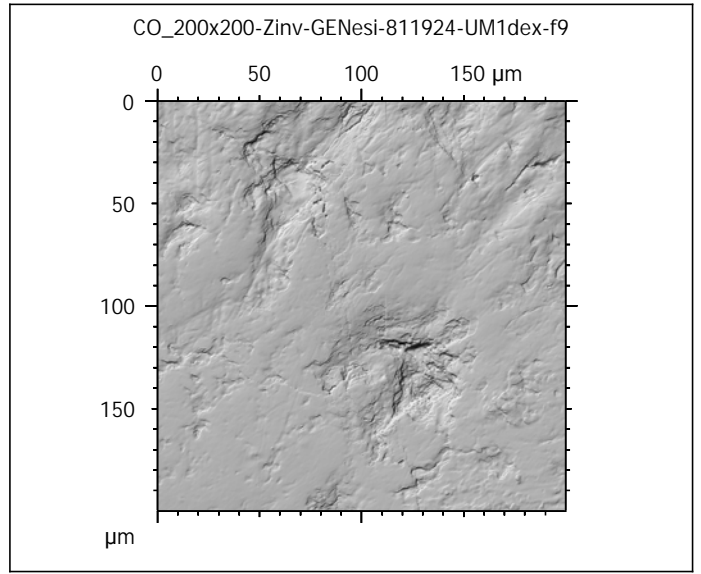
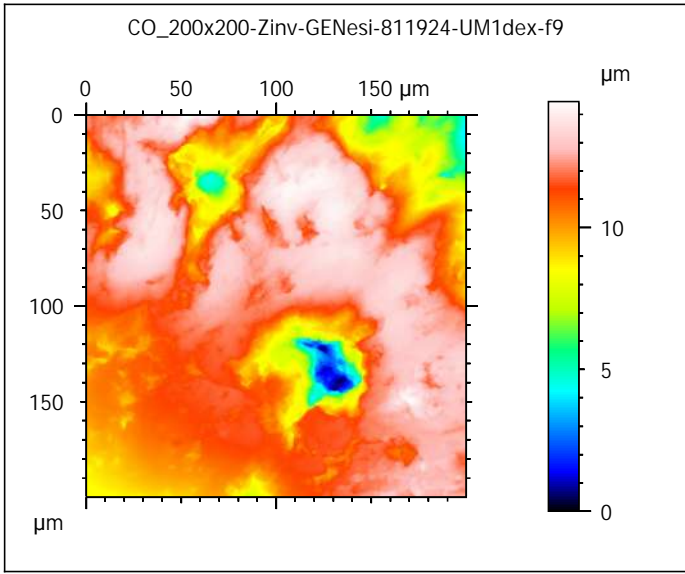
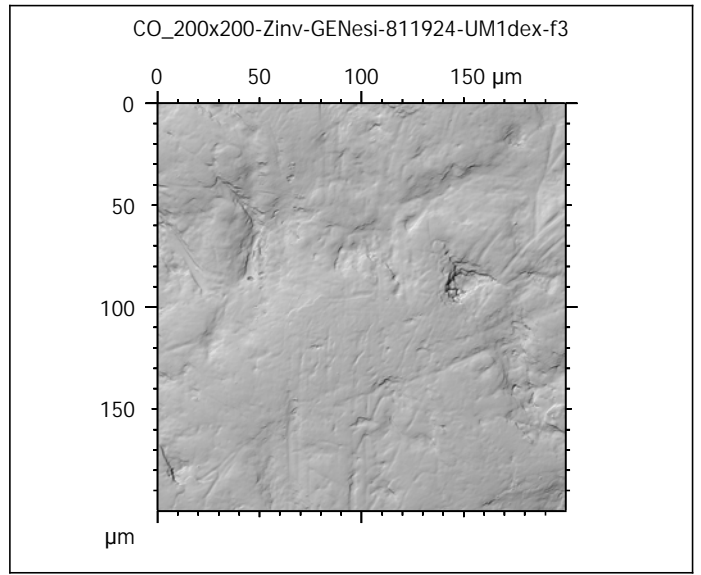
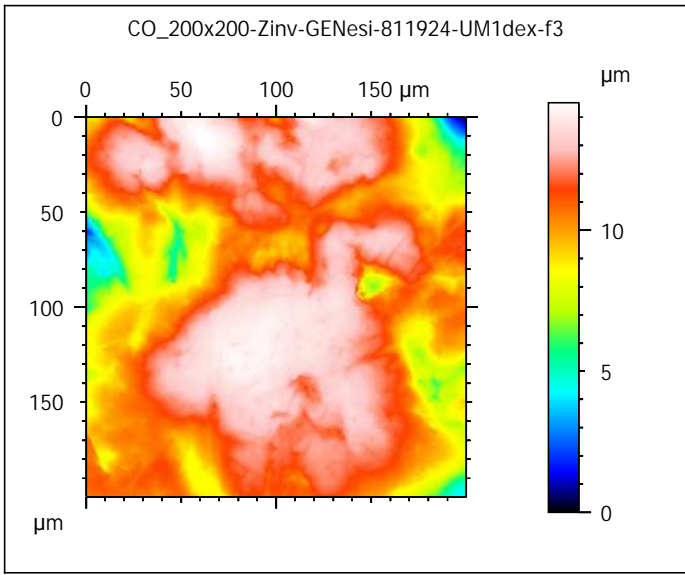




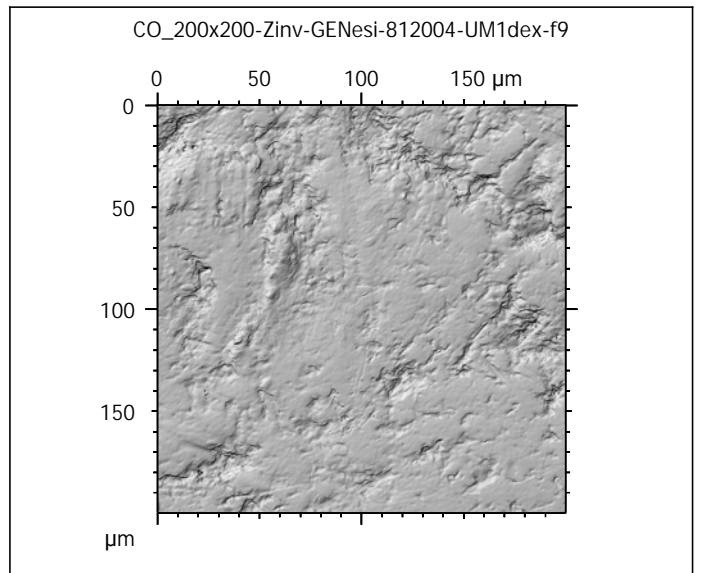
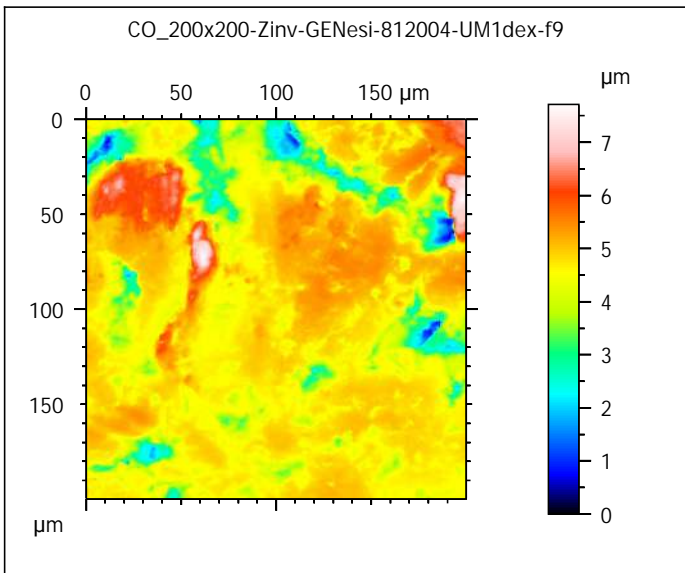
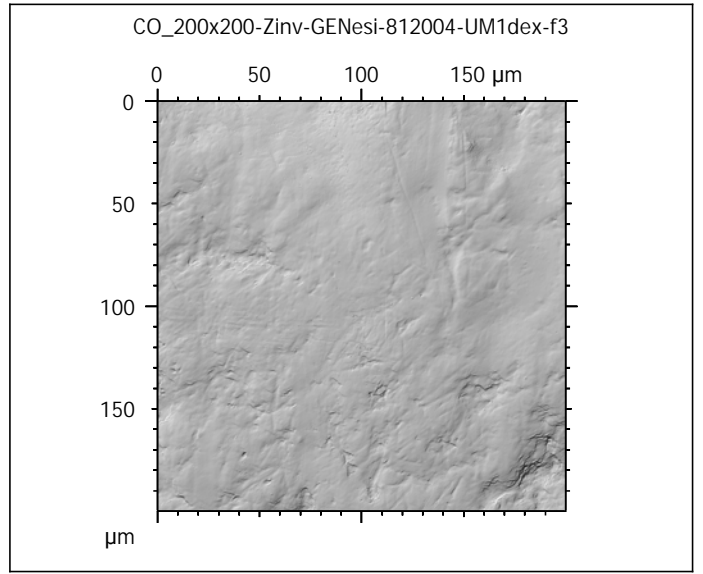
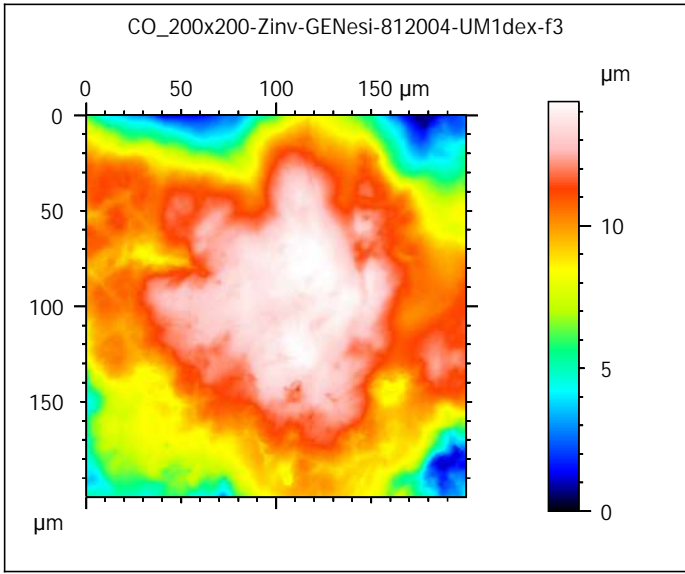
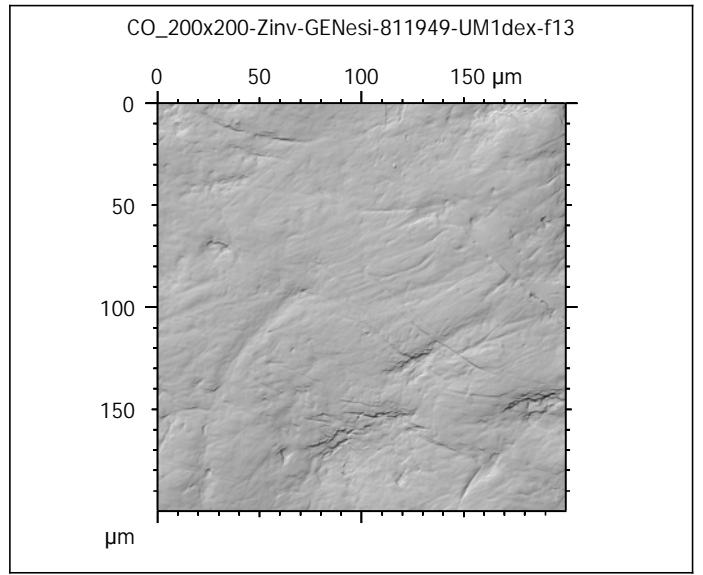
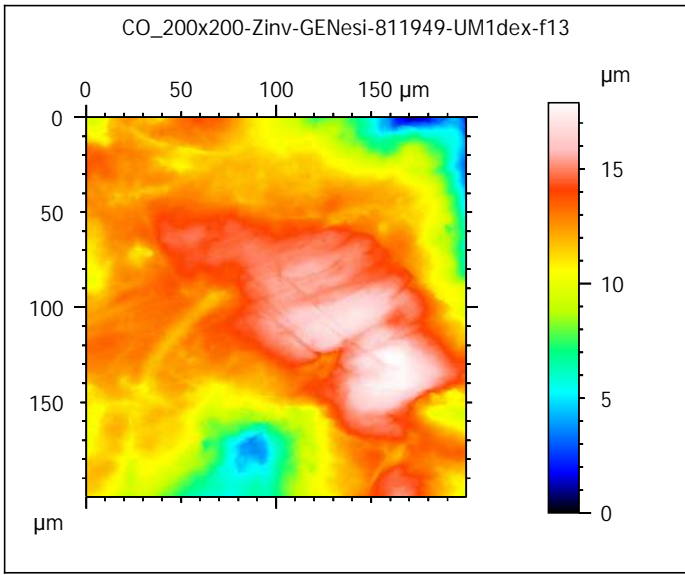


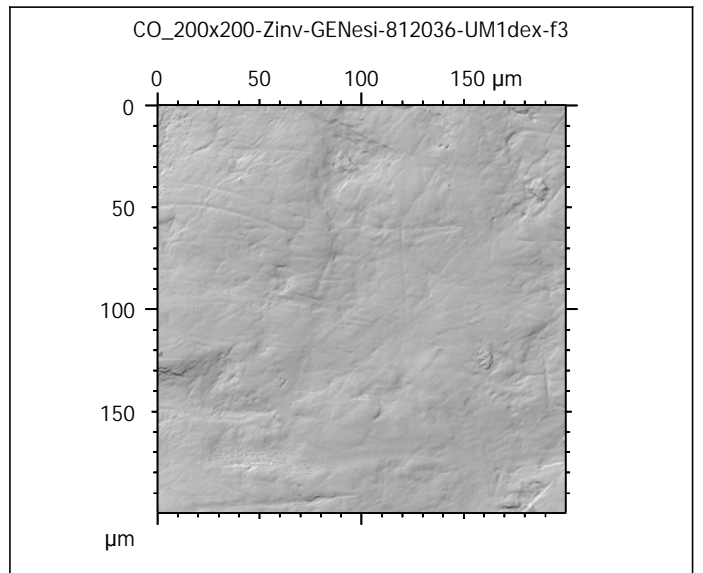
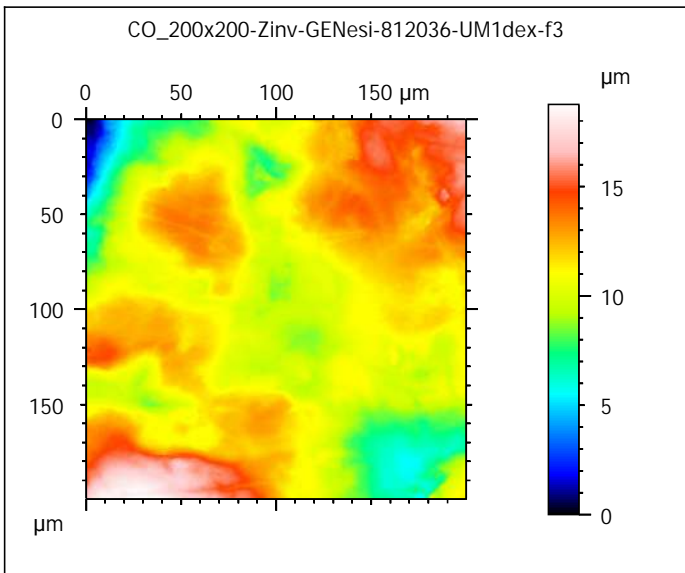
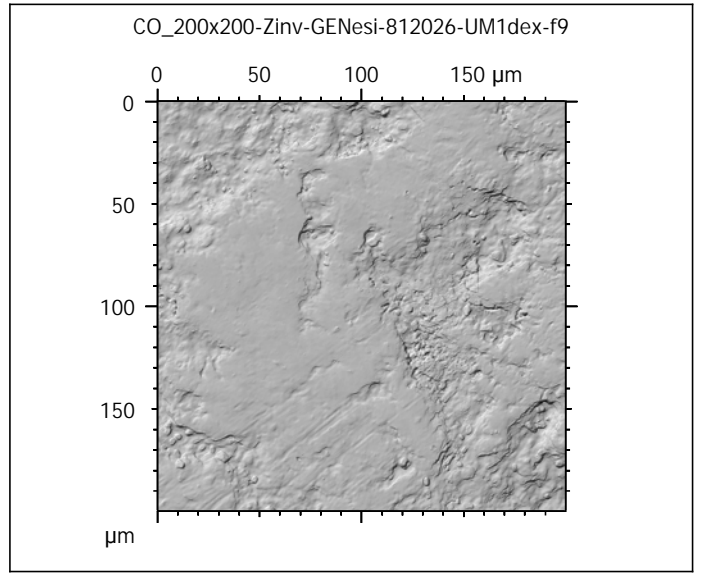
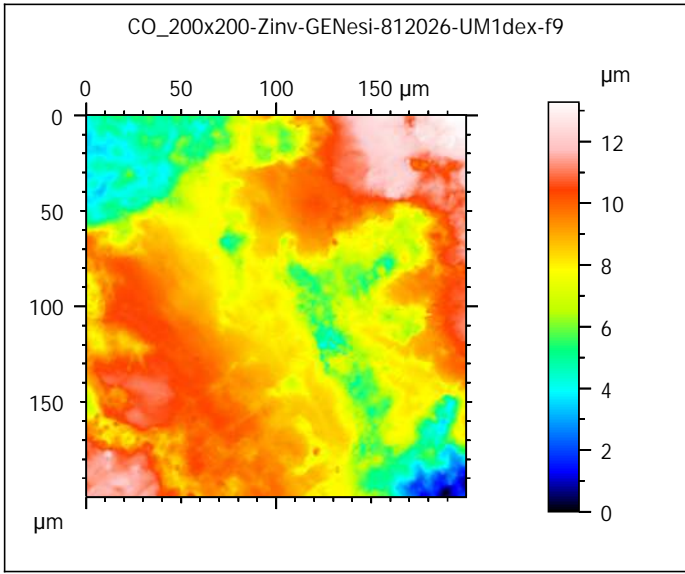
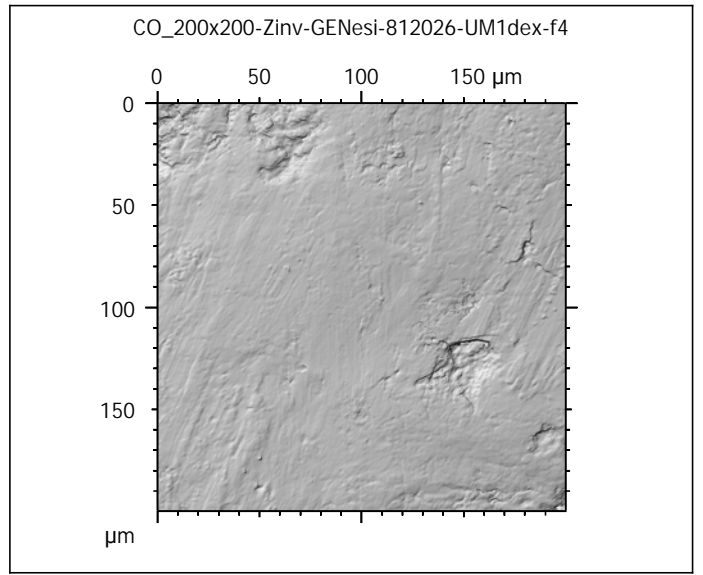
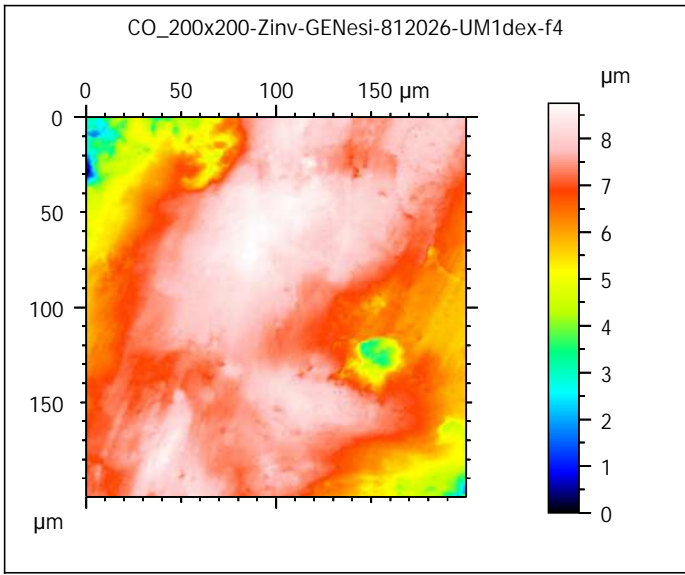


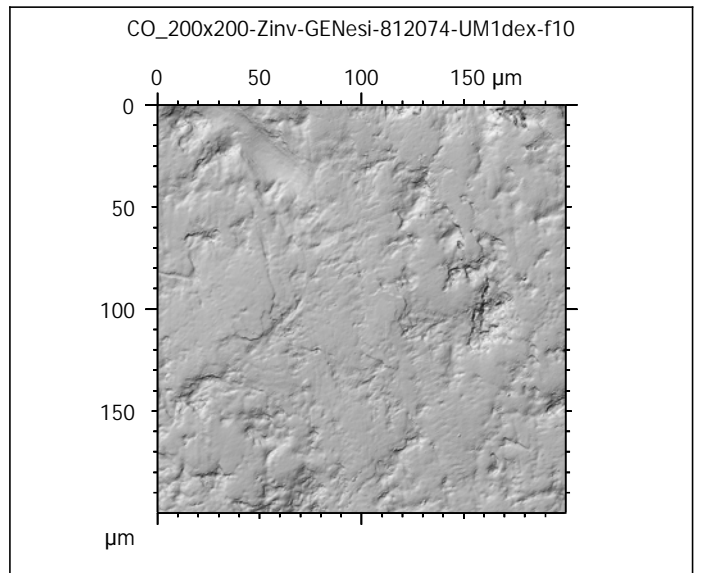
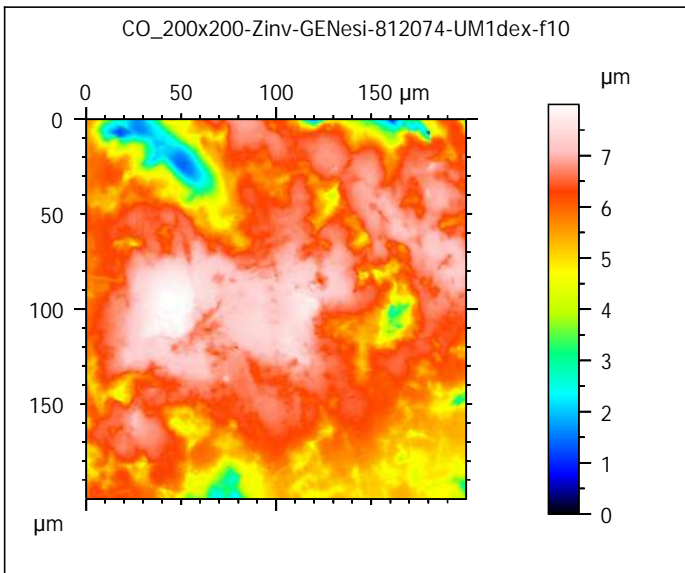
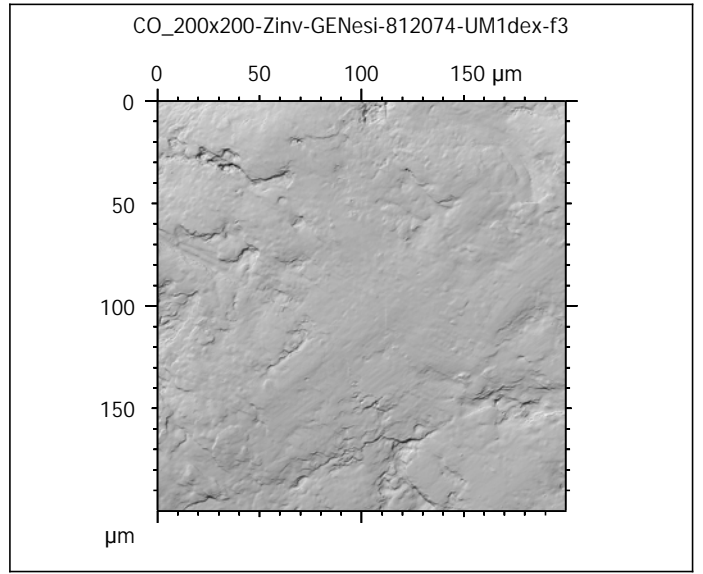
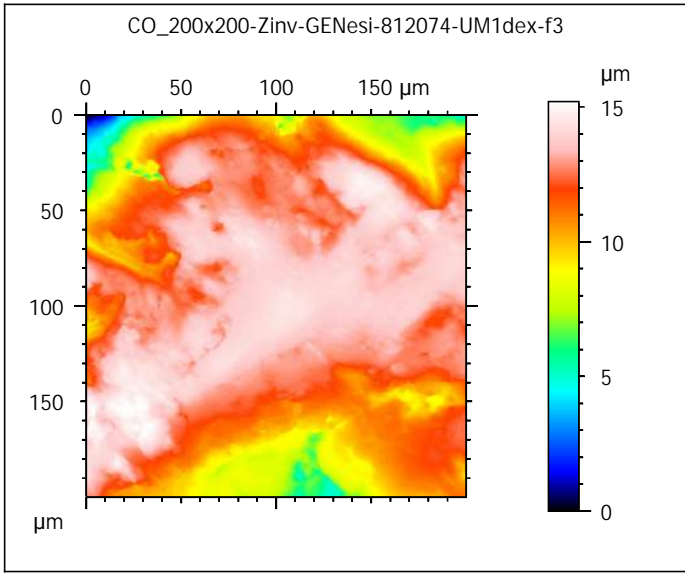
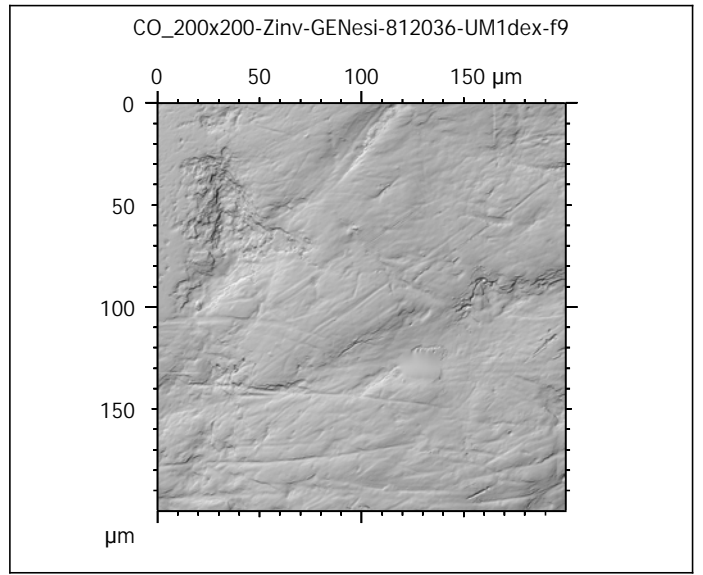
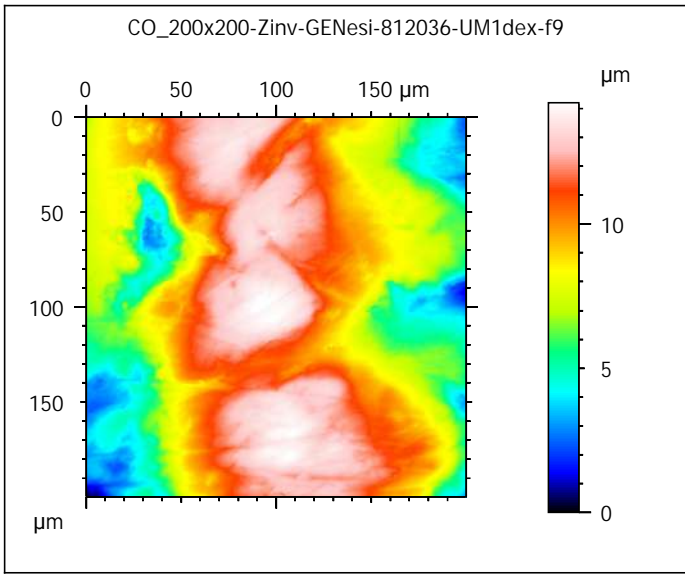




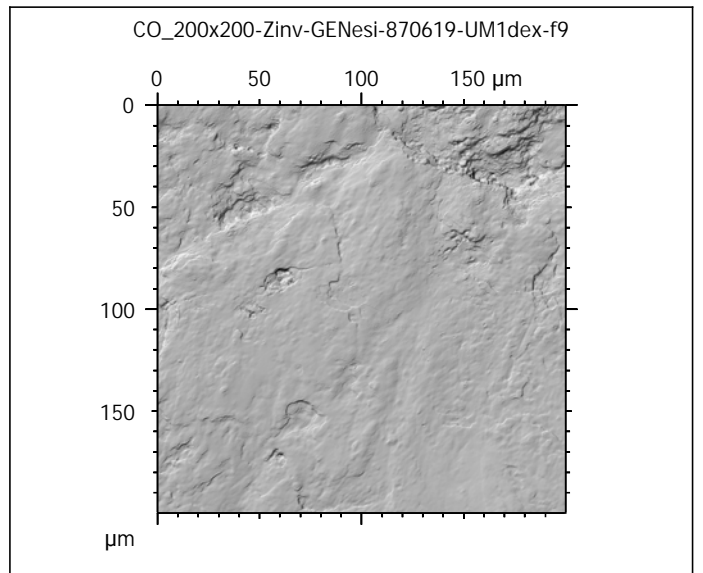
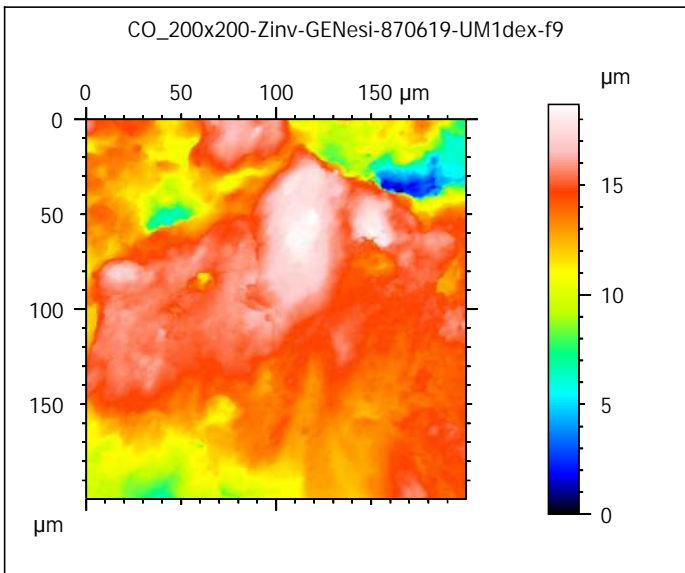
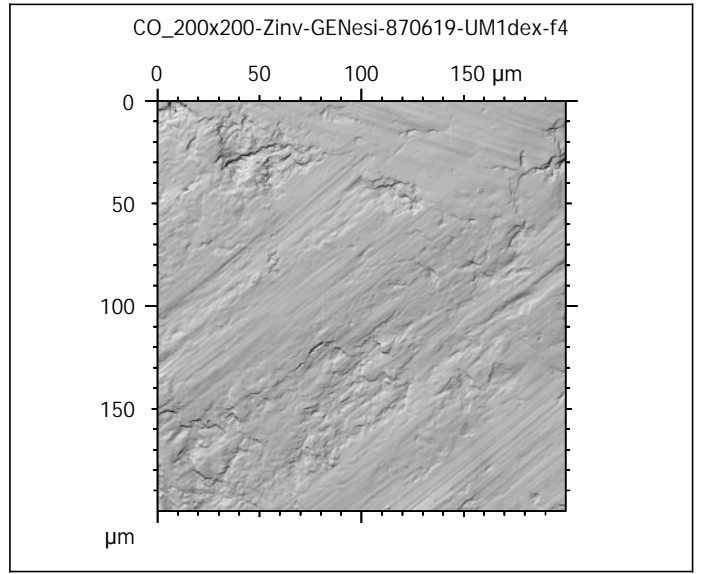
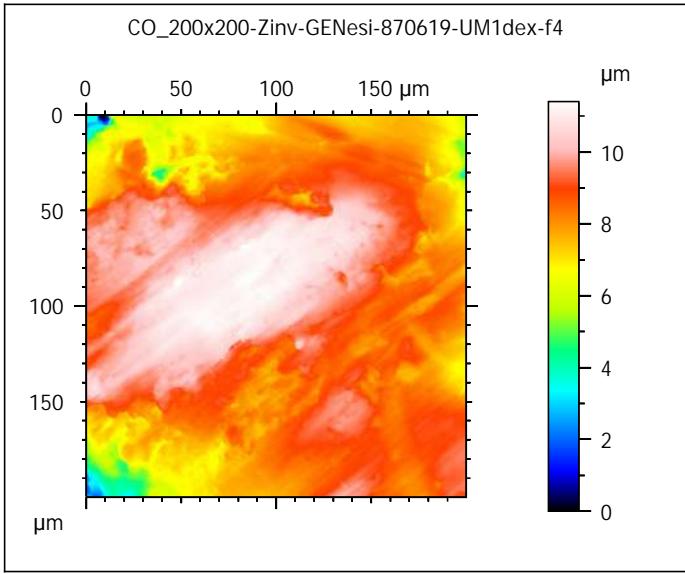
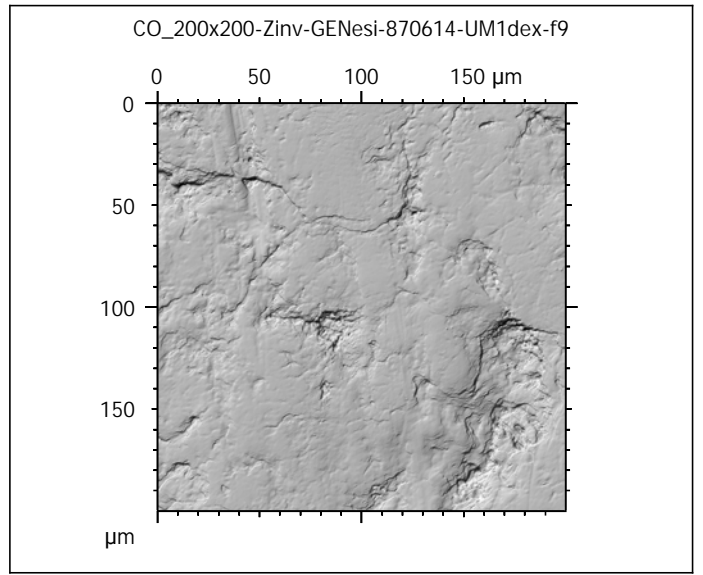
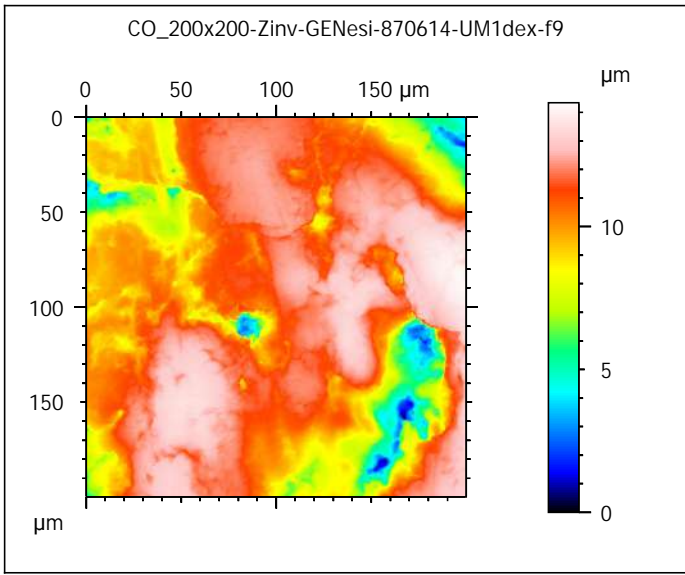


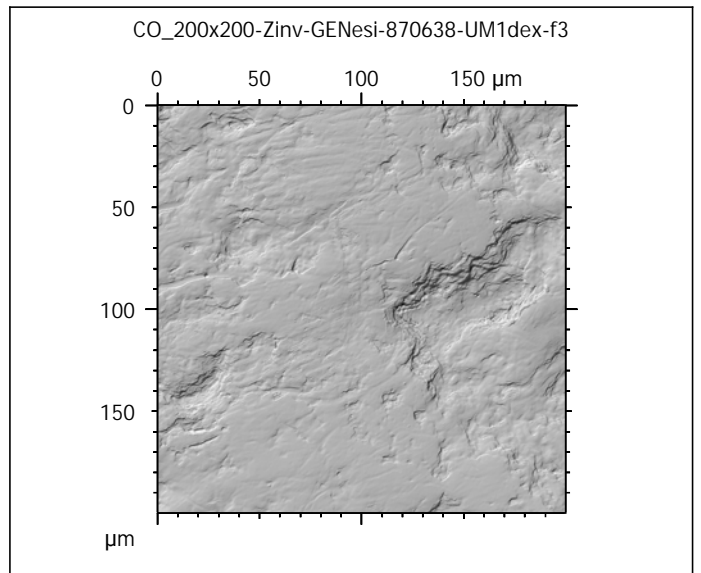
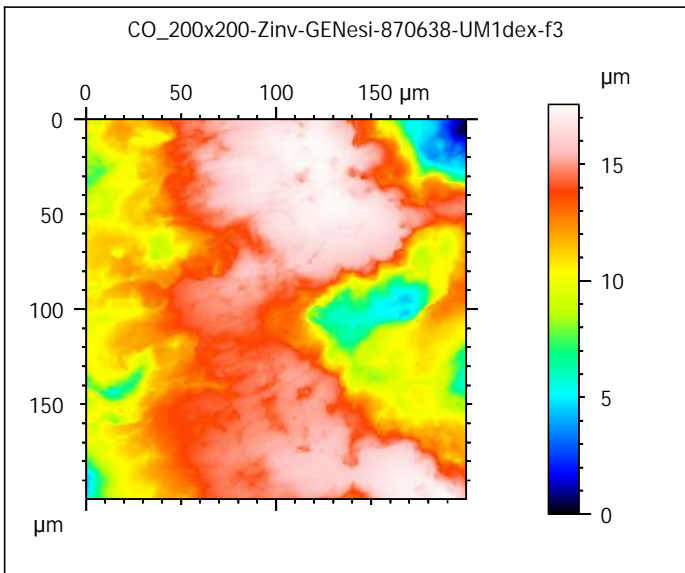
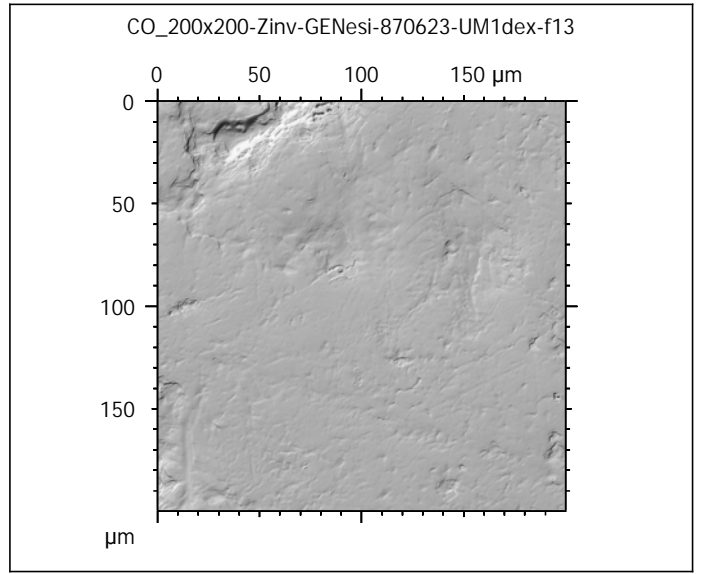
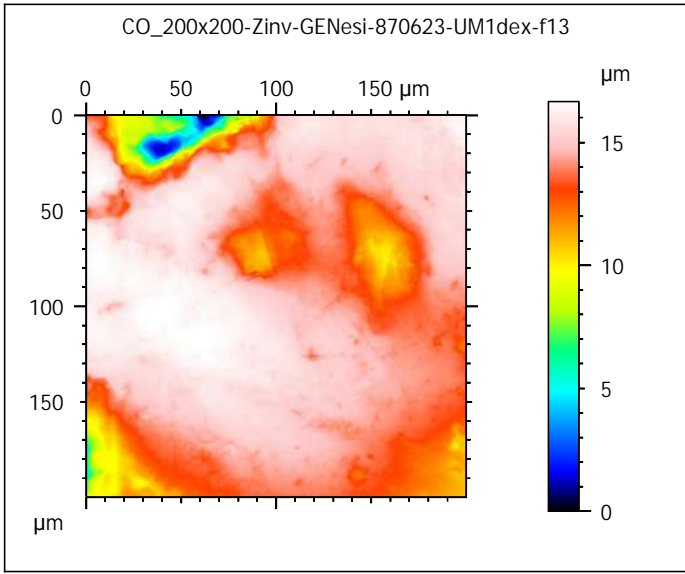
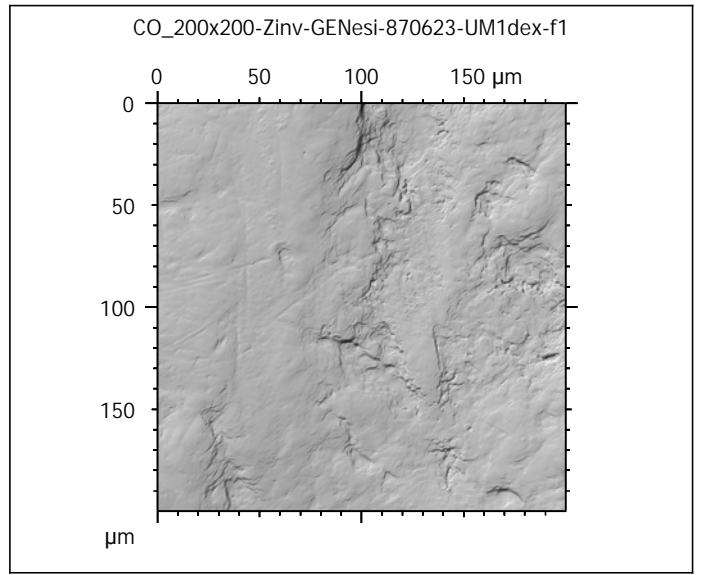
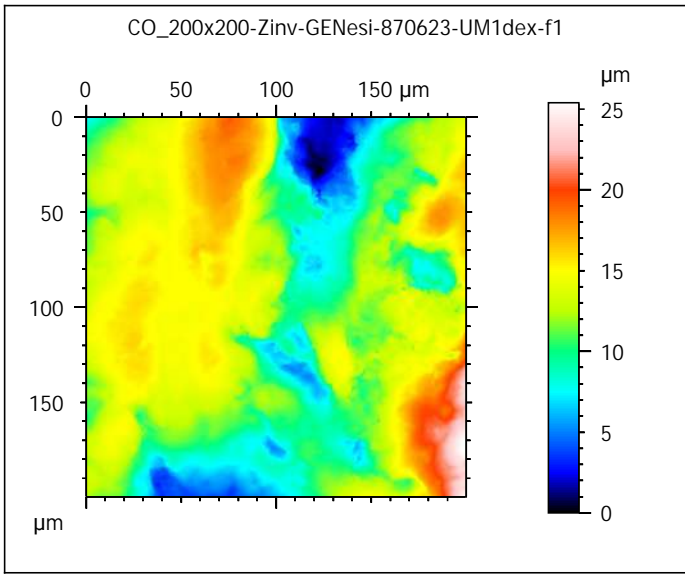


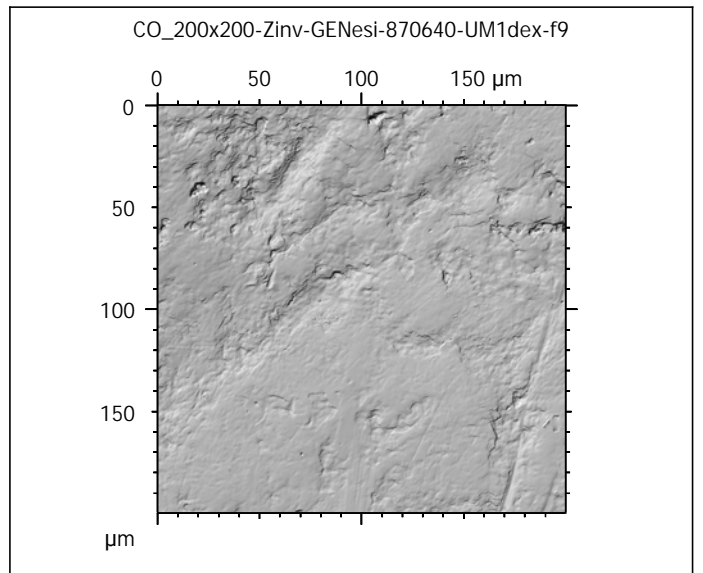
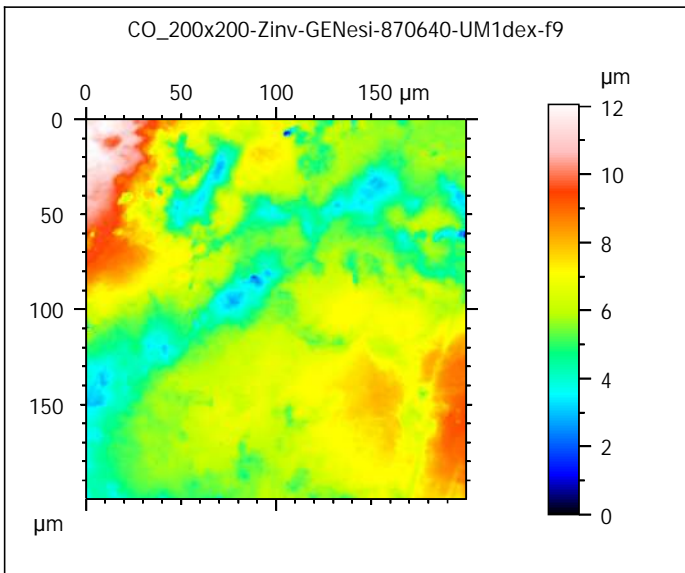
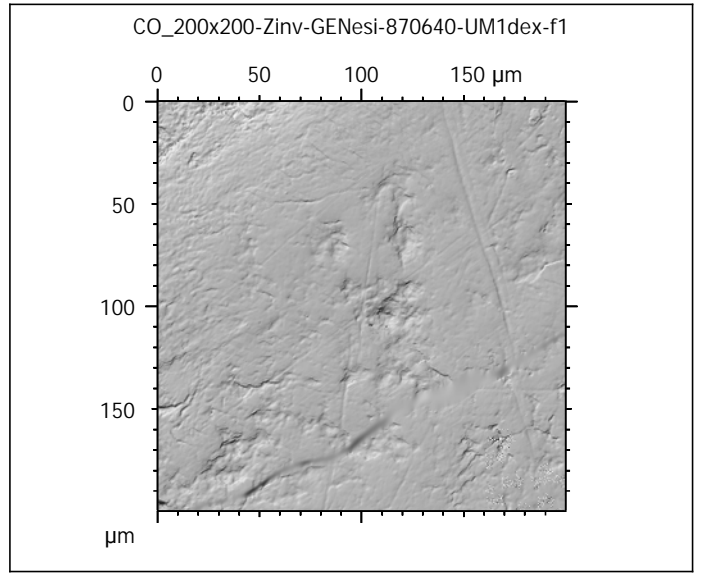
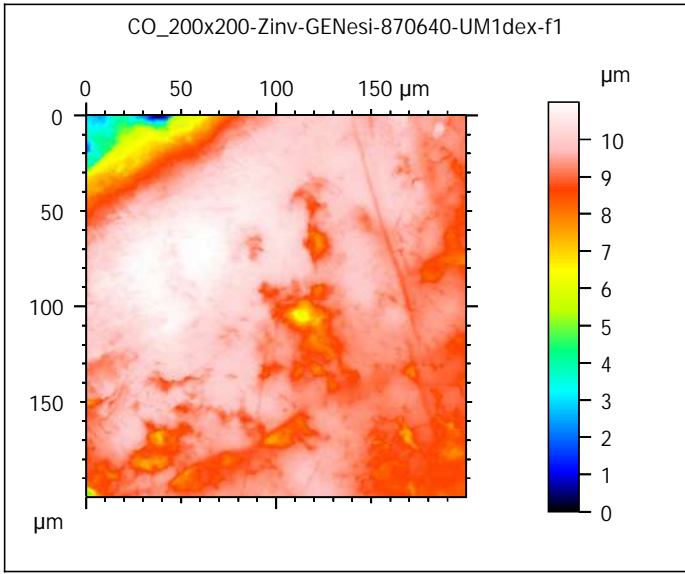
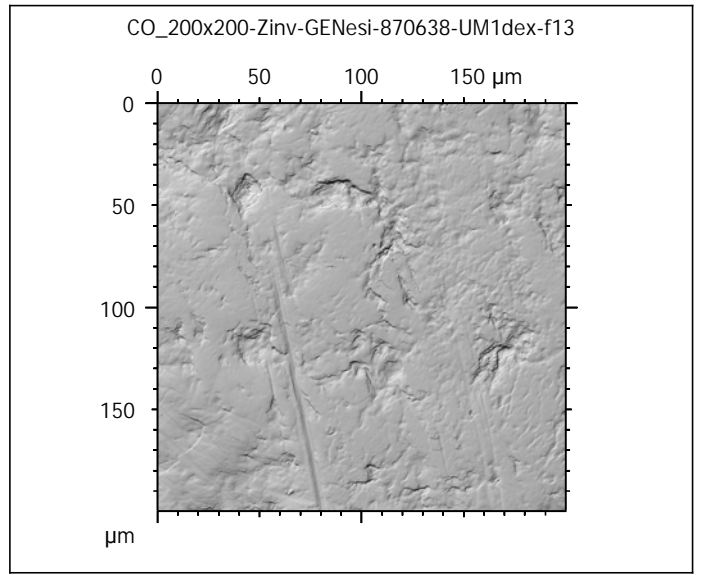
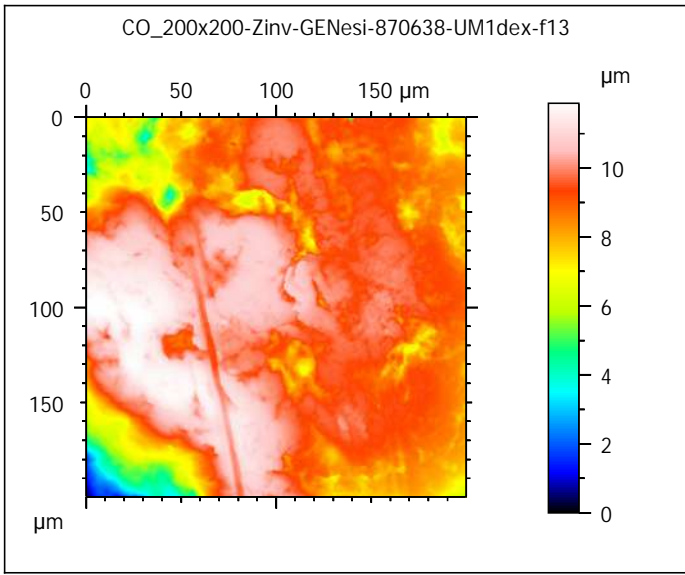




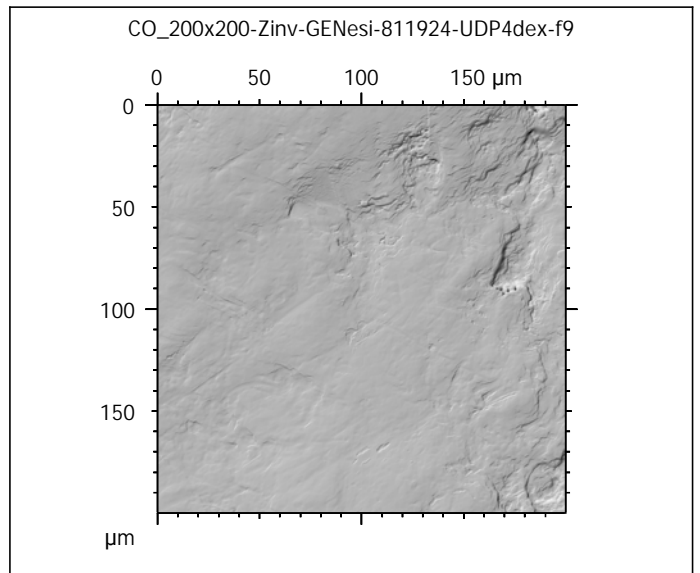
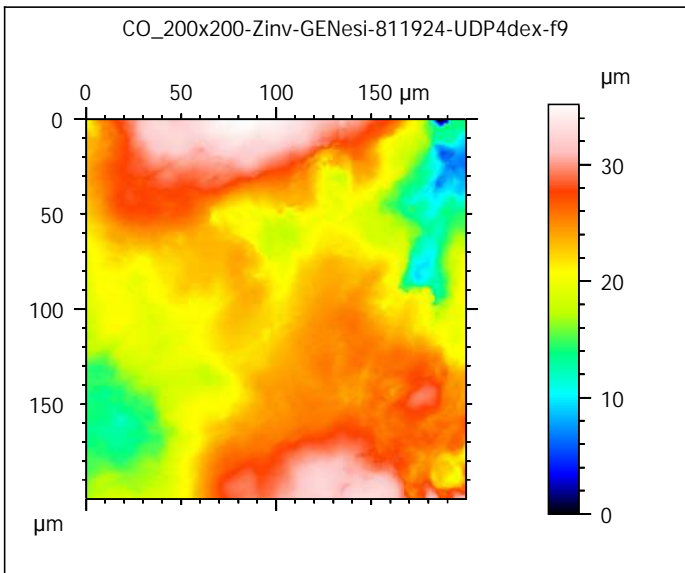
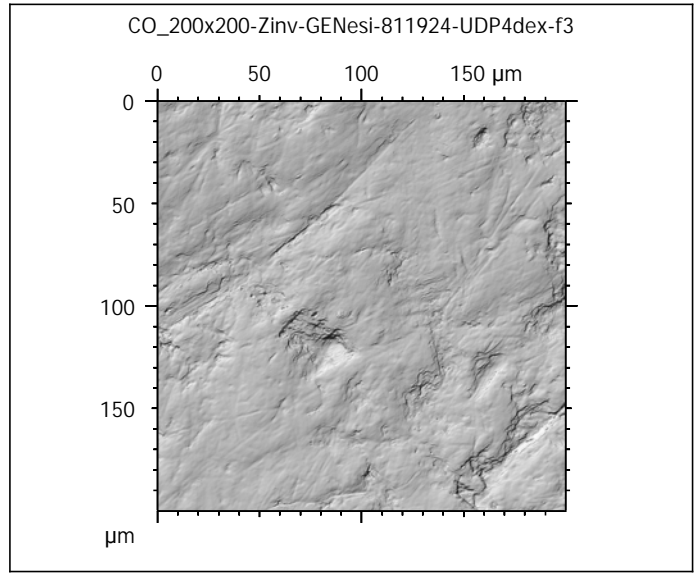
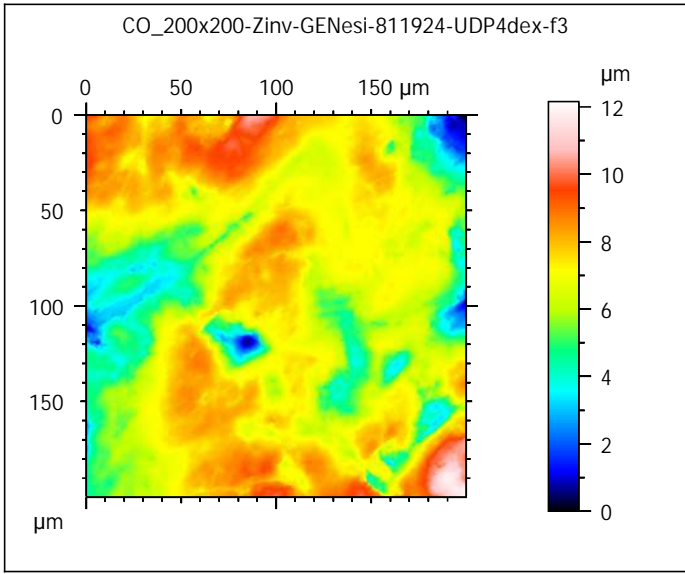
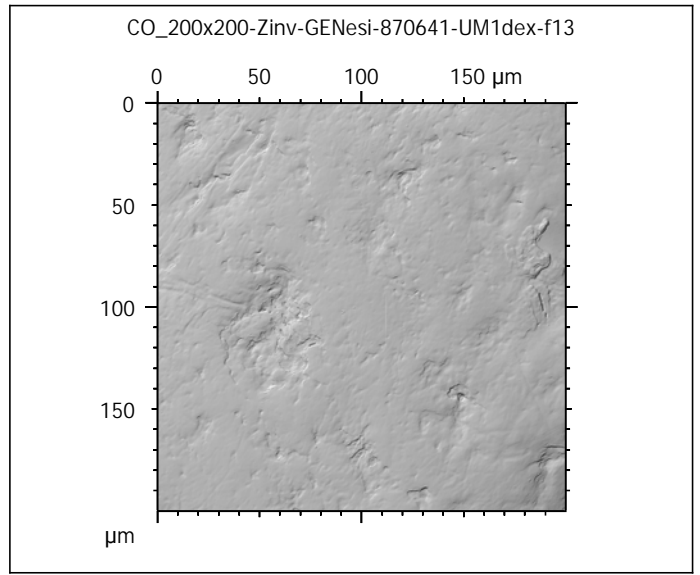
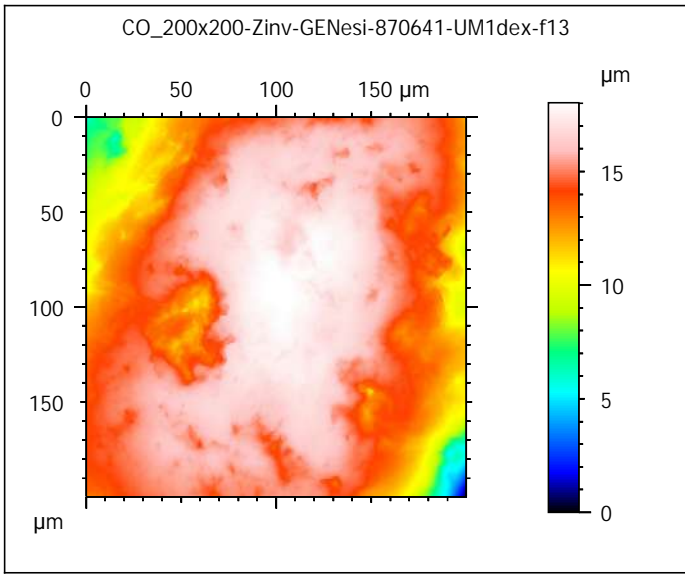


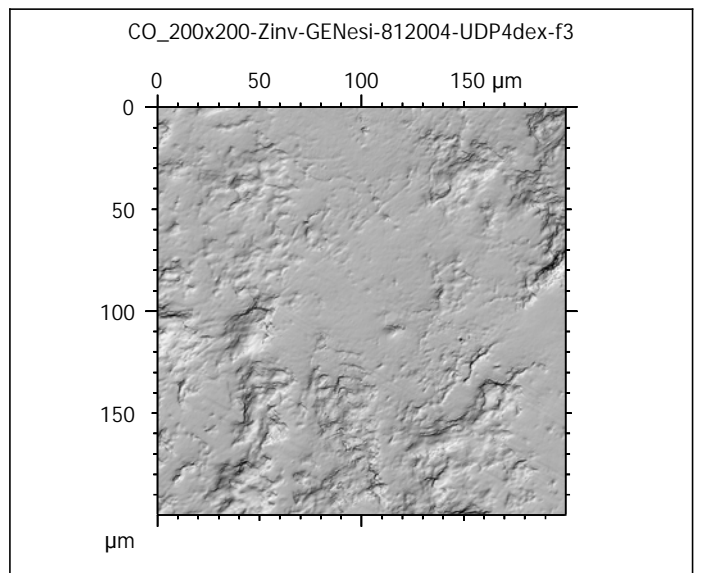
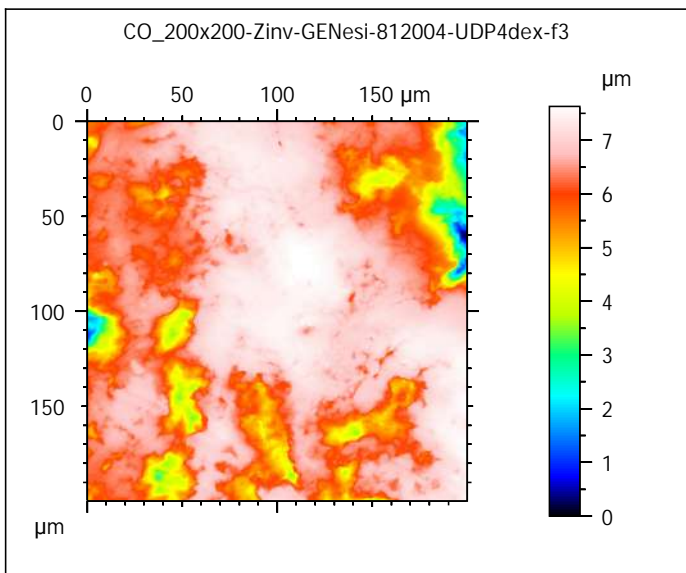
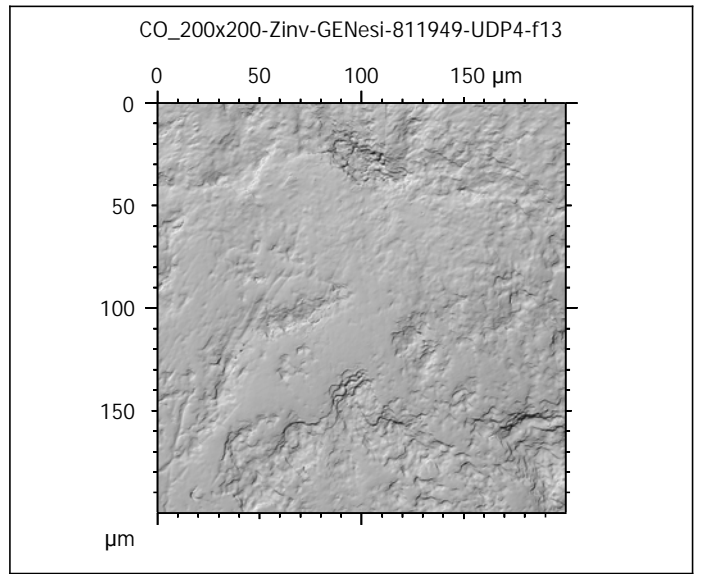
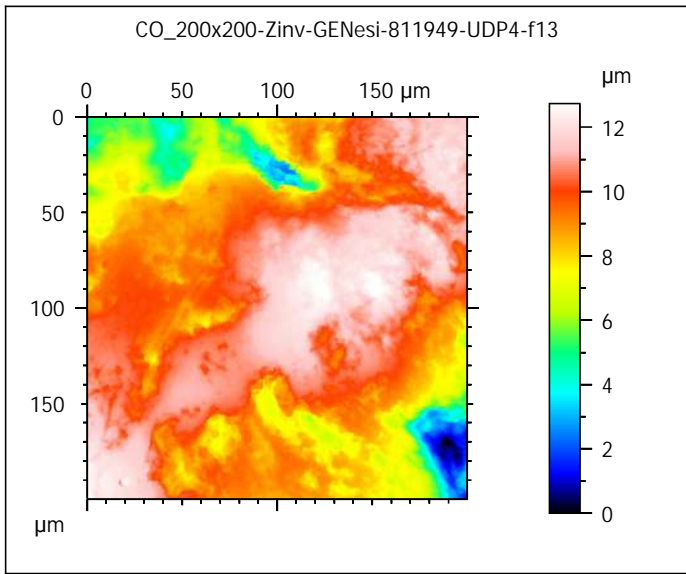
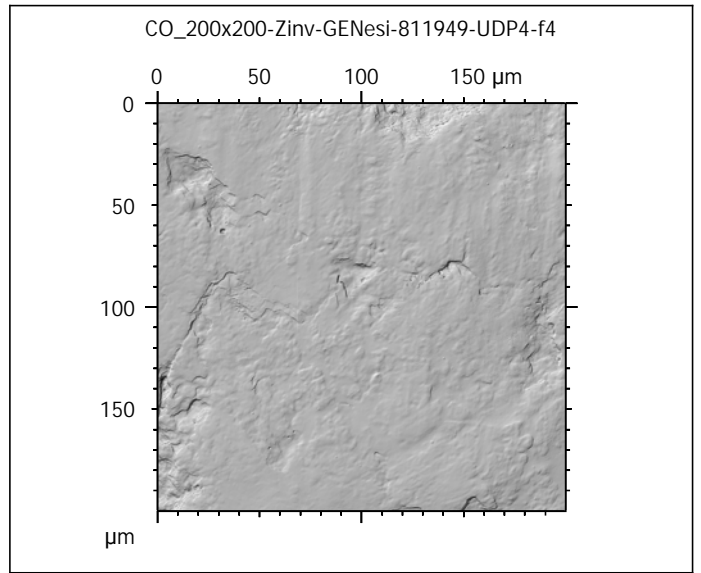
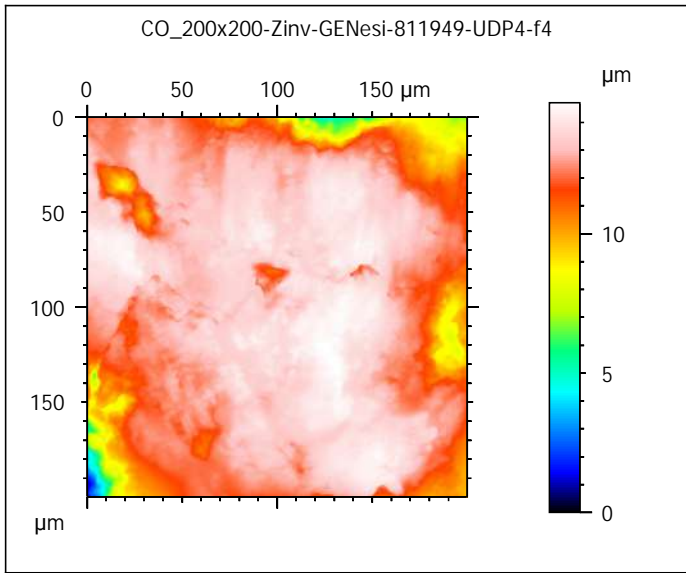




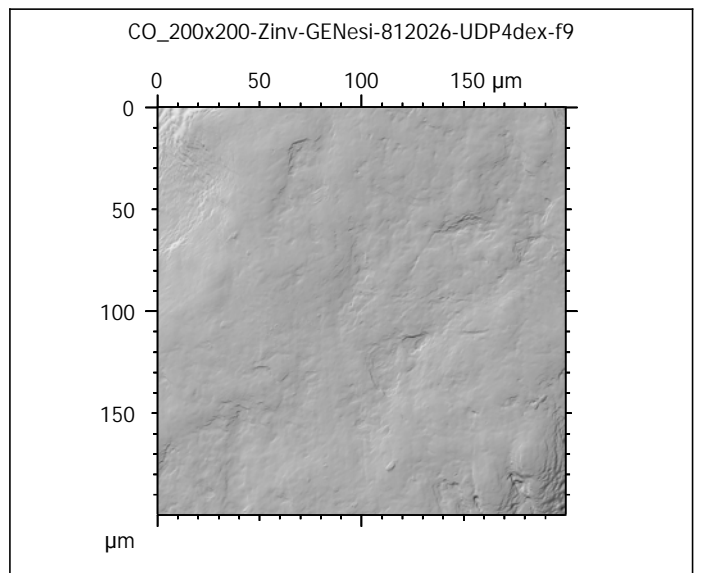
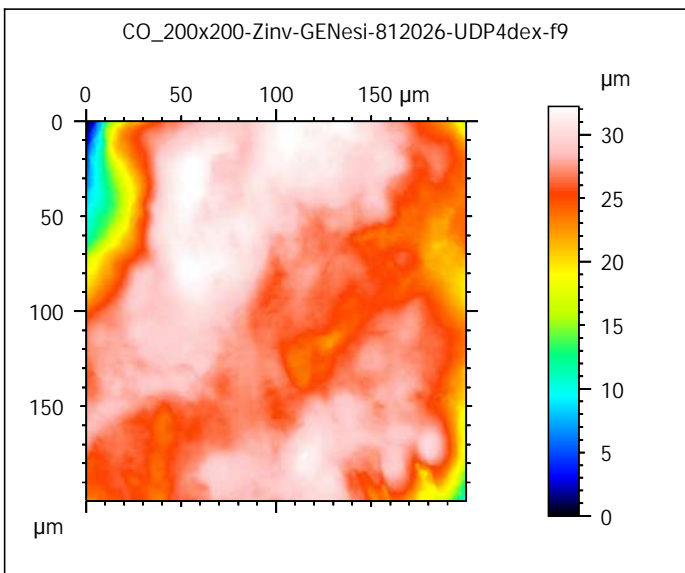
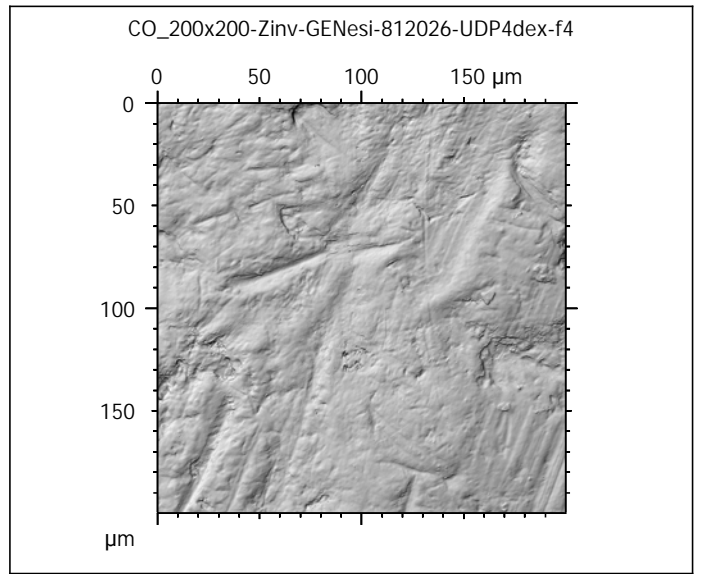
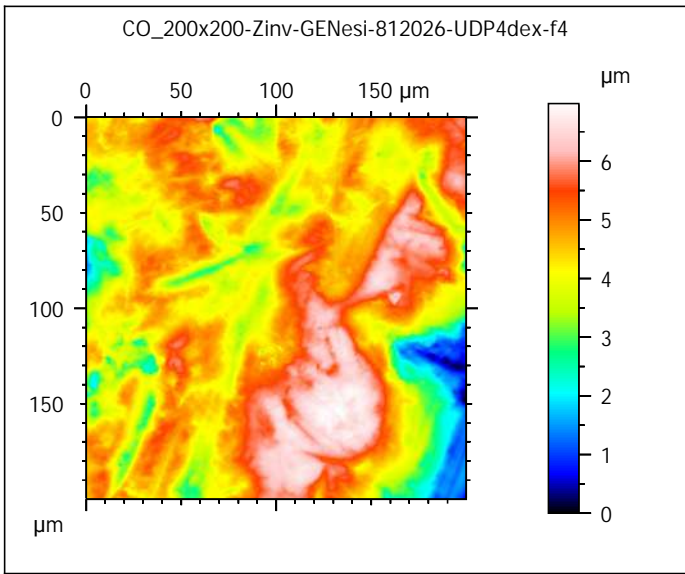
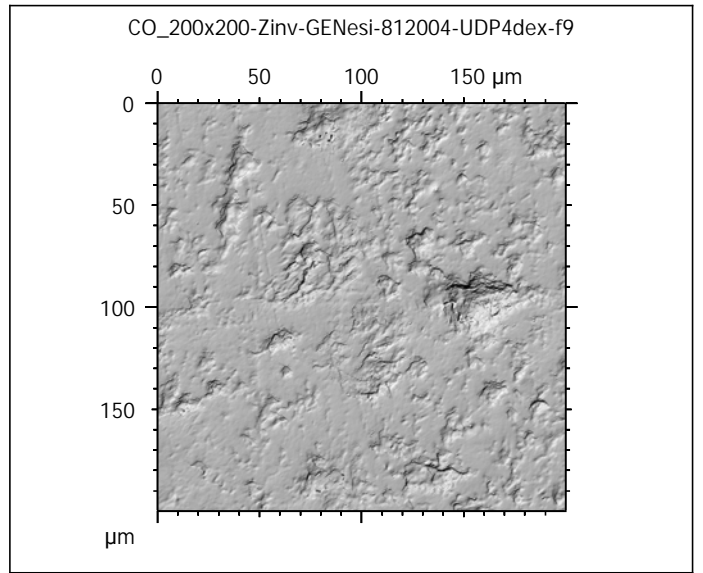
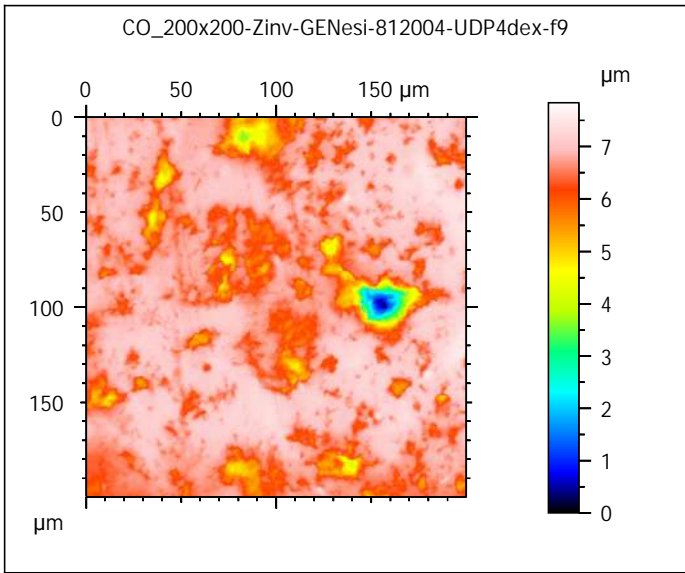


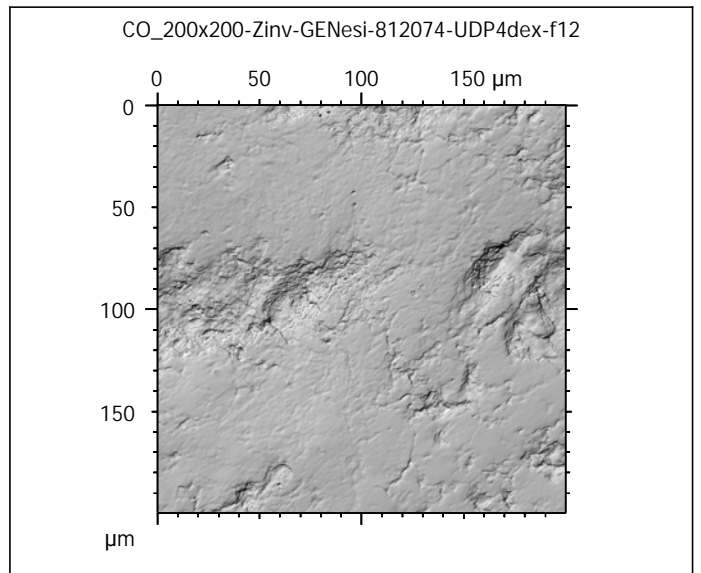
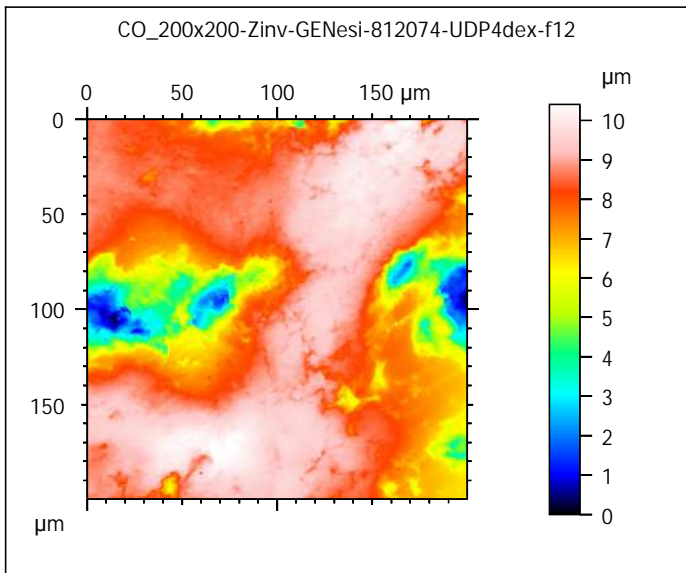
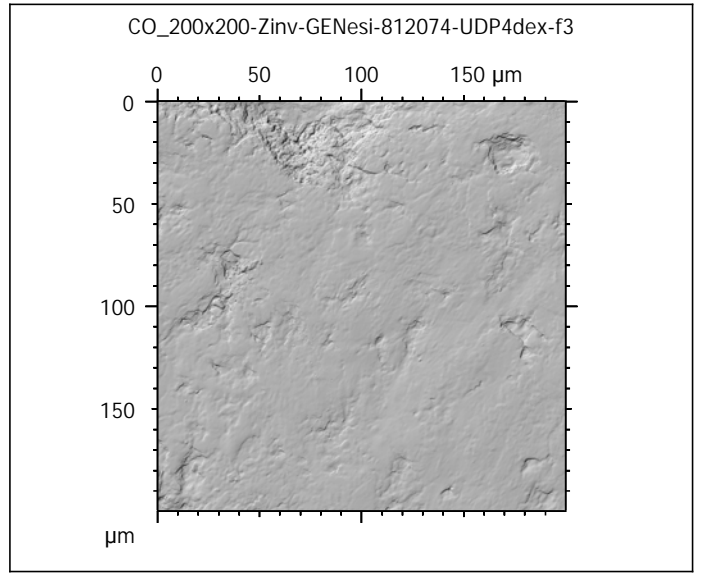
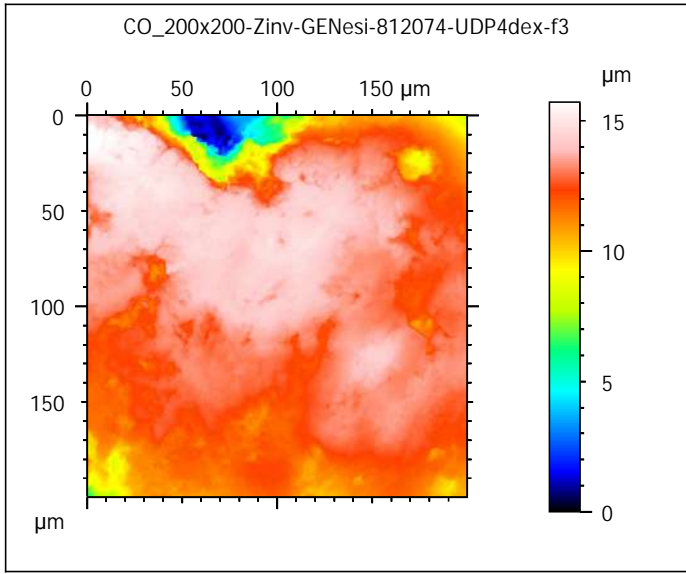
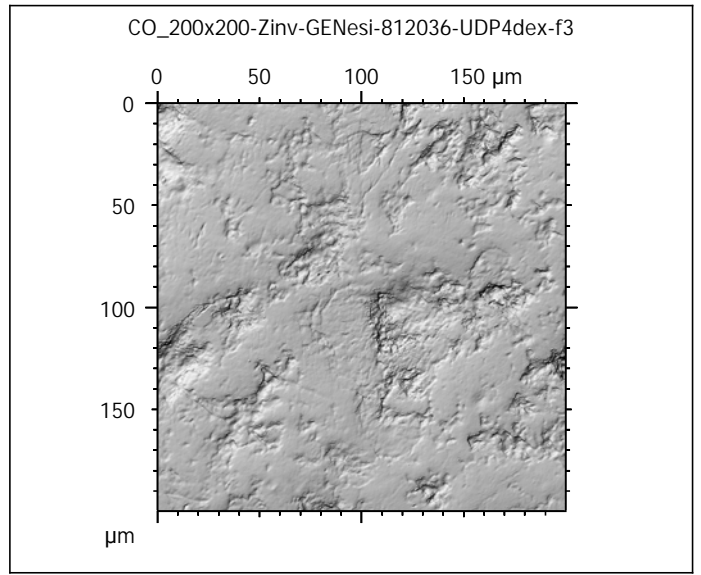
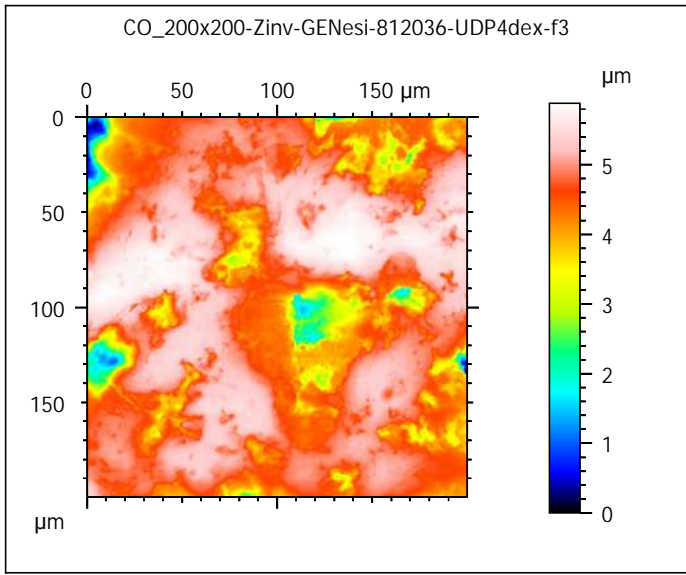


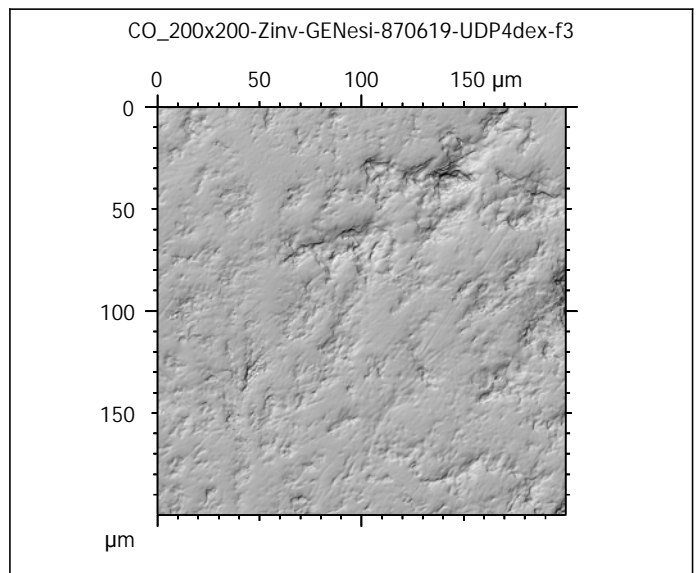
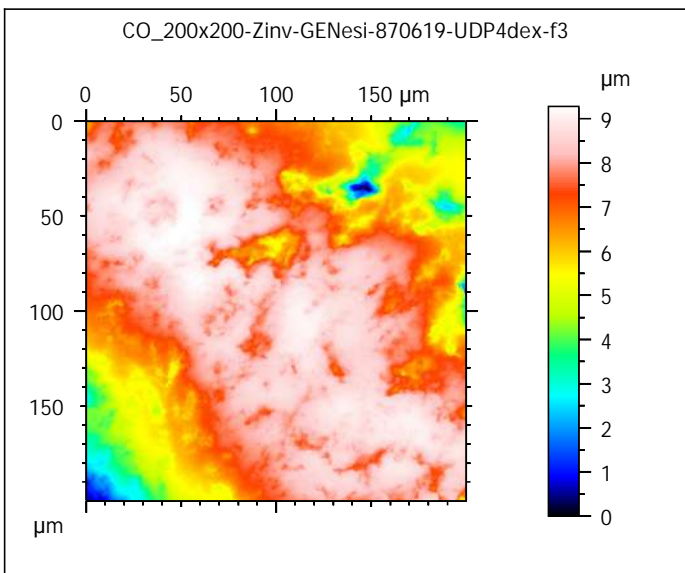
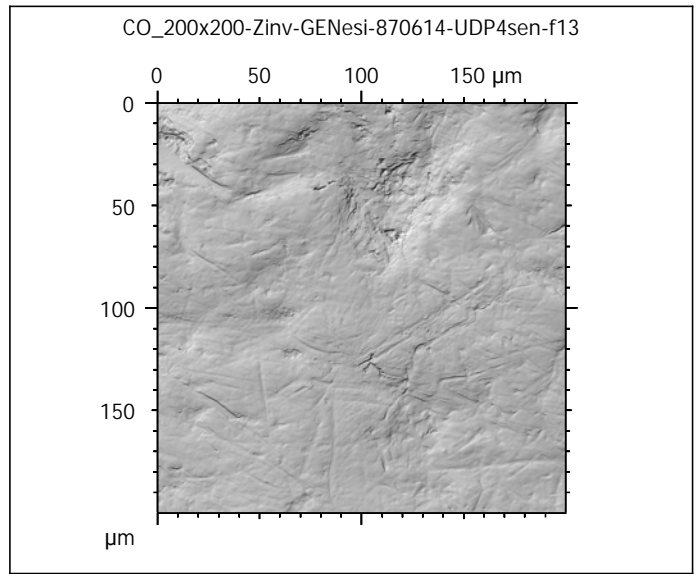
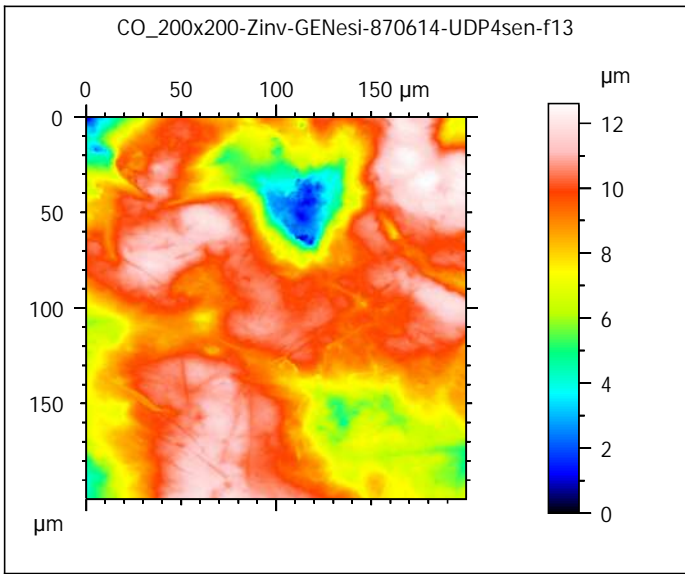
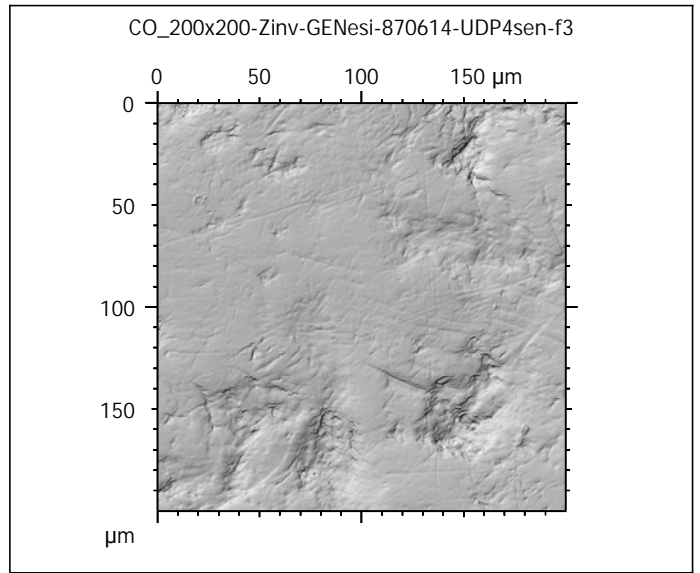
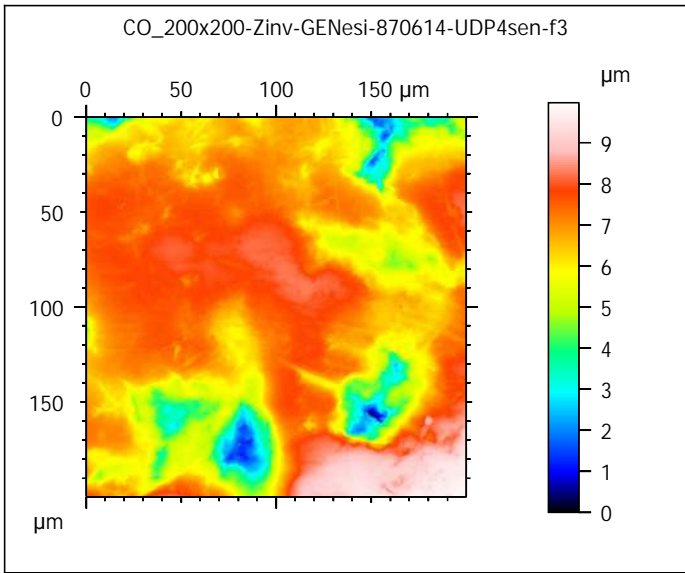




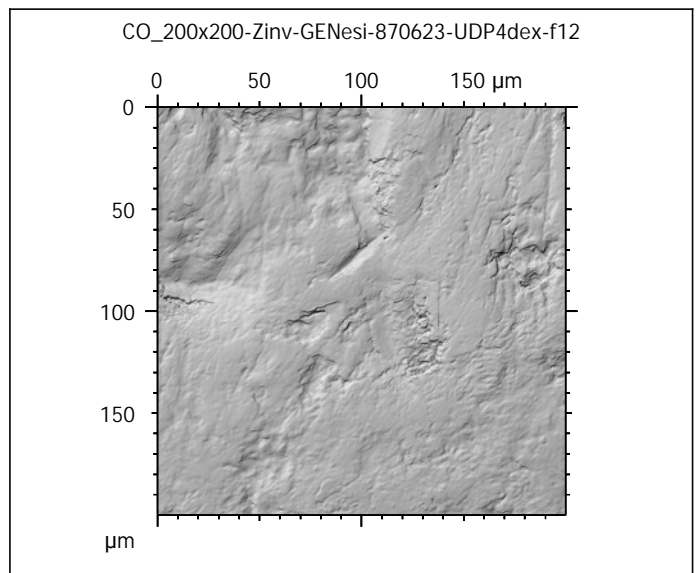
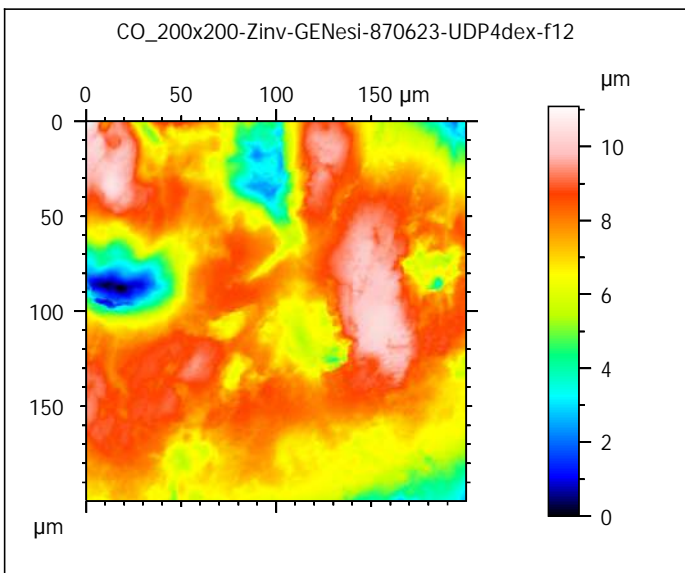
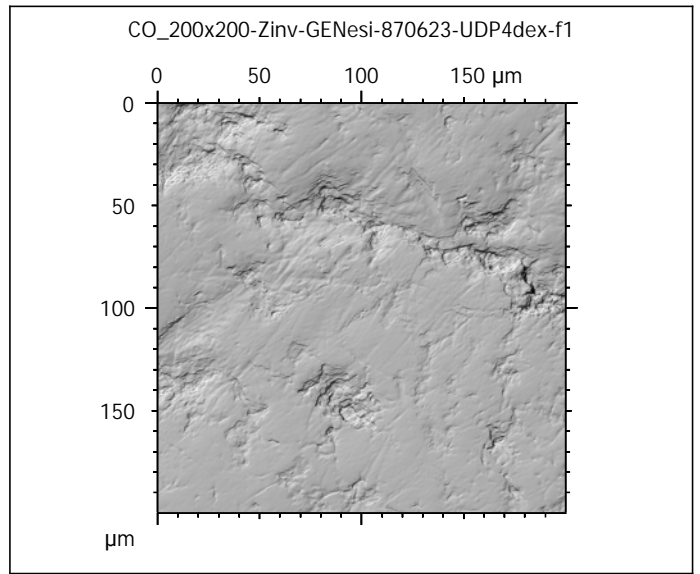
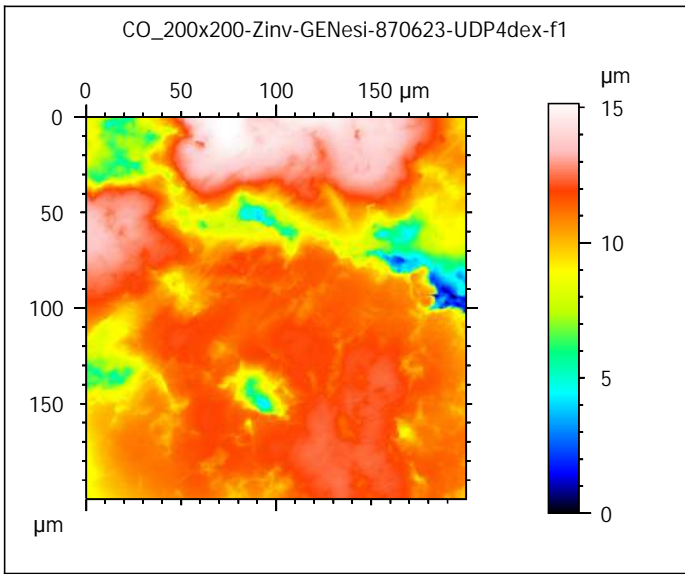
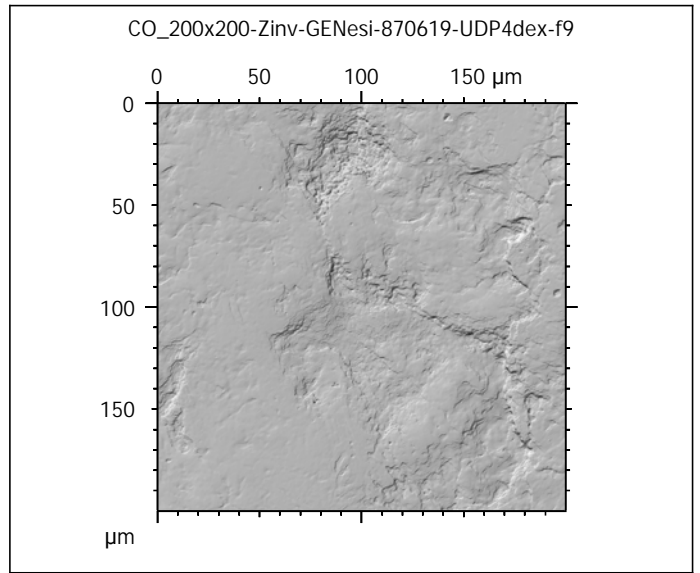
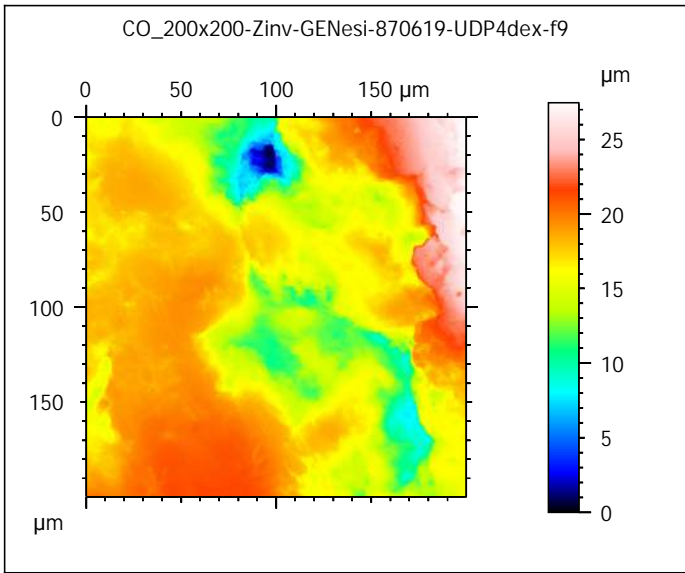


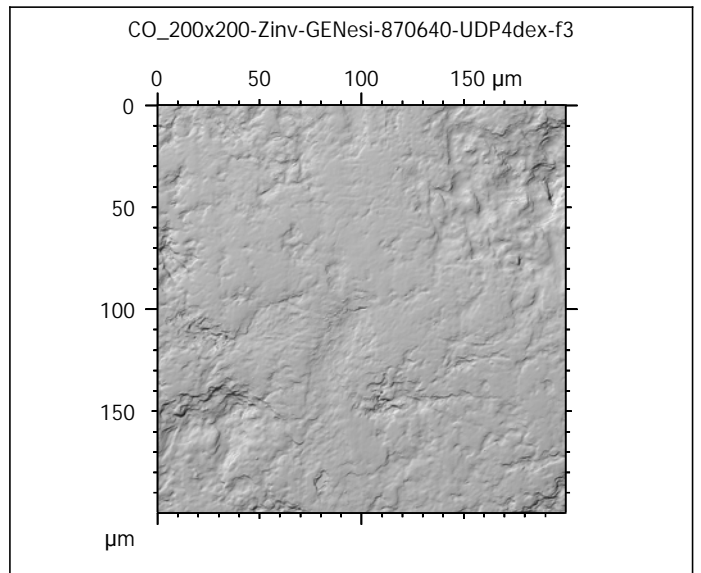
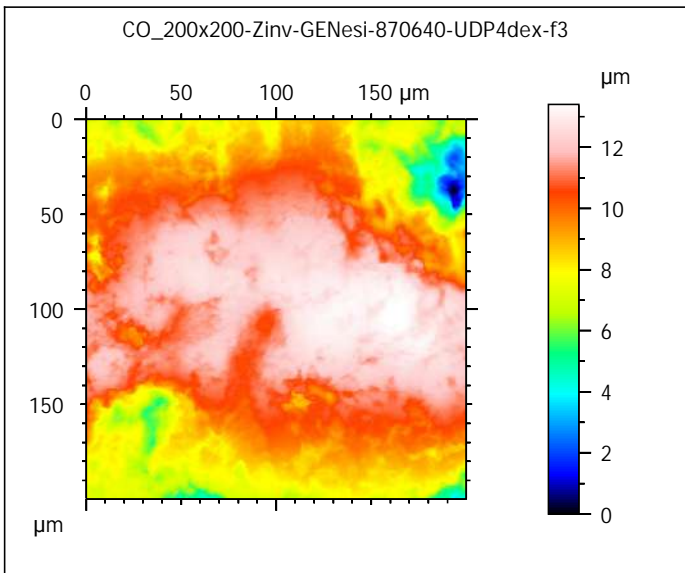
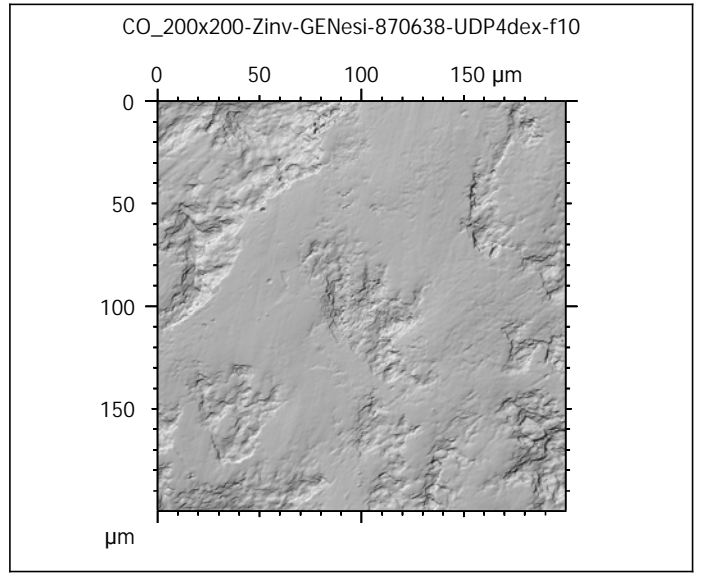
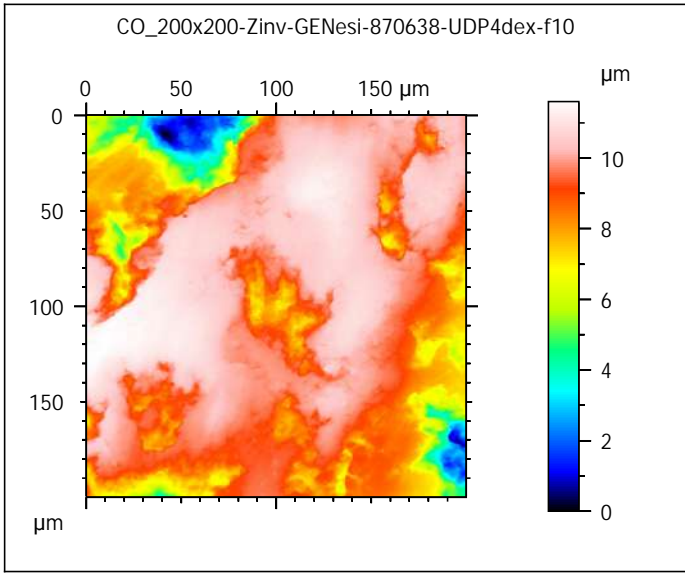
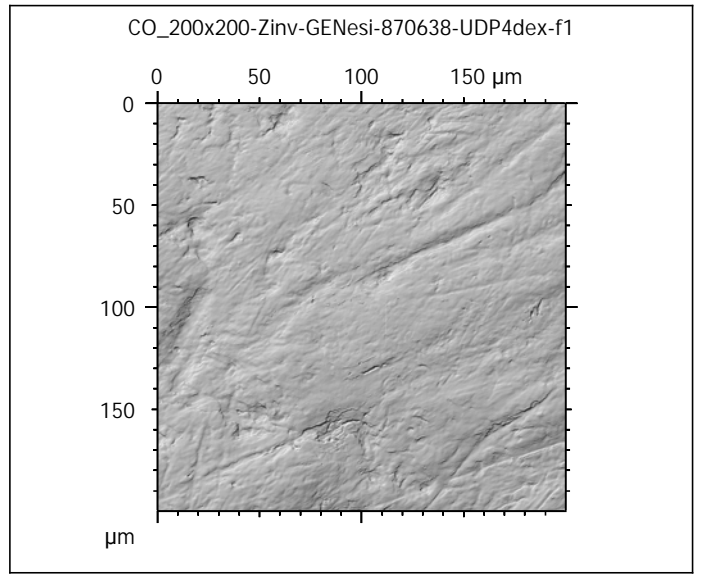
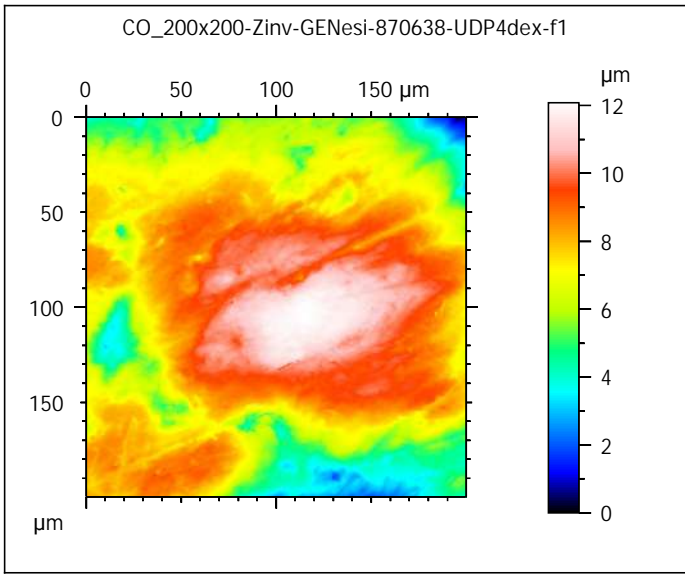


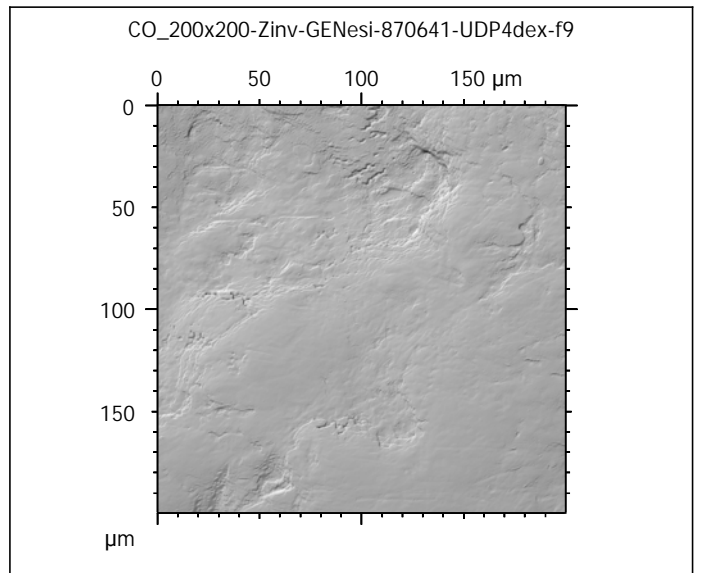
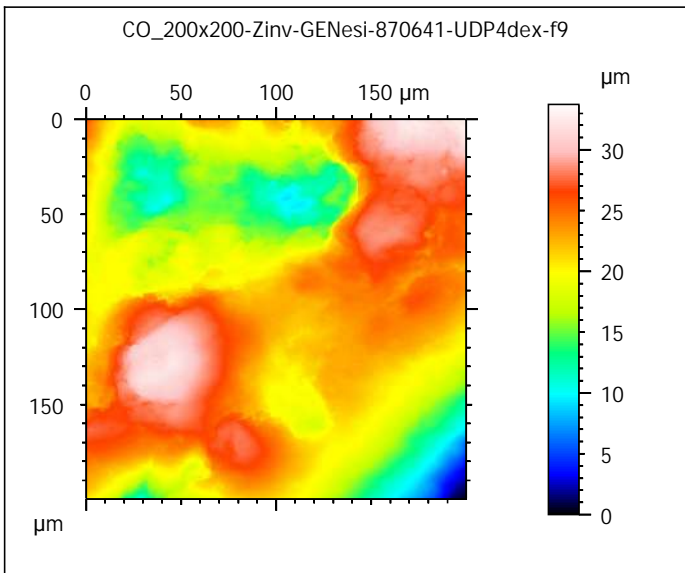
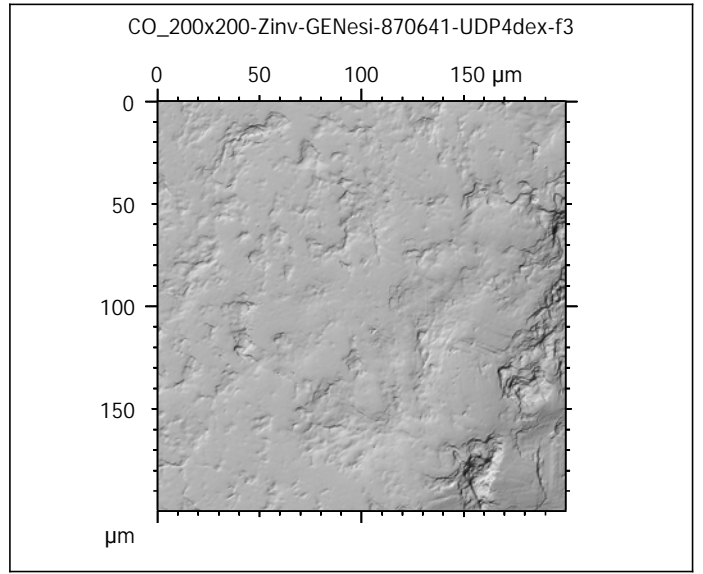
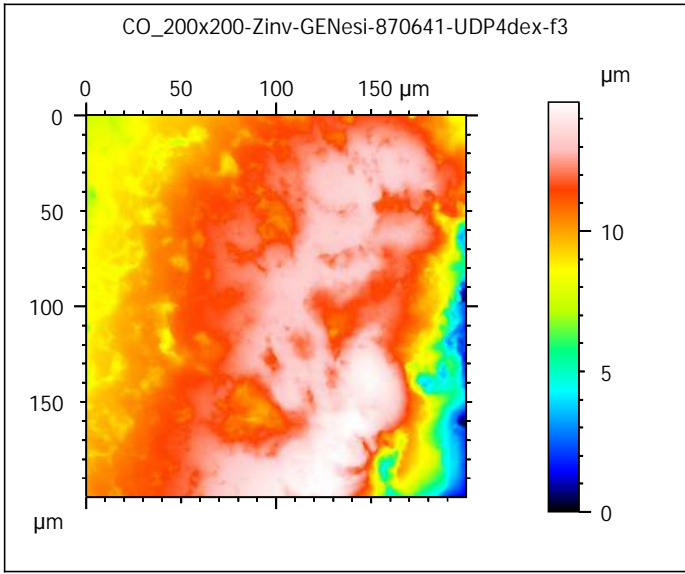
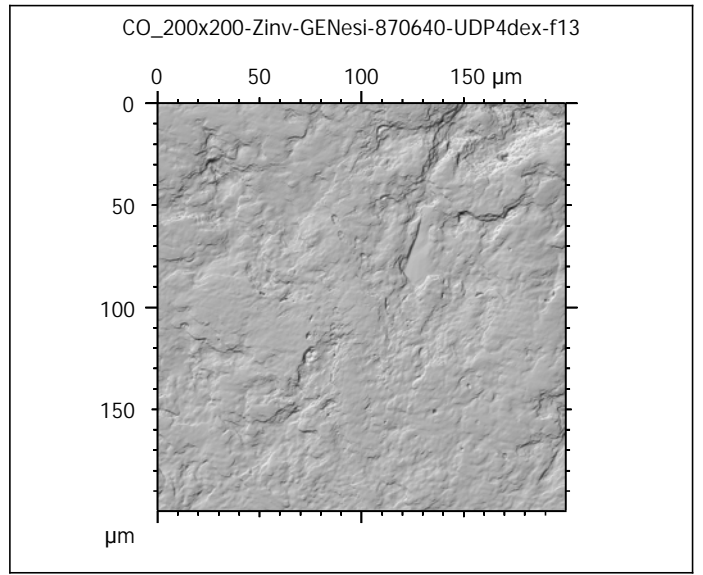
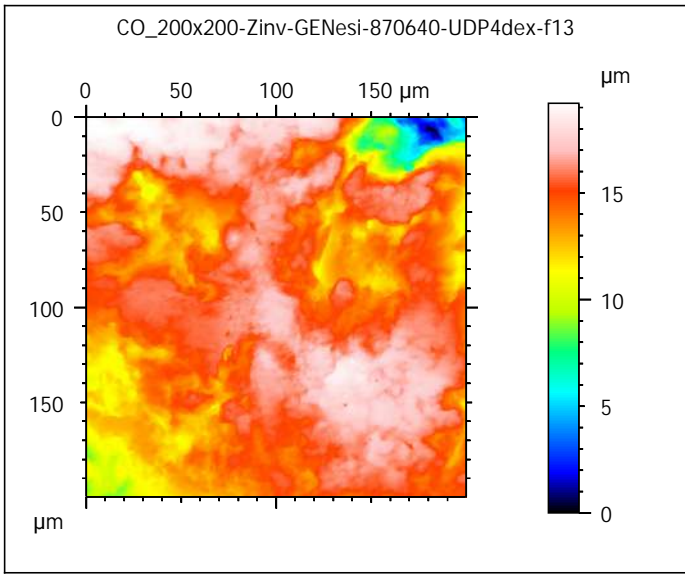














Photosimulations and false color elevation maps of scanned shearing and crushing facets on molars and deciduous premolars of the **barley group** (70% base diet + 30% barley seeds)

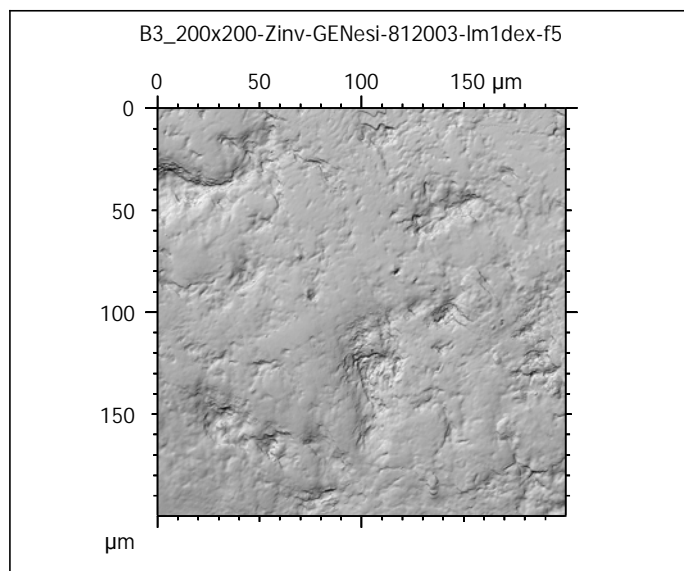
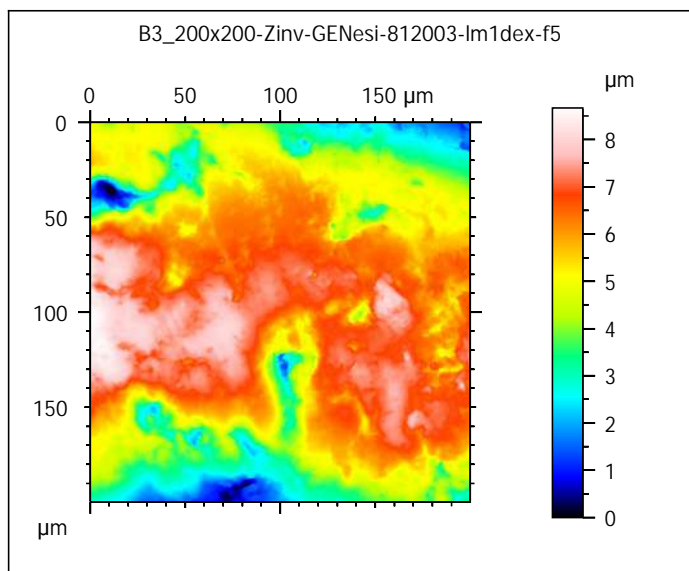
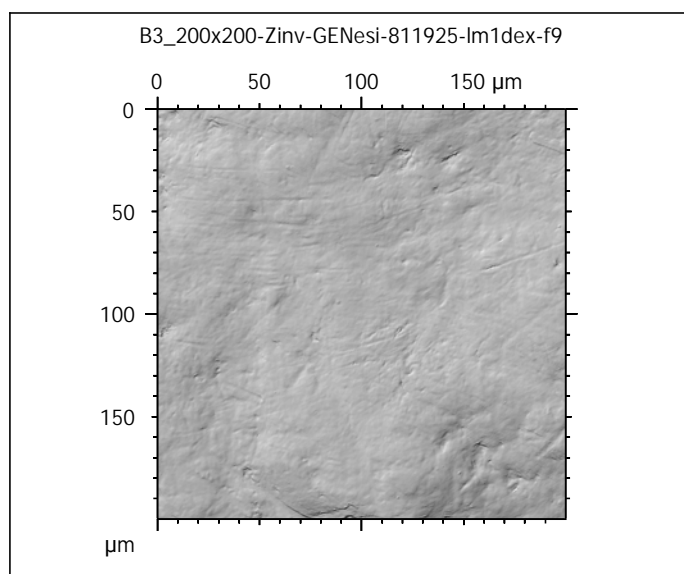
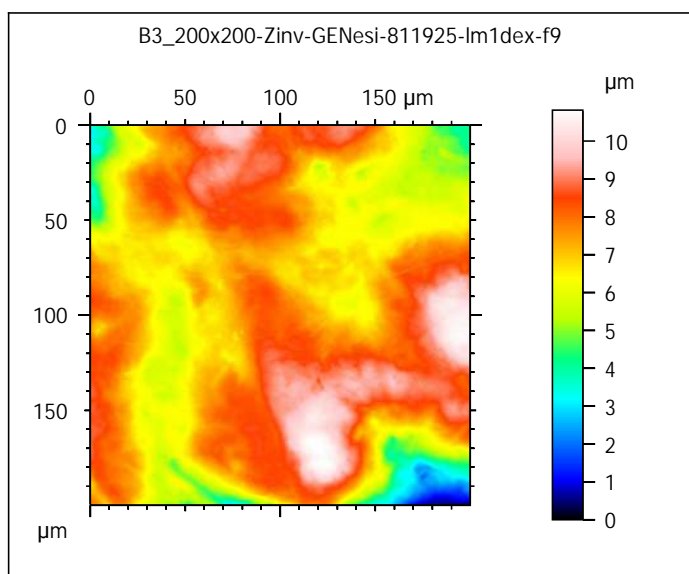
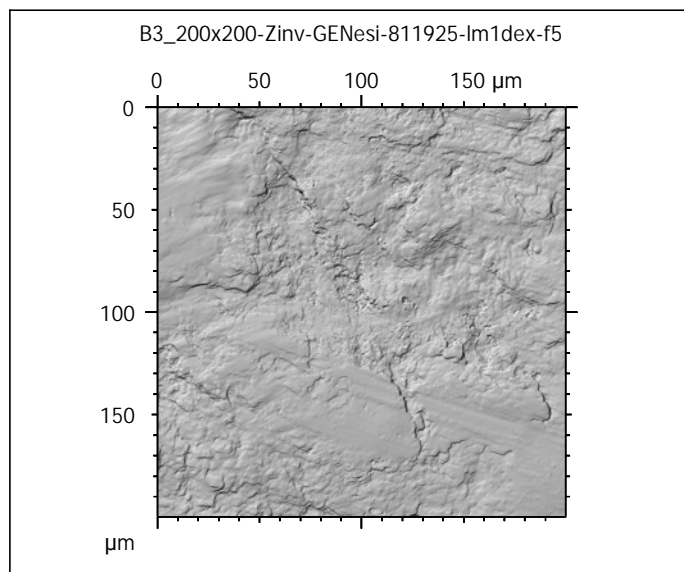
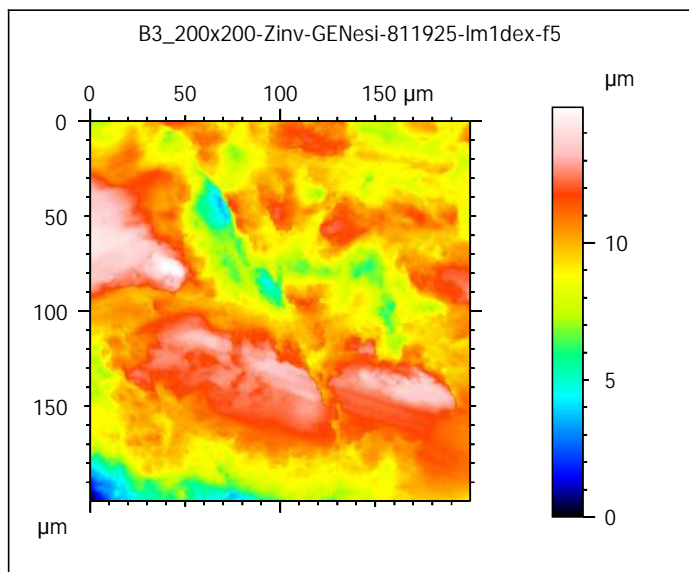
scanned at the PALEVOPRIM lab by M. Louail, University of Poitiers, France with "TRIDENT", white light confocal microscope Leica DCM8 - April 2020

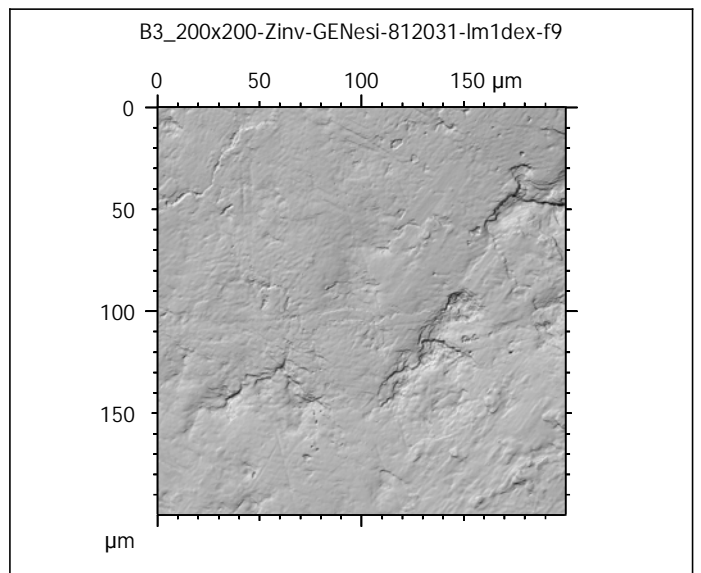
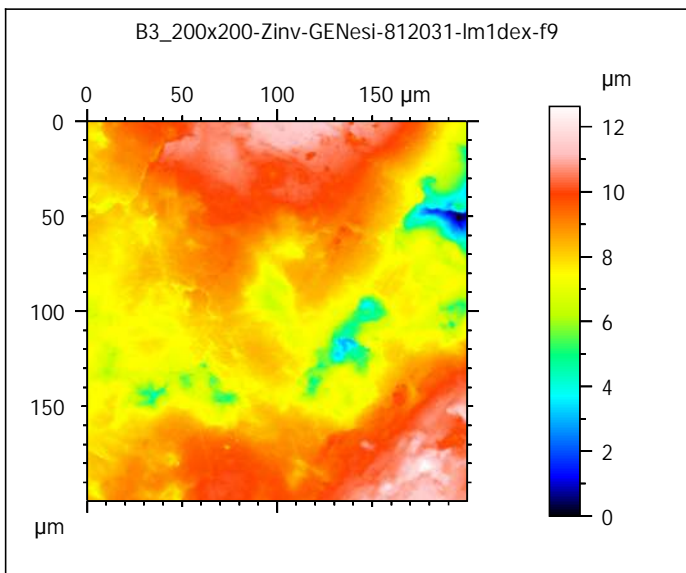
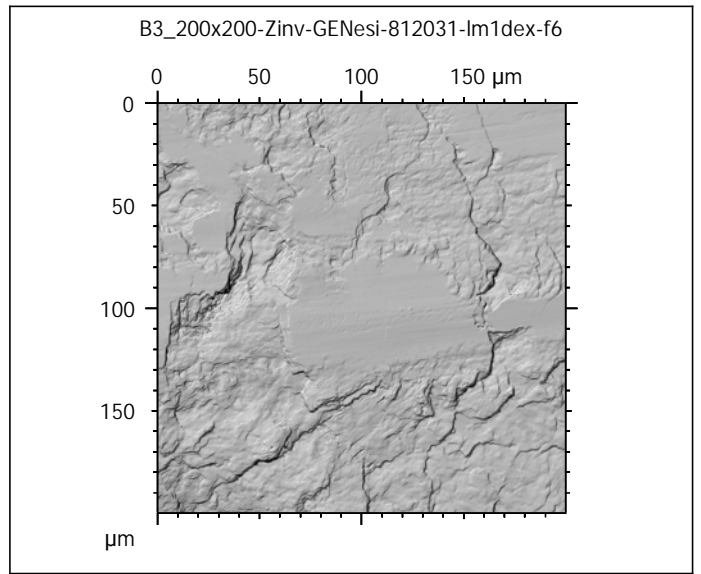
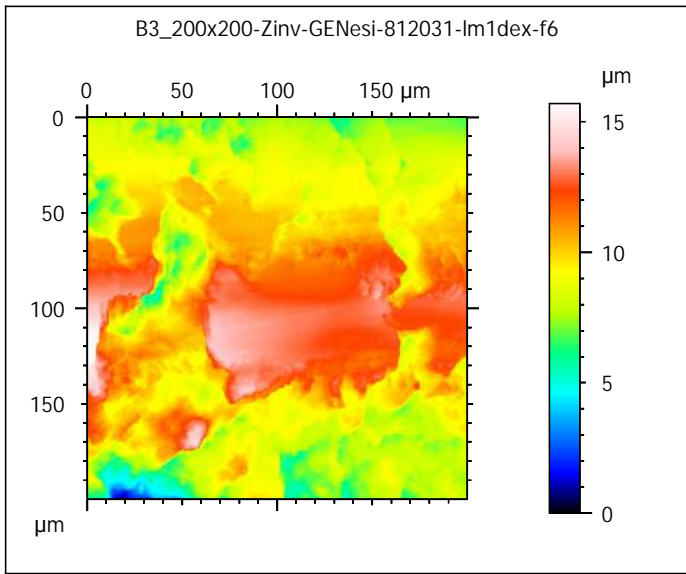
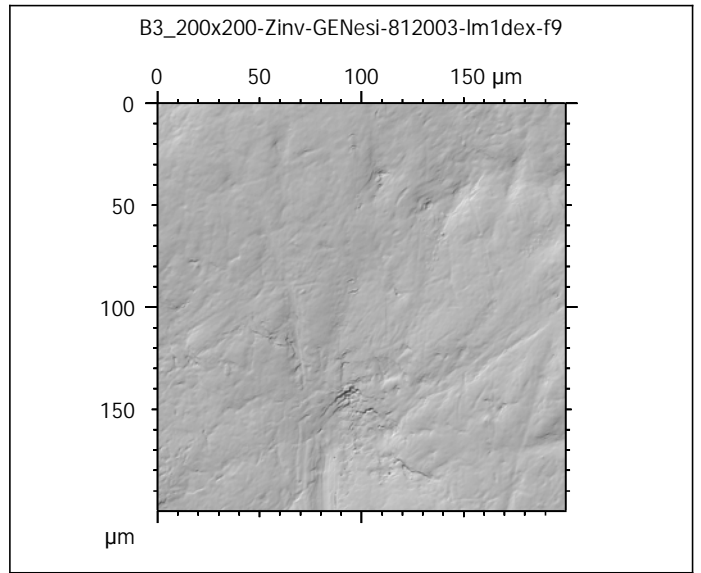
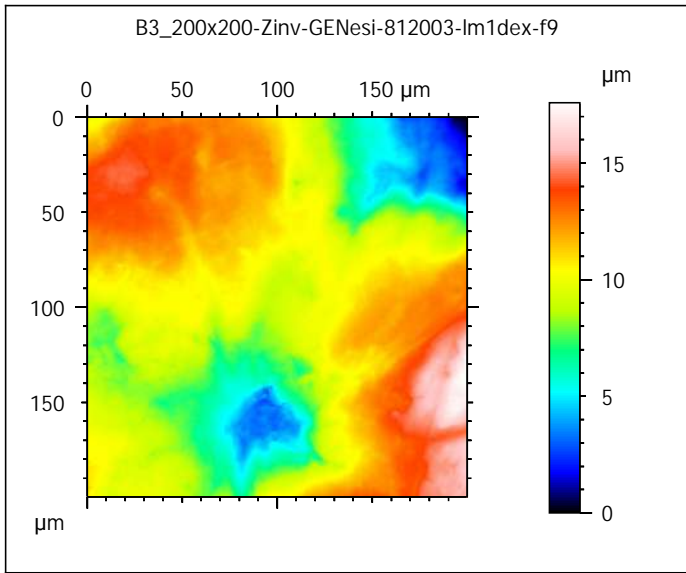
ALIHOM Project (Région Nouvelle Aquitaine, France), ANR Diet-Scratches

**DIET-SCRATCHES**

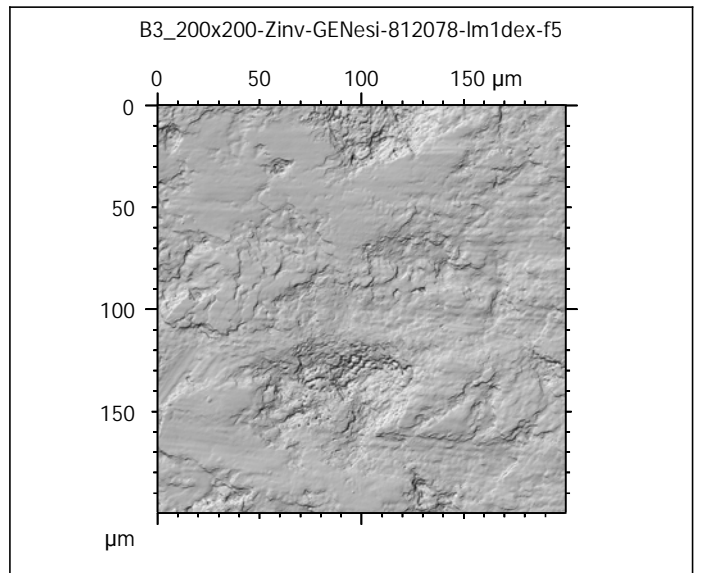
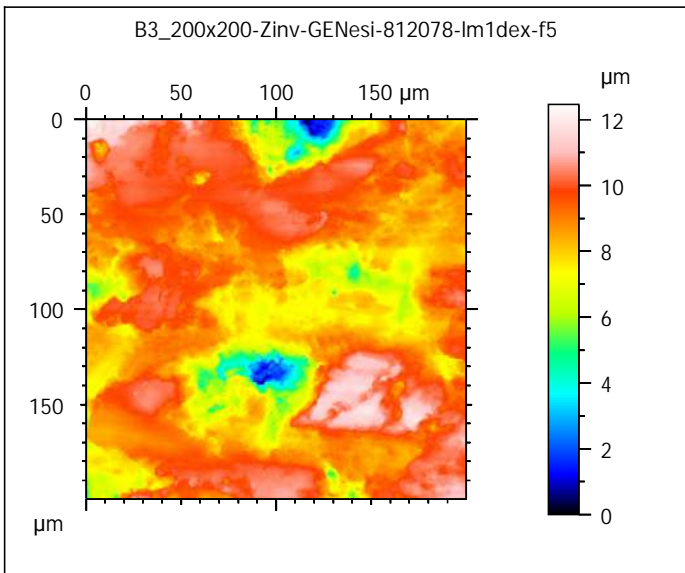
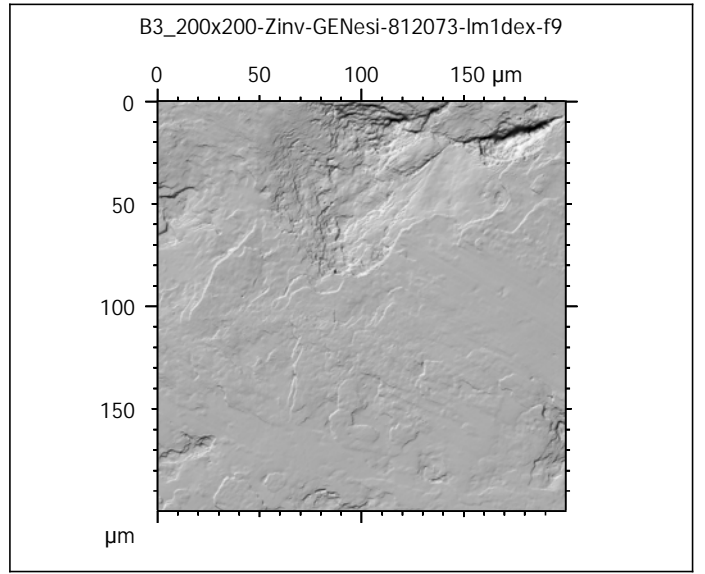
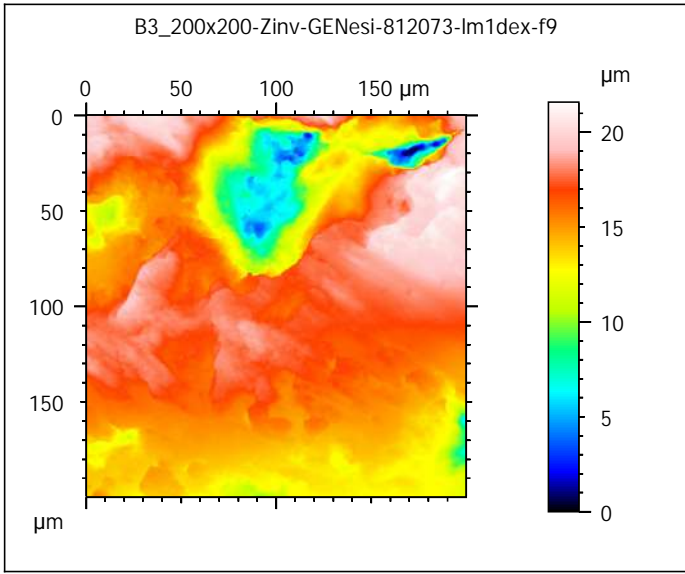
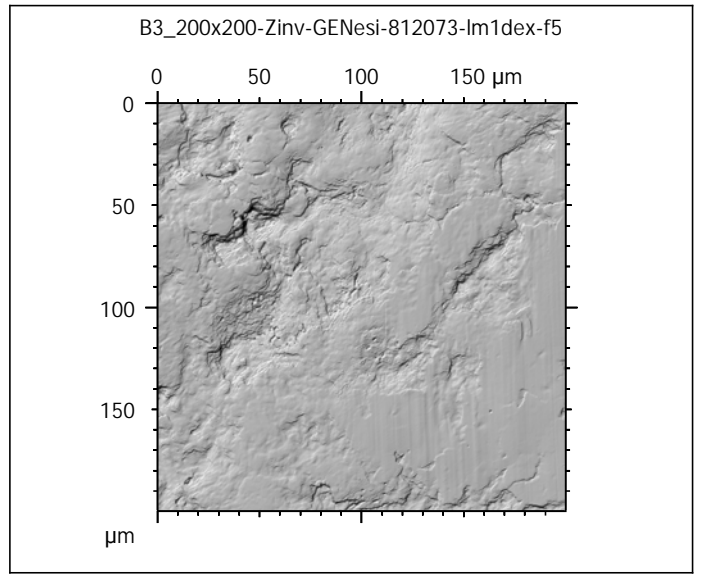
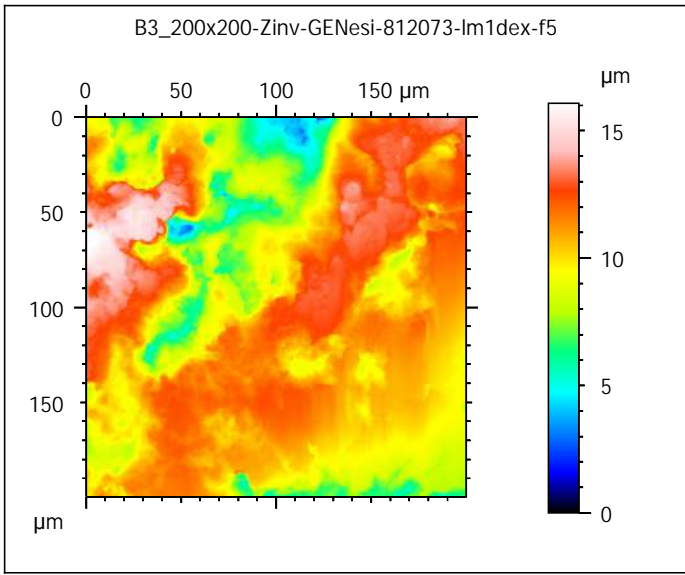
ANR-17-CE27-0002

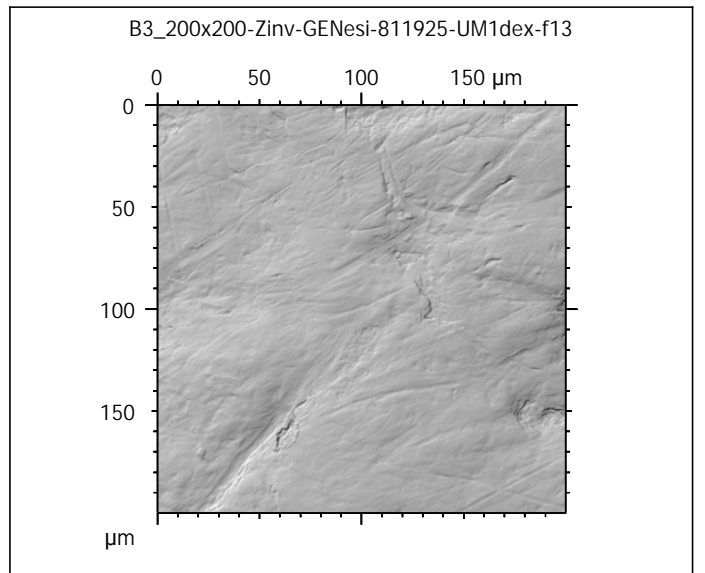
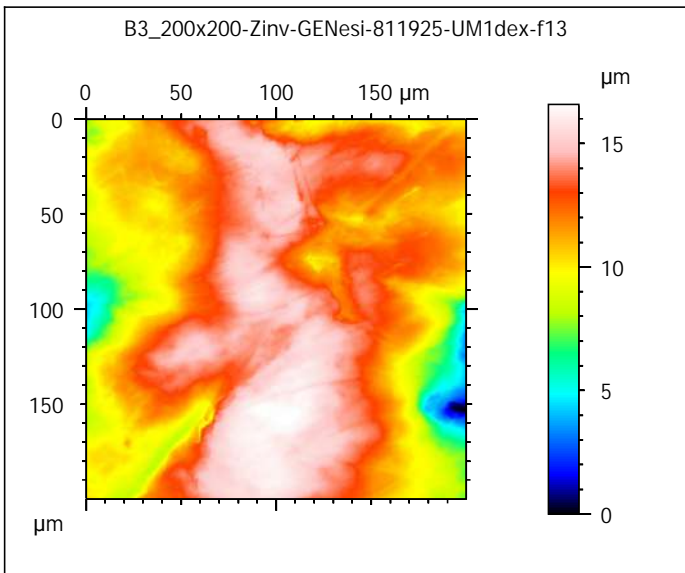
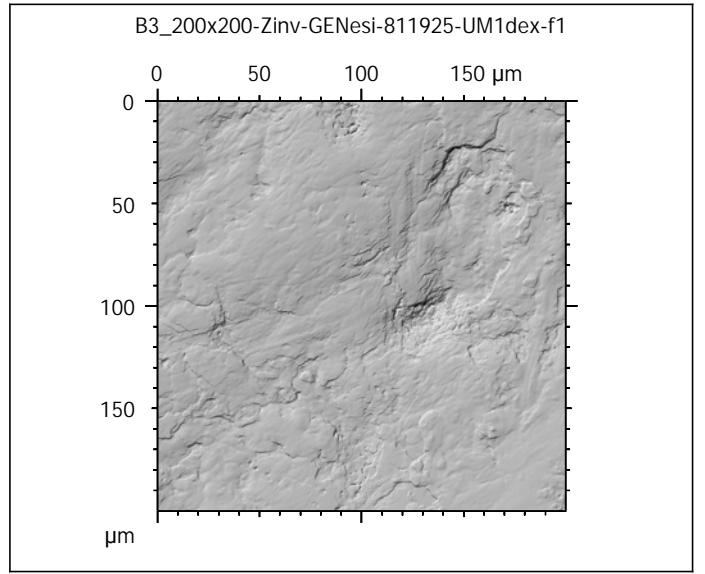
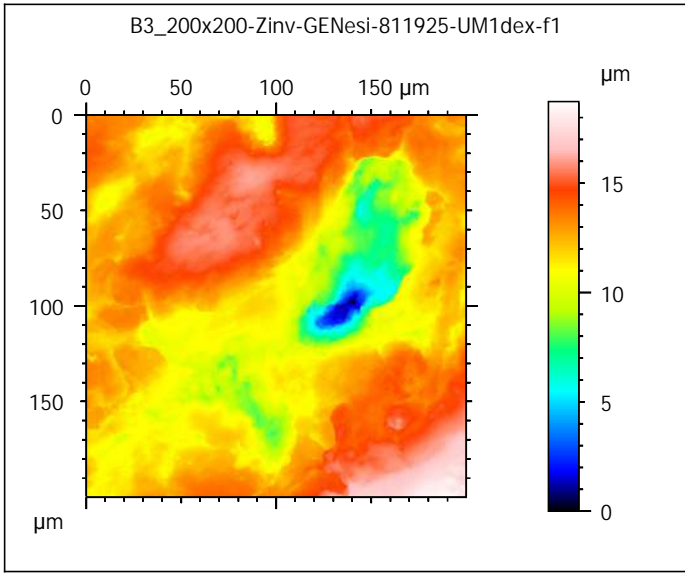
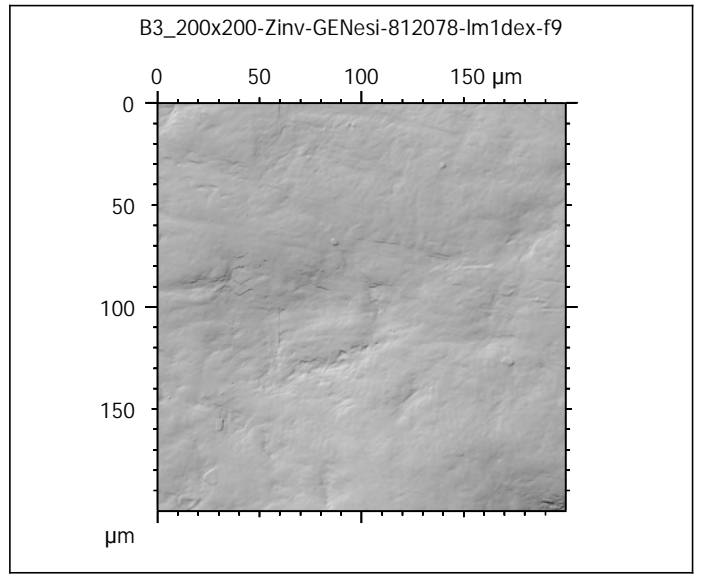
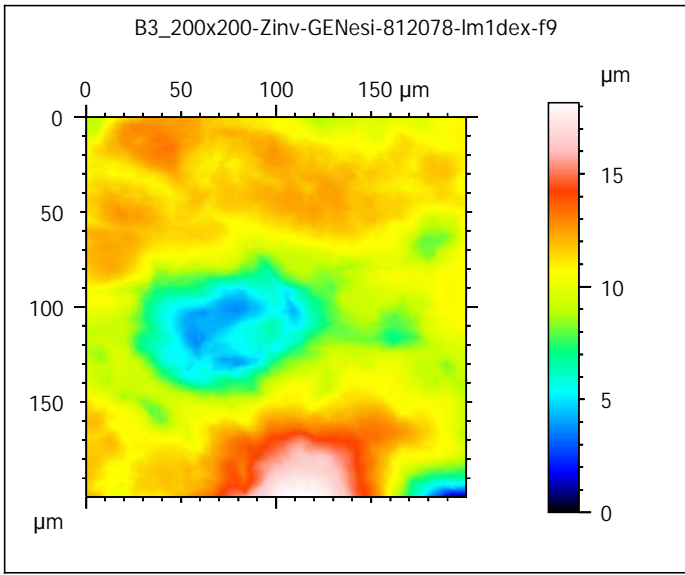
PIs: G. Merceron & S. Ferchaud

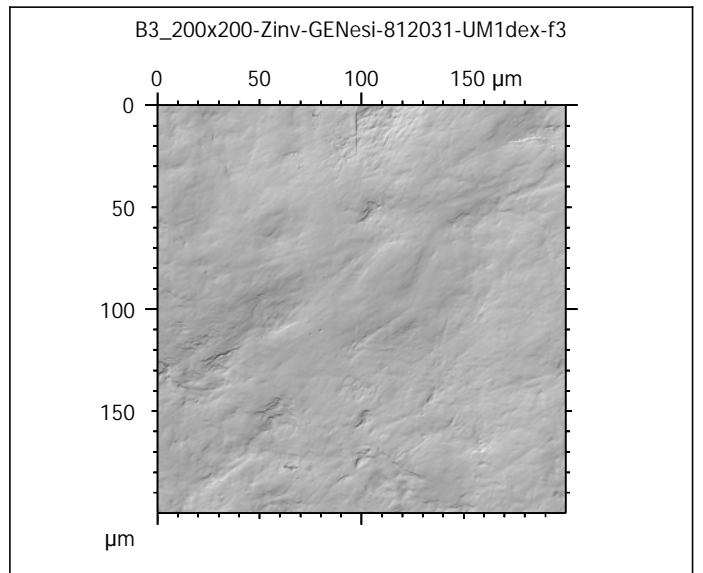
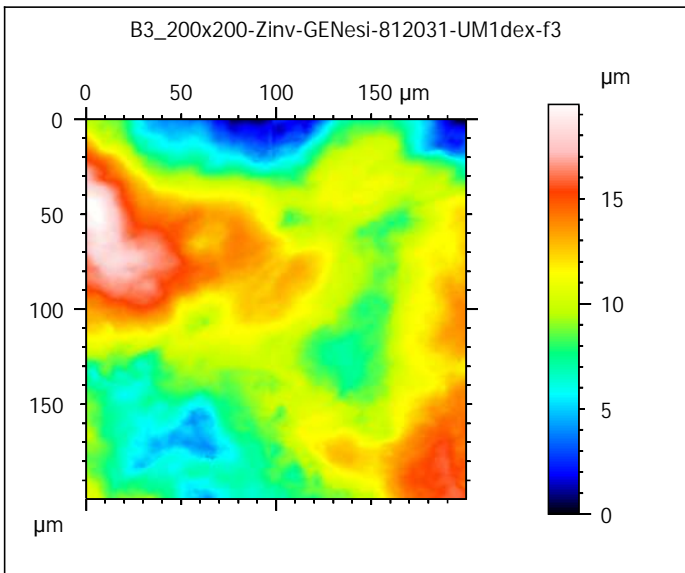
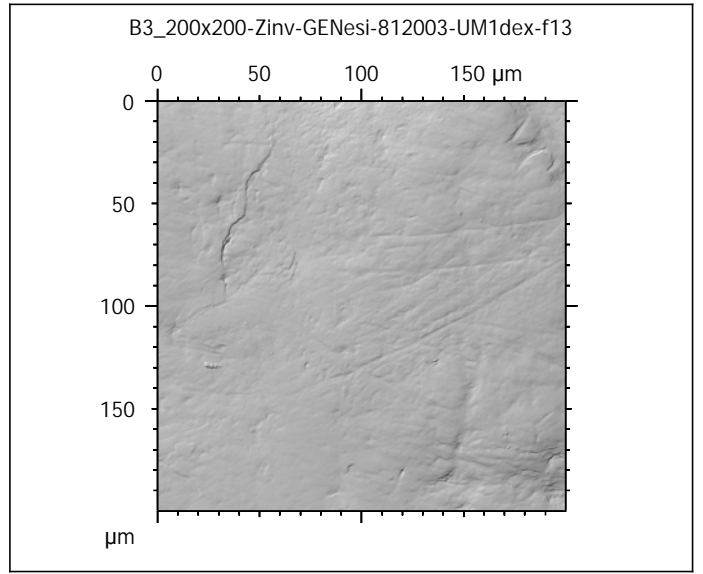
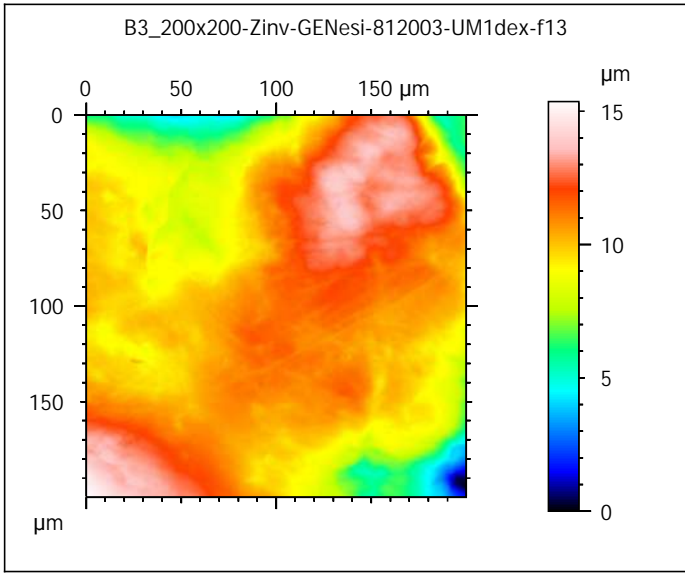
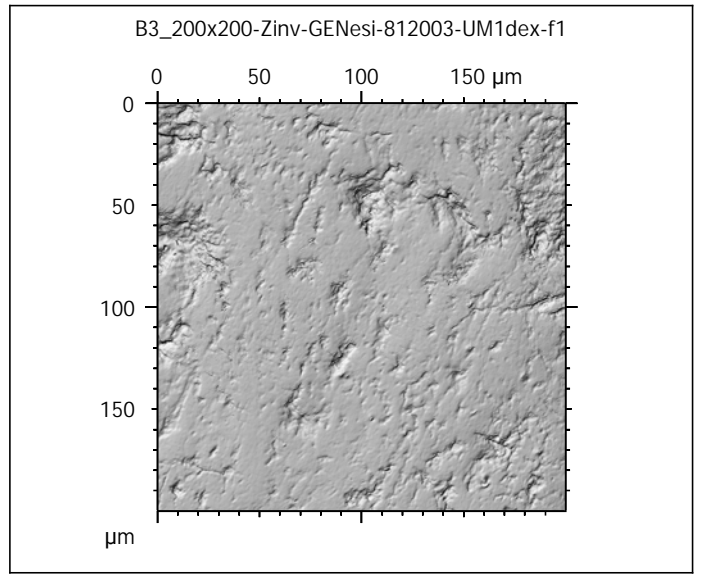
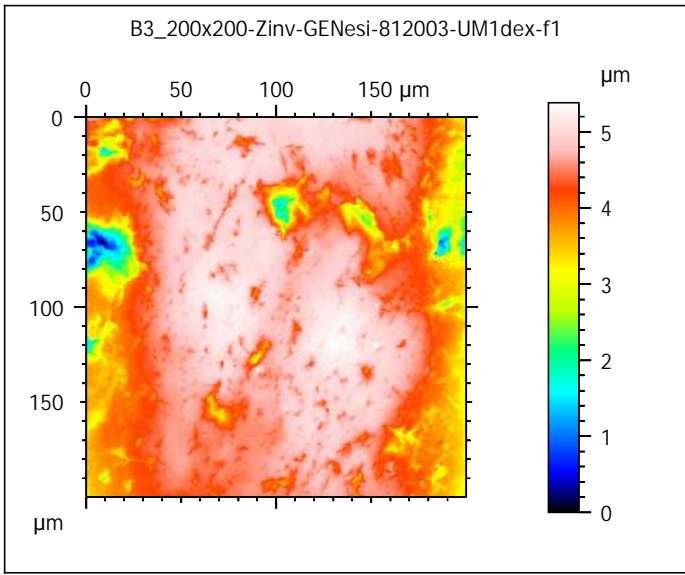




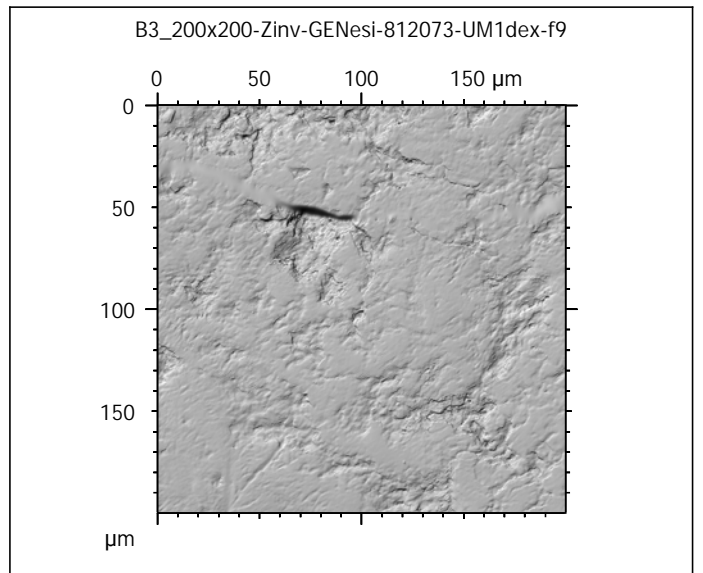
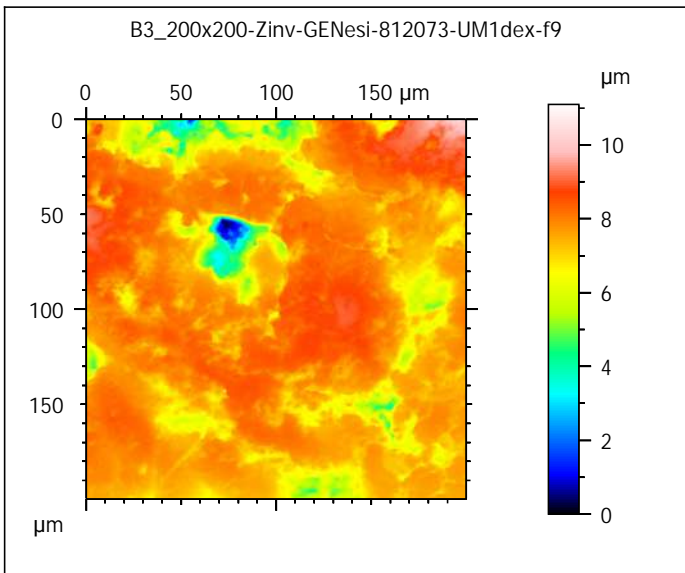
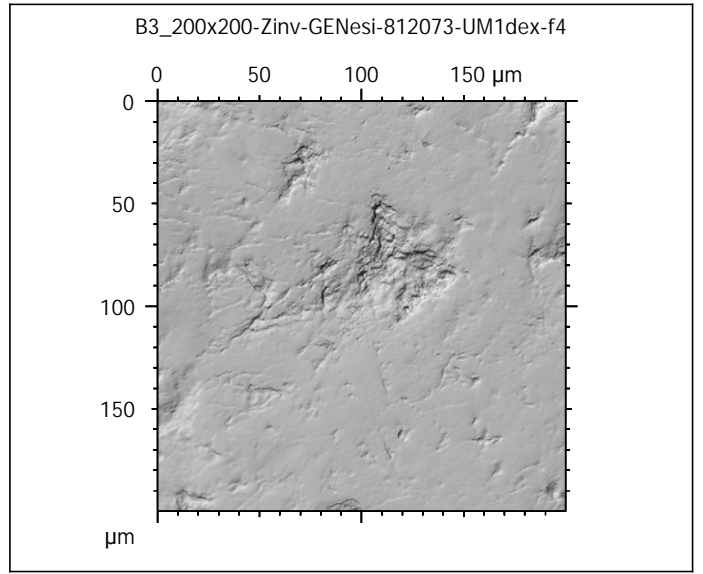
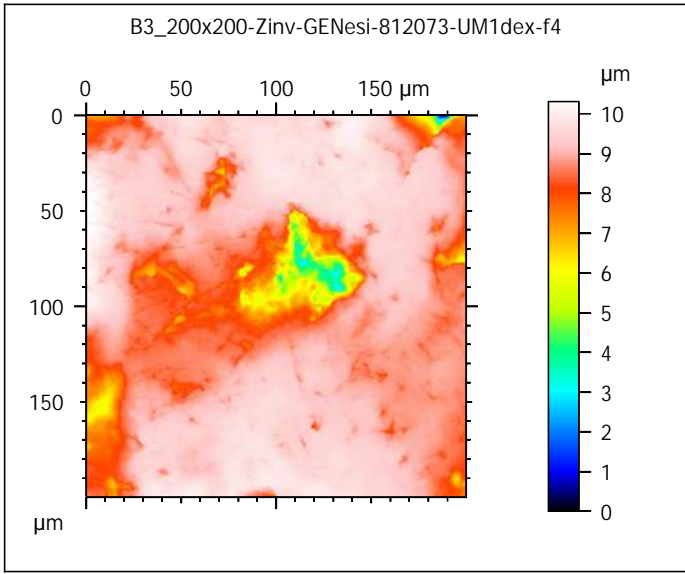
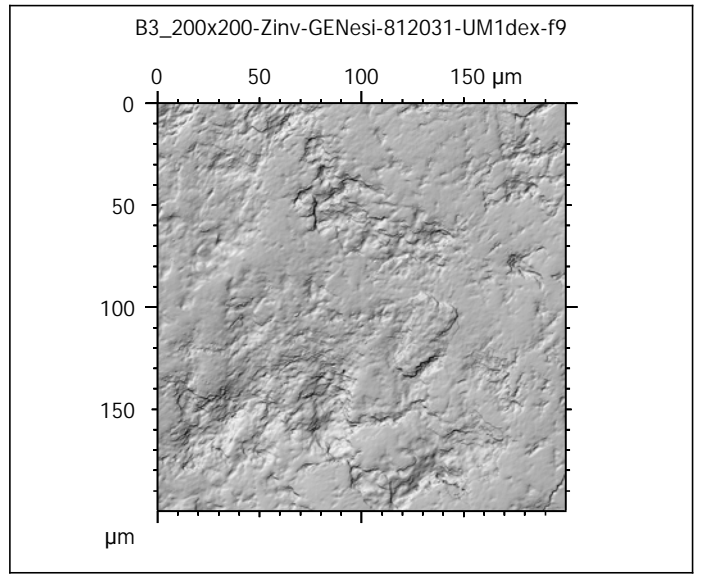
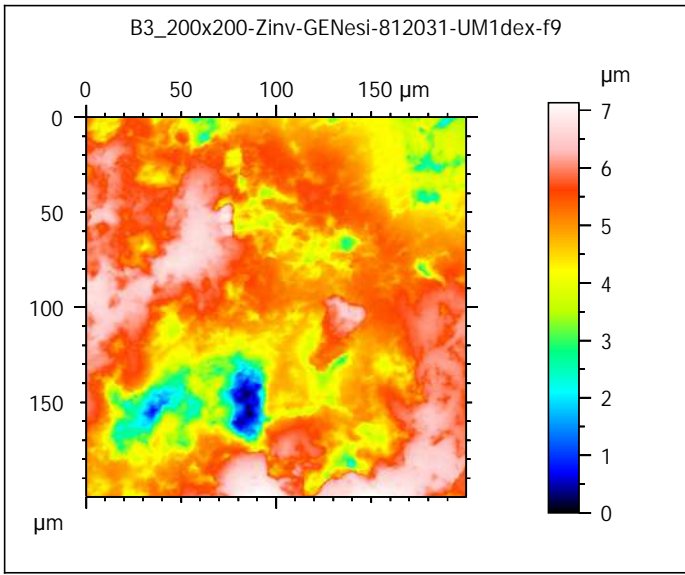


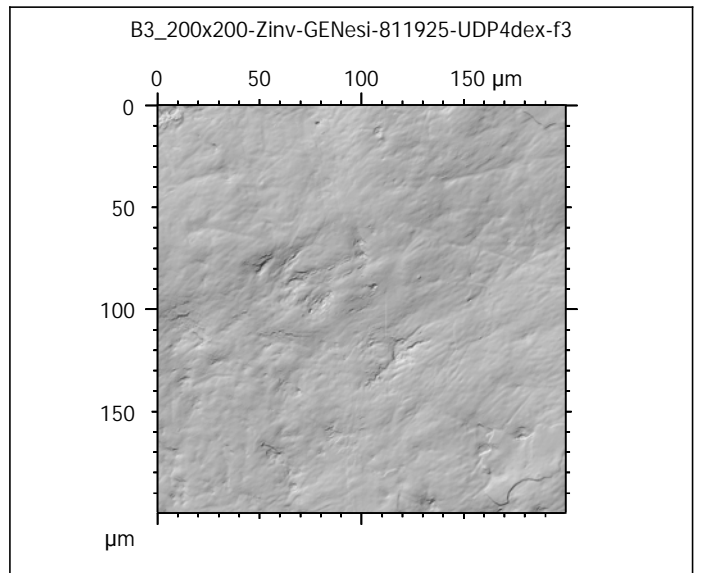
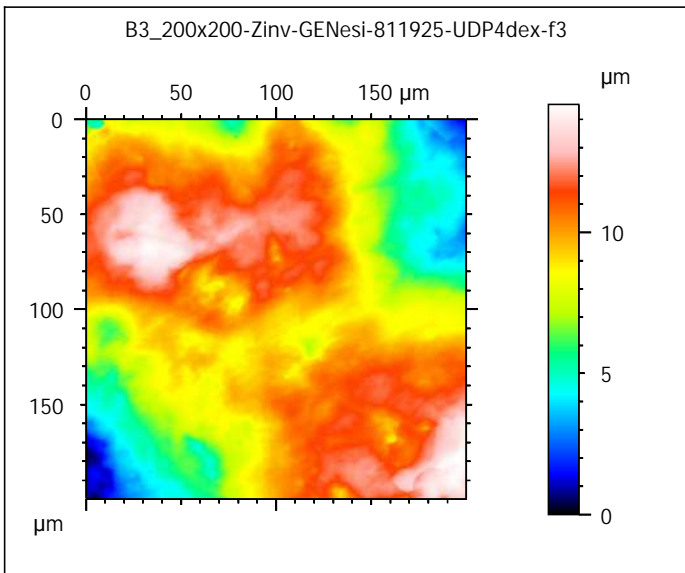
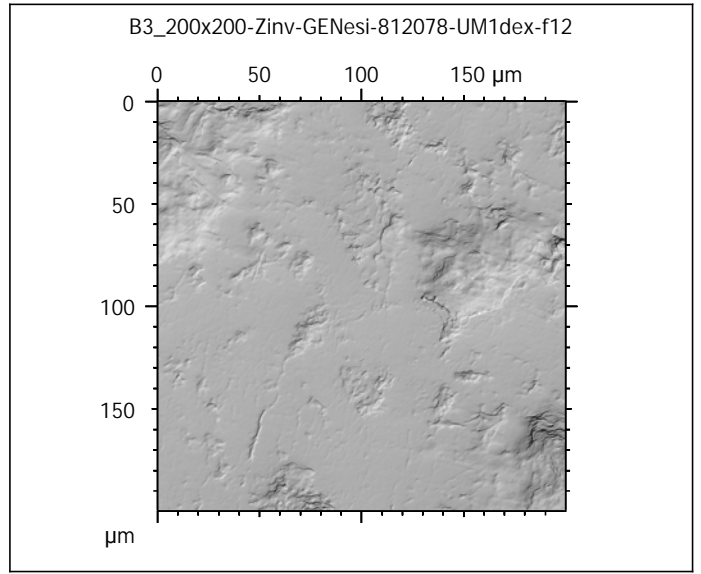
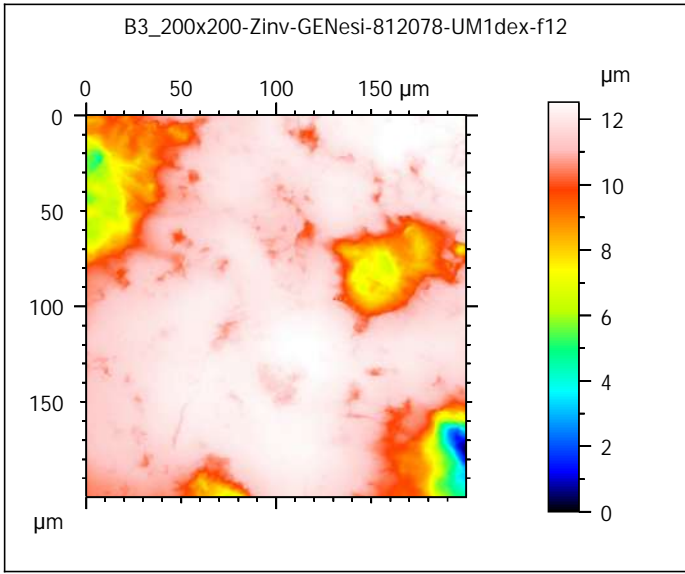
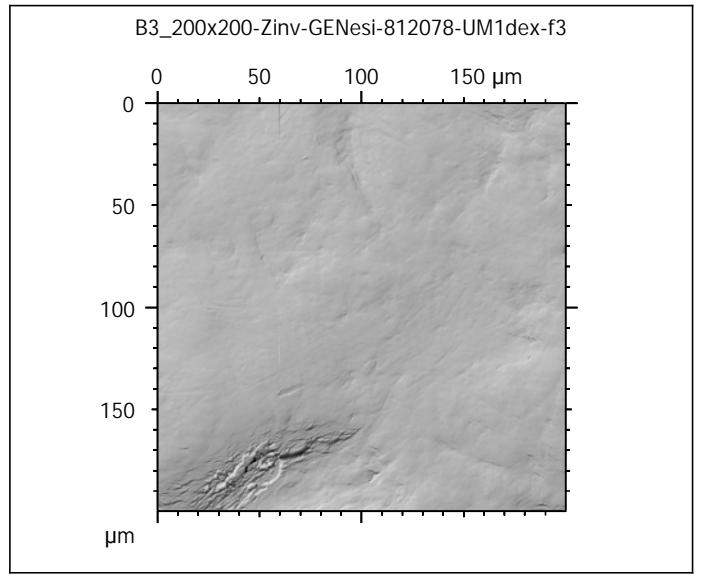
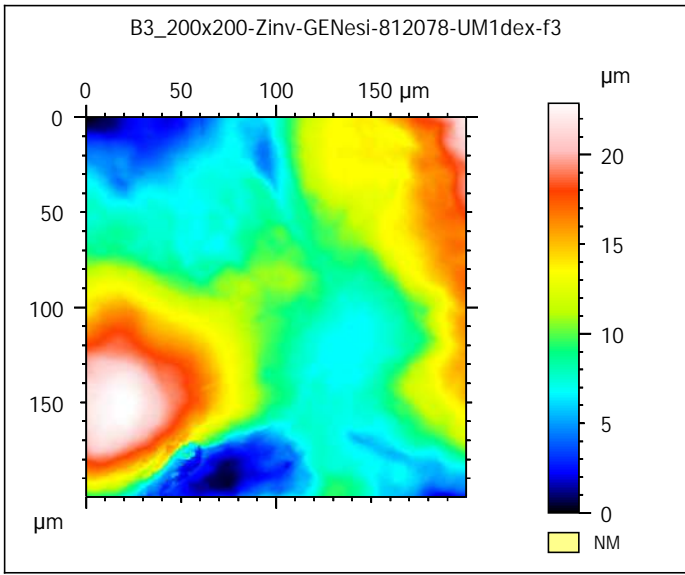


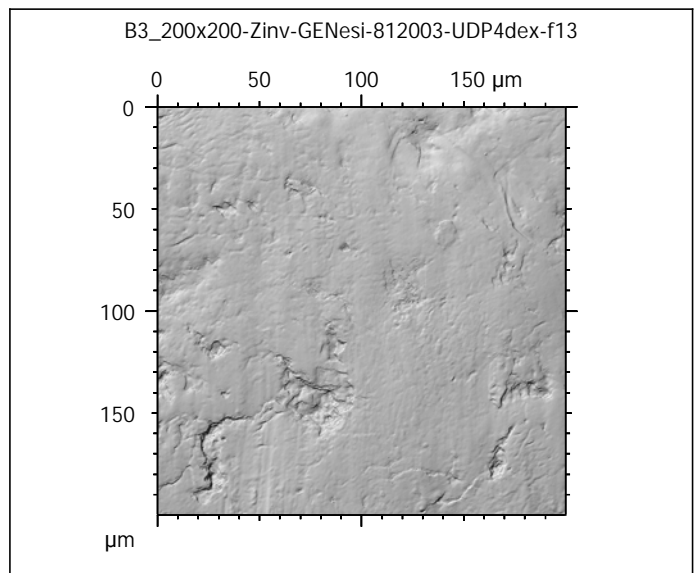
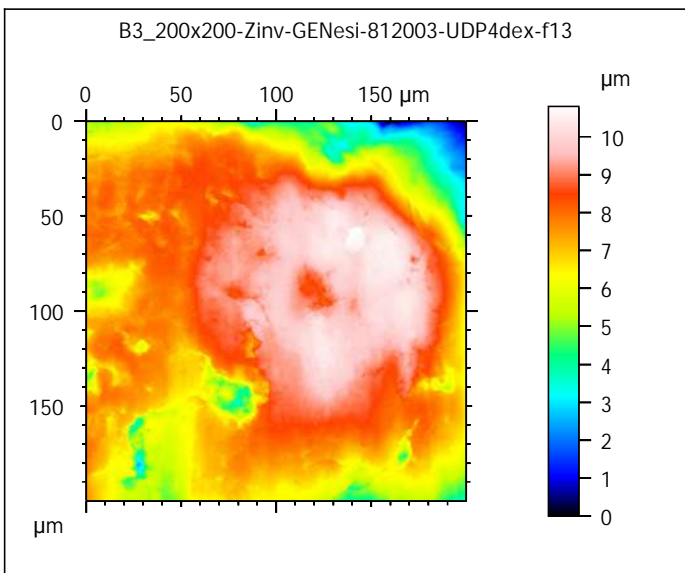
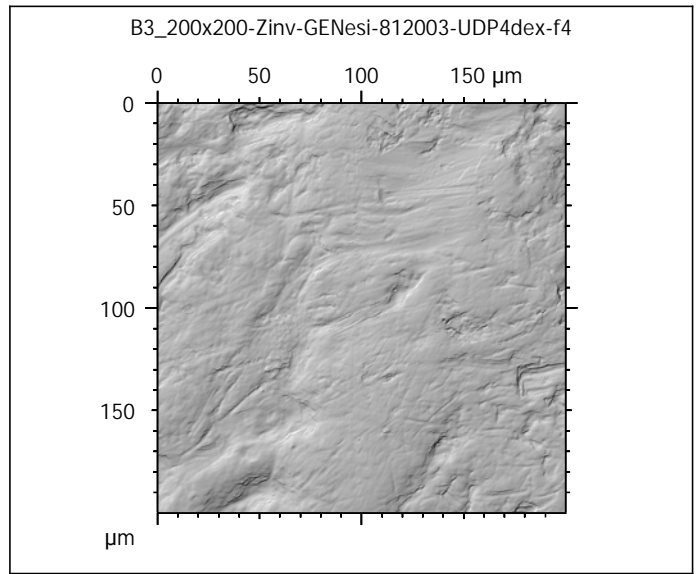
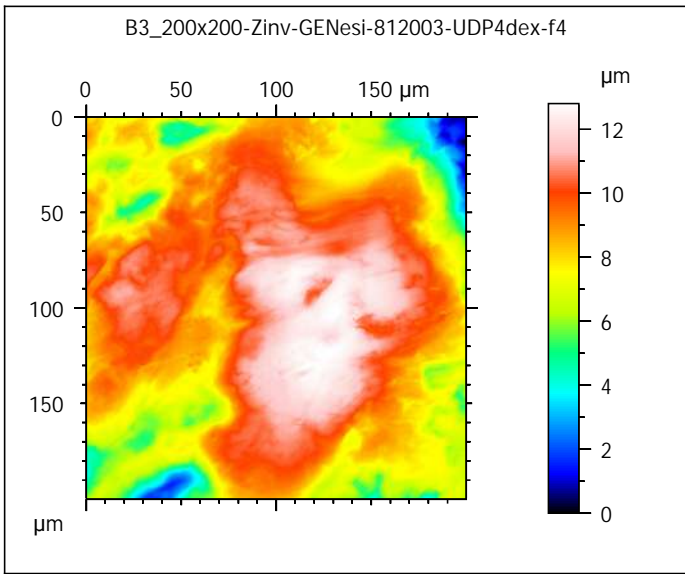
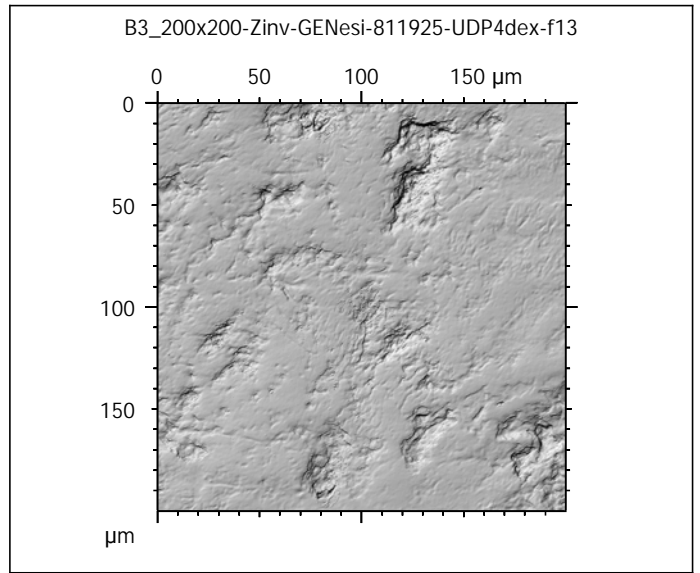
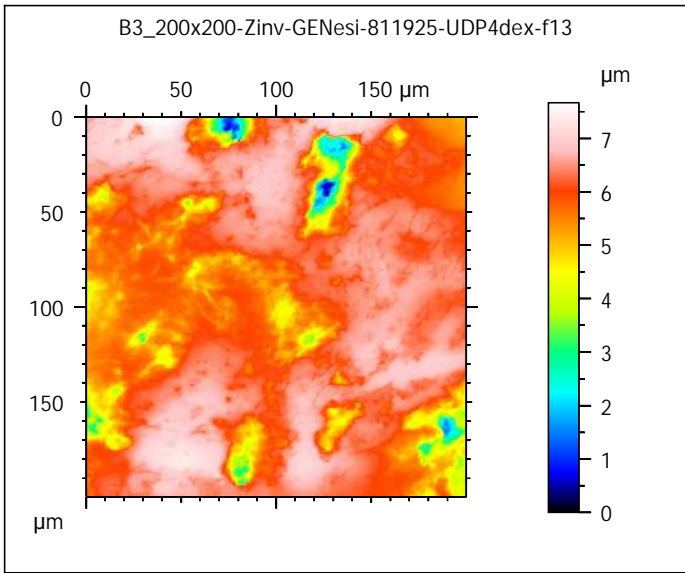




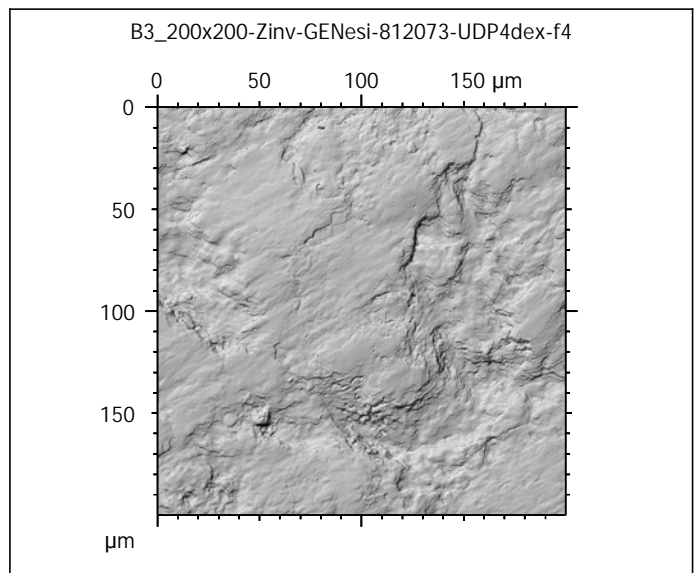
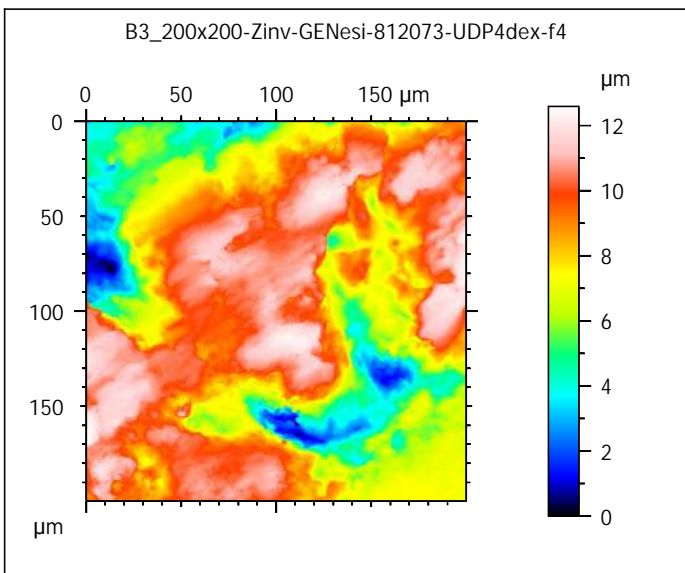
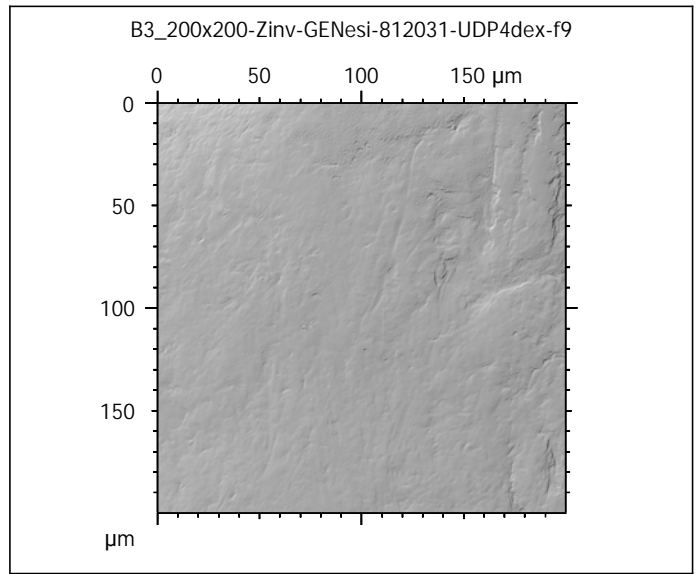
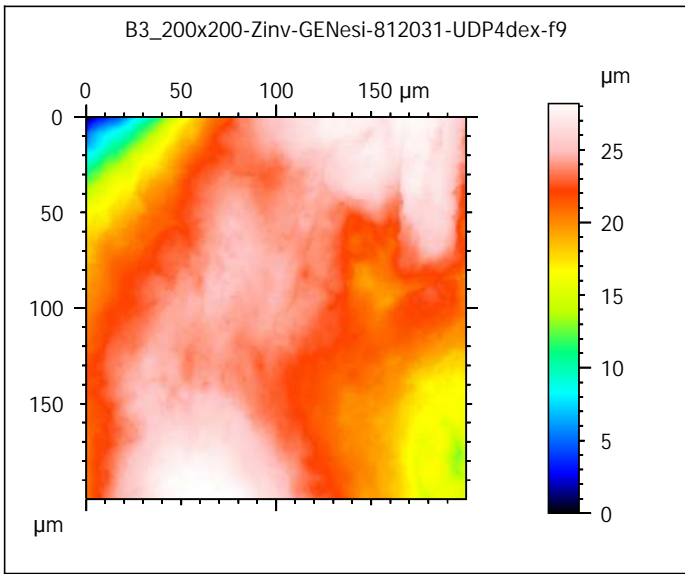
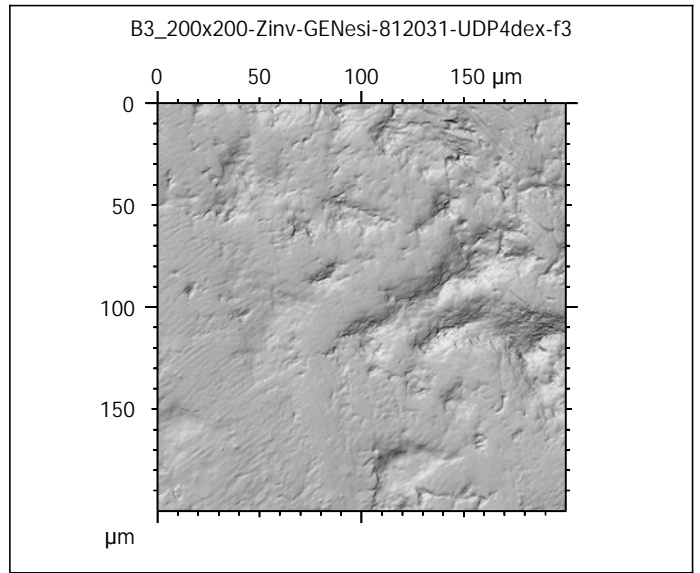
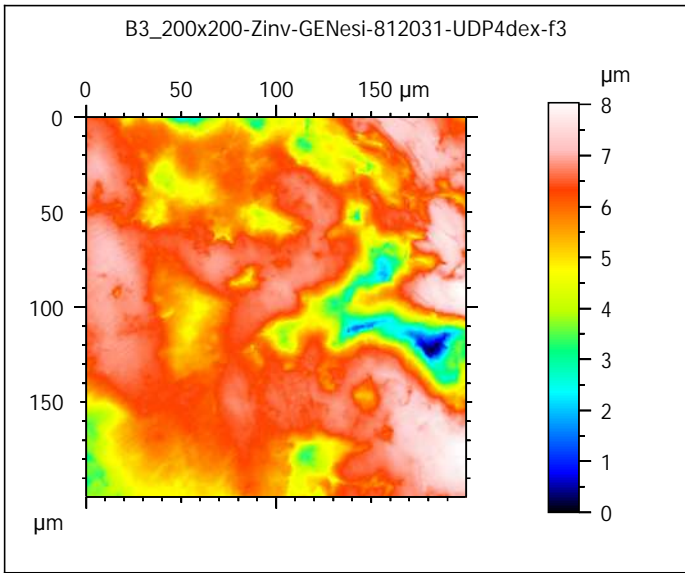


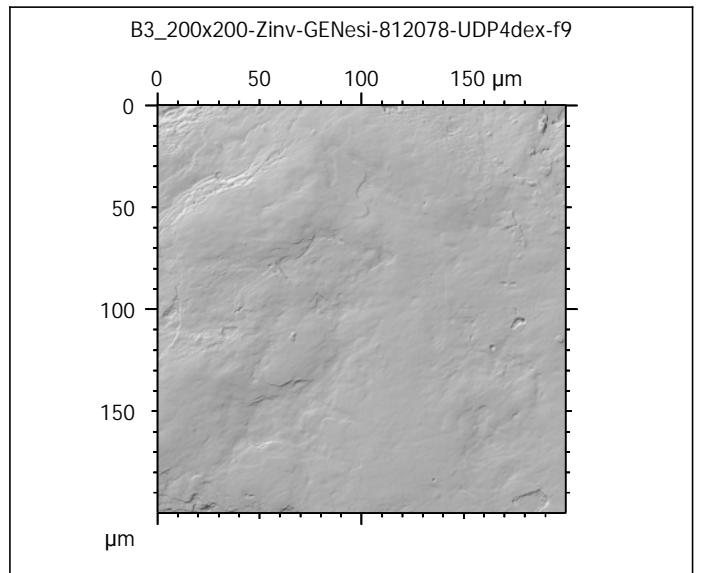
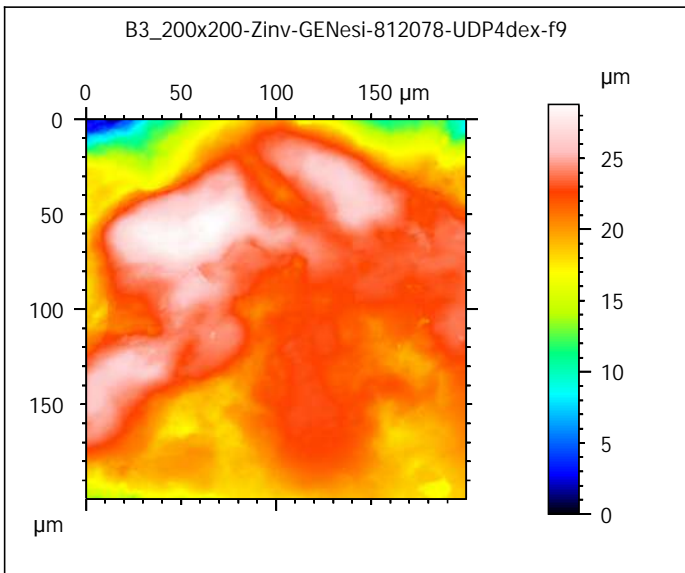
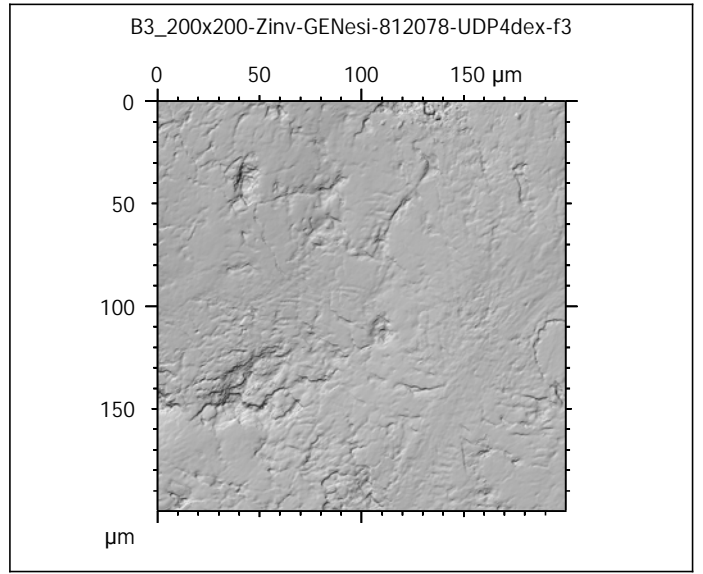
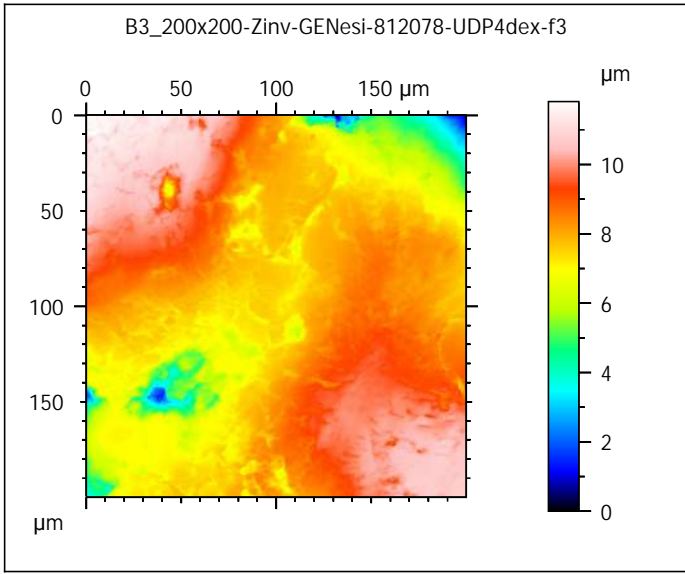
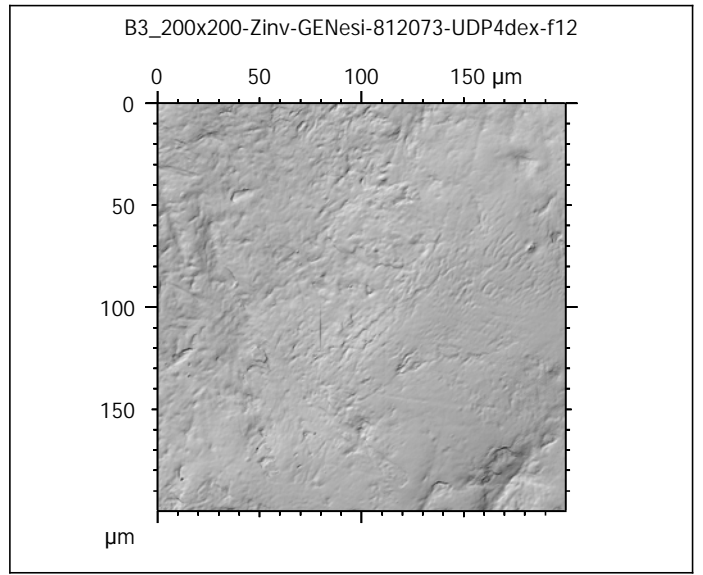
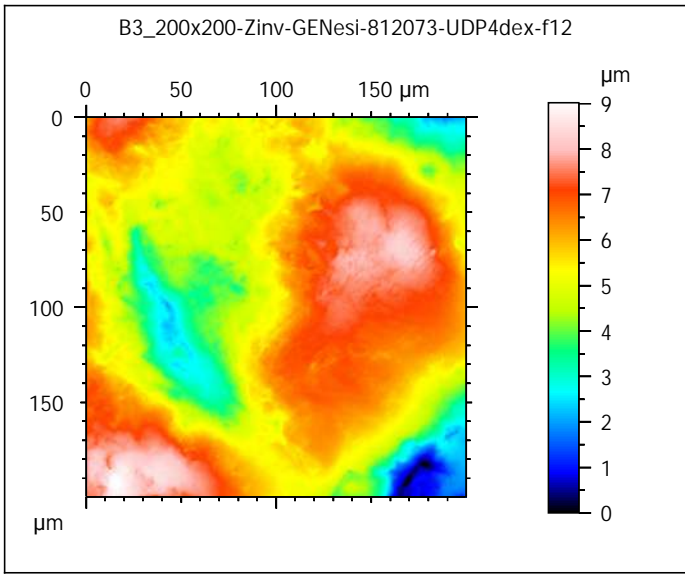














Photosimulations and false color elevation maps of scanned shearing and crushing facets on molars and deciduous premolars of the **corn group** (60% base diet + 20% corn flour + 20% corn kernels)

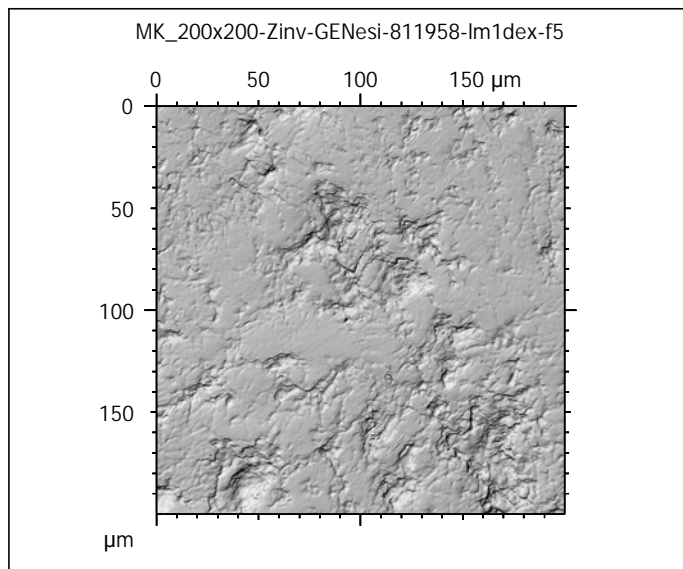
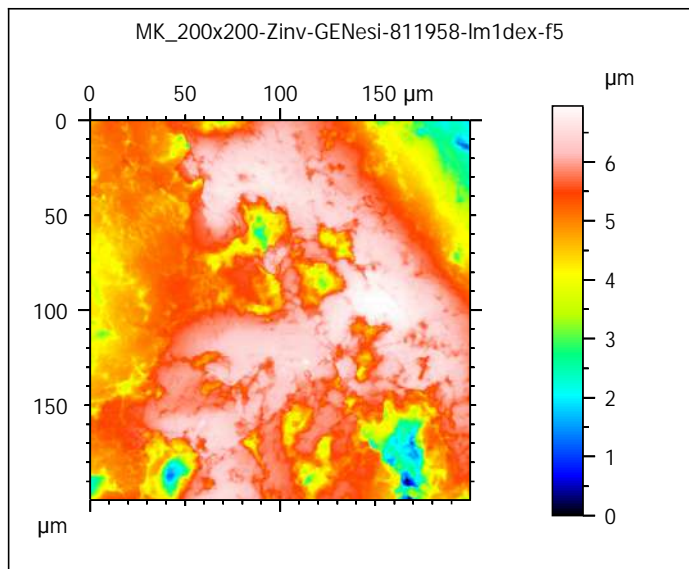
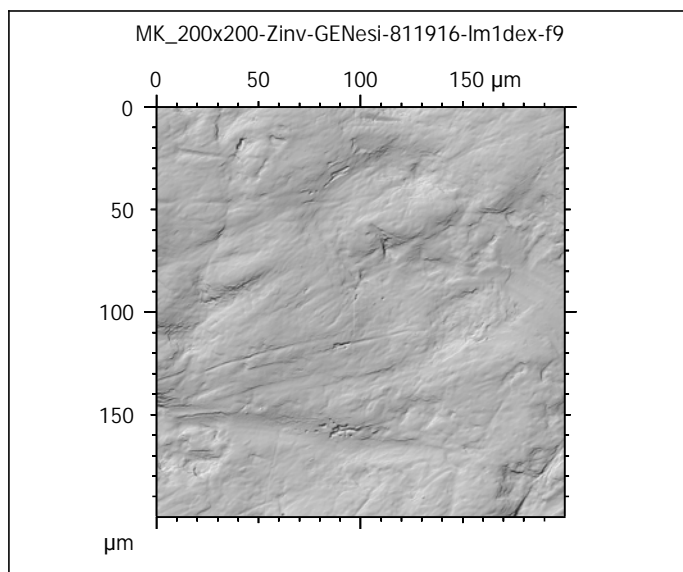
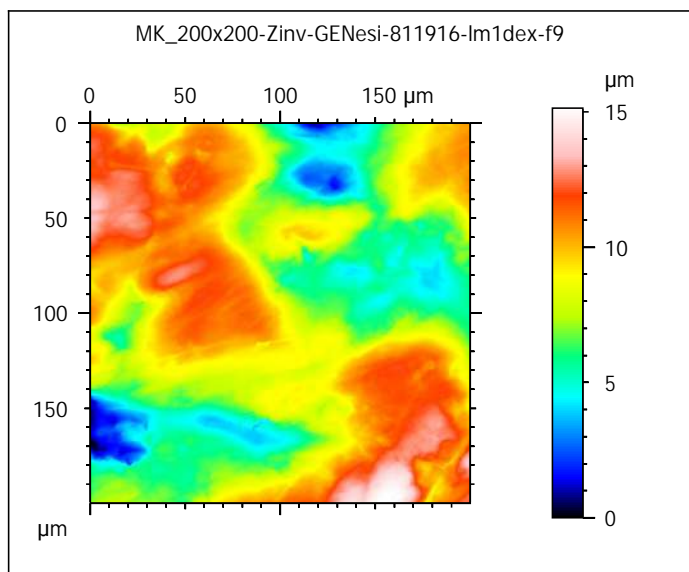
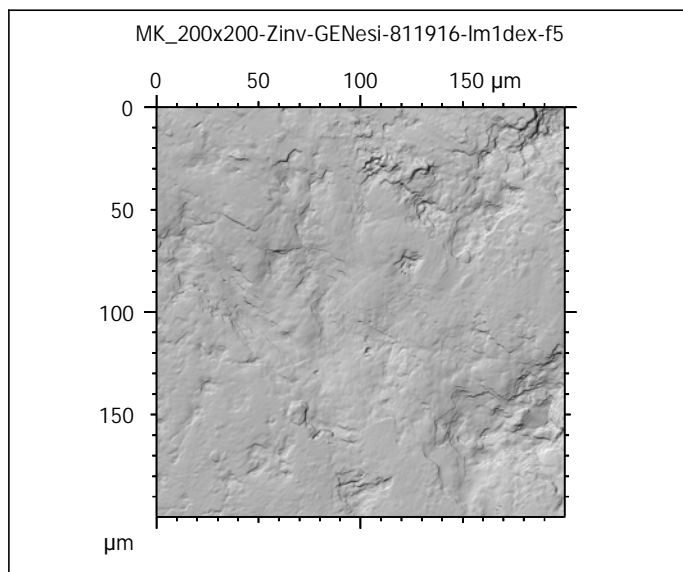
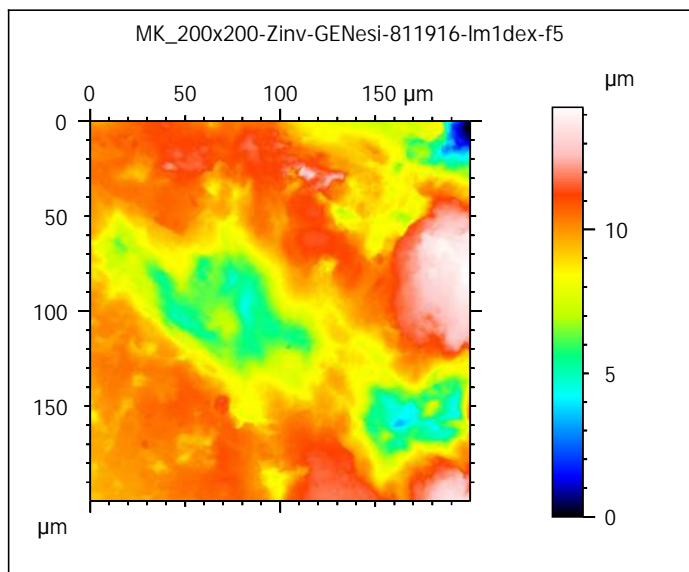
scanned at the PALEVOPRIM lab by M. Louail, University of Poitiers, France with "TRIDENT", white light confocal microscope Leica DCM8 - April 2020

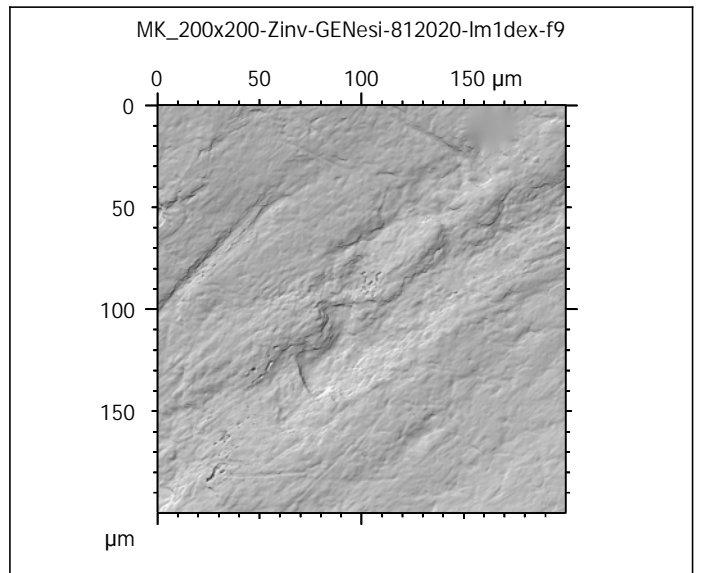
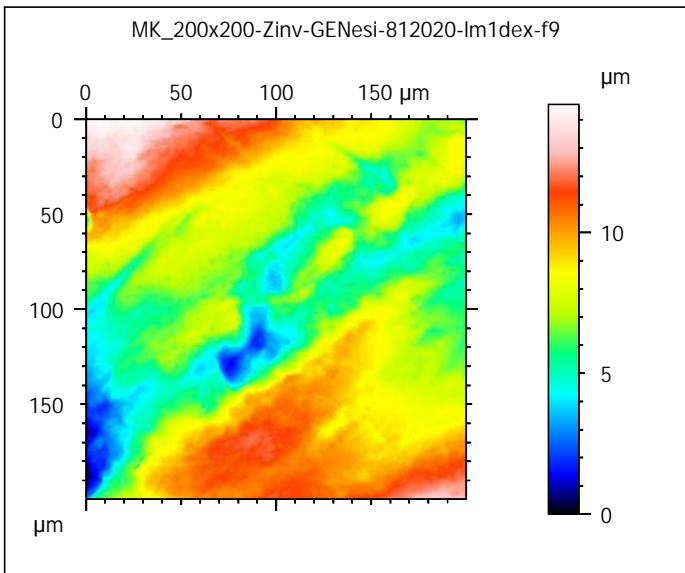
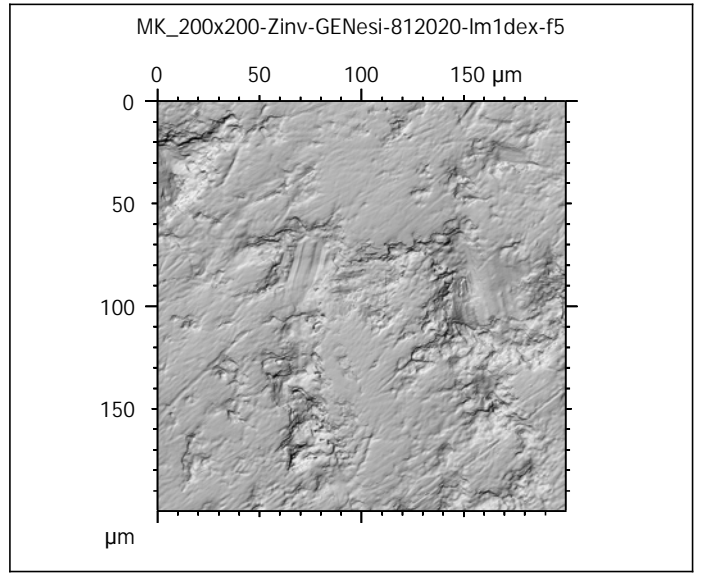
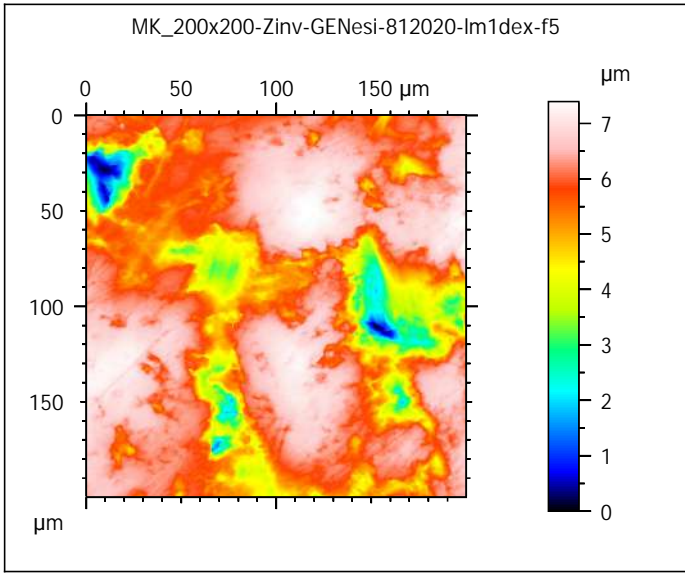
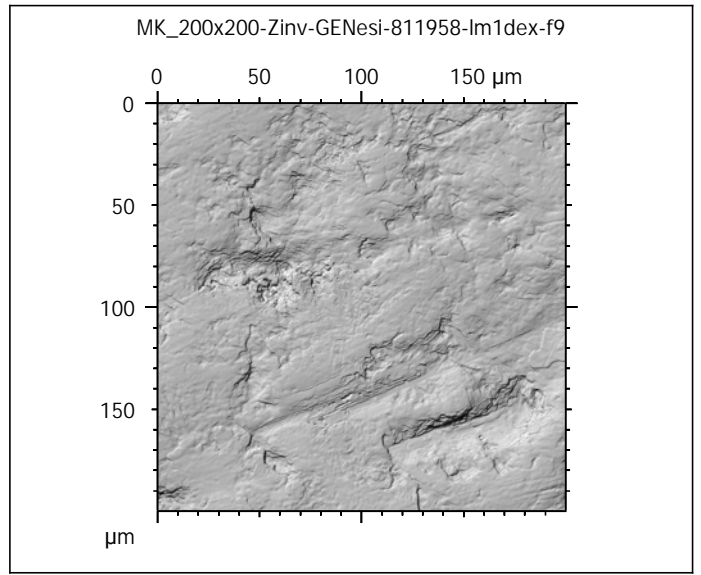
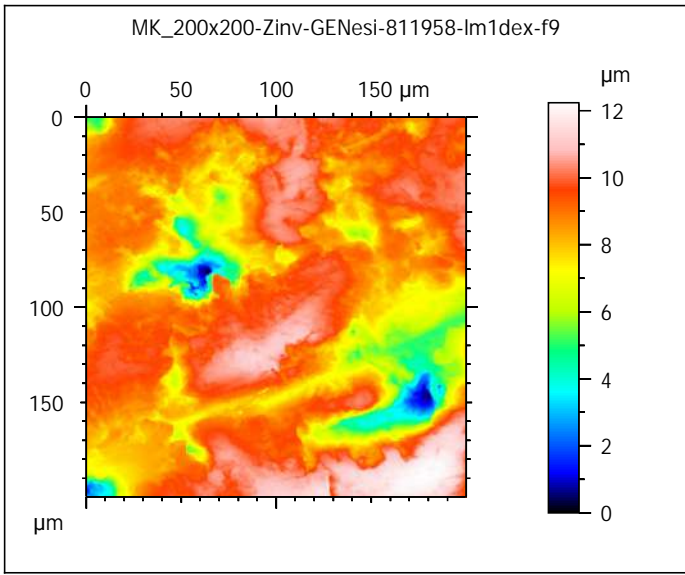
ALIHOM Project (Région Nouvelle Aquitaine, France), ANR Diet-Scratches

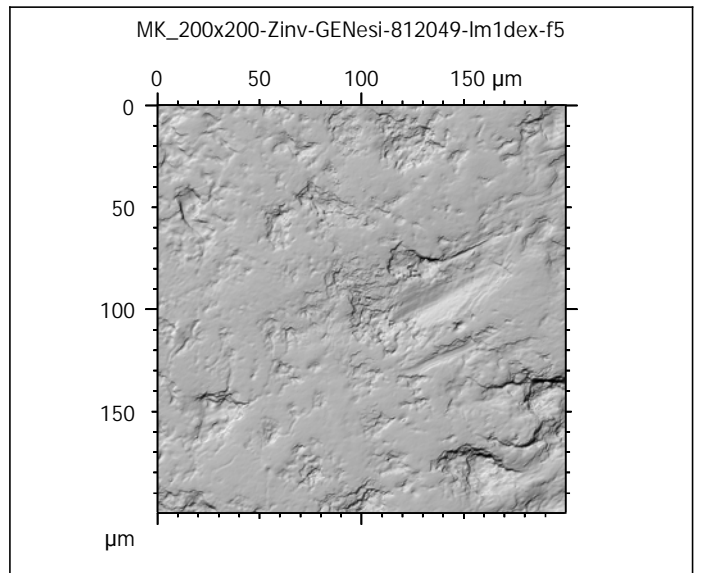
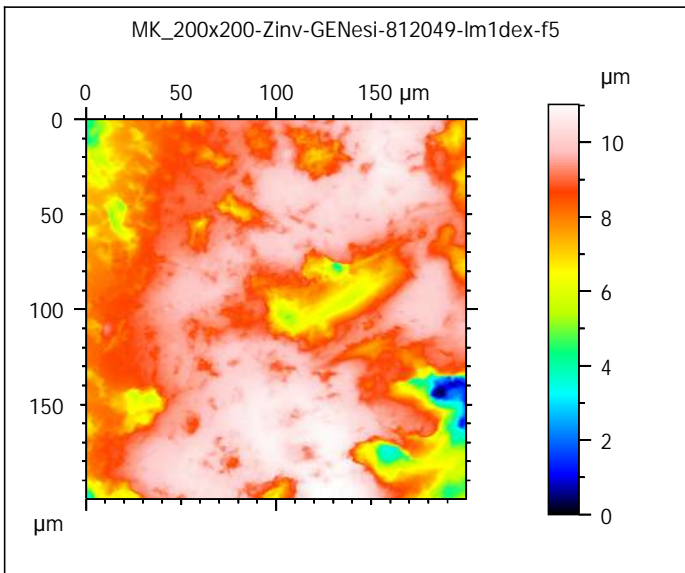
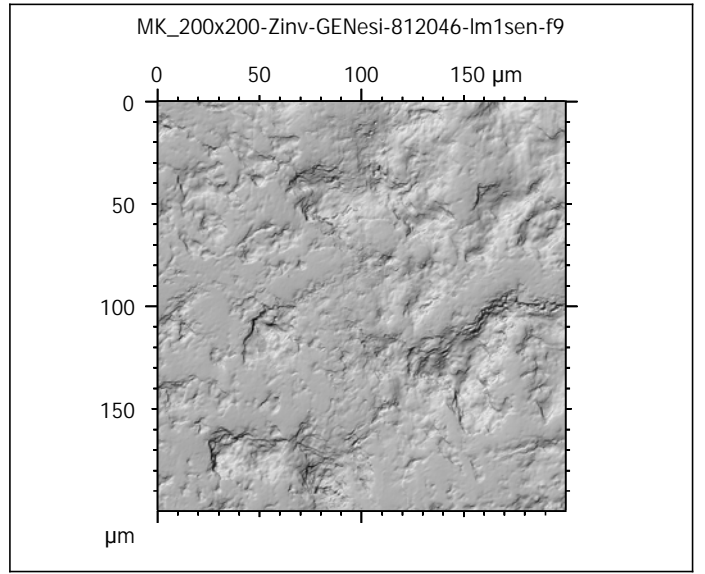
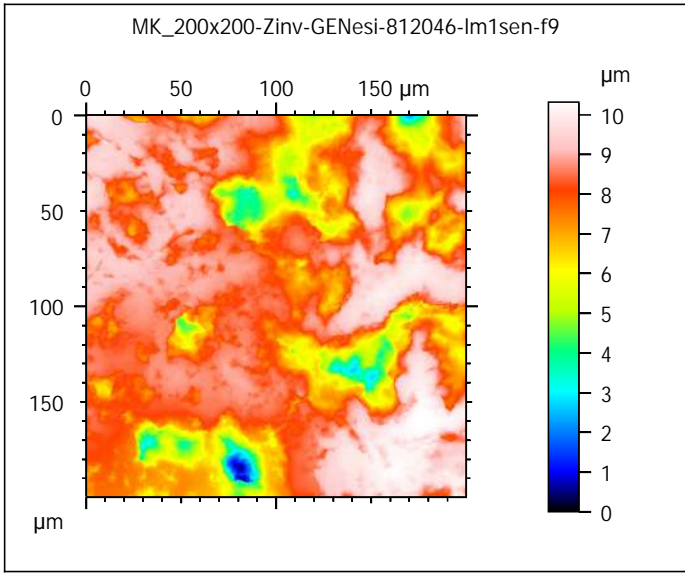
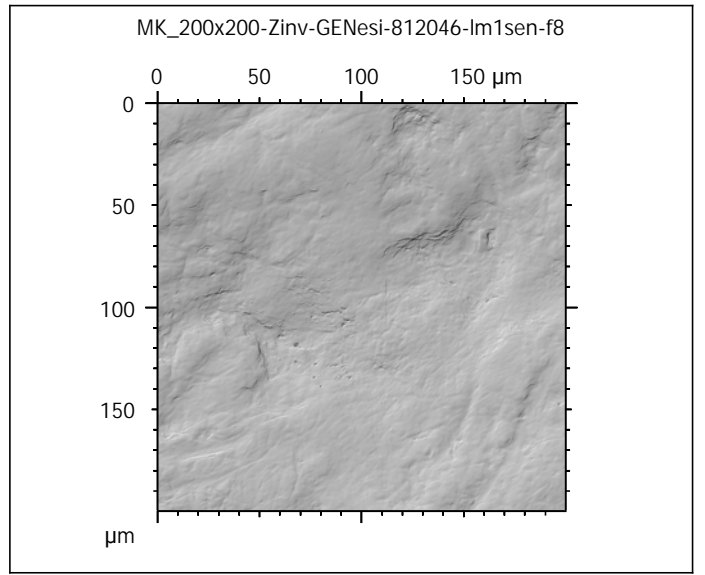
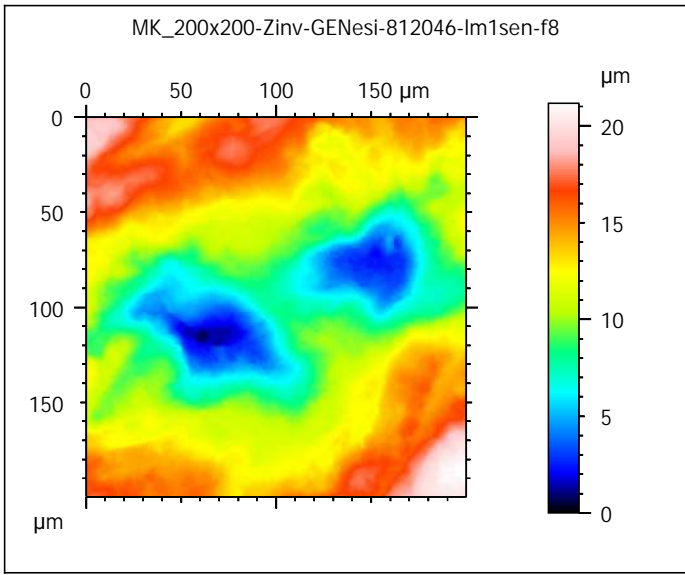
**DIET-SCRATCHES**

ANR-17-CE27-0002

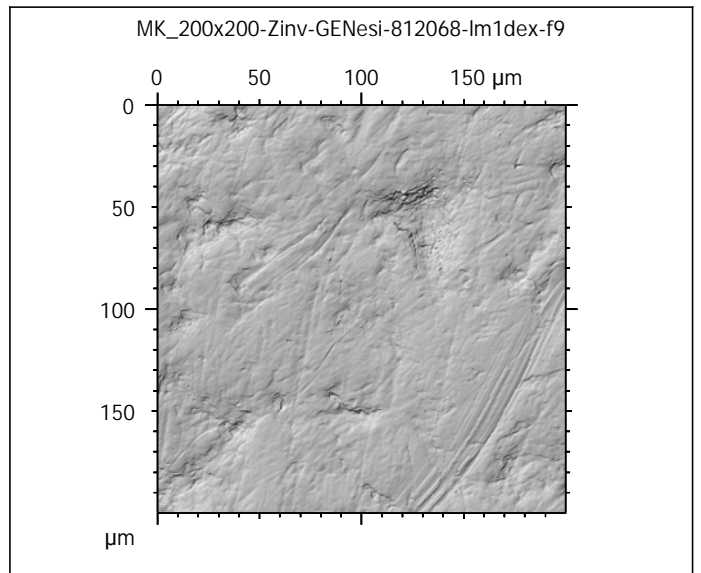
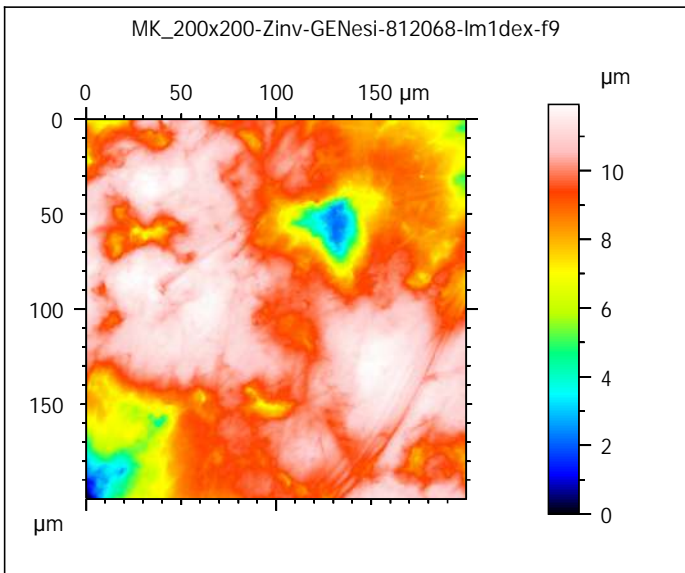
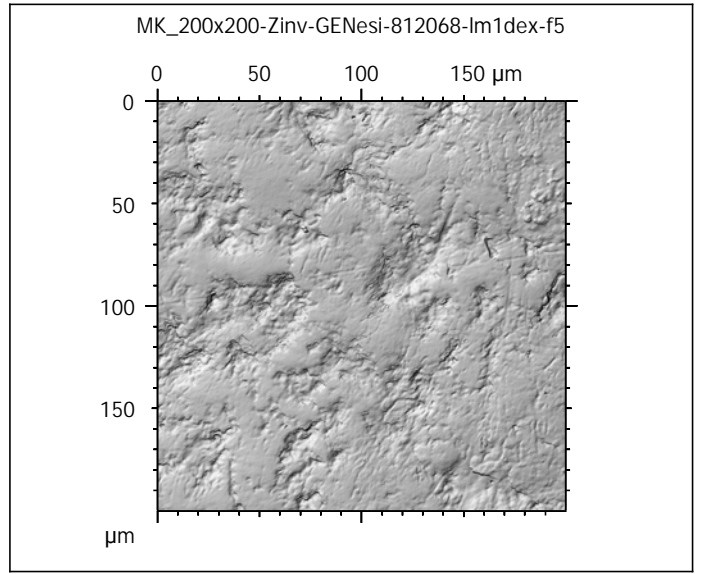
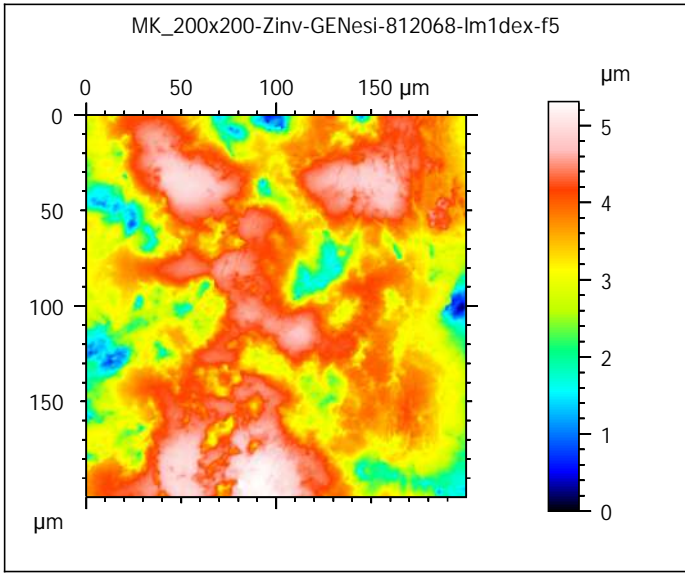
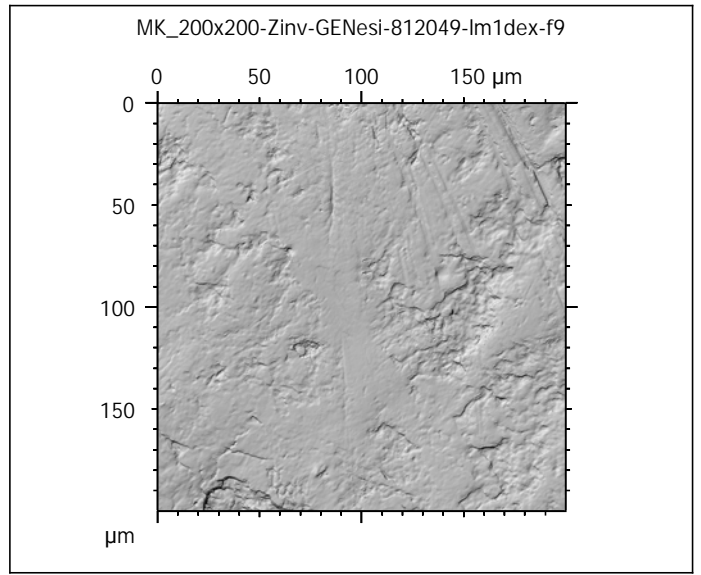
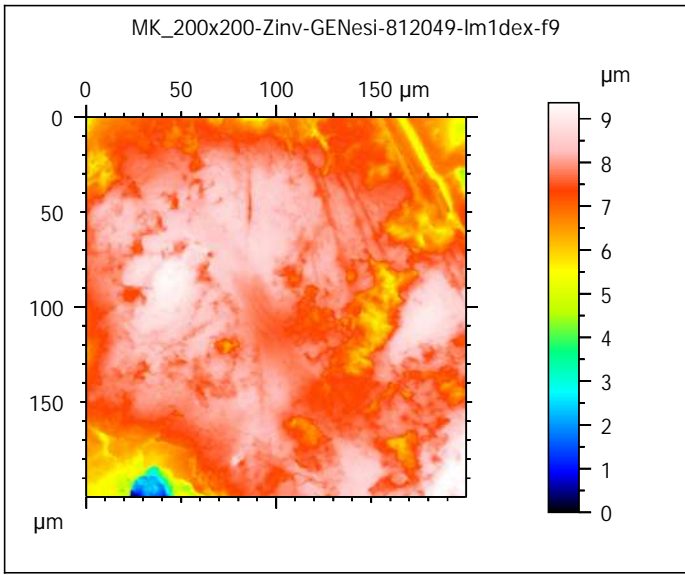
PIs: G. Merceron & S. Ferchaud

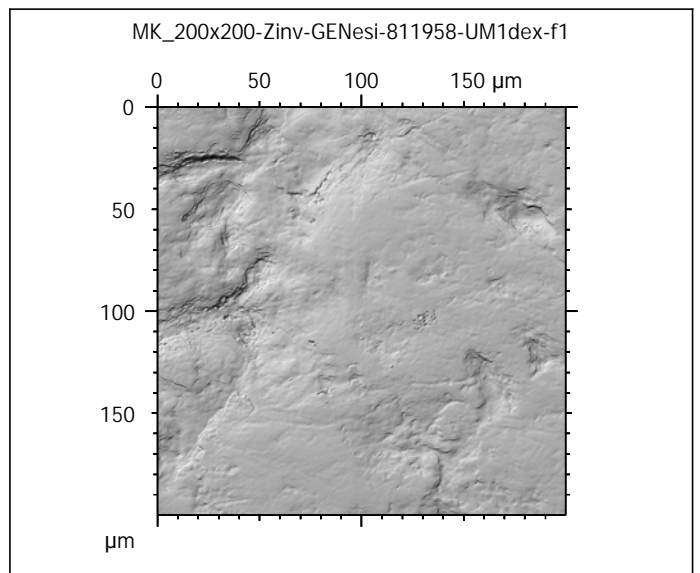
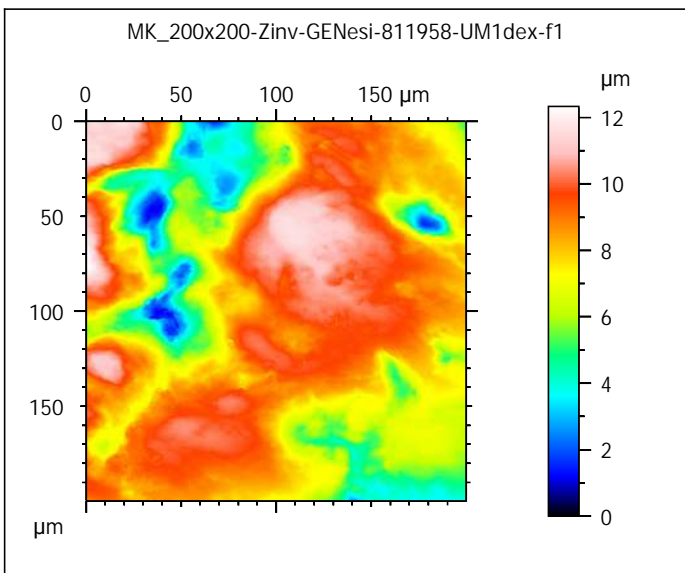
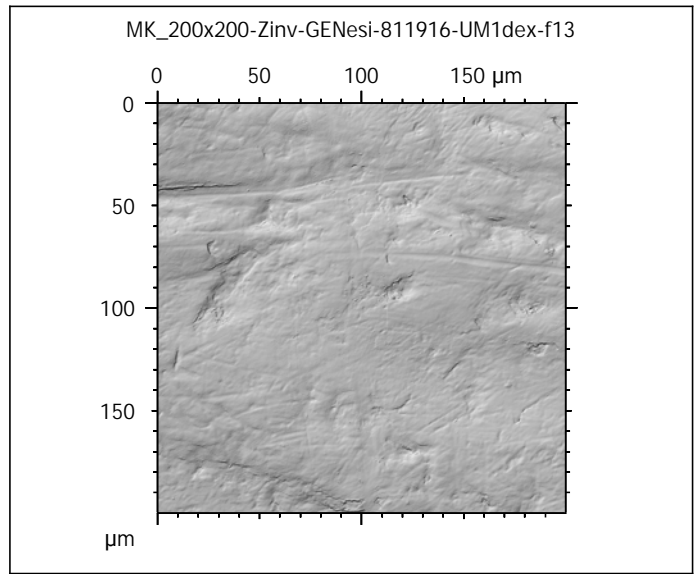
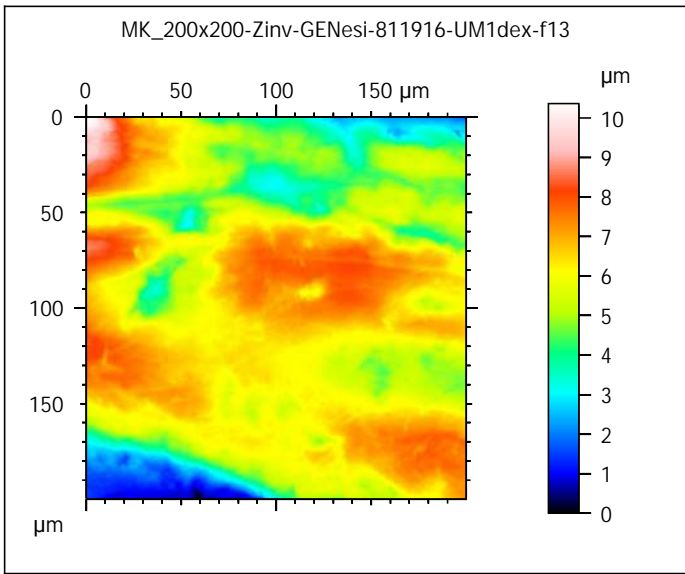
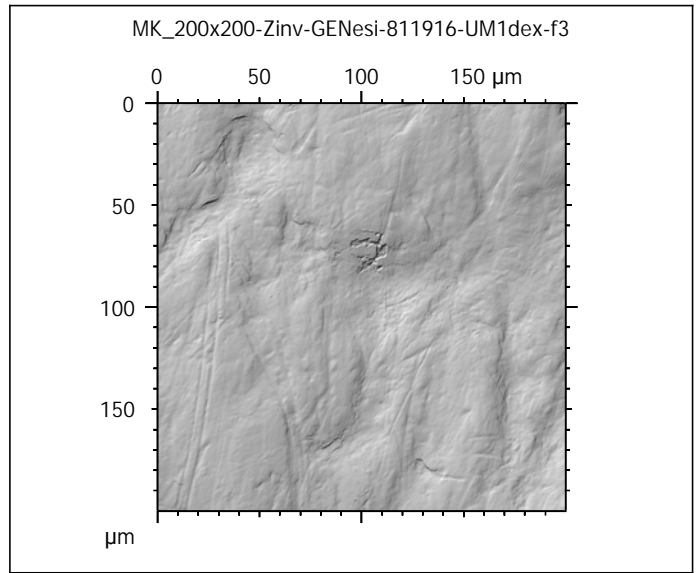
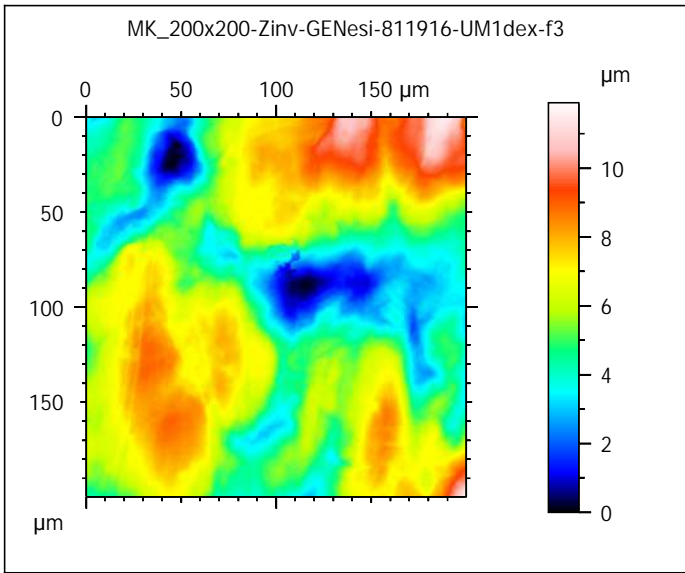


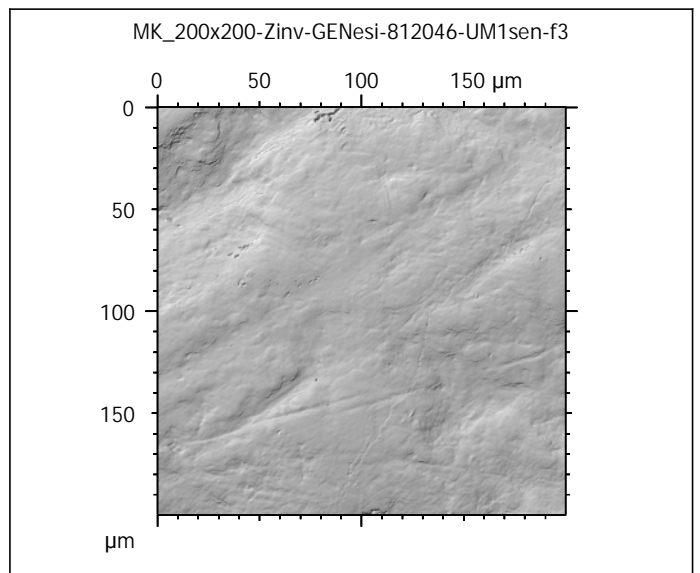
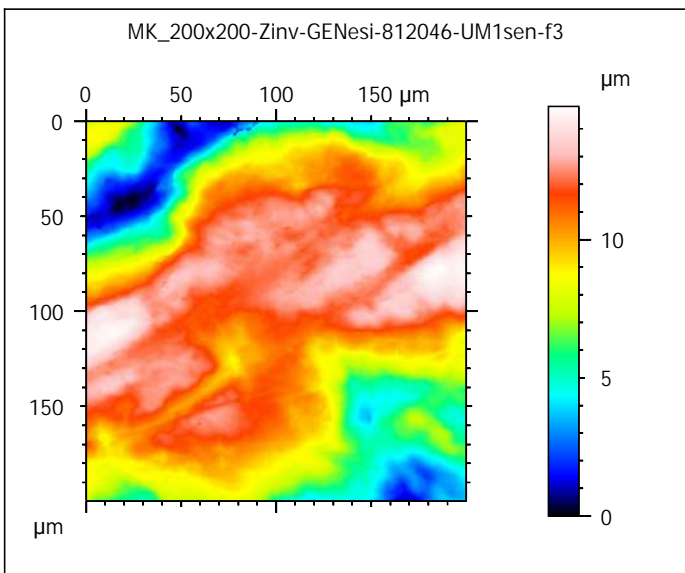
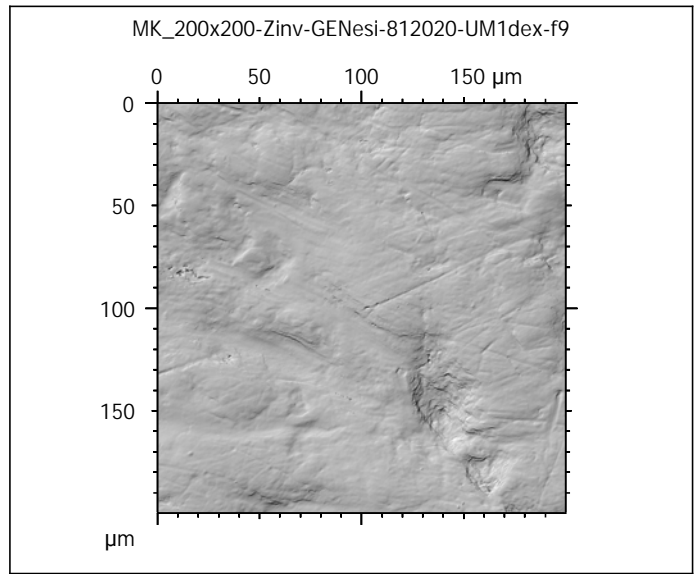
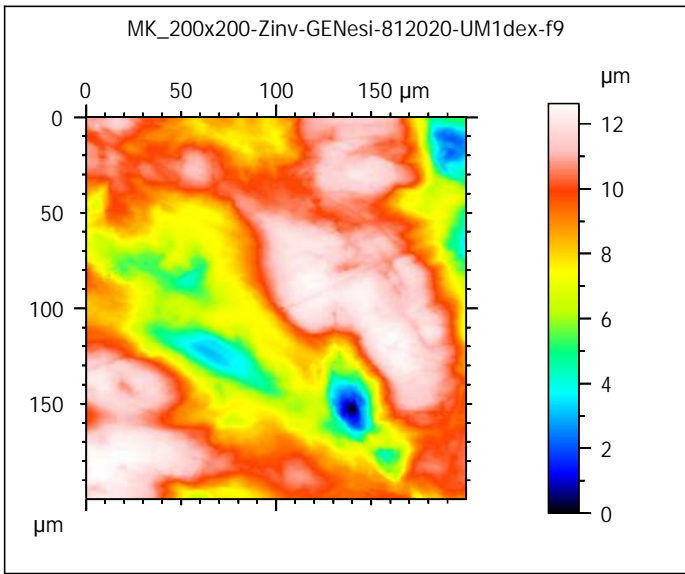
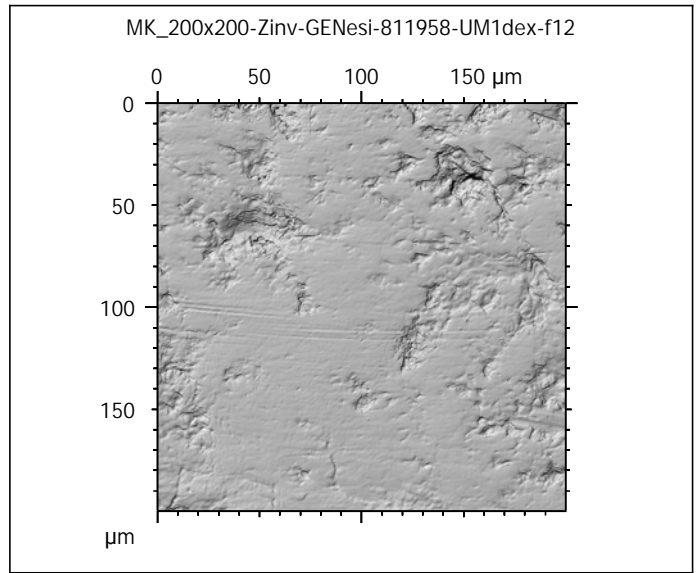
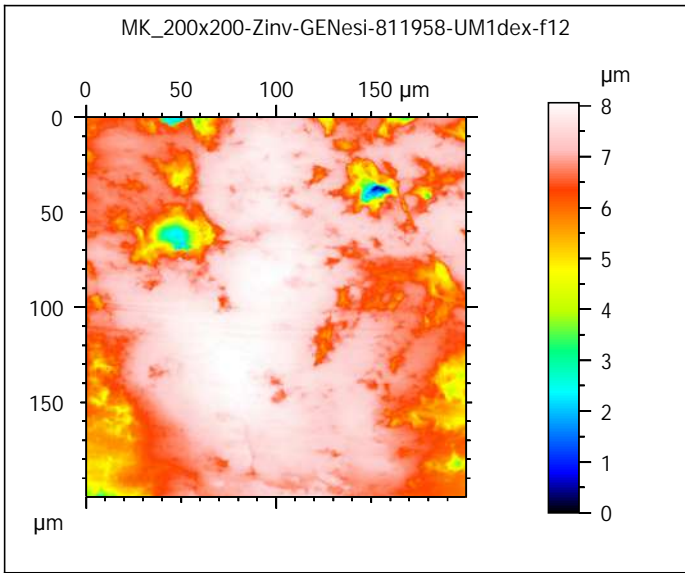




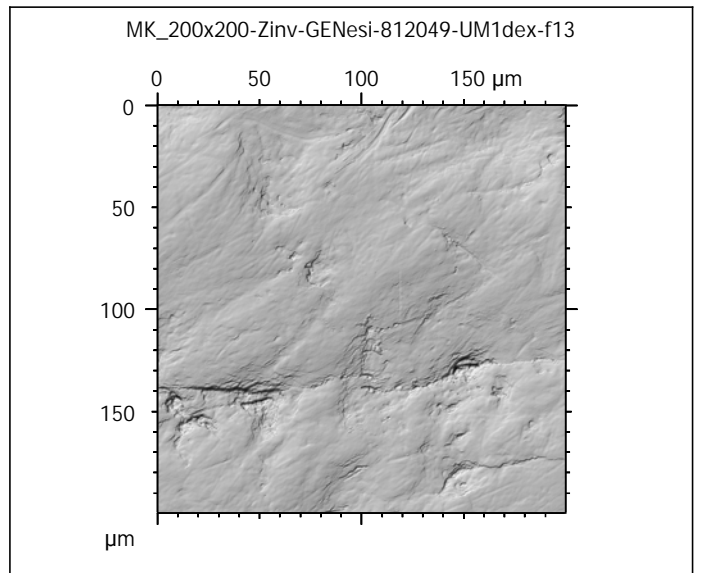
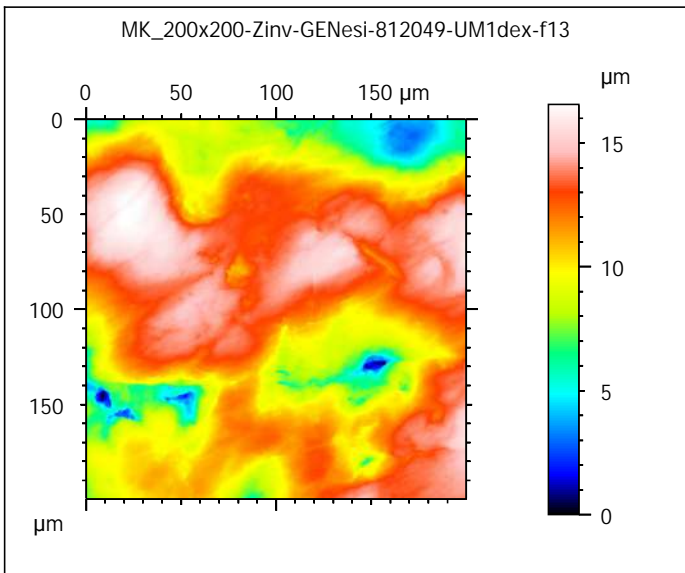
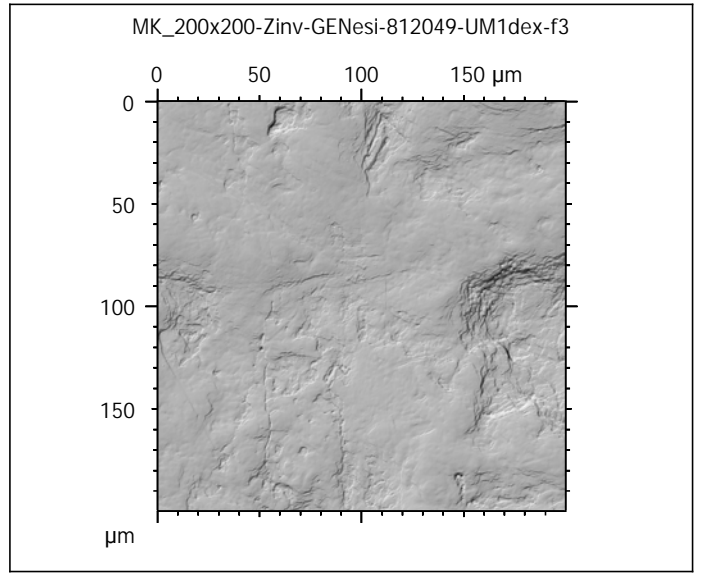
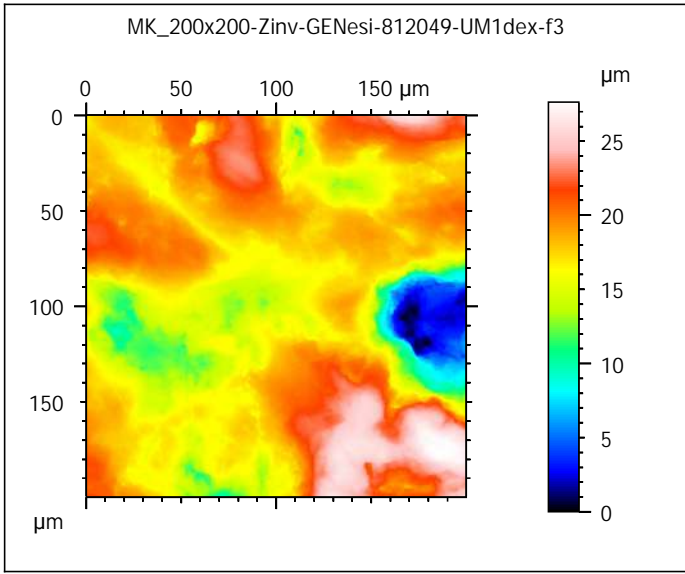
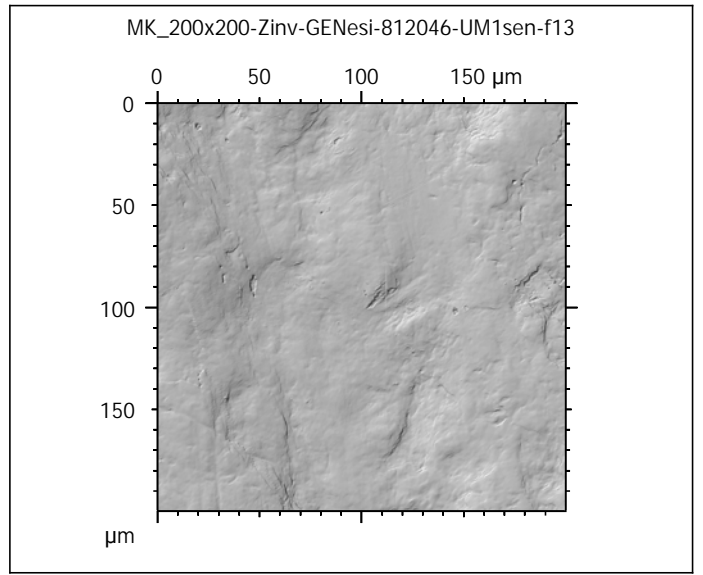
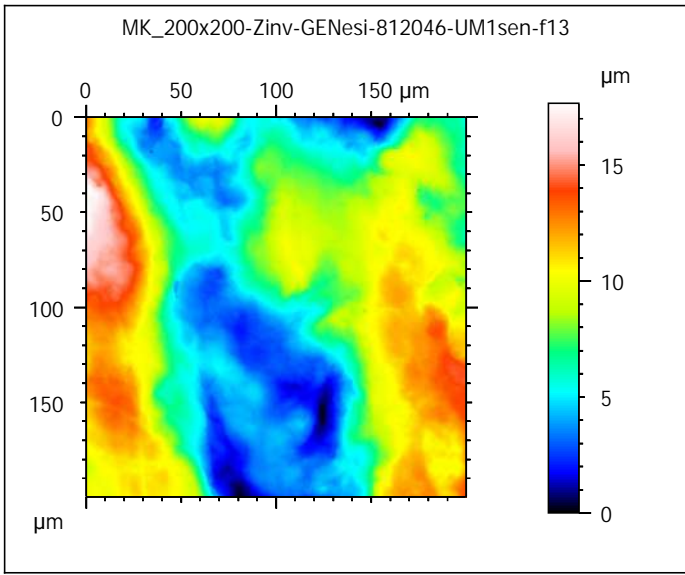




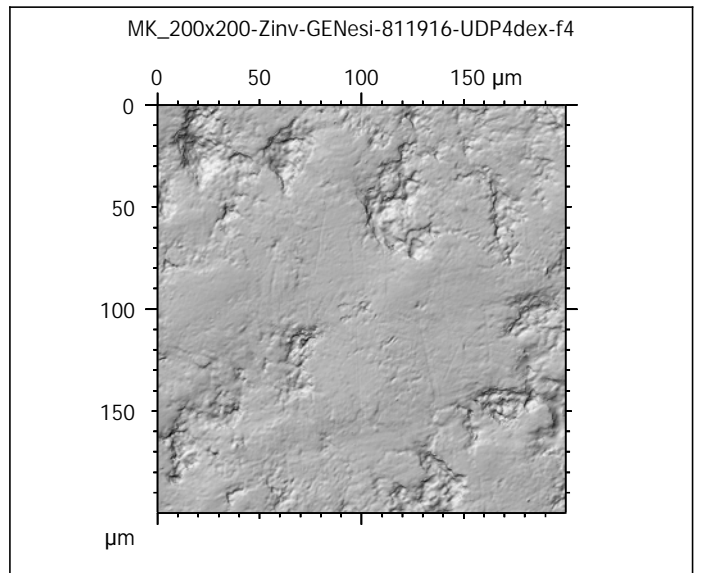
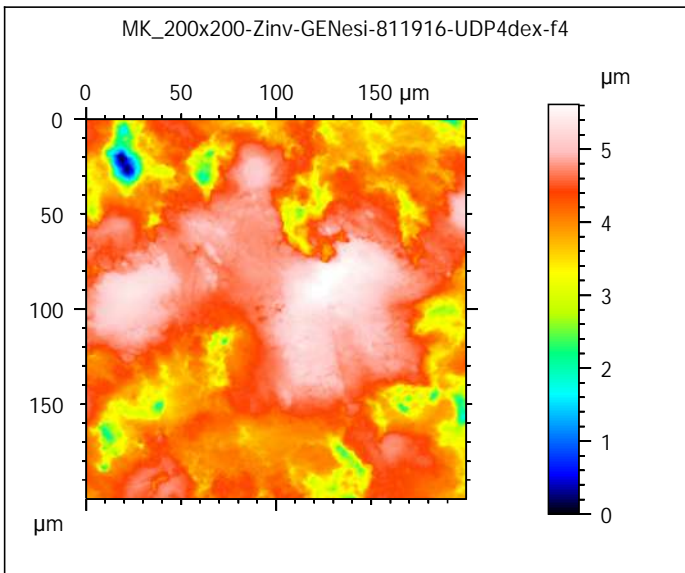
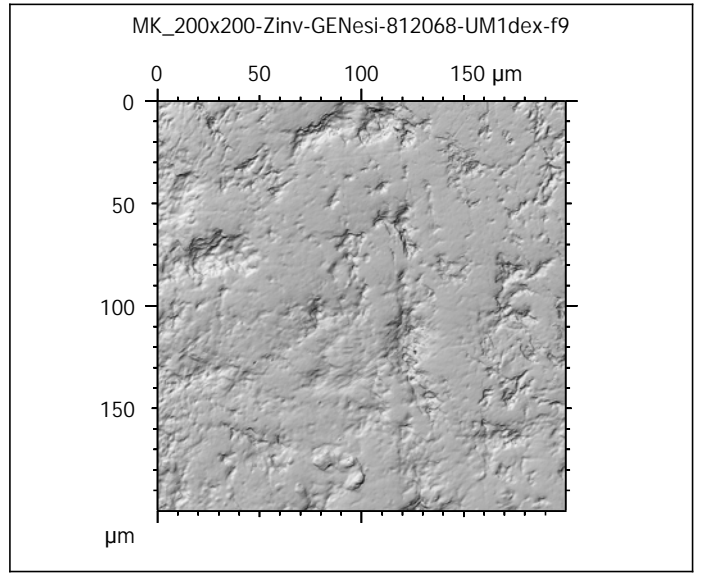
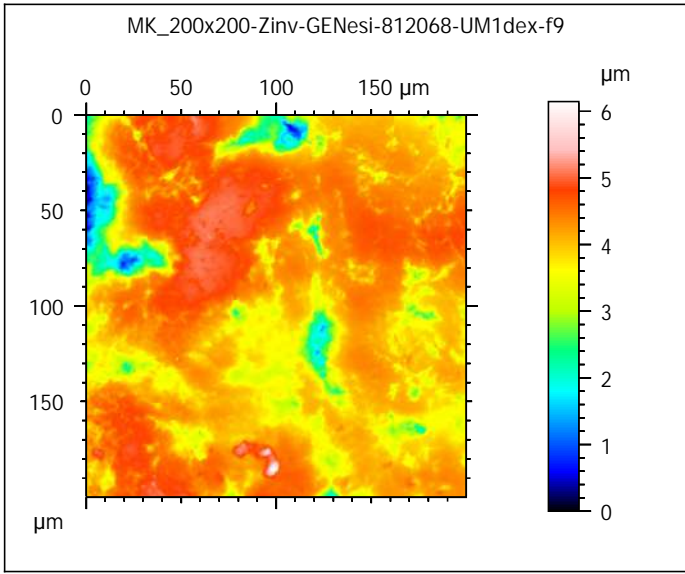
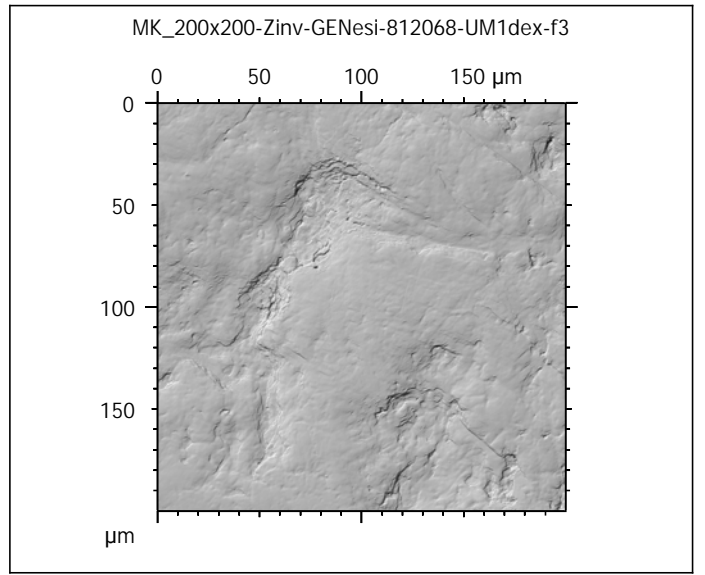
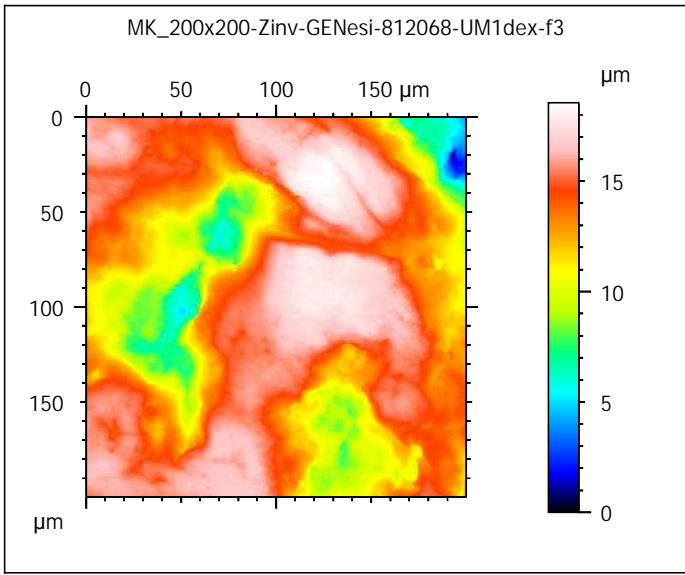


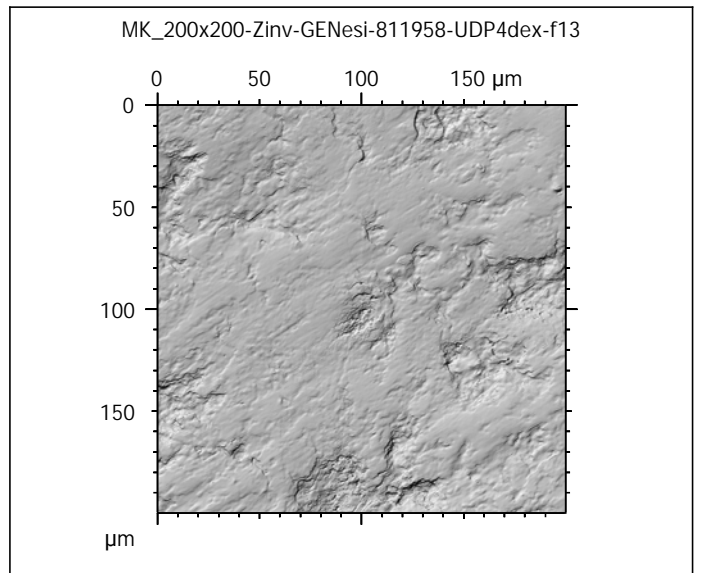
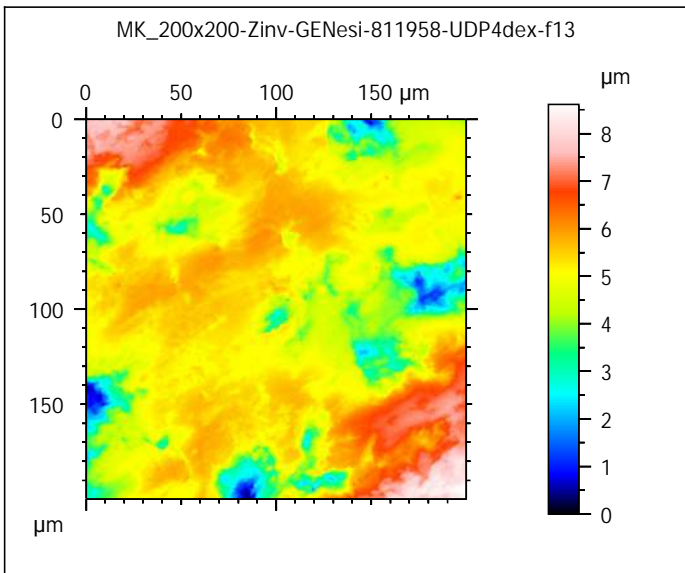
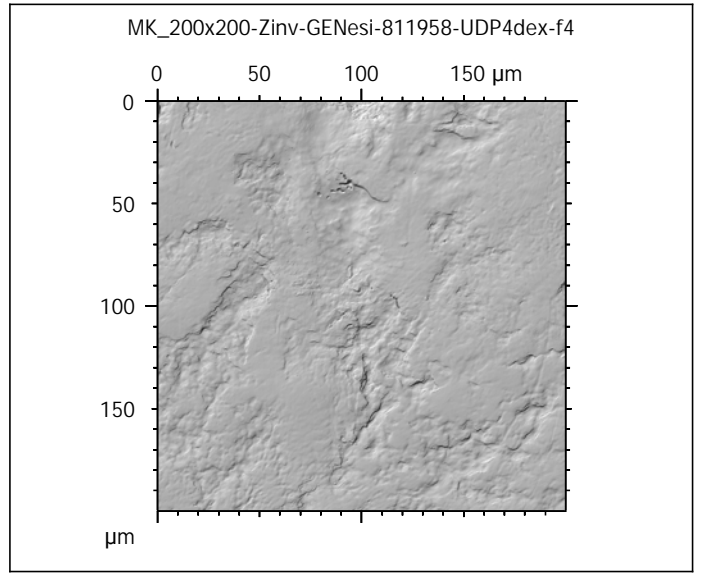
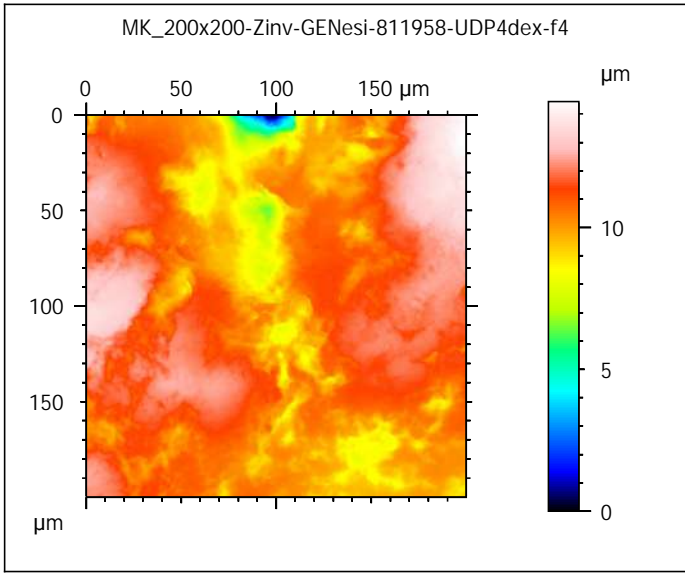
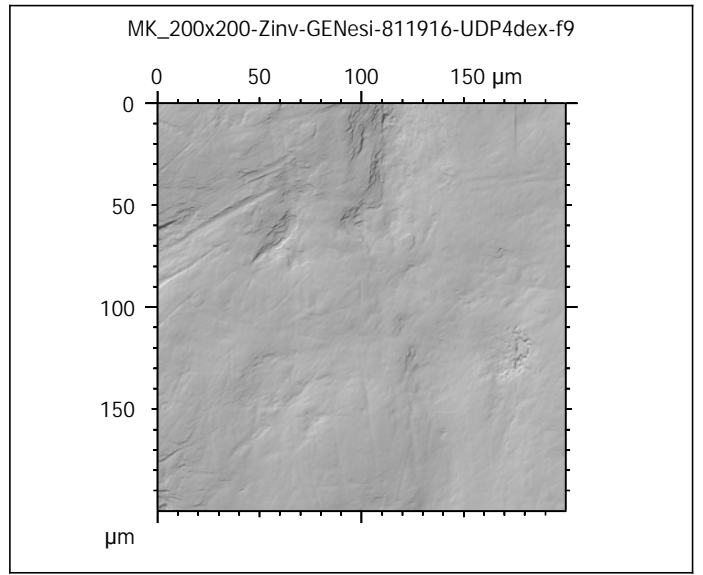
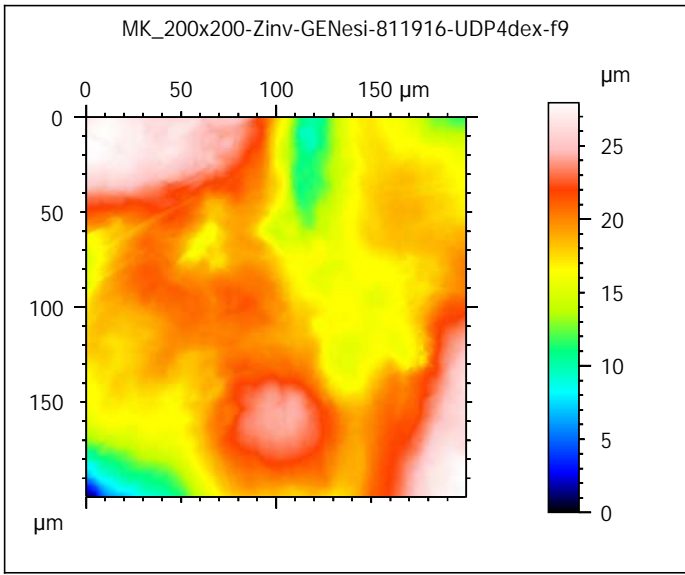


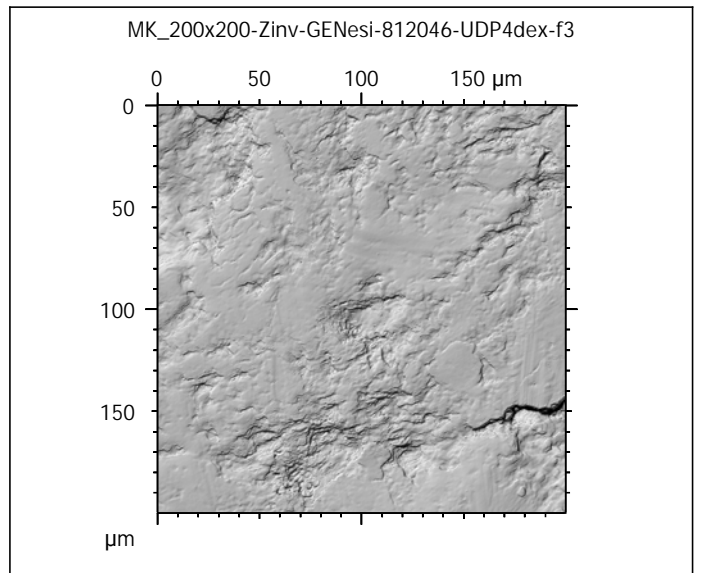
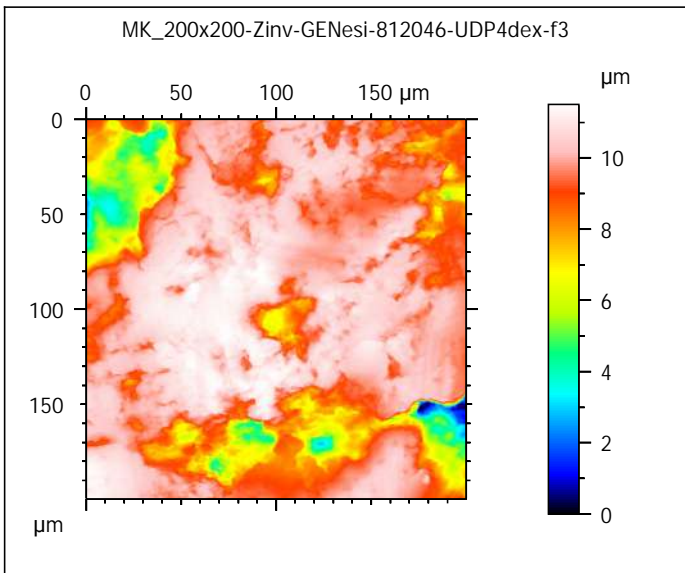
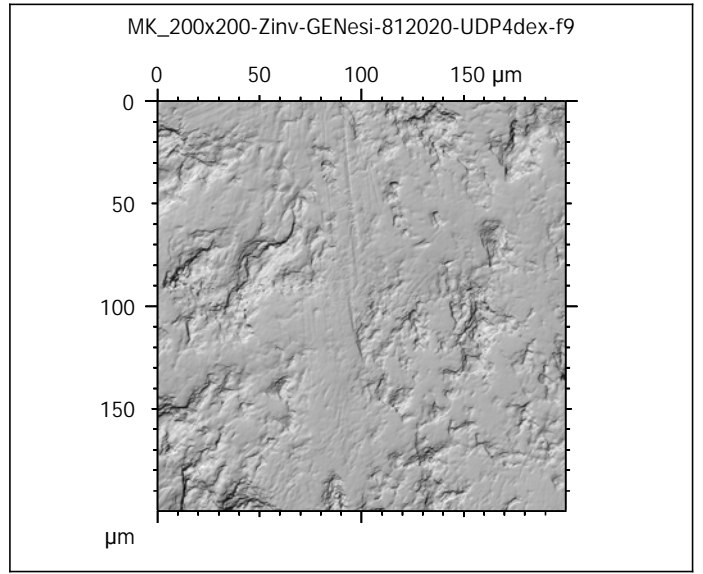
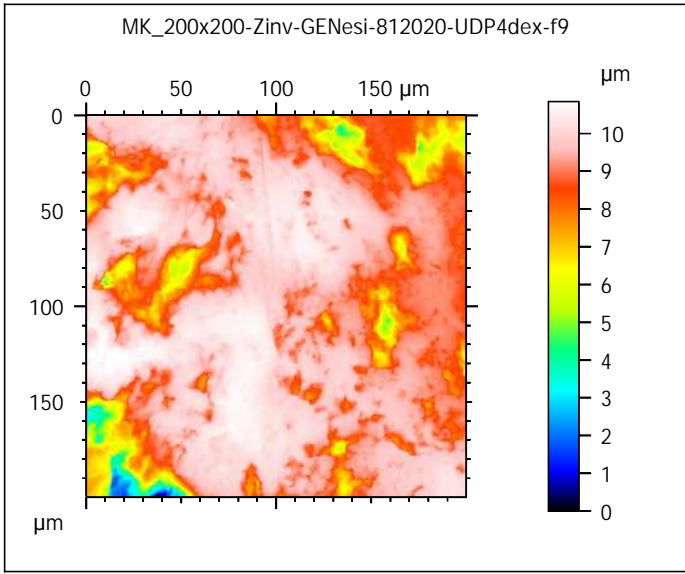
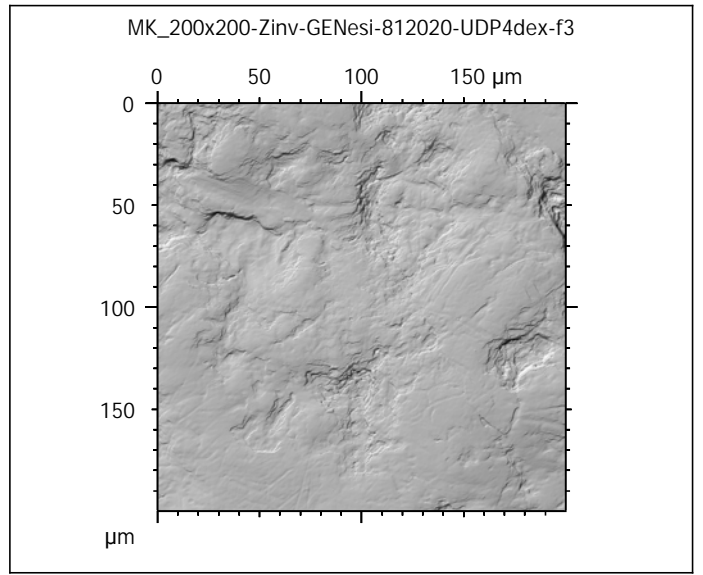
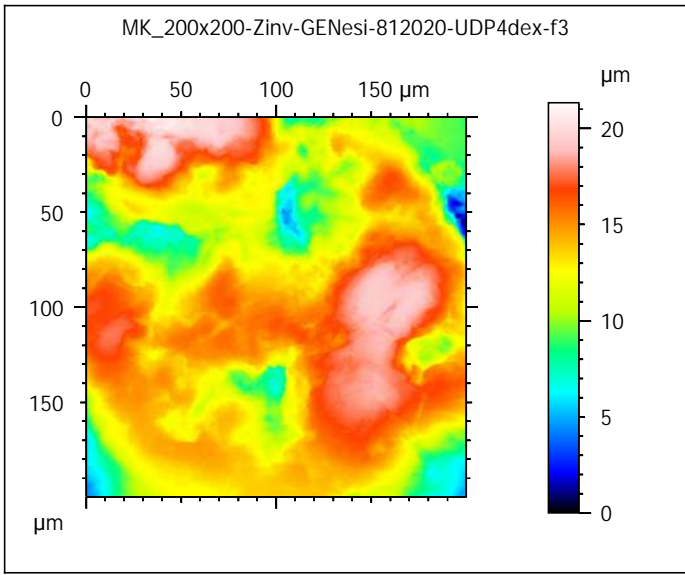




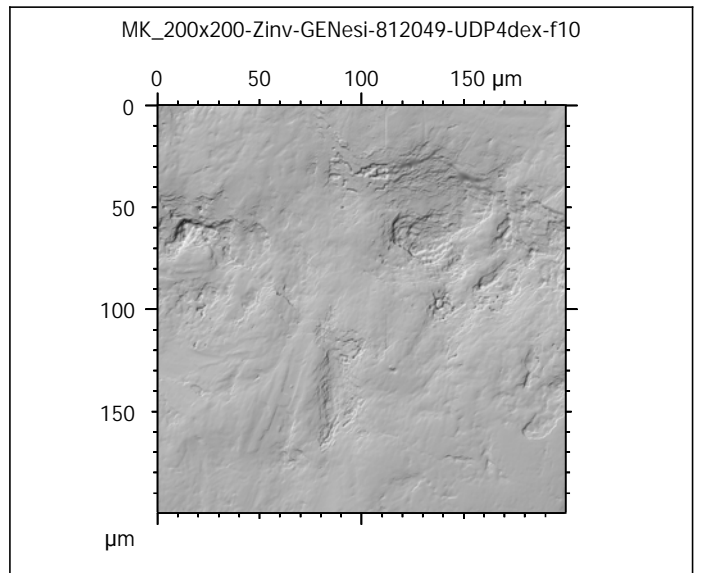
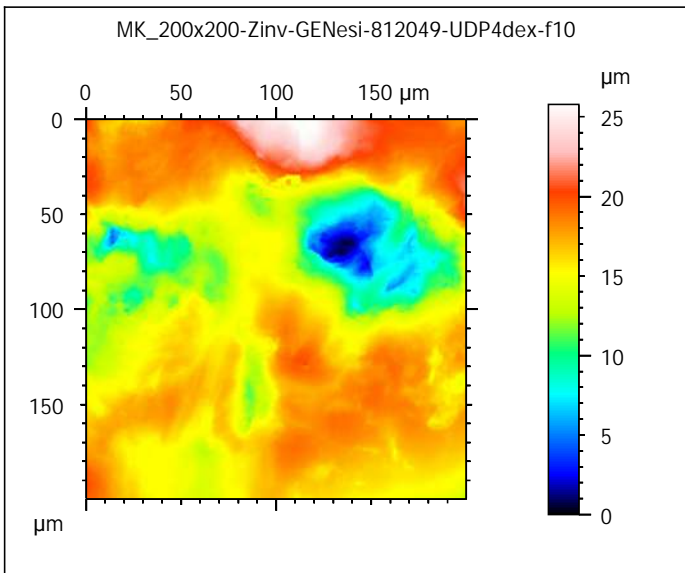
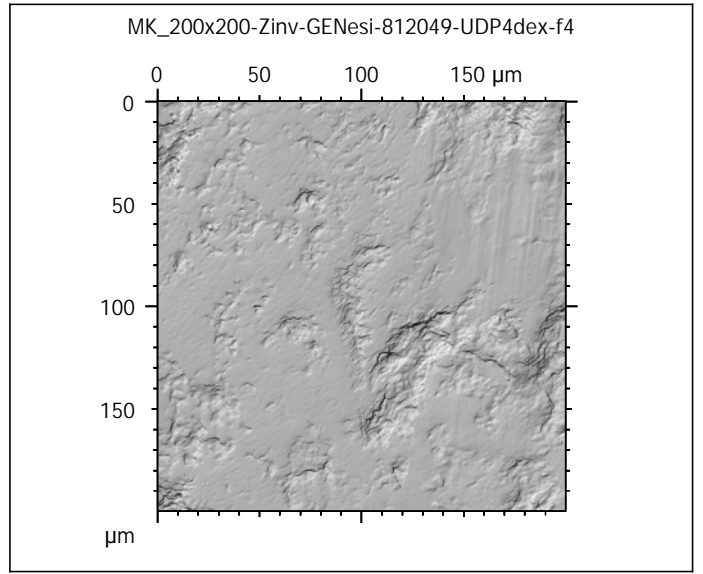
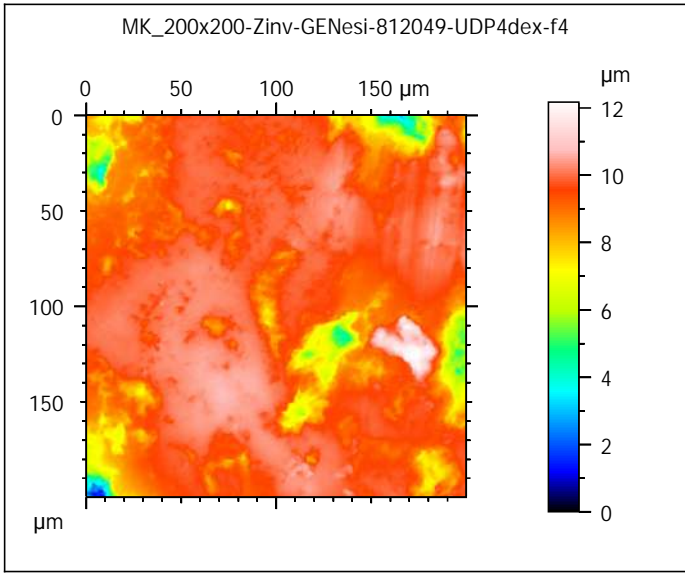
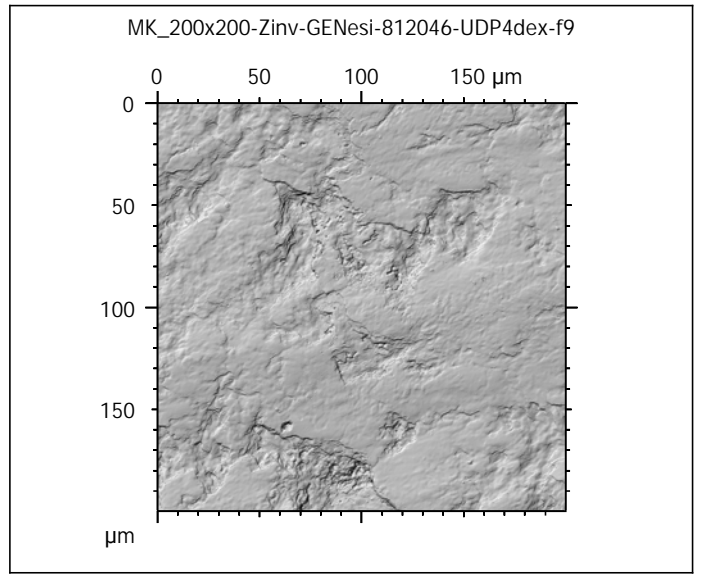
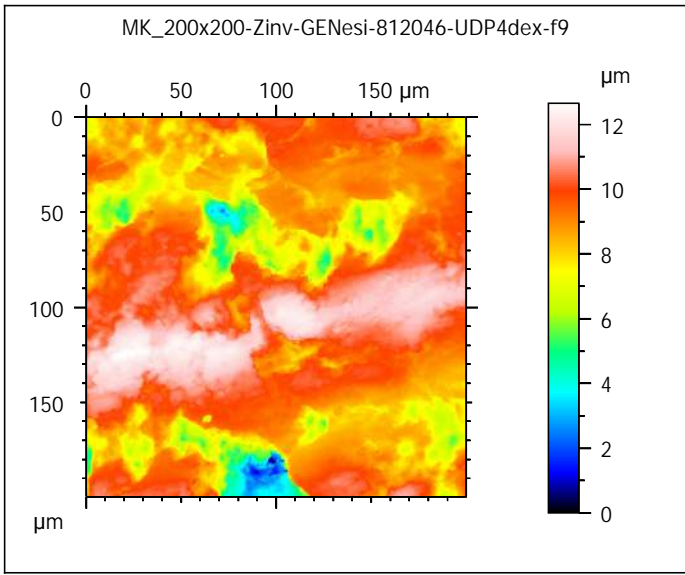


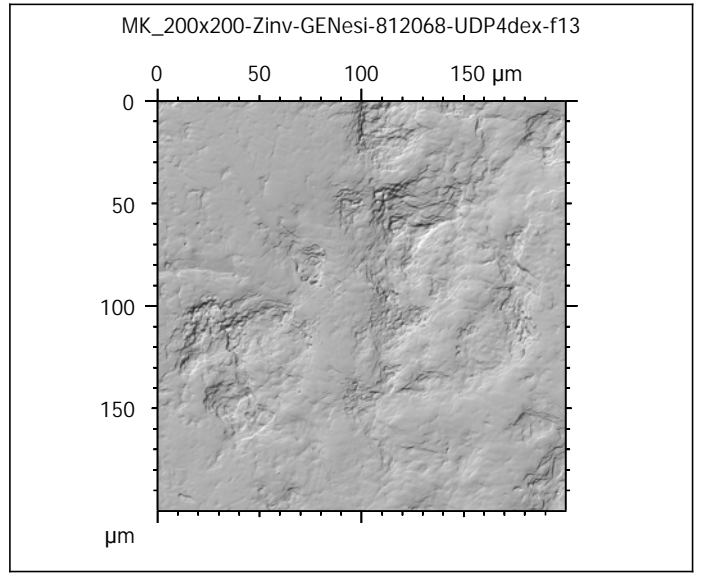
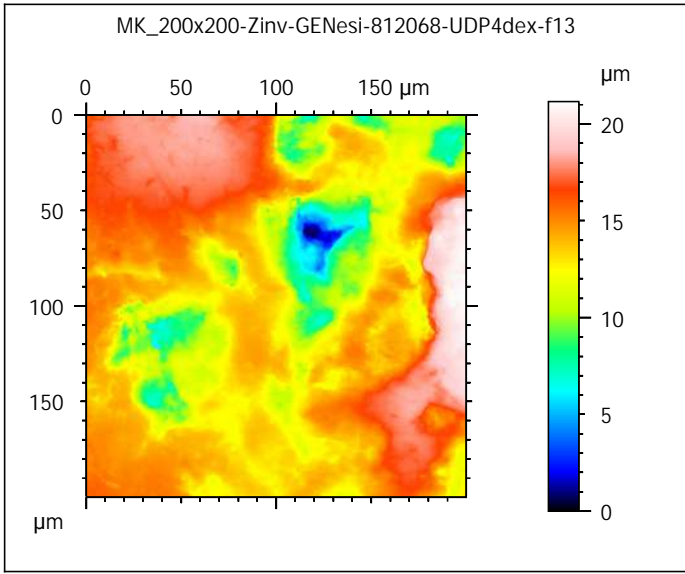
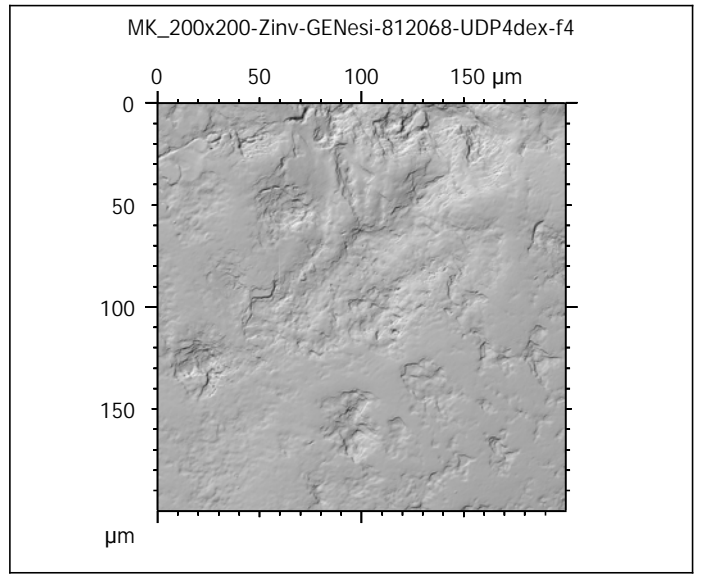
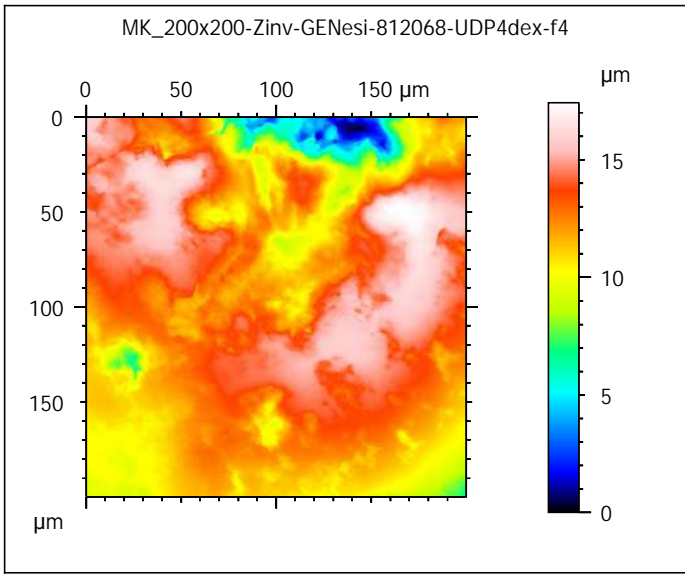












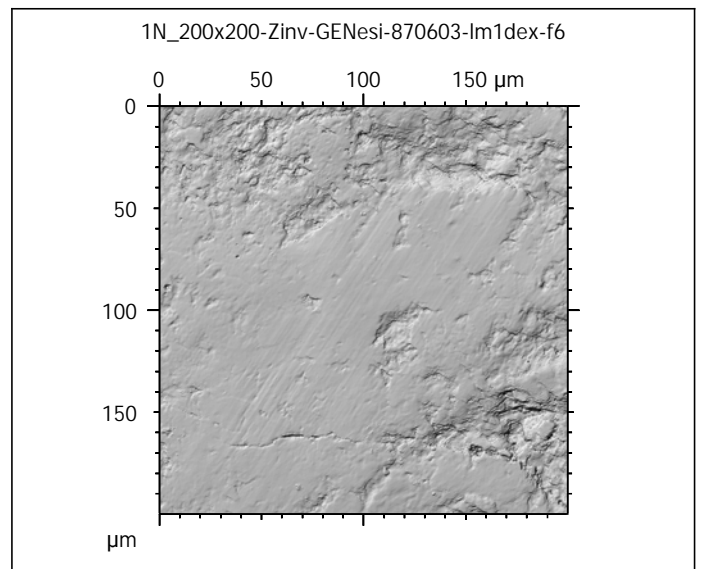
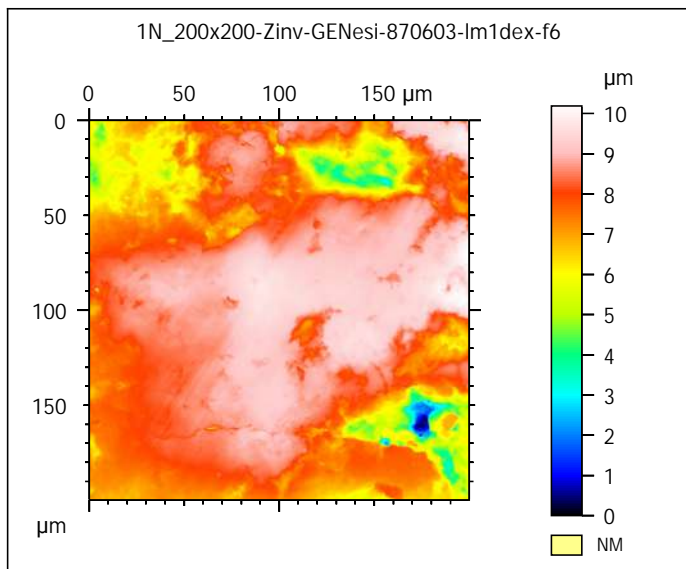
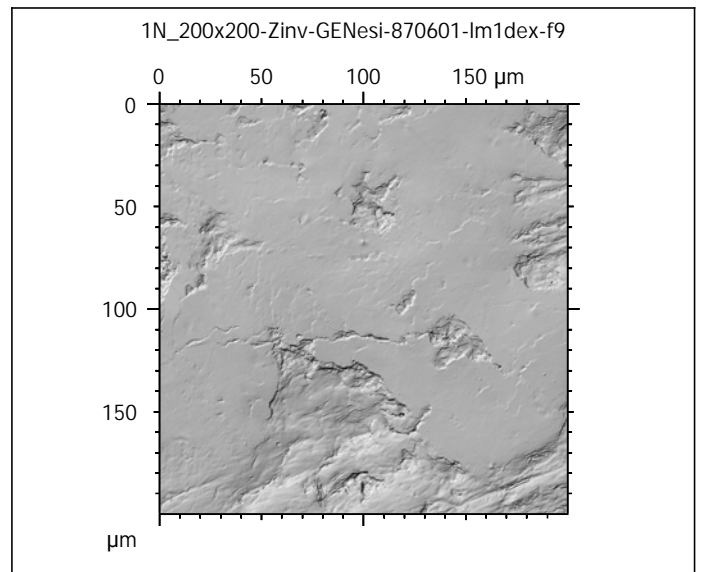
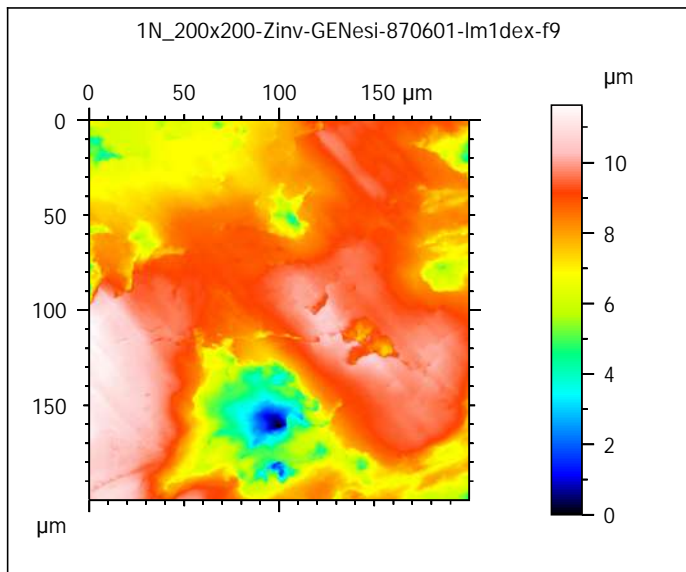
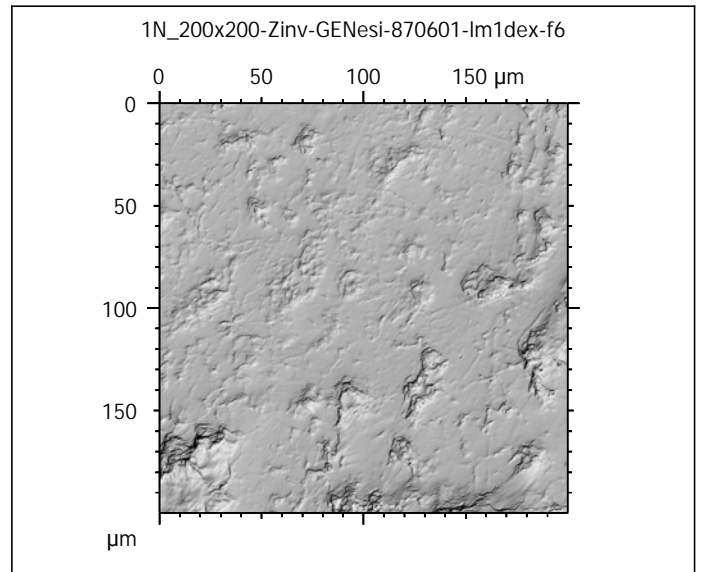
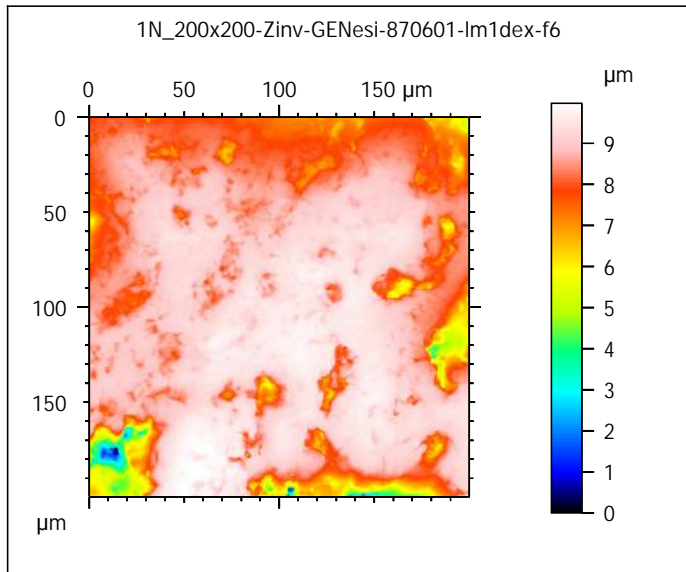
Photosimulations and false color elevation maps of scanned shearing and crushing facets on molars and deciduous premolars of the **hazelnut group** (100% base diet + 10 hazelnuts in shell per day)

scanned at the PALEVOPRIM lab by M. Louail, University of Poitiers, France with "TRIDENT", white light confocal microscope Leica DCM8 - April 2020  
ALIHOM Project (Région Nouvelle Aquitaine, France), ANR Diet-Scratches

**DIET-SCRATCHES**

ANR-17-CE27-0002

PIs: G. Merceron & S. Ferchaud



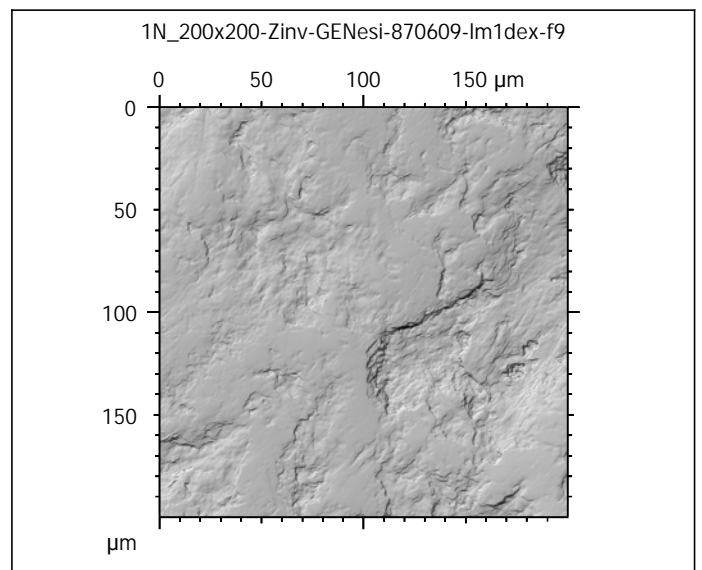
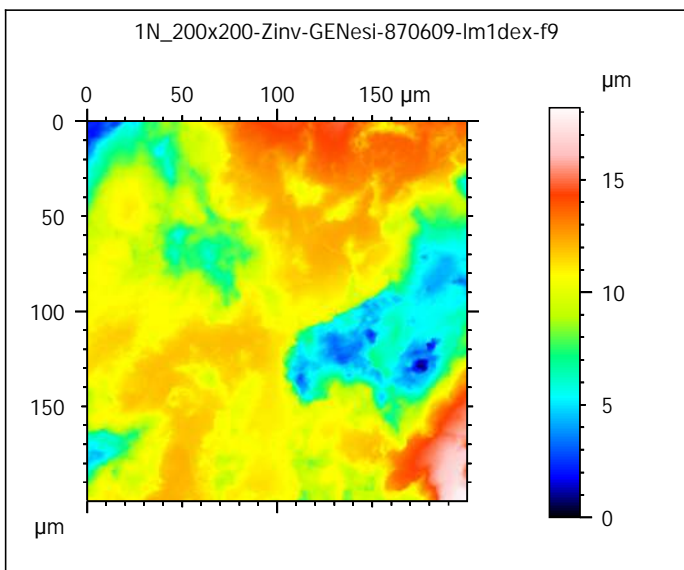
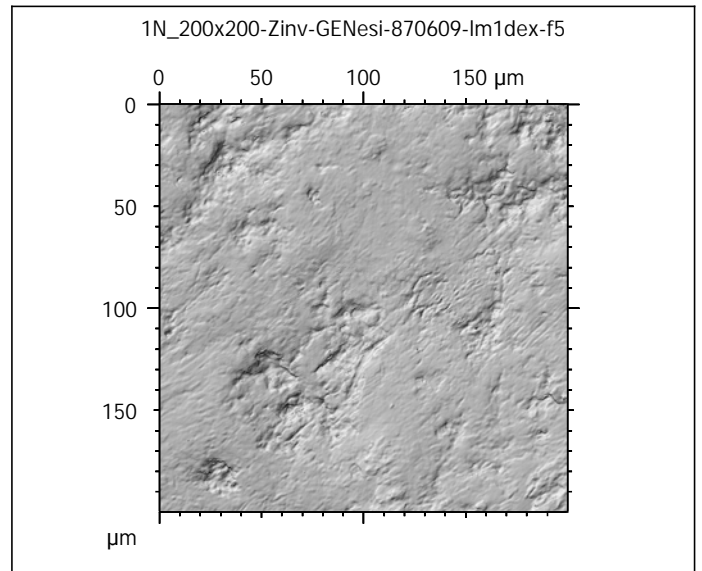
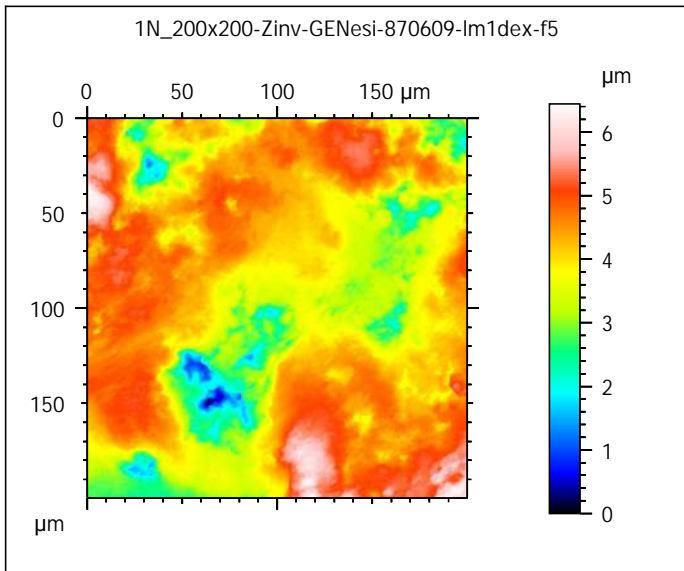
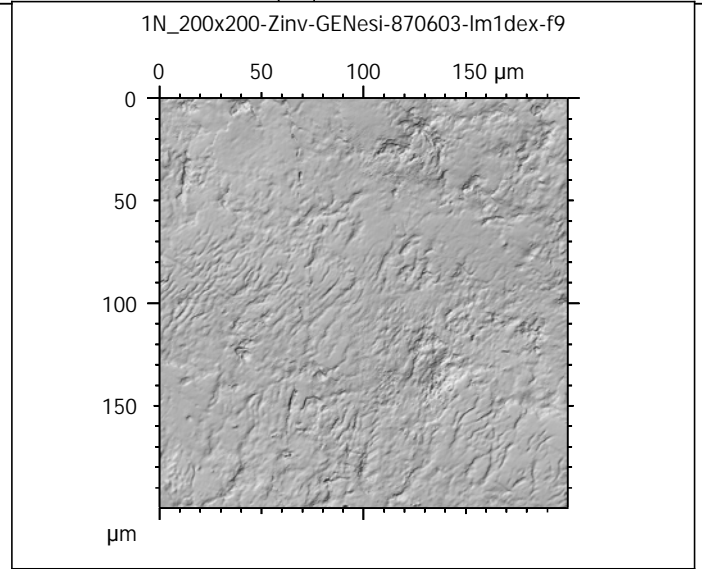
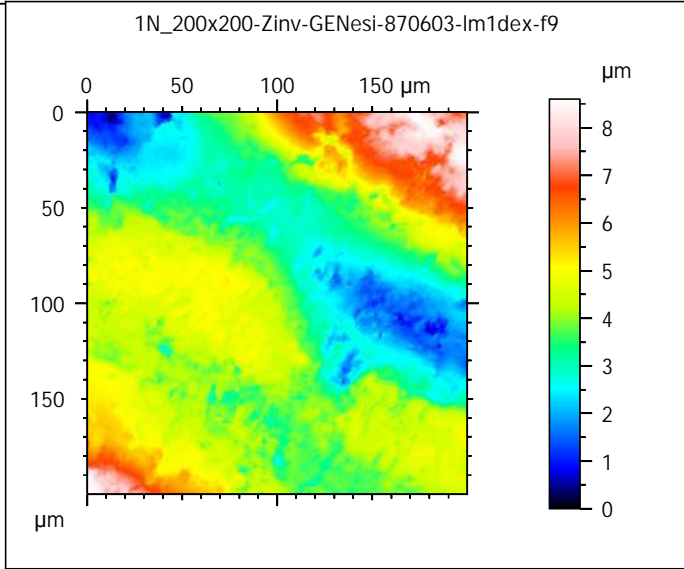


Photosimulations and false color elevation maps of scanned shearing and crushing facets on molars and deciduous premolars of the **hazelnut group** (100% base diet + 10 hazelnuts in shell per day)

scanned at the PALEVOPRIM lab by M. Louail, University of Poitiers, France with "TRIDENT", white light confocal microscope Leica DCM8 - April 2020  
ALIHOM Project (Région Nouvelle Aquitaine, France), ANR Diet-Scratches

**DIET-SCRATCHES**

ANR-17-CE27-0002  
PIs: G. Merceron & S. Ferchaud





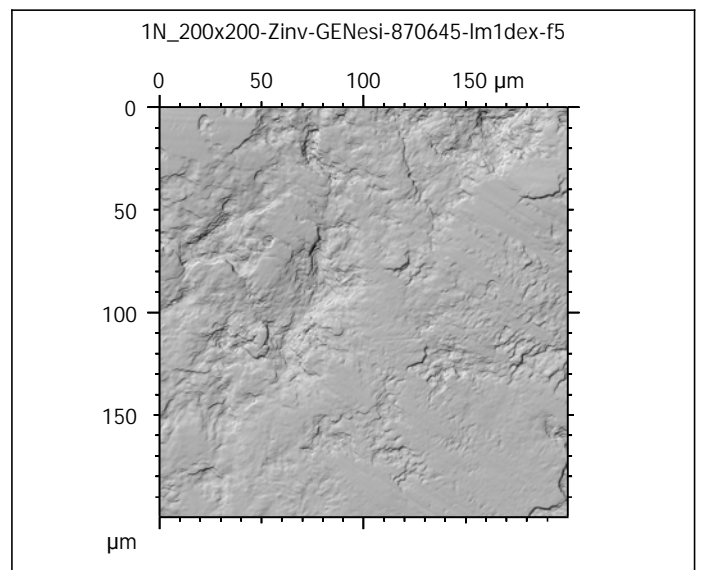
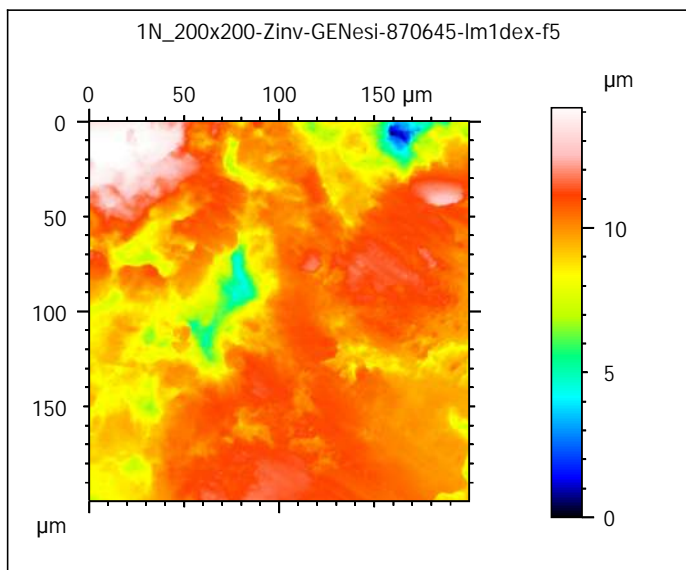
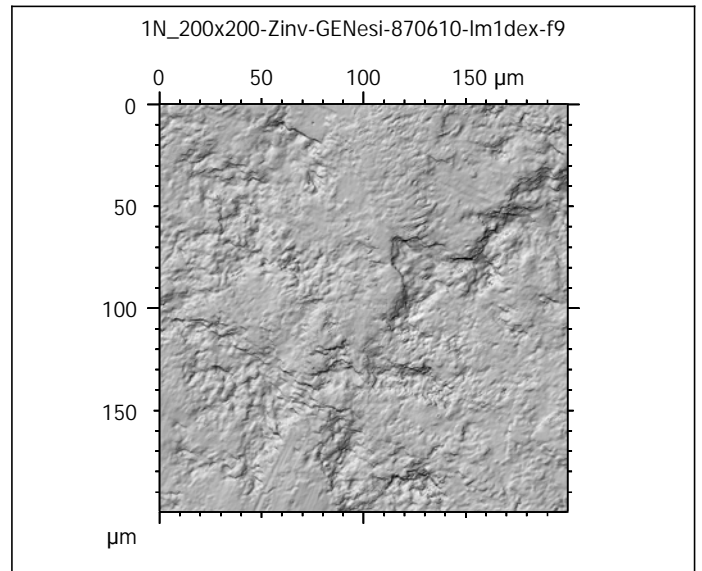
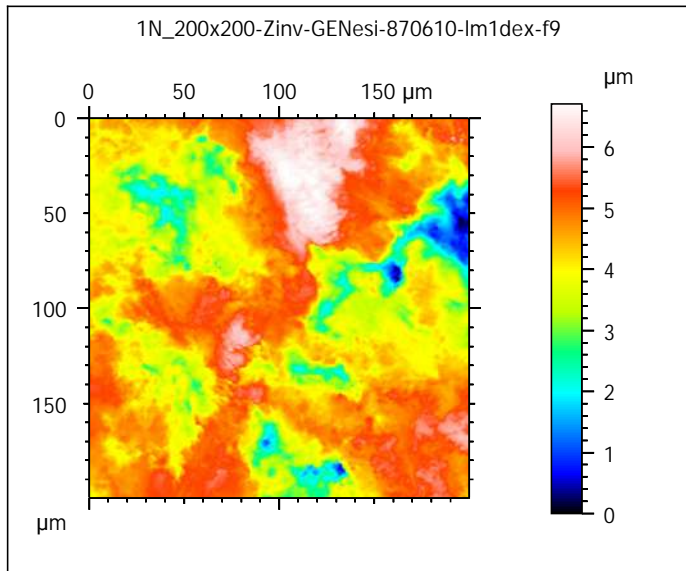
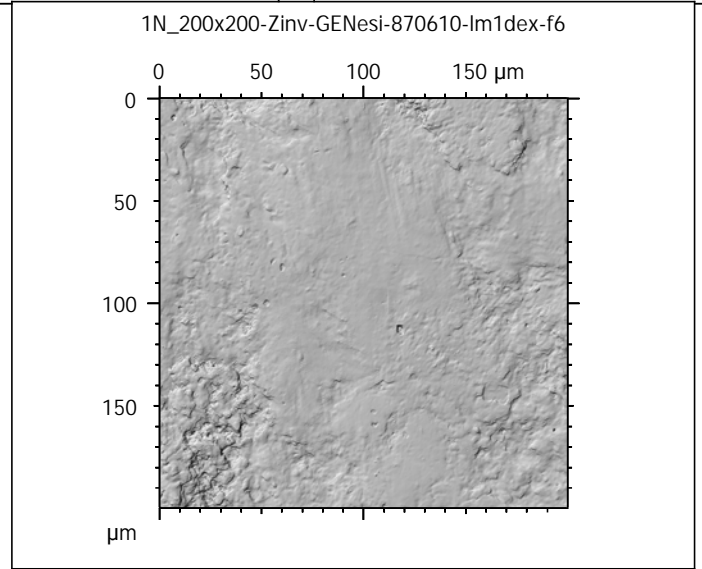
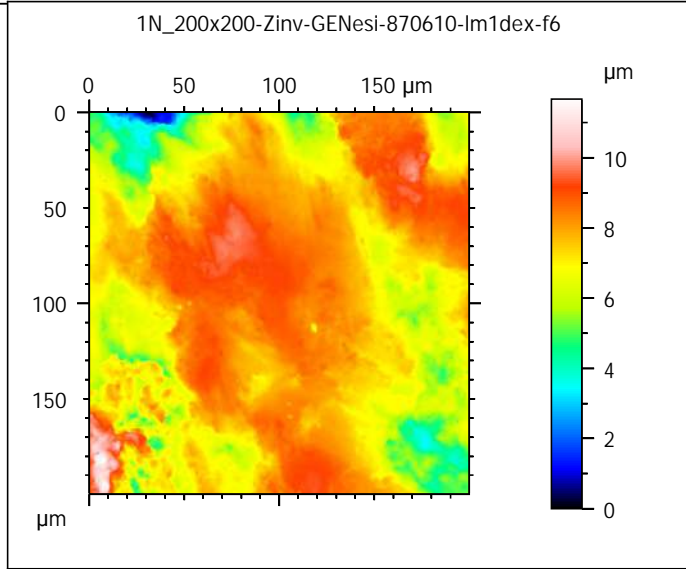
Photosimulations and false color elevation maps of scanned shearing and crushing facets on molars and deciduous premolars of the **hazelnut group** (100% base diet + 10 hazelnuts in shell per day)

scanned at the PALEVOPRIM lab by M. Louail, University of Poitiers, France with "TRIDENT", white light confocal microscope Leica DCM8 - April 2020  
ALIHOM Project (Région Nouvelle Aquitaine, France), ANR Diet-Scratches

**DIET-SCRATCHES**

ANR-17-CE27-0002

PIs: G. Merceron & S. Ferchaud



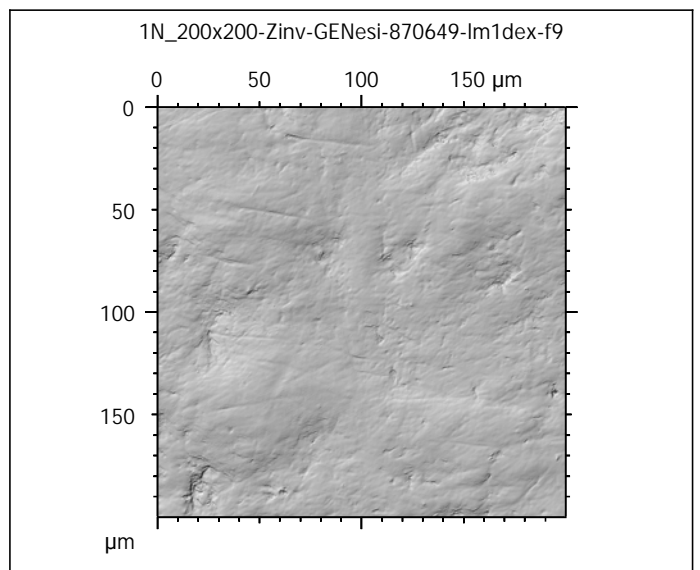
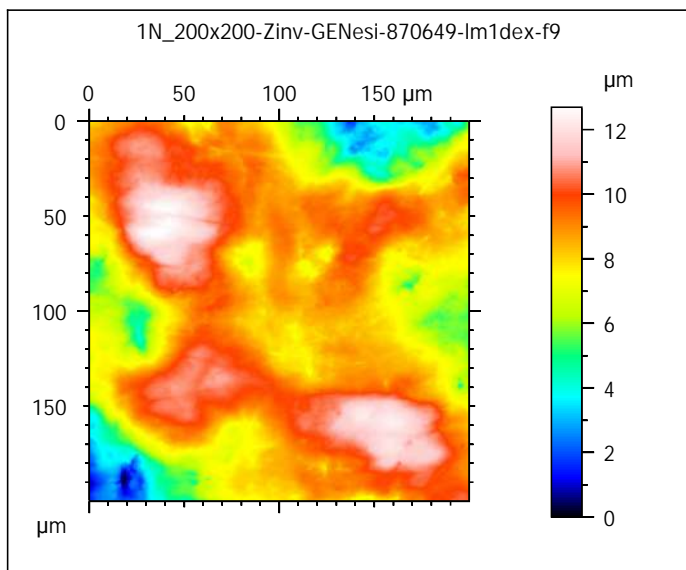
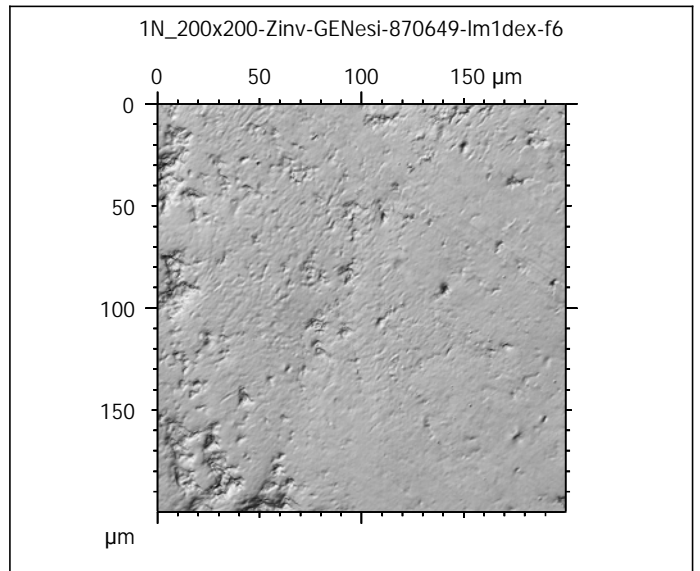
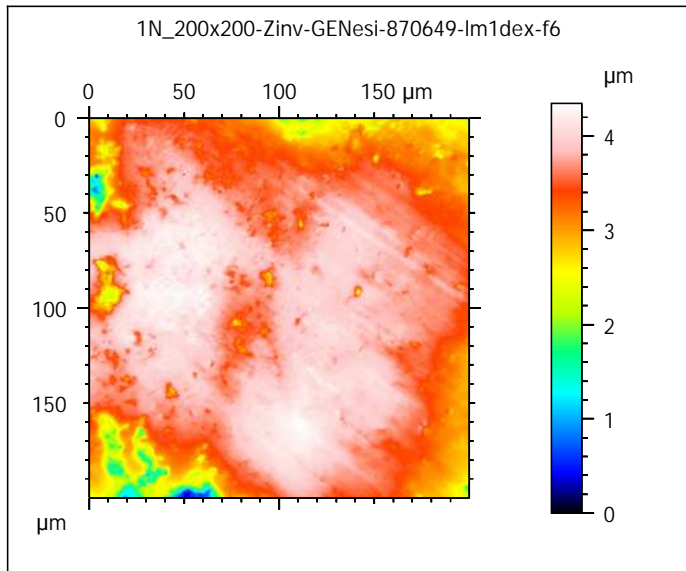
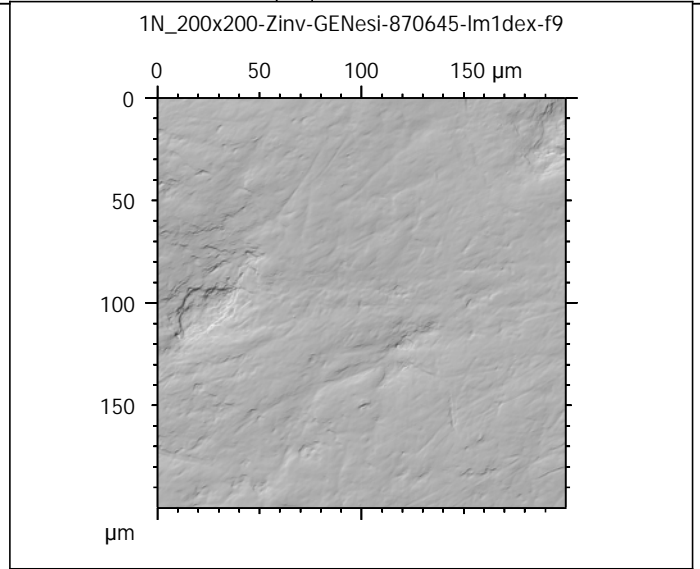
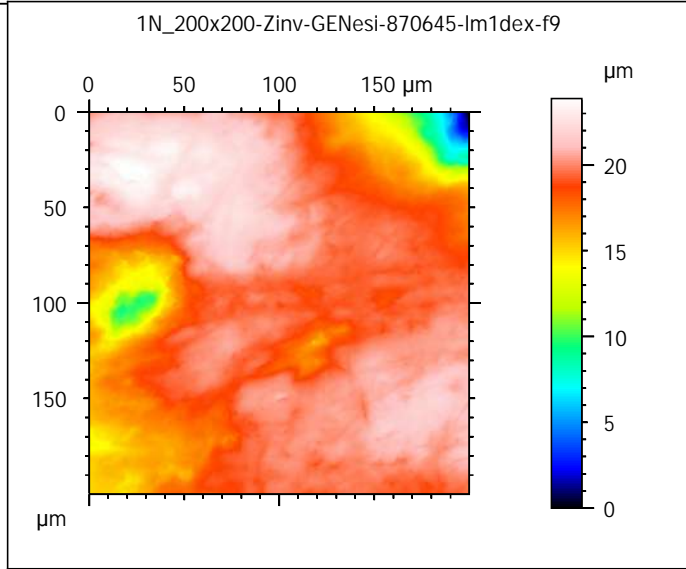
Photosimulations and false color elevation maps of scanned shearing and crushing facets on molars and deciduous premolars of the **hazelnut group** (100% base diet + 10 hazelnuts in shell per day)

scanned at the PALEVOPRIM lab by M. Louail, University of Poitiers, France with "TRIDENT", white light confocal microscope Leica DCM8 - April 2020  
ALIHOM Project (Région Nouvelle Aquitaine, France), ANR Diet-Scratches

**DIET-SCRATCHES**

ANR-17-CE27-0002

PIs: G. Merceron & S. Ferchaud





Photosimulations and false color elevation maps of scanned shearing and crushing facets on molars and deciduous premolars of the **hazelnut group** (100% base diet + 10 hazelnuts in shell per day)

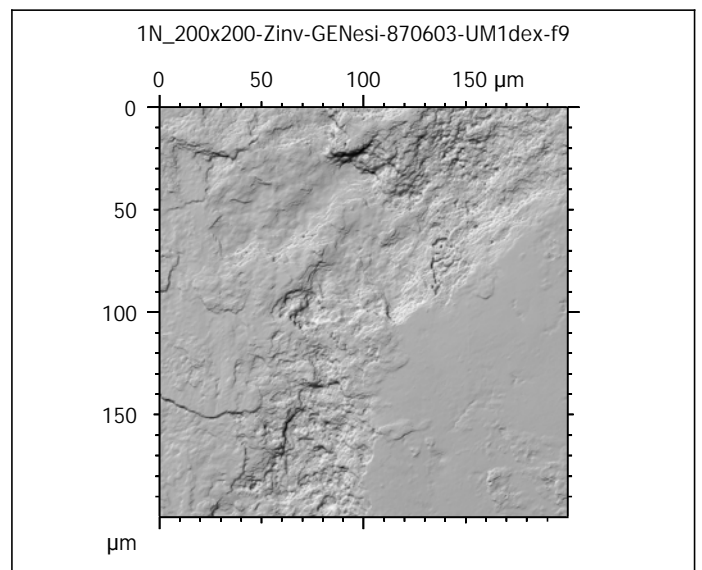
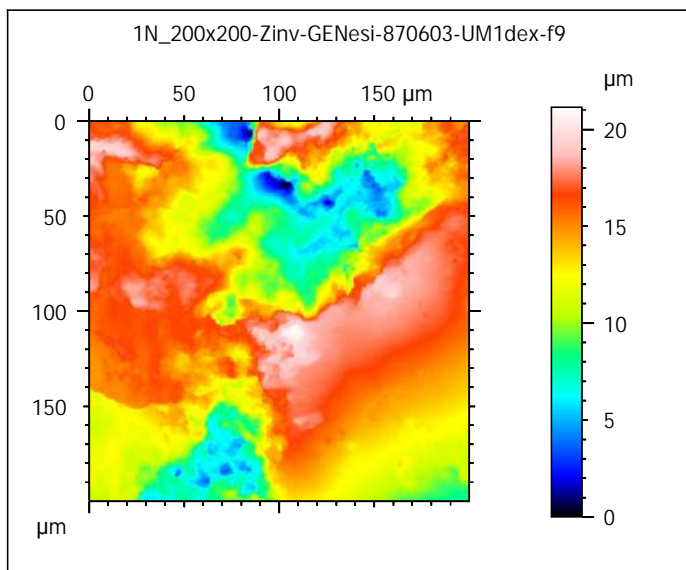
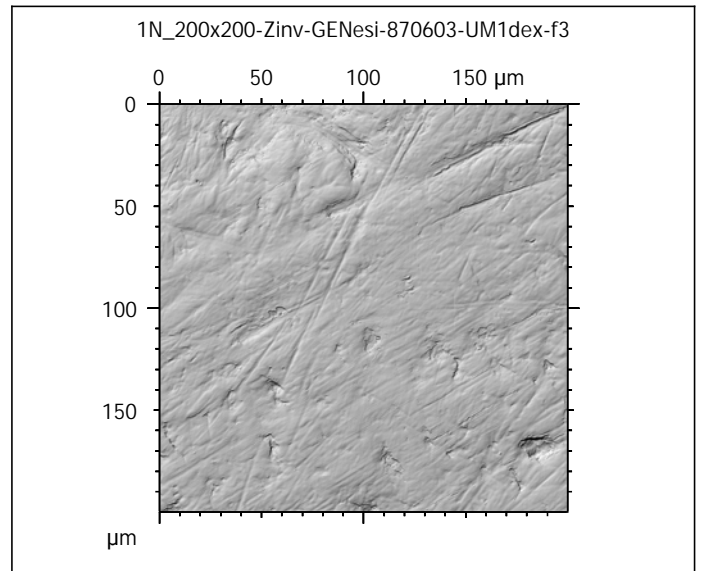
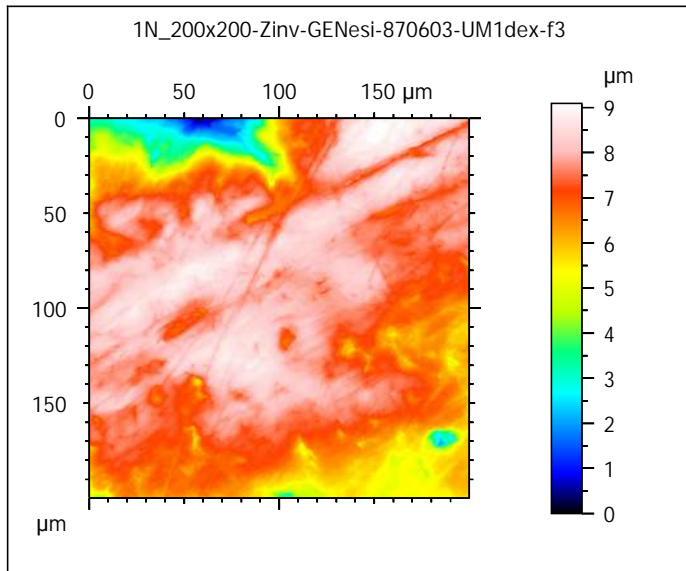
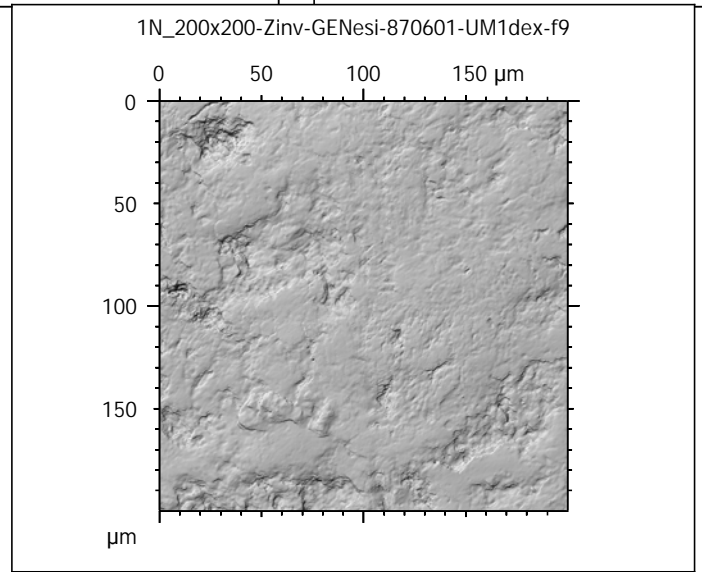
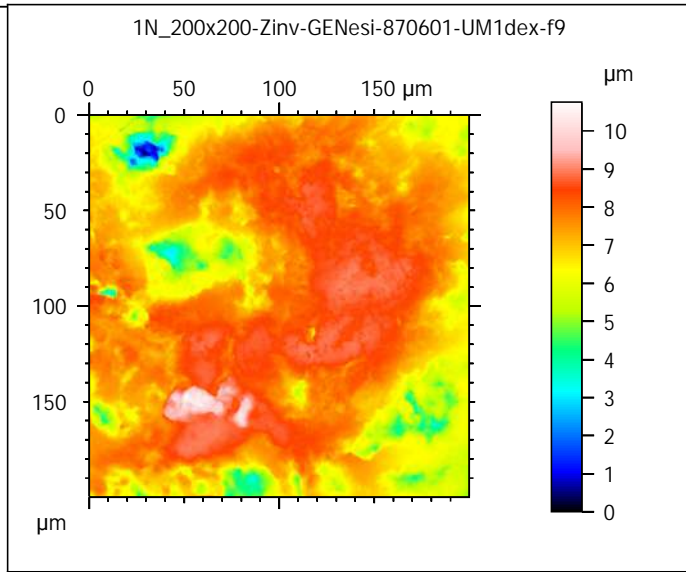
scanned at the PALEVOPRIM lab by M. Louail, University of Poitiers, France with "TRIDENT", white light confocal microscope Leica DCM8 - April 2020

ALIHOM Project (Région Nouvelle Aquitaine, France), ANR Diet-Scratches

**DIET-SCRATCHES**

ANR-17-CE27-0002

PIs: G. Merceron & S. Ferchaud



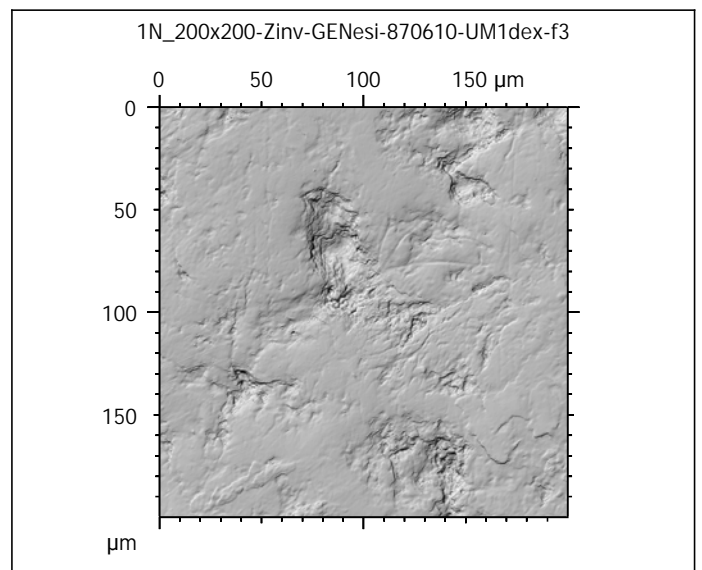
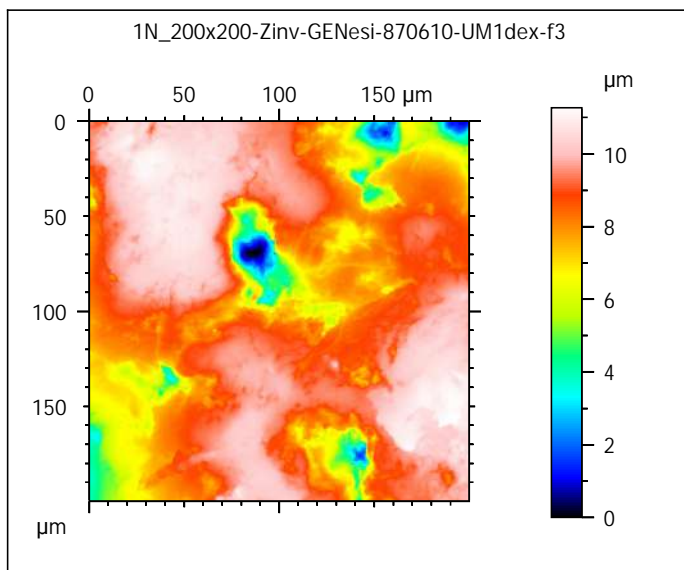
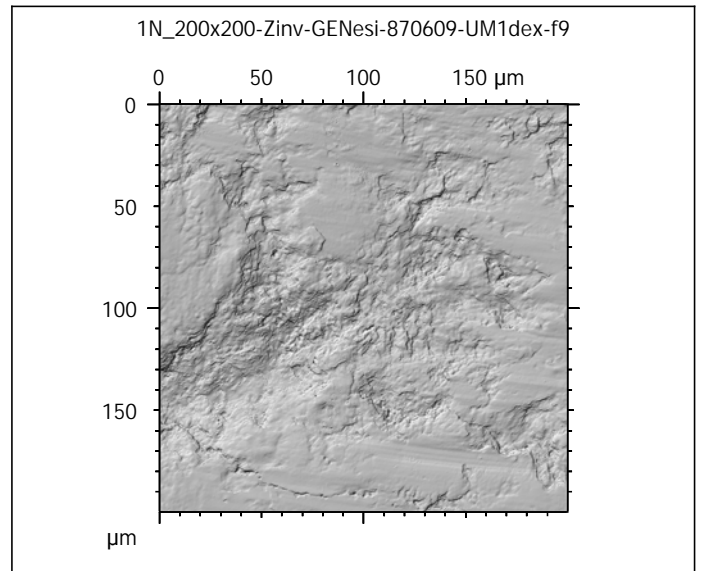
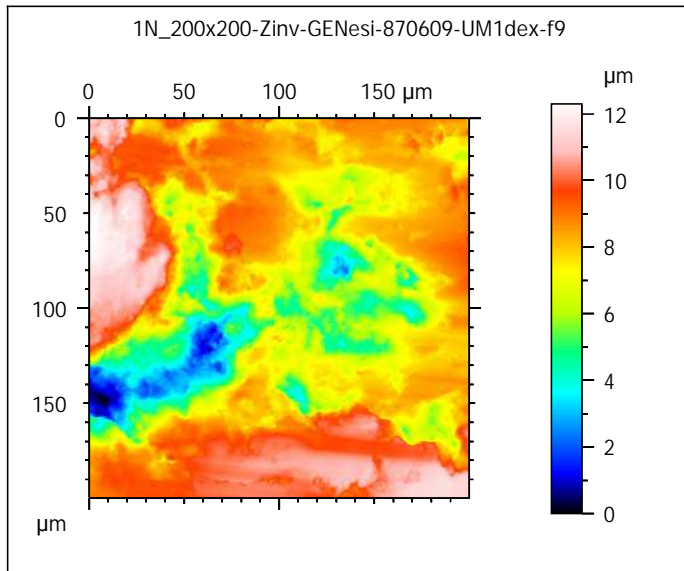
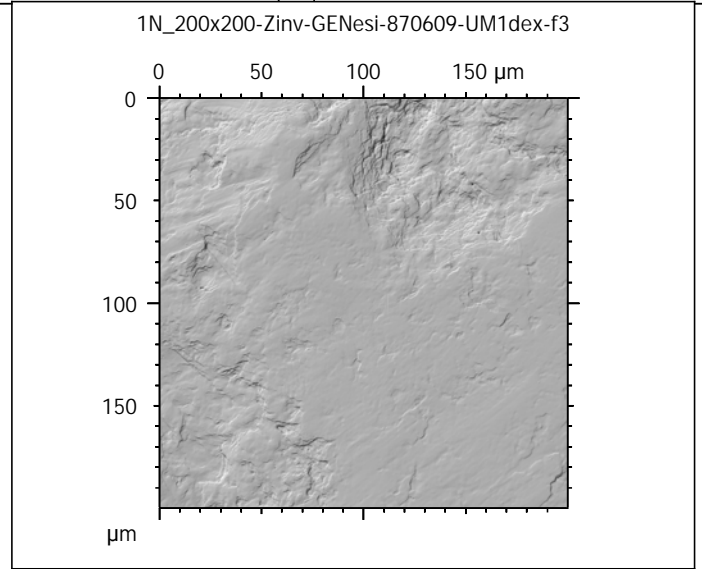
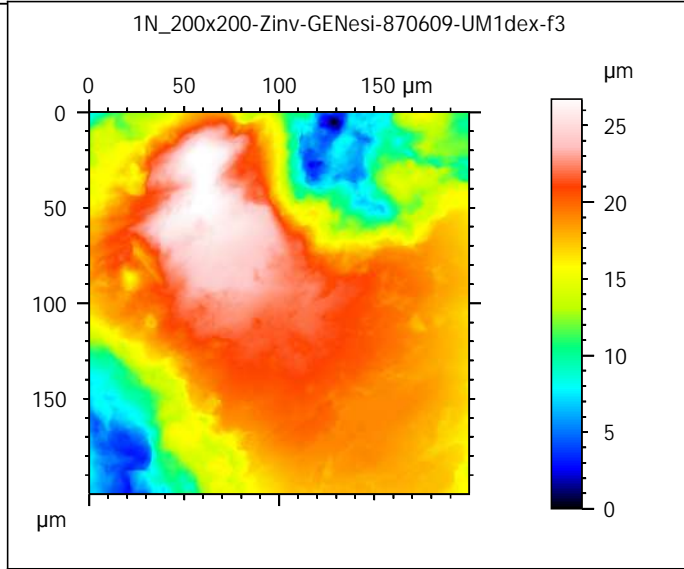
Photosimulations and false color elevation maps of scanned shearing and crushing facets on molars and deciduous premolars of the **hazelnut group** (100% base diet + 10 hazelnuts in shell per day)

scanned at the PALEVOPRIM lab by M. Louail, University of Poitiers, France with "TRIDENT", white light confocal microscope Leica DCM8 - April 2020  
ALIHOM Project (Région Nouvelle Aquitaine, France), ANR Diet-Scratches

**DIET-SCRATCHES**

ANR-17-CE27-0002

PIs: G. Merceron & S. Ferchaud





Photosimulations and false color elevation maps of scanned shearing and crushing facets on molars and deciduous premolars of the **hazelnut group** (100% base diet + 10 hazelnuts in shell per day)

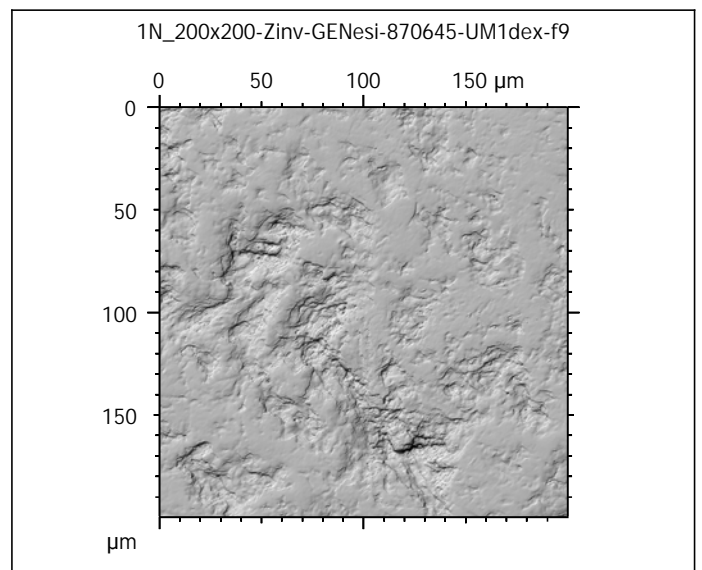
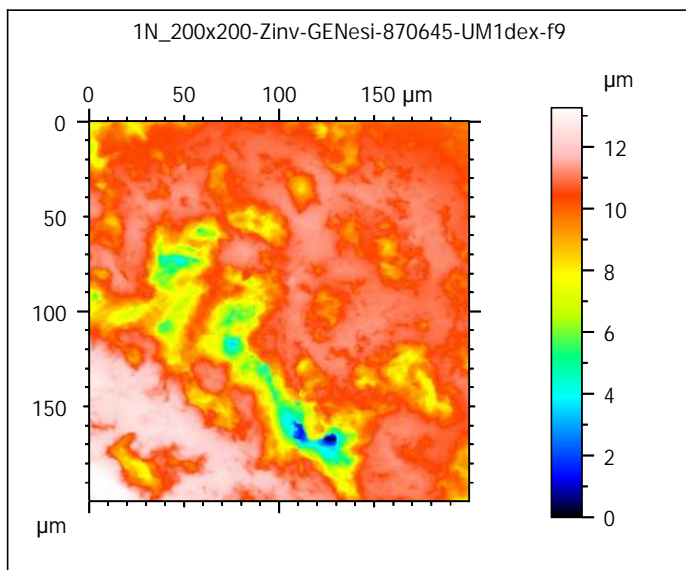
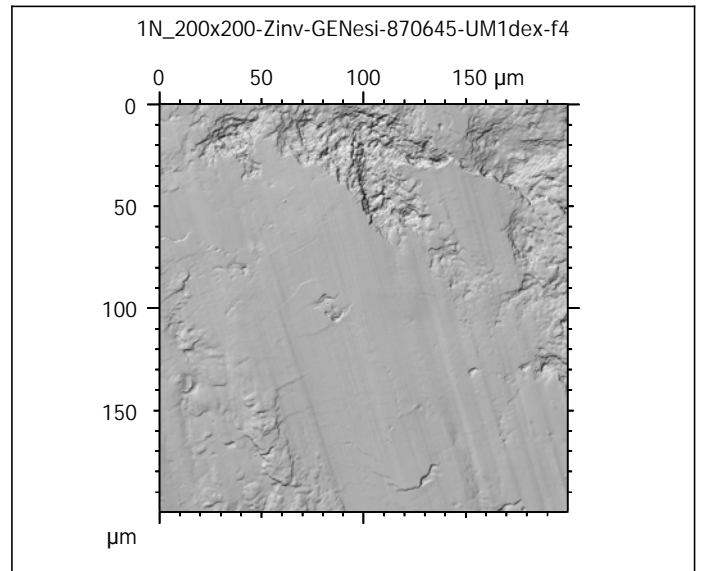
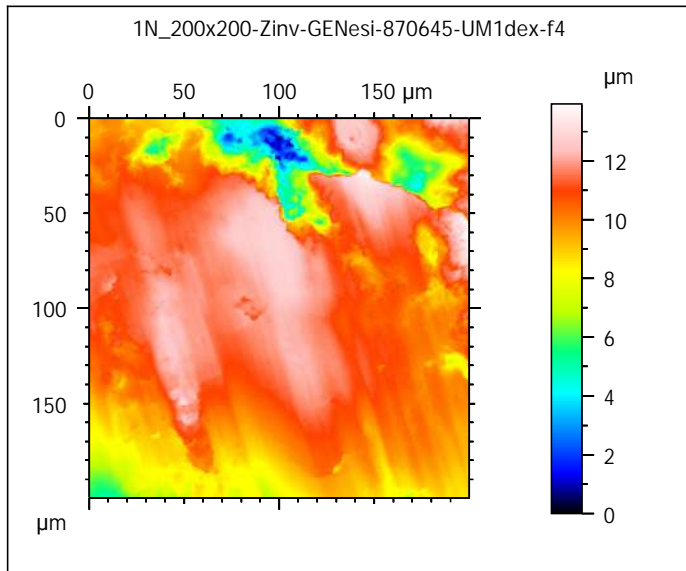
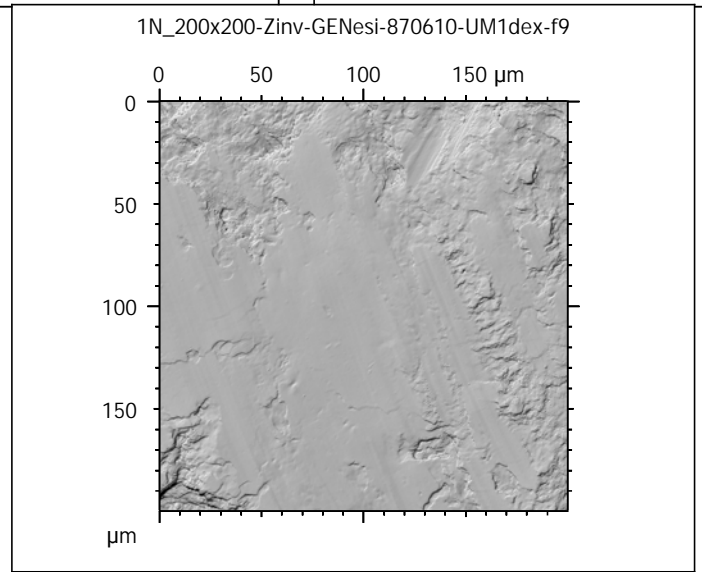
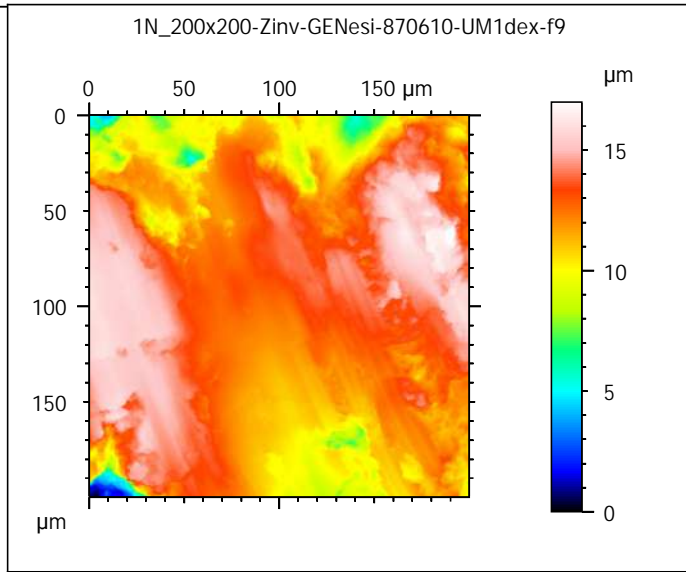
scanned at the PALEVOPRIM lab by M. Louail, University of Poitiers, France with "TRIDENT", white light confocal microscope Leica DCM8 - April 2020

ALIHOM Project (Région Nouvelle Aquitaine, France), ANR Diet-Scratches

**DIET-SCRATCHES**

ANR-17-CE27-0002

PIs: G. Merceron & S. Ferchaud



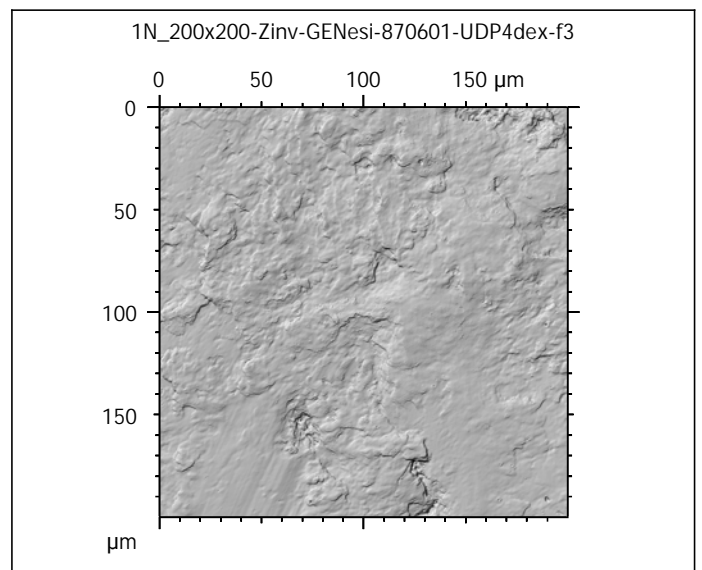
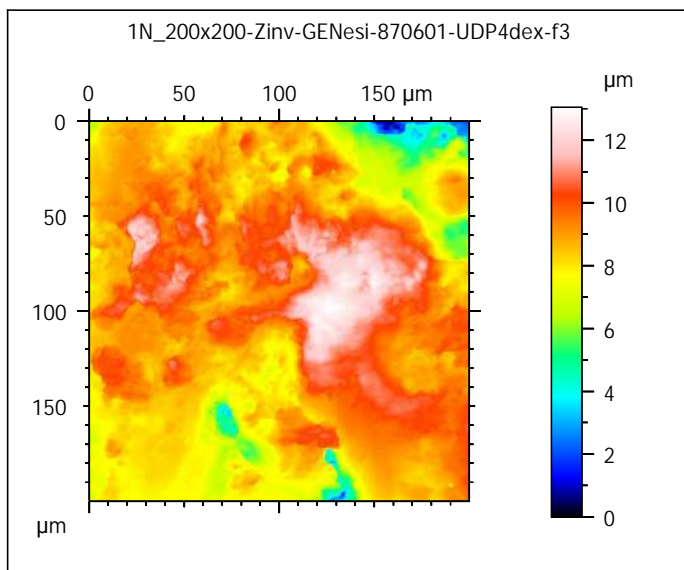
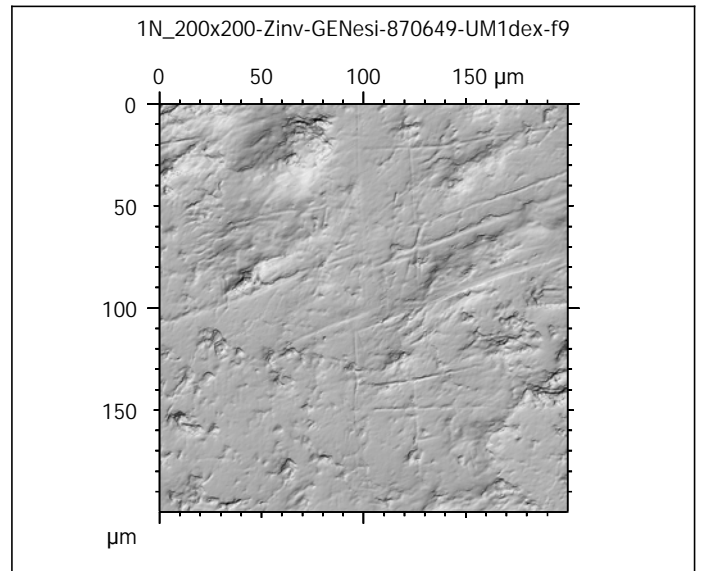
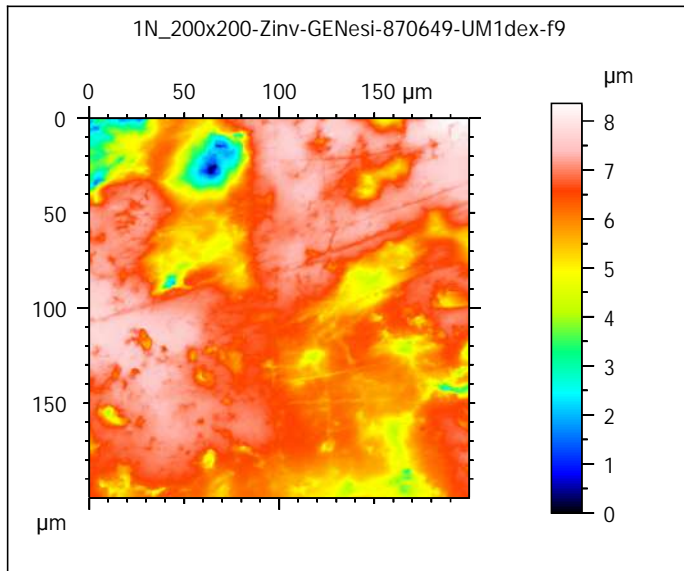
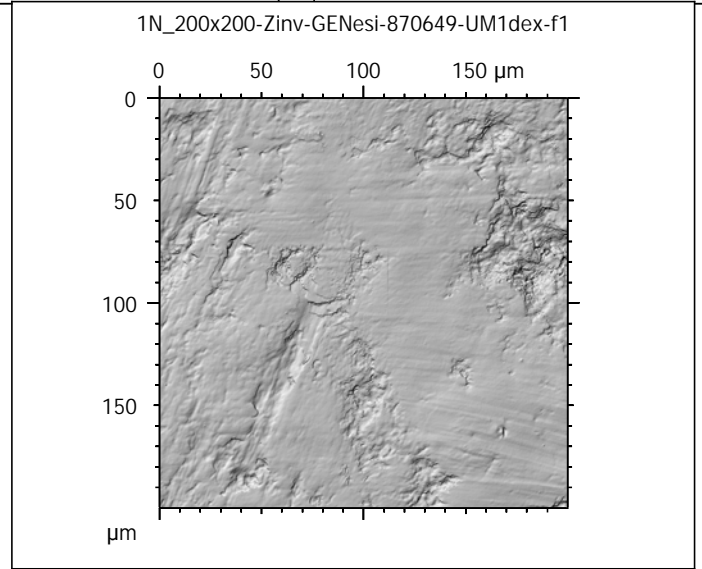
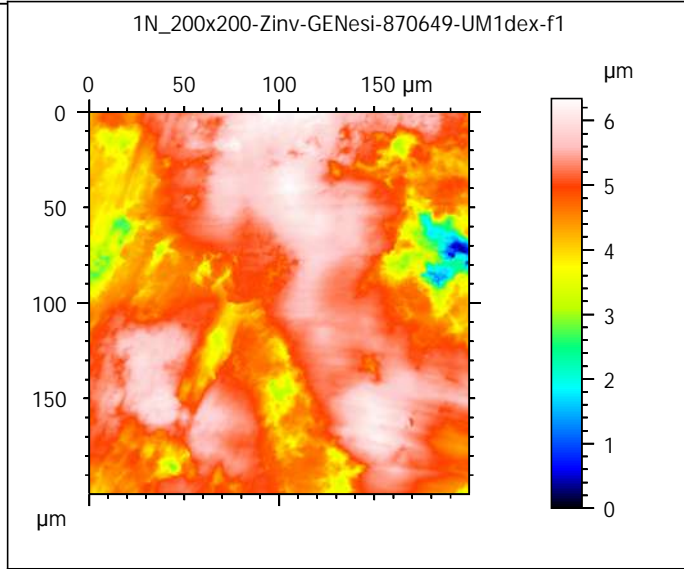
Photosimulations and false color elevation maps of scanned shearing and crushing facets on molars and deciduous premolars of the **hazelnut group** (100% base diet + 10 hazelnuts in shell per day)

scanned at the PALEVOPRIM lab by M. Louail, University of Poitiers, France with "TRIDENT", white light confocal microscope Leica DCM8 - April 2020  
ALIHOM Project (Région Nouvelle Aquitaine, France), ANR Diet-Scratches

**DIET-SCRATCHES**

ANR-17-CE27-0002

PIs: G. Merceron & S. Ferchaud



Photosimulations and false color elevation maps of scanned shearing and crushing facets on molars and deciduous premolars of the **hazelnut group** (100% base diet + 10 hazelnuts in shell per day)

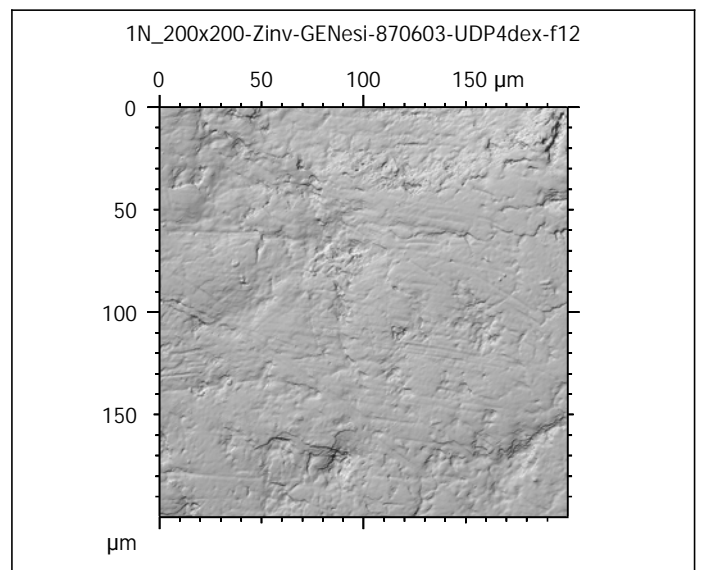
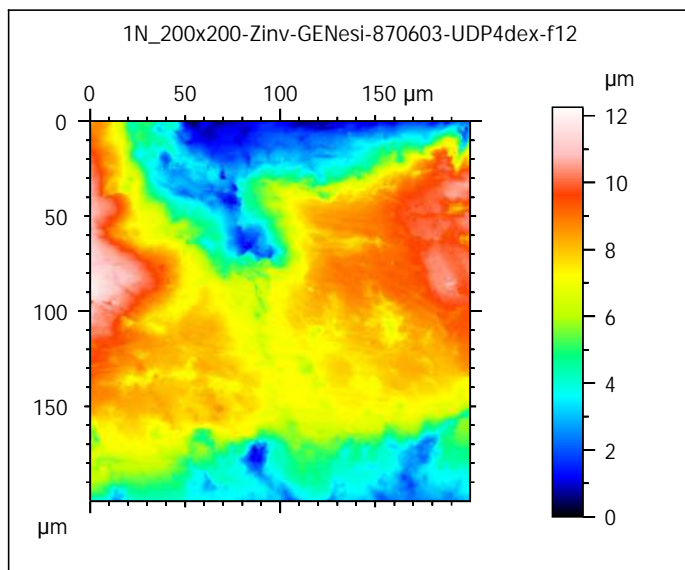
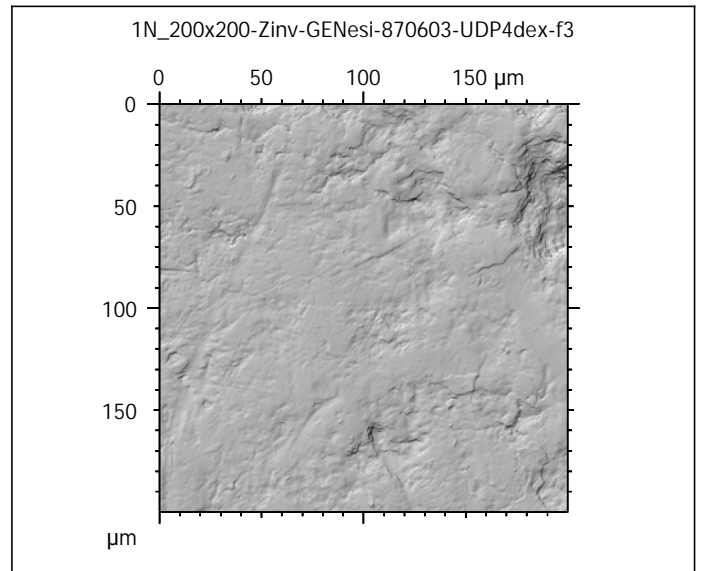
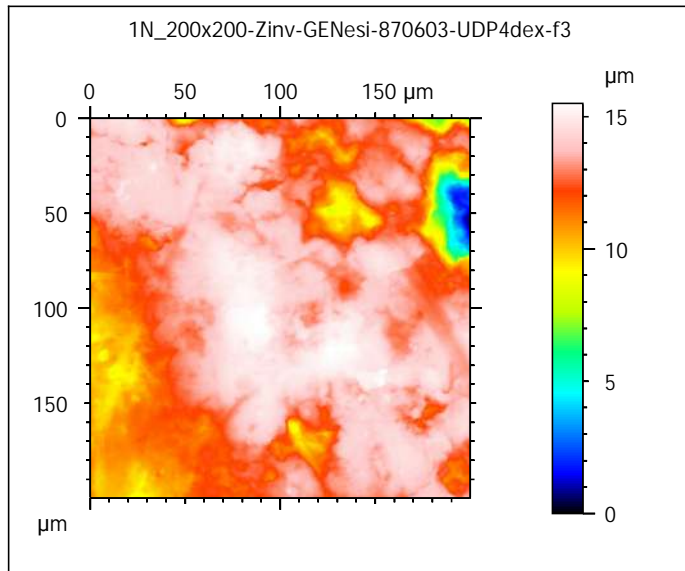
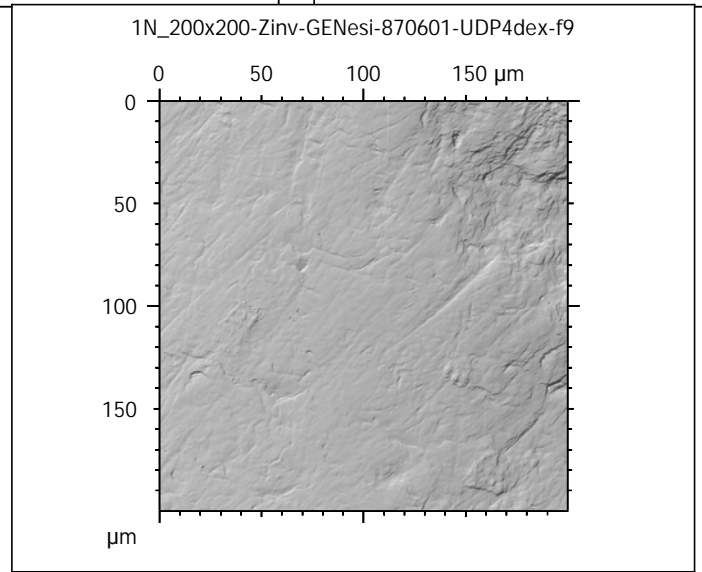
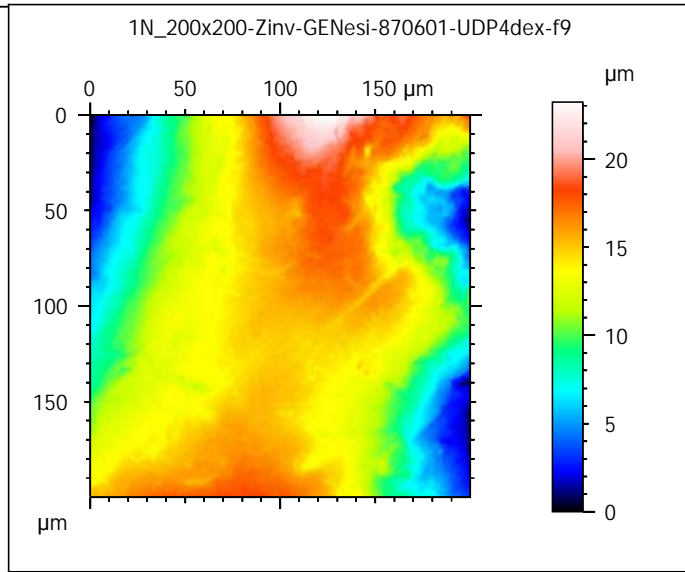
scanned at the PALEVOPRIM lab by M. Louail, University of Poitiers, France with "TRIDENT", white light confocal microscope Leica DCM8 - April 2020

ALIHOM Project (Région Nouvelle Aquitaine, France), ANR Diet-Scratches

**DIET-SCRATCHES**

ANR-17-CE27-0002

PIs: G. Merceron & S. Ferchaud





Photosimulations and false color elevation maps of scanned shearing and crushing facets on molars and deciduous premolars of the **hazelnut group** (100% base diet + 10 hazelnuts in shell per day)

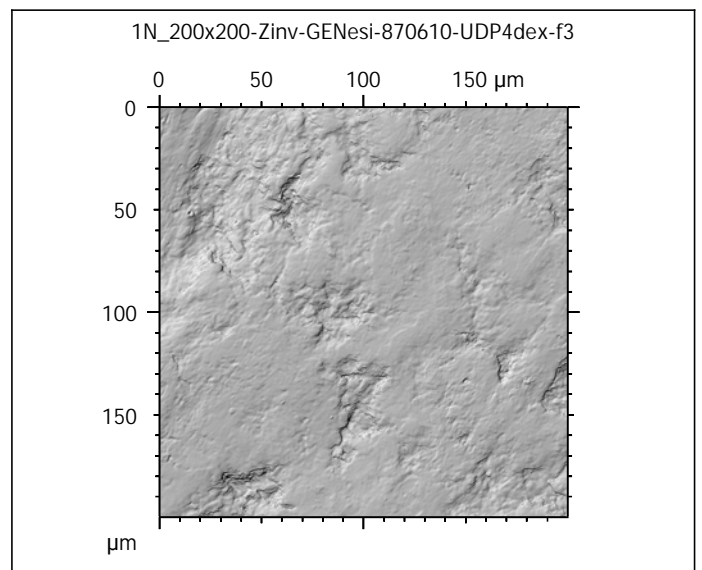
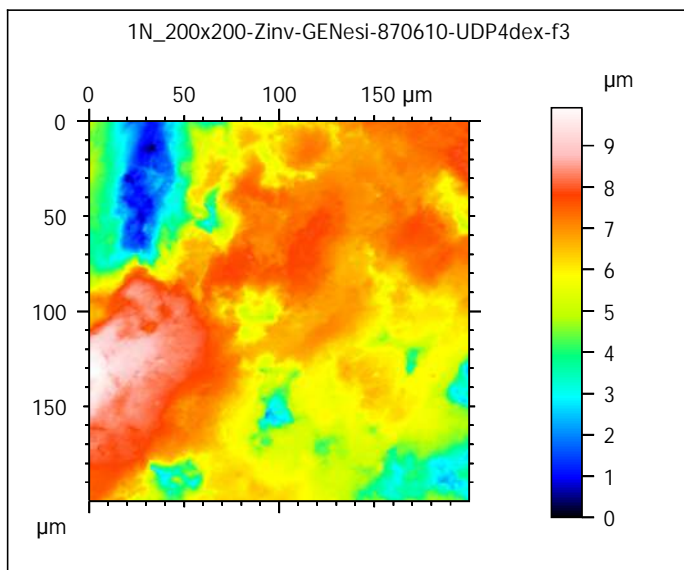
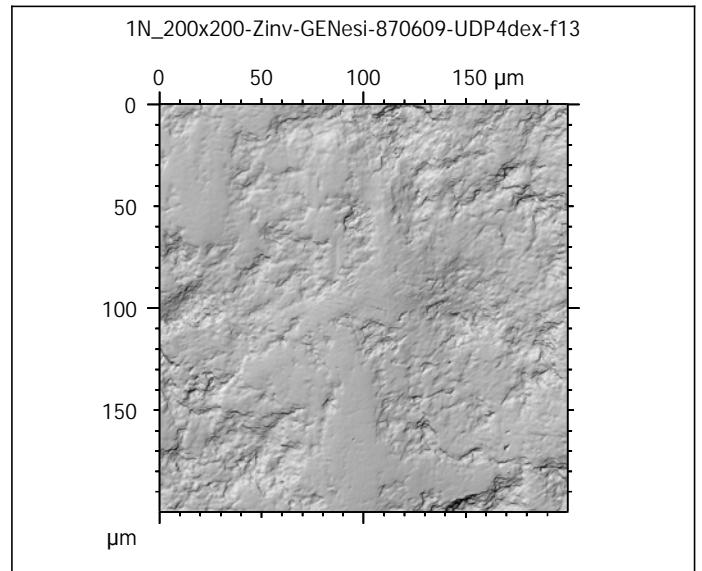
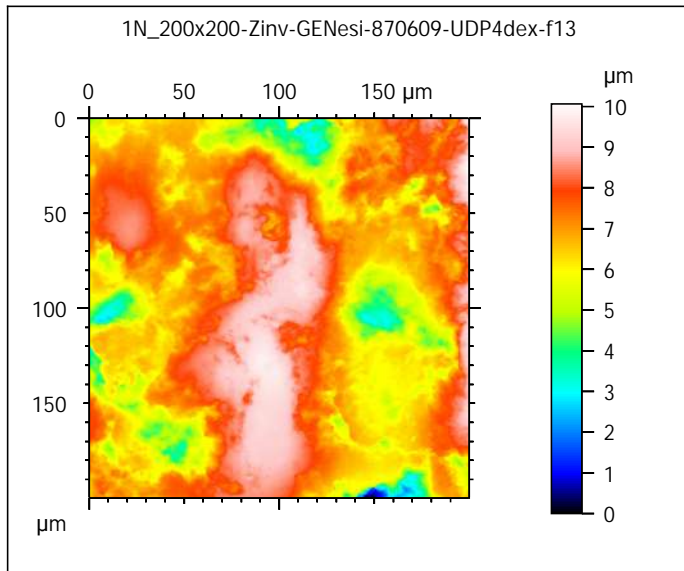
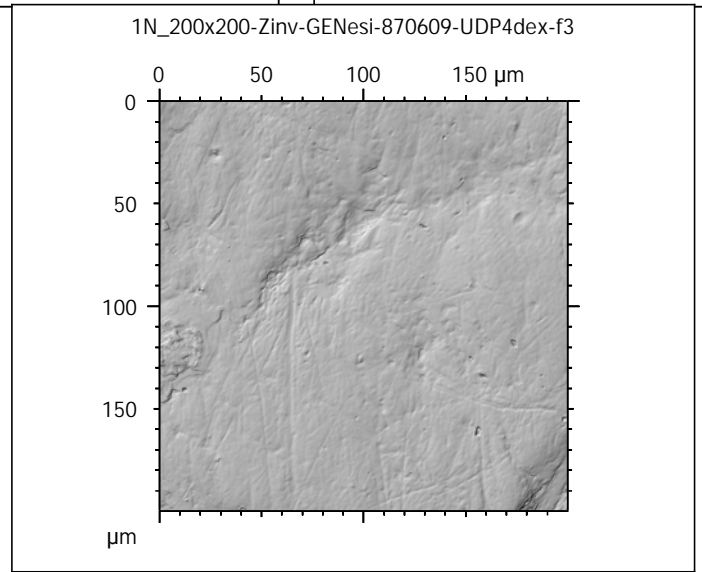
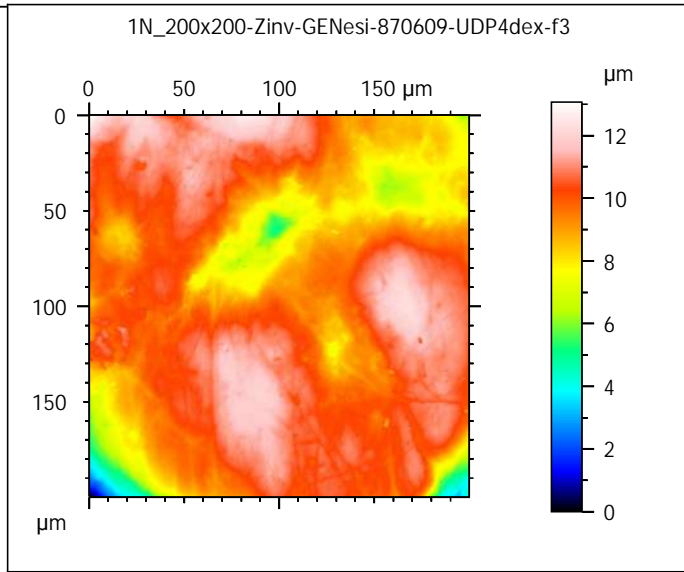
scanned at the PALEVOPRIM lab by M. Louail, University of Poitiers, France with "TRIDENT", white light confocal microscope Leica DCM8 - April 2020

ALIHOM Project (Région Nouvelle Aquitaine, France), ANR Diet-Scratches

**DIET-SCRATCHES**

ANR-17-CE27-0002

PIs: G. Merceron & S. Ferchaud



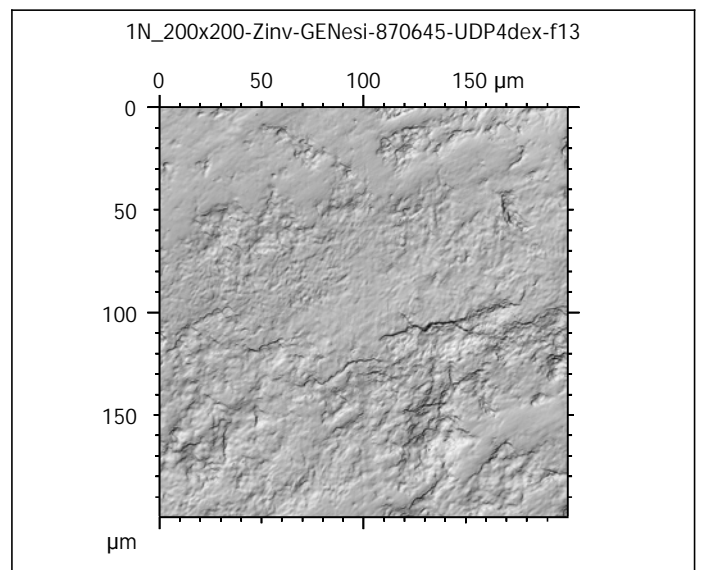
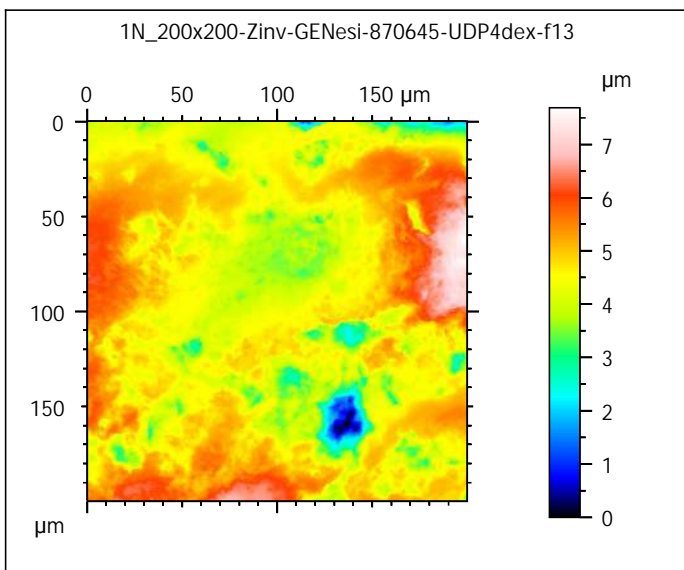
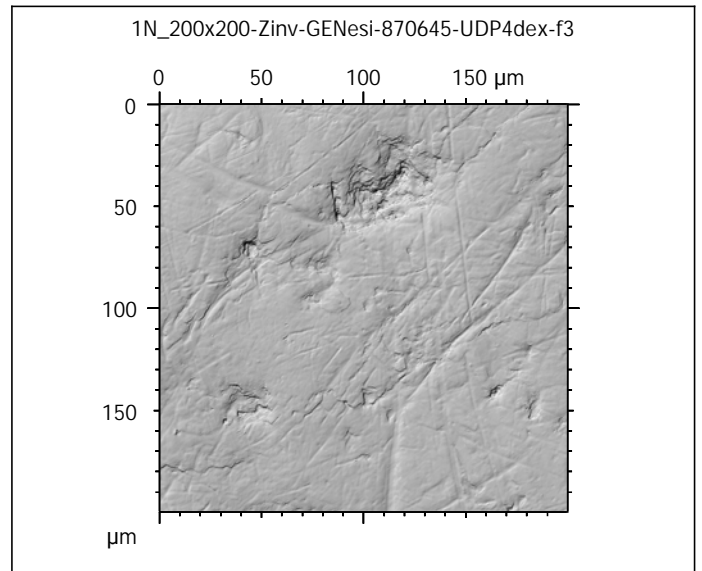
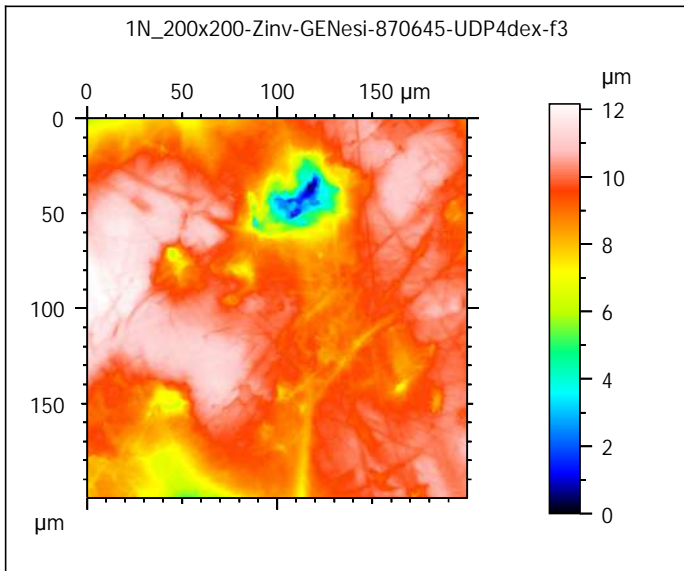
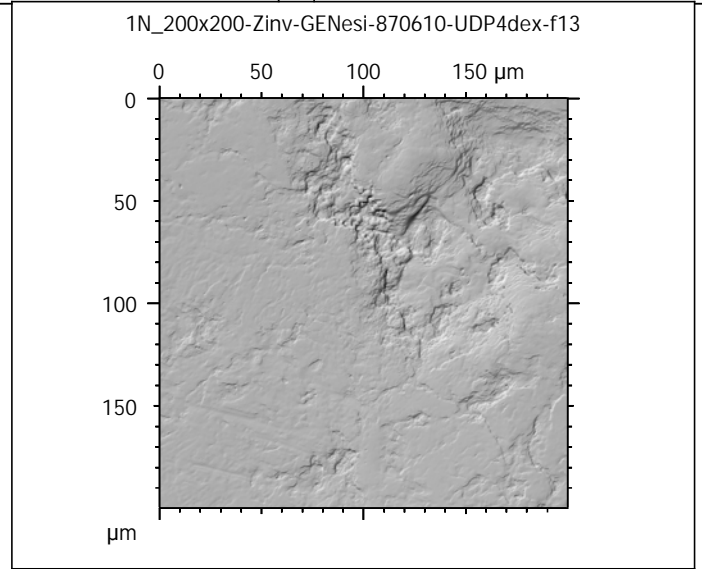
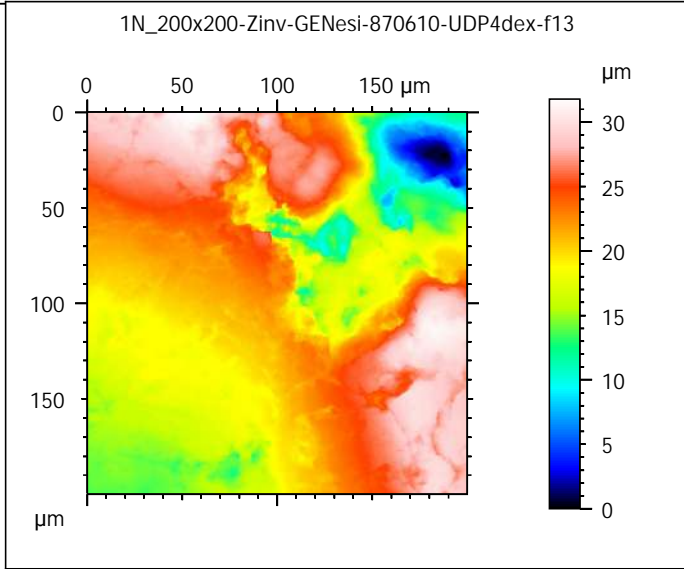
Photosimulations and false color elevation maps of scanned shearing and crushing facets on molars and deciduous premolars of the **hazelnut group** (100% base diet + 10 hazelnuts in shell per day)

scanned at the PALEVOPRIM lab by M. Louail, University of Poitiers, France with "TRIDENT", white light confocal microscope Leica DCM8 - April 2020  
ALIHOM Project (Région Nouvelle Aquitaine, France), ANR Diet-Scratches

**DIET-SCRATCHES**

ANR-17-CE27-0002

PIs: G. Merceron & S. Ferchaud



Photosimulations and false color elevation maps of scanned shearing and crushing facets on molars and deciduous premolars of the **hazelnut group** (100% base diet + 10 hazelnuts in shell per day)

scanned at the PALEVOPRIM lab by M. Louail, University of Poitiers, France with "TRIDENT", white light confocal microscope Leica DCM8 - April 2020

ALIHOM Project (Région Nouvelle Aquitaine, France), ANR Diet-Scratches

**DIET-SCRATCHES**

ANR-17-CE27-0002

PIs: G. Merceron & S. Ferchaud

